Mathematical Problems in Engineering

Applications of Fuzzy Sets and their Extensions in Engineering 2021

Lead Guest Editor: Mingwei Lin
Guest Editors: Zhen-Song Chen, Xindong Peng, and Bahram Farhadinia

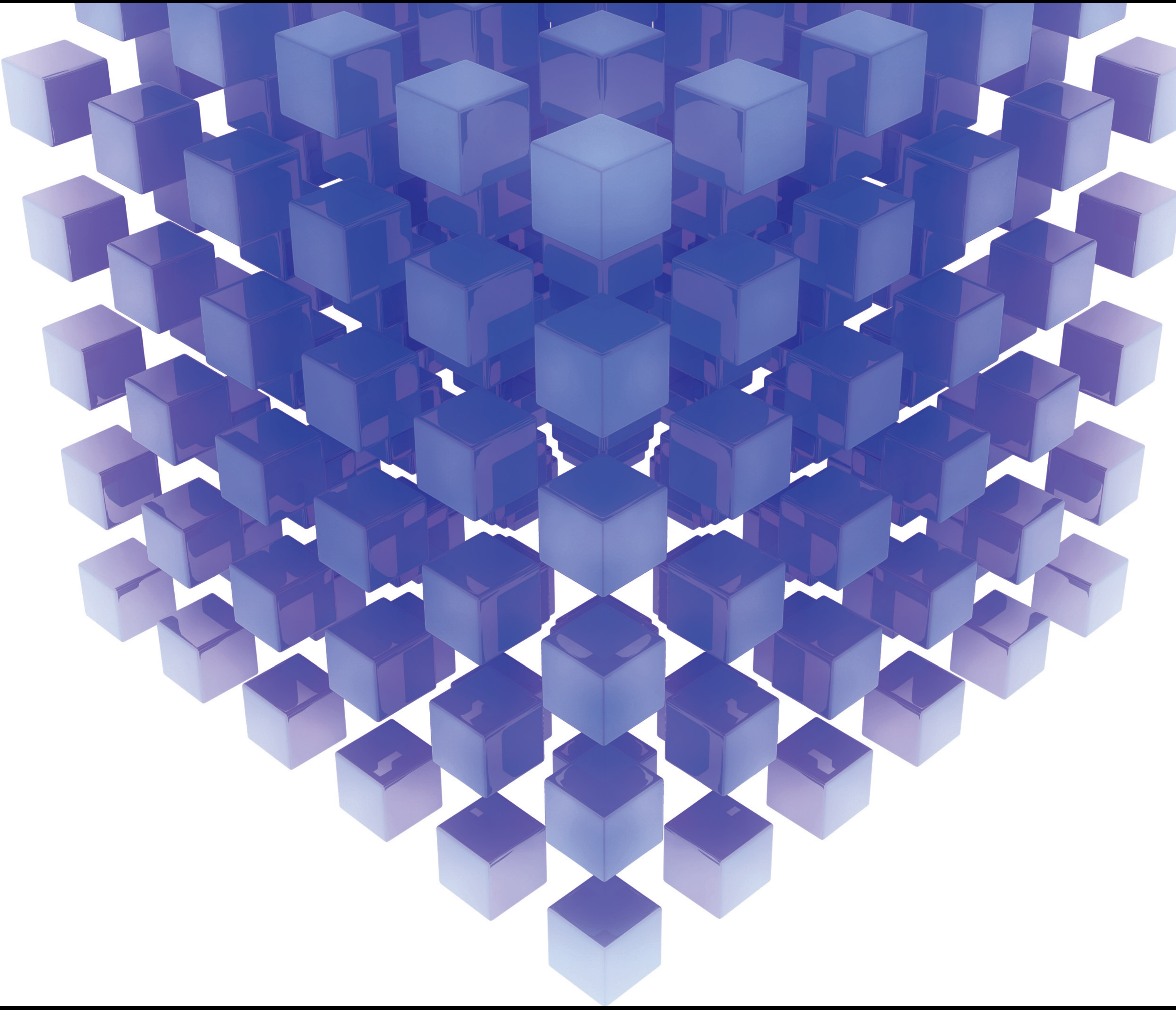

Applications of Fuzzy Sets and their Extensions in Engineering 2021

Mathematical Problems in Engineering

Applications of Fuzzy Sets and their Extensions in Engineering 2021

Lead Guest Editor: Mingwei Lin
Guest Editors: Zhen-Song Chen, Xindong Peng, and Bahram Farhadinia

Paolo Boscariol, Italy
Daniela Boso, Italy
Guillermo Botella-Juan, Spain
Abdesselem Boulkroune, Algeria
Boulaïd Boulkroune, Belgium
Fabio Bovenga, Italy
Francesco Braghin, Italy
Ricardo Branco, Portugal
Julien Bruchon, France
Matteo Bruggi, Italy
Michele Brun, Italy
Maria Elena Bruni, Italy
Maria Angela Butturi, Italy
Bartłomiej Błachowski, Poland
Dhanamjayulu C, India
Raquel Caballero-Águila, Spain
Filippo Cacace, Italy
Salvatore Caddemi, Italy
Zuowei Cai, China
Roberto Caldelli, Italy
Francesco Cannizzaro, Italy
Maosen Cao, China
Ana Carpio, Spain
Rodrigo Carvajal, Chile
Caterina Casavola, Italy
Sara Casciati, Italy
Federica Caselli, Italy
Carmen Castillo, Spain
Inmaculada T. Castro, Spain
Miguel Castro, Portugal
Giuseppe Catalanotti, United Kingdom
Alberto Cavallo, Italy
Gabriele Cazzulani, Italy
Fatih Vehbi Celebi, Turkey
Miguel Cerrolaza, Venezuela
Gregory Chagnon, France
Ching-Ter Chang, Taiwan
Kuei-Lun Chang, Taiwan
Qing Chang, USA
Xiaoheng Chang, China
Prasenjit Chatterjee, Lithuania
Kacem Chehdi, France
Peter N. Cheimets, USA
Chih-Chiang Chen, Taiwan
He Chen, China
Kebing Chen, China
Mengxin Chen, China
Shyi-Ming Chen, Taiwan
Xizhong Chen, Ireland
Xue-Bo Chen, China
Zhiwen Chen, China
Qiang Cheng, USA
Zeyang Cheng, China
Luca Chiapponi, Italy
Francisco Chicano, Spain
Tirivanhu Chinyoka, South Africa
Adrian Chmielewski, Poland
Seongim Choi, USA
Gautam Choubey, India
Hung-Yuan Chung, Taiwan
Yusheng Ci, China
Simone Cinquemani, Italy
Roberto G. Citarella, Italy
Joaquim Ciurana, Spain
John D. Clayton, USA
Piero Colajanni, Italy
Giuseppina Colicchio, Italy
Vassilios Constantoudis, Greece
Enrico Conte, Italy
Alessandro Contento, USA
Mario Cools, Belgium
Gino Cortellessa, Italy
Carlo Cosentino, Italy
Paolo Crippa, Italy
Erik Cuevas, Mexico
Guozeng Cui, China
Mehmet Cunkas, Turkey
Giuseppe D'Aniello, Italy
Peter Dabnichki, Australia
Weizhong Dai, USA
Zhifeng Dai, China
Purushothaman Damodaran, USA
Sergey Dashkovskiy, Germany
Adiel T. De Almeida-Filho, Brazil
Fabio De Angelis, Italy
Samuele De Bartolo, Italy
Stefano De Miranda, Italy
Filippo De Monte, Italy

José António Fonseca De Oliveira Correia, Portugal
Jose Renato De Sousa, Brazil
Michael Defoort, France
Alessandro Della Corte, Italy
Laurent Dewasme, Belgium
Sanku Dey, India
Gianpaolo Di Bona, Italy
Roberta Di Pace, Italy
Francesca Di Puccio, Italy
Ramón I. Diego, Spain
Yannis Dimakopoulos, Greece
Hasan Dinçer, Turkey
José M. Domínguez, Spain
Georgios Dounias, Greece
Bo Du, China
Emil Dumic, Croatia
Madalina Dumitriu, United Kingdom
Premraj Durairaj, India
Saeed Eftekhar Azam, USA
Said El Kafhali, Morocco
Antonio Elipe, Spain
R. Emre Erkmen, Canada
John Escobar, Colombia
Leandro F. F. Miguel, Brazil
FRANCESCO FOTI, Italy
Andrea L. Facci, Italy
Shahla Faisal, Pakistan
Giovanni Falsone, Italy
Hua Fan, China
Jianguang Fang, Australia
Nicholas Fantuzzi, Italy
Muhammad Shahid Farid, Pakistan
Hamed Faroqi, Iran
Yann Favennec, France
Fiorenzo A. Fazzolari, United Kingdom
Giuseppe Fedele, Italy
Roberto Fedele, Italy
Baowei Feng, China
Mohammad Ferdows, Bangladesh
Arturo J. Fernández, Spain
Jesus M. Fernandez Oro, Spain
Francesco Ferrise, Italy
Eric Feulvarch, France
Thierry Floquet, France
Eric Florentin, France
Gerardo Flores, Mexico
Antonio Forcina, Italy
Alessandro Formisano, Italy
Francesco Franco, Italy
Elisa Francomano, Italy
Juan Frausto-Solis, Mexico
Shujun Fu, China
Juan C. G. Prada, Spain
HECTOR GOMEZ, Chile
Matteo Gaeta, Italy
Mauro Gaggero, Italy
Zoran Gajic, USA
Jaime Gallardo-Alvarado, Mexico
Mosè Gallo, Italy
Akemi Gálvez, Spain
Maria L. Gandarias, Spain
Hao Gao, Hong Kong
Xingbao Gao, China
Yan Gao, China
Zhiwei Gao, United Kingdom
Giovanni Garcea, Italy
José García, Chile
Harish Garg, India
Alessandro Gasparetto, Italy
Stylianos Georgantzinos, Greece
Fotios Georgiades, India
Parviz Ghadimi, Iran
Ștefan Cristian Gherghina, Romania
Georgios I. Giannopoulos, Greece
Agathoklis Giaralis, United Kingdom
Anna M. Gil-Lafuente, Spain
Ivan Giorgio, Italy
Gaetano Giunta, Luxembourg
Jefferson L.M.A. Gomes, United Kingdom
Emilio Gómez-Déniz, Spain
Antonio M. Gonçalves de Lima, Brazil
Qunxi Gong, China
Chris Goodrich, USA
Rama S. R. Gorla, USA
Veena Goswami, India
Xunjie Gou, Spain
Jakub Grabski, Poland

Antoine Grall, France
George A. Gravvanis, Greece
Fabrizio Greco, Italy
David Greiner, Spain
Jason Gu, Canada
Federico Guarracino, Italy
Michele Guida, Italy
Muhammet Gul, Turkey
Dong-Sheng Guo, China
Hu Guo, China
Zhaoxia Guo, China
Yusuf Gurefe, Turkey
Salim HEDDAM, Algeria
ABID HUSSANAN, China
Quang Phuc Ha, Australia
Li Haitao, China
Petr Hájek, Czech Republic
Mohamed Hamdy, Egypt
Muhammad Hamid, United Kingdom
Renke Han, United Kingdom
Weimin Han, USA
Xingsi Han, China
Zhen-Lai Han, China
Thomas Hanne, Switzerland
Xinan Hao, China
Mohammad A. Hariri-Ardebili, USA
Khalid Hattaf, Morocco
Defeng He, China
Xiao-Qiao He, China
Yanchao He, China
Yu-Ling He, China
Ramdane Hedjar, Saudi Arabia
Jude Hemanth, India
Reza Hemmati, Iran
Nicolae Herisanu, Romania
Alfredo G. Hernández-Diaz, Spain
M.I. Herreros, Spain
Eckhard Hitzer, Japan
Paul Honeine, France
Jaromir Horacek, Czech Republic
Lei Hou, China
Yingkun Hou, China
Yu-Chen Hu, Taiwan
Yunfeng Hu, China
Can Huang, China
Gordon Huang, Canada
Linsheng Huo, China
Sajid Hussain, Canada
Asier Ibeas, Spain
Orest V. Iftime, The Netherlands
Przemyslaw Ignaciuk, Poland
Giacomo Innocenti, Italy
Emilio Insfran Pelozo, Spain
Azeem Irshad, Pakistan
Alessio Ishizaka, France
Benjamin Ivorra, Spain
Breno Jacob, Brazil
Reema Jain, India
Tushar Jain, India
Amin Jajarmi, Iran
Chiranjibe Jana, India
Łukasz Jankowski, Poland
Samuel N. Jator, USA
Juan Carlos Jáuregui-Correa, Mexico
Kandasamy Jayakrishna, India
Reza Jazar, Australia
Khalide Jbilou, France
Isabel S. Jesus, Portugal
Chao Ji, China
Qing-Chao Jiang, China
Peng-fei Jiao, China
Ricardo Fabricio Escobar Jiménez, Mexico
Emilio Jiménez Macías, Spain
Maolin Jin, Republic of Korea
Zhuo Jin, Australia
Ramash Kumar K, India
BHABEN KALITA, USA
MOHAMMAD REZA KHEDMATI, Iran
Viacheslav Kalashnikov, Mexico
Mathiyalagan Kalidass, India
Tamas Kalmar-Nagy, Hungary
Rajesh Kaluri, India
Jyotheeswara Reddy Kalvakurthi, India
Zhao Kang, China
Ramani Kannan, Malaysia
Tomasz Kapitaniak, Poland
Julius Kaplunov, United Kingdom
Konstantinos Karamanos, Belgium
Michal Kawulok, Poland

Francisco J. Martos, Spain
Elio Masciari, Italy
Paolo Massioni, France
Alessandro Mauro, Italy
Jonathan Mayo-Maldonado, Mexico
Pier Luigi Mazzeo, Italy
Laura Mazzola, Italy
Driss Mehdi, France
Zahid Mehmood, Pakistan
Roderick Melnik, Canada
Xiangyu Meng, USA
Jose Merodio, Spain
Alessio Merola, Italy
Mahmoud Mesbah, Iran
Luciano Mescia, Italy
Laurent Mevel, France
Constantine Michailides, Cyprus
Mariusz Michta, Poland
Prankul Middha, Norway
Aki Mikkola, Finland
Giovanni Minafò, Italy
Edmondo Minisci, United Kingdom
Hiroyuki Mino, Japan
Dimitrios Mitsotakis, New Zealand
Ardashir Mohammadzadeh, Iran
Francisco J. Montáns, Spain
Francesco Montefusco, Italy
Gisele Mophou, France
Rafael Morales, Spain
Marco Morandini, Italy
Javier Moreno-Valenzuela, Mexico
Simone Morganti, Italy
Caroline Mota, Brazil
Aziz Moukrim, France
Shen Mouquan, China
Dimitris Mourtzis, Greece
Emiliano Mucchi, Italy
Taseer Muhammad, Saudi Arabia
Ghulam Muhiuddin, Saudi Arabia
Amitava Mukherjee, India
Josefa Mula, Spain
Jose J. Muñoz, Spain
Giuseppe Muscolino, Italy
Marco Mussetta, Italy
Hariharan Muthusamy, India
Alessandro Naddeo, Italy
Raj Nandkeolyar, India
Keivan Navaie, United Kingdom
Soumya Nayak, India
Adrian Neagu, USA
Erivelton Geraldo Nepomuceno, Brazil
AMA Neves, Portugal
Ha Quang Thinh Ngo, Vietnam
Nhon Nguyen-Thanh, Singapore
Papakostas Nikolaos, Ireland
Jelena Nikolic, Serbia
Tatsushi Nishi, Japan
Shanzhou Niu, China
Ben T. Nohara, Japan
Mohammed Nouari, France
Mustapha Nourelfath, Canada
Kazem Nouri, Iran
Ciro Núñez-Gutiérrez, Mexico
Wlodzimierz Ogryczak, Poland
Roger Ohayon, France
Krzysztof Okarma, Poland
Mitsuhiro Okayasu, Japan
Murat Olgun, Turkey
Diego Oliva, Mexico
Alberto Olivares, Spain
Enrique Onieva, Spain
Calogero Orlando, Italy
Susana Ortega-Cisneros, Mexico
Sergio Ortobelli, Italy
Naohisa Otsuka, Japan
Sid Ahmed Ould Ahmed Mahmoud, Saudi Arabia
Taoreed Owolabi, Nigeria
EUGENIA PETROPOULOU, Greece
Arturo Pagano, Italy
Madhumangal Pal, India
Pasquale Palumbo, Italy
Dragan Pamučar, Serbia
Weifeng Pan, China
Chandan Pandey, India
Rui Pang, United Kingdom
Jürgen Pannek, Germany
Elena Panteley, France
Achille Paolone, Italy

George A. Papakostas, Greece
Xosé M. Pardo, Spain
You-Jin Park, Taiwan
Manuel Pastor, Spain
Pubudu N. Pathirana, Australia
Surajit Kumar Paul, India
Luis Payá, Spain
Igor Pažanin, Croatia
Libor Pekař, Czech Republic
Francesco Pellicano, Italy
Marcello Pellicciari, Italy
Jian Peng, China
Mingshu Peng, China
Xiang Peng, China
Xindong Peng, China
Yuexing Peng, China
Marzio Pennisi, Italy
Maria Patrizia Pera, Italy
Matjaz Perc, Slovenia
A. M. Bastos Pereira, Portugal
Wesley Peres, Brazil
F. Javier Pérez-Pinal, Mexico
Michele Perrella, Italy
Francesco Pesavento, Italy
Francesco Petrini, Italy
Hoang Vu Phan, Republic of Korea
Lukasz Pieczonka, Poland
Dario Piga, Switzerland
Marco Pizzarelli, Italy
Javier Plaza, Spain
Goutam Pohit, India
Dragan Poljak, Croatia
Jorge Pomares, Spain
Hiram Ponce, Mexico
Sébastien Poncet, Canada
Volodymyr Ponomaryov, Mexico
Jean-Christophe Ponsart, France
Mauro Pontani, Italy
Sivakumar Poruran, India
Francesc Pozo, Spain
Aditya Rio Prabowo, Indonesia
Anchasa Pramuanjaroenkij, Thailand
Leonardo Primavera, Italy
B Rajanarayan Prusty, India
Krzysztof Puszynski, Poland
Chuan Qin, China
Dongdong Qin, China
Jianlong Qiu, China
Giuseppe Quaranta, Italy
DR. RITU RAJ, India
Vitomir Racic, Italy
Carlo Rainieri, Italy
Kumbakonam Ramamani Rajagopal, USA
Ali Ramazani, USA
Angel Manuel Ramos, Spain
Higinio Ramos, Spain
Muhammad Afzal Rana, Pakistan
Muhammad Rashid, Saudi Arabia
Manoj Rastogi, India
Alessandro Rasulo, Italy
S.S. Ravindran, USA
Abdolrahman Razani, Iran
Alessandro Reali, Italy
Jose A. Reinoso, Spain
Oscar Reinoso, Spain
Haijun Ren, China
Carlo Renno, Italy
Fabrizio Renno, Italy
Shahram Rezapour, Iran
Ricardo Riaza, Spain
Francesco Riganti-Fulginei, Italy
Gerasimos Rigatos, Greece
Francesco Ripamonti, Italy
Jorge Rivera, Mexico
Eugenio Roanes-Lozano, Spain
Ana Maria A. C. Rocha, Portugal
Luigi Rodino, Italy
Francisco Rodríguez, Spain
Rosana Rodríguez López, Spain
Francisco Rossomando, Argentina
Jose de Jesus Rubio, Mexico
Weiguo Rui, China
Rubén Ruiz, Spain
Ivan D. Rukhlenko, Australia
Dr. Eswaramoorthi S., India
Weichao SHI, United Kingdom
Chaman Lal Sabharwal, USA
Andrés Sáez, Spain

Bekir Sahin, Turkey
Laxminarayan Sahoo, India
John S. Sakellariou, Greece
Michael Sakellariou, Greece
Salvatore Salamone, USA
Jose Vicente Salcedo, Spain
Alejandro Salcido, Mexico
Alejandro Salcido, Mexico
Nunzio Salerno, Italy
Rohit Salgotra, India
Miguel A. Salido, Spain
Sinan Salih, Iraq
Alessandro Salvini, Italy
Abdus Samad, India
Sovan Samanta, India
Nikolaos Samaras, Greece
Ramon Sancibrian, Spain
Giuseppe Sanfilippo, Italy
Omar-Jacobo Santos, Mexico
J Santos-Reyes, Mexico
José A. Sanz-Herrera, Spain
Musavarah Sarwar, Pakistan
Shahzad Sarwar, Saudi Arabia
Marcelo A. Savi, Brazil
Andrey V. Savkin, Australia
Tadeusz Sawik, Poland
Roberta Sburlati, Italy
Gustavo Scaglia, Argentina
Thomas Schuster, Germany
Hamid M. Sedighi, Iran
Mijanur Rahaman Seikh, India
Tapan Senapati, China
Lotfi Senhadji, France
Junwon Seo, USA
Michele Serpilli, Italy
Silvestar Šesnić, Croatia
Gerardo Severino, Italy
Ruben Sevilla, United Kingdom
Stefano Sfarra, Italy
Dr. Ismail Shah, Pakistan
Leonid Shaikhet, Israel
Vimal Shanmuganathan, India
Prayas Sharma, India
Bo Shen, Germany
Hang Shen, China
Xin Pu Shen, China
Dimitri O. Shepelsky, Ukraine
Jian Shi, China
Amin Shokrollahi, Australia
Suzanne M. Shontz, USA
Babak Shotorban, USA
Zhan Shu, Canada
Angelo Sifaleras, Greece
Nuno Simões, Portugal
Mehakpreet Singh, Ireland
Piyush Pratap Singh, India
Rajiv Singh, India
Seralathan Sivamani, India
S. Sivasankaran, Malaysia
Christos H. Skiadas, Greece
Konstantina Skouri, Greece
Neale R. Smith, Mexico
Bogdan Smolka, Poland
Delfim Soares Jr., Brazil
Alba Sofi, Italy
Francesco Soldovieri, Italy
Raffaele Solimene, Italy
Yang Song, Norway
Jussi Sopanen, Finland
Marco Spadini, Italy
Paolo Spagnolo, Italy
Ruben Specogna, Italy
Vasilios Spitas, Greece
Ivanka Stamova, USA
Rafał Stanisławski, Poland
Miladin Stefanović, Serbia
Salvatore Strano, Italy
Yakov Strelniker, Israel
Kangkang Sun, China
Qiuqin Sun, China
Shuaishuai Sun, Australia
Yanchao Sun, China
Zong-Yao Sun, China
Kumarasamy Suresh, India
Sergey A. Suslov, Australia
D.L. Suthar, Ethiopia
D.L. Suthar, Ethiopia
Andrzej Swierniak, Poland
Andras Szekrenyes, Hungary
Kumar K. Tamma, USA

Contents

Hindawi
Mathematical Problems in Engineering
Volume 2023, Article ID 9851279, 1 page
https://doi.org/10.1155/2023/9851279

Retraction

Retracted: Method for Fuzzy Number Intuitionistic Fuzzy Multiple Attribute Decision Making and Its Application to Blended Classroom Teaching Reform Effect Evaluation

Mathematical Problems in Engineering

Received 26 September 2023; Accepted 26 September 2023; Published 27 September 2023

This article has been retracted by Hindawi following an investigation undertaken by the publisher [1]. This investigation has uncovered evidence of one or more of the following indicators of systematic manipulation of the publication process:

(1) Discrepancies in scope
(2) Discrepancies in the description of the research reported
(3) Discrepancies between the availability of data and the research described
(4) Inappropriate citations
(5) Incoherent, meaningless and/or irrelevant content included in the article
(6) Peer-review manipulation

The presence of these indicators undermines our confidence in the integrity of the article's content and we cannot, therefore, vouch for its reliability. Please note that this notice is intended solely to alert readers that the content of this article is unreliable. We have not investigated whether authors were aware of or involved in the systematic manipulation of the publication process.

Wiley and Hindawi regrets that the usual quality checks did not identify these issues before publication and have since put additional measures in place to safeguard research integrity.

We wish to credit our own Research Integrity and Research Publishing teams and anonymous and named external researchers and research integrity experts for contributing to this investigation.

The corresponding author, as the representative of all authors, has been given the opportunity to register their agreement or disagreement to this retraction. We have kept a record of any response received.

References

[1] X. Sun, "Method for Fuzzy Number Intuitionistic Fuzzy Multiple Attribute Decision Making and Its Application to Blended Classroom Teaching Reform Effect Evaluation," *Mathematical Problems in Engineering*, vol. 2022, Article ID 3907871, 14 pages, 2022.

Hindawi
Mathematical Problems in Engineering
Volume 2022, Article ID 3179688, 30 pages
https://doi.org/10.1155/2022/3179688

Research Article

MULTIMOORA Method for Addressing Security Algorithms Evaluation Problem under *q*-Rung Orthopair Fuzzy Environment

Rongguo Wang,[1] **Xinmei Li**,[2] **Mingwei Lin**,[2] **and Zhanpeng Lin**[2]

[1]*School of Technology, Fuzhou Technology and Business University, Fuzhou 350715, Fujian, China*
[2]*College of Computer and Cyber Security, Fujian Normal University, Fuzhou 350117, Fujian, China*

Correspondence should be addressed to Rongguo Wang; dfxywrg@163.com, Xinmei Li; li_zn_mg@163.com, Mingwei Lin; linmwcs@163.com, and Zhanpeng Lin; linzhanpeng9912@163.com

Received 15 October 2021; Revised 14 November 2021; Accepted 19 November 2021; Published 9 August 2022

Academic Editor: Amin Jajarmi

How to determine a suitable security algorithm for a special application scenario is a complex problem. In this paper, this complex problem is formulated as a multicriteria decision-making (MCDM) problem, and we propose a novel MULTIMOORA (multiobjective optimization on the basis of a ratio analysis plus the full MULTIpevaluation information in the security algorithms evaluation problem. The MULTIMOORA method is an excellent decision method, which owns strong robustness. However, it has not been used to process the complex information structure of *q*-rung orthopair fuzzy sets. Moreover, it cannot solve the problem that the extreme values negatively influence the ranking results, and it also cannot capture the interrelationship hiding behind the criteria. To overcome the above challenges, we propose novel *q*-rung orthopair fuzzy **Dombi power Heronian mean** (DPHM) operator and *q*-rung orthopair fuzzy **Dombi power geometric Heronian mean** (DPGHM) operator. Based on these two operators, the MULTIMOORA method is improved for solving the security algorithms' evaluation problem. Finally, a practical example for evaluating five security algorithms is used to illustrate the decision process of the proposed *q*-rung orthopair fuzzy MULTIMOORA method.

1. Introduction

With the quick development of multiple information technologies including cloud computing, Internet of Things, and edge computing [1], more and more companies and personals choose to upload their private data to the network [2]. However, as the scale of network becomes larger, the whole network becomes more complicated [3]. The network shows massive security loophole [4]. The companies and personals also own the special software to improve their business. The software also has massive security loophole and risks. To ensure the reliability of software and network, researchers and scholars have provided some solutions. For example, Abdel-Basset et al. [5] have put forward a neutrosophic decision-making model for evaluating the e-government website according to the quality, security, and accessibility. Wang et al. [6] have combined the TOPSIS (technique for order of preference by similarity to ideal solution) approach with the 0-1 integer programming method to choose an intelligent web service for improving the reliability of network.

Researchers and scholars also designed a number of efficient security algorithms to ensure the security requirements of network [7–9]. However, these security algorithms usually own different characteristics and advantages [10]. For a special application scenario, a suitable security algorithm should be selected for satisfying the requirements of this application scenario. How to choose the most suitable security algorithm for a special application scenario is a big challenge. To address this problem, Ning et al. [11] formulated this problem as a multicriteria decision-making (MCDM) problem and proposed a hybrid model for selecting the best encryption algorithm according to several requirements such as the performance, physical, and security. However, the study [11] still has some shortcomings.

(1) In the study [11], crisp values are used to evaluate security algorithms. Since the security algorithm evaluation problem becomes more and more complex, it is not easy for decision makers to use accurate crisp values for evaluating security algorithms [13]. The birth of fuzzy sets (FSs) [14] provides decision makers with a new way to express uncertain evaluation information. However, FSs only describe the membership degree (MD) information. To enhance the uncertain information modeling capability, intuitionistic fuzzy sets (IFSs) [15] were proposed to express the MD and nonmembership degree (NMD) information. In IFSs, the sum of MD and NMD values is not larger than 1. To provide the decision makers with more freedom for expressing the evaluation information, the concept of Pythagorean fuzzy sets (PFSs) was proposed by Yager and Abbasov [16], where the square sum of MD and NMD is not larger than 1. To generalize the concepts of IFSs and PFSs, a generic version, called q-rung orthopair fuzzy set (q-ROFS), was proposed by Yager [17]. In this study, we intend to use q-ROFSs to express the uncertain information. The significance of q-ROFSs is that this information representation way is flexible, and it provides the decision makers with more freedom than PFSs and IFSs.

(2) q-ROFSs have attracted many researchers since its birth. For example, linguistic q-ROFSs [18–20] and interval-valued q-ROFSs [21] are the qualitative and uncertain versions of q-ROFSs. To fuse q-ROFSs' information, various aggregation operators have been proposed [22–28], such as Archimedean Bonferroni mean operators [22], partitioned Bonferroni mean operators [23], Heronian mean operators [24], Maclaurin symmetric mean operators [25, 26], Hamy mean operators [27], and Choquet integral operators [28]. They are the value measurement MCDM methods [29–31], which do not consider the distance between each criterion value and maximum criterion value.

(3) As one of the efficient decision methods, the MULTIMOORA (multiobjective optimization on the basis of a ratio analysis plus the full MULTIplicative form) method [32] consists of three submodels for comprehensively determining the decision results. As shown in Table 1, the decision results that are obtained from the MULTIMOORA method are robust and the MULTIMOORA method outperforms than some other decision methods [12]. Because of its excellent characteristics, the MULTIMOORA method has been used to process various evaluation information, such as interval numbers [33], IFSs [34], picture fuzzy sets [35], and probabilistic linguistic term sets [36]. To the best of our knowledge, there have been no research results on the combination of q-ROFSs and MULTIMOORA method to date. In this paper, we intend to extend the MULTIMOORA method for processing the q-ROFS information in the MCDM problems. Nevertheless, the MULTIMOORA method cannot handle the case that extreme values influence the reliability of the decision results. Moreover, it is incapable of processing the complex interrelationships hiding behind criteria values.

Hence, the motivations of this study are summarized as

(1) A more flexible way of q-ROFSs is used to express the uncertain and vague evaluation information for the security algorithms evaluation problems

(2) A novel decision-making method is developed to solve the security algorithms evaluation problems and select an appropriate algorithm for a special application scenario

To overcome the challenges, a novel q-rung orthopair fuzzy MULTIMOORA method based on Dombi power Heronian mean aggregation operators is proposed in this paper, and it is applied to solve the security algorithms' evaluation problem.

(1) The Dombi operational laws, special forms of t-norms and t-conorms, show strong flexibility when computing input values. The power average (PA) operator has the ability of alleviating negative influences of extreme input values on the decision results. The Heronian mean (HM) acts as a mapping function that can capture the complex interrelationships among input values. Considering the excellent characteristics, in this paper, some Dombi power Heronian mean aggregation operators are proposed to fuse q-rung orthopair fuzzy numbers (q-ROFNs), which are q-rung orthopair fuzzy Dombi power Heronian mean (q-ROFDPHM) operator and q-rung orthopair fuzzy Dombi power geometric Heronian mean (q-ROFDPGHM) operator, as well as their weighted forms. Afterwards, their features are discussed.

(2) The weighted forms of the q-ROFDPHM and q-ROFDPGHM operators are applied to improve the MULTIMOORA method so that a novel q-rung orthopair fuzzy MULTIMOORA method is put forward for handling the security algorithms' evaluation problem. After that, the detailed decision-making procedure of the proposed q-rung orthopair fuzzy MULTIMOORA method is provided.

(3) A case concerning the evaluation of five security algorithms is provided to show the implementation processes of the proposed q-rung orthopair fuzzy MULTIMOORA method. Afterwards, the influences of the parameters on the ranking results are analyzed. Then, the q-rung orthopair fuzzy MULTIMOORA method is compared with the existing decision methods that handle the q-ROFS information.

Table 1: Performance comparison among decision-making methods [12].

Methods	Computational time	Simplicity	Mathematical calculations	Stability
MULTIMOORA	Very less	Very simple	Minimum	Good
TOPSIS	Moderate	Moderately critical	Moderate	Poor
VIKOR	Less	Simple	Moderate	Medium
ELECTRE	High	Moderately critical	Moderate	Medium

The rest content of this paper is organized as follows. The basic knowledge of q-rung orthopair fuzzy sets, PA, Dombi T-conorm and T-norm, HM operator, and MULTIMOORA method is provided in Section 2. In Section 3, the q-ROFDPHM operator and its weighted form are put forward. Section 4 puts forward the q-ROFDPGHM operator and its weighted form. In Section 5, we apply the proposed operators to propose a novel q-rung orthopair fuzzy MULTIMOORA method and also present the decision procedure. In Section 6, an illustrative example of evaluating of security algorithms is provided to show the implementation process of the proposed q-rung orthopair fuzzy MULTIMOORA method. In Section 7, some valuable conclusions are listed.

2. Preliminaries

In this paper, the basic information of q-ROFSs, PA, Dombi T-conorm and T-norm, HM operator, and MULTIMOORA method is provided.

2.1. q-Rung Orthopair Fuzzy Sets. The concept of q-ROFSs was proposed based on IFSs and PFSs. The q-ROFSs show higher flexibility and larger value range than IFSs and PFSs [37–39].

Definition 1 (see [17]). Let $X = \{x_1, x_2, \ldots, x_n\}$ be a finite universe of discourse (UoD); then, a q-ROFS A on X is mathematically expressed as

$$A = \{\langle x, \mu_A(x), \nu_A(x)\rangle | x \in X\}, \tag{1}$$

where $\mu_A: X \longrightarrow [0,1]$ and $\nu_A: X \longrightarrow [0,1]$ are the membership degree (MD) and nonmembership degree (NMD) of the element x belonging to the q-ROFS A, respectively. The constraint conditions for q-ROFS are $0 \le \mu_A(x) \le 1$, $0 \le \nu_A(x) \le 1$, and $0 \le \mu_A^q(x) + \nu_A^q(x) \le 1$, for all $q \ge 1$. The parameter q is a positive integer. The value of $\pi_A(x) = \sqrt[q]{(1 - (\mu_A(x))^q - (\nu_A(x))^q)}$ is defined to be the hesitant degree (HD) of the element x belonging to the q-ROFS A. For convenience, the two-tuple $(\mu_A(x), \nu_A(x))$ is simplified as (μ_A, ν_A), which is also called q-rung orthopair fuzzy number (q-ROFN) by Liu and Wang [40].

For comparing q-ROFNs, the definitions of score function and accuracy function were given by Liu and Wang [40] for q-ROFNs as follows.

Definition 2 (see [40]). Given a q-ROFN $o = (\mu, \nu)$, then its score function and accuracy function are defined as $s(o) = \mu^q - \nu^q$ and $h(o) = \mu^q + \nu^q$, in which $s(o) \in [-1, 1]$ denotes the score function and $h(o) \in [0, 1]$ is the accuracy function.

Based on the above score function and accuracy function presented in Definition 2, Liu and Wang [40] gave a method for comparing two q-ROFNs as follows.

Definition 3 (see [40]). Given two q-ROFNs $o_1 = (\mu_1, \nu_1)$ and $o_2 = (\mu_2, \nu_2)$, $s(o_1)$ and $s(o_2)$ are their score function values, and $h(o_1)$ and $h(o_2)$ are their accuracy function values,

(1) If $s(o_1) > s(o_2)$, then it can be considered that $o_1 > o_2$.

(2) If $s(o_1) = s(o_2)$, then their accuracy function values should be further compared as follows:

  (1) If $h(o_1) > h(o_2)$, then $o_1 > o_2$.

  (2) If $h(o_1) = h(o_2)$, then $o_1 = o_2$.

To measure the deviation degree between any two q-ROFNs, Liu et al. [41] provided the definition of distance between them as follows.

Definition 4 (see [41]). For q-ROFNs, $o_1 = (\mu_1, \nu_1)$ and $o_2 = (\mu_2, \nu_2)$, the distance between them is computed as

$$d(o_1, o_2) = \frac{1}{2}\left(\left|\mu_1^q - \mu_2^q\right| + \left|\nu_1^q - \nu_2^q\right| + \left|\pi_1^q - \pi_2^q\right|\right), \tag{2}$$

where π_1 and π_2 are the HD values of q-ROFNs o_1 and o_2, respectively.

2.2. Power Average Operator. The power average (PA) is a useful aggregation operator that was put forward by Yager [42]. The PA operator has the ability of alleviating negative influences of extreme input values on the calculation results. The original PA operator was devised to process crisp values. Its mathematical definition is given as follows:

Definition 5 (see [42]). Let $o_i\,(i = 1, 2, \ldots, n)$ be a series of nonnegative crisp values; then, the PA operator really acts as a function that

$$\mathrm{PA}(o_1, o_2, \ldots, o_n) = \sum_{i=1}^{n}\left(\frac{(1 + S(o_i))}{\sum_{k=1}^{n}(1 + S(o_k))} o_i\right), \tag{3}$$

where $S(o_i) = \sum_{j=1, j\ne i}^{n} \mathrm{Sup}(o_i, o_j)$ is the support degree for o_i from o_j and $\mathrm{Sup}(o_i, o_j) = 1 - d(o_i, o_j)$.

The support degree satisfies the following features:

(1) $\mathrm{Sup}(o_i, o_j) \in [0, 1]$

(2) $\mathrm{Sup}(o_i, o_j) = \mathrm{Sup}(o_j, o_i)$

(3) If $d(o_i, o_j) < d(o_r, o_k)$, then $\mathrm{Sup}(o_i, o_j) > \mathrm{Sup}(o_r, o_k)$, where $d(o_i, o_j)$ denotes the distance between o_i and o_j

2.3. Dombi T-Norm and T-Conorm. The Dombi T-norm (TNM) and T-conorm (TCNM), which were proposed by Dombi [43], are referred to as special forms of t-norms and t-conorms. Their mathematical expressions are provided as follows.

Definition 6 (see [43]). Given any two real values, m and n, then the Dombi TNM and Dombi TCNM act as two functions, which are mathematically defined as

$$D(m,n) = \frac{1}{1+\left(((1-m)/m)^{\aleph} + ((1-n)/n)^{\aleph}\right)^{(1/\aleph)}},$$

$$D^{*}(m,n) = 1 - \frac{1}{1+\left((m/(1-m))^{\aleph} + (n/(1-n))^{\aleph}\right)^{(1/\aleph)}}, \tag{4}$$

where $\aleph > 0$, $m, n \in [0,1]$.

Based on the above Dombi TNM and Dombi TCNM, Jana et al. [44] gave the Dombi operational laws for computing q-ROFNs as follows.

Definition 7 (see [44]). Given two q-ROFNs $o_1 = (\mu_1, \nu_1)$ and $o_2 = (\mu_2, \nu_2)$, then the Dombi operational laws of q-ROFNs are defined as

(1) $o_1 \oplus o_2 = ((1-(1/(1+((\mu_1^q/(1-\mu_1^q))^{\aleph} + (\mu_2^q/(1-\mu_2^q))^{\aleph})^{(1/\aleph)})))^{(1/q)}, (1/(1+(((1-\nu_1^q)/\nu_1^q)^{\aleph} + ((1-\nu_2^q)/\nu_2^q)^{\aleph})^{(1/\aleph)}))^{(1/q)})$

(2) $o_1 \otimes o_2 = ((1/(1+(((1-\mu_1^q)/\mu_1^q)^{\aleph} + ((1-\mu_2^q)/\mu_2^q)^{\aleph})^{(1/\aleph)}))(1/q), (1-(1/(1+((\nu_1^q/(1-\nu_1^q))^{\aleph} + (\nu_2^q/(1-\nu_2^q))^{\aleph})^{(1/\aleph)})))^{(1/q)})$

(3) $lo_1 = ((1-(1/(1+(l(\mu_1^q/(1-\mu_1^q))^{\aleph})^{(1/\aleph)})))^{(1/q)}, (1/1+(l((1-\nu_1^q)/\nu_1^q)^{\aleph})^{(1/\aleph)})^{(1/q)})$

(4) $o_1^l = ((1/(1+(l((1-\mu_1^q)/\mu_1^q)^{\aleph})^{(1/\aleph)}))^{(1/q)}, (1-(1/(1+(l(\nu_1^q/(1-\nu_1^q))^{\aleph})^{(1/\aleph)})))^{(1/q)})$, where $\aleph > 0$

2.4. Heronian Mean and Geometric Heronian Mean Operators. The aggregation operators (AOs) [45–47] are value measurement MCDM methods. It is very simple and easy to perform AOs. The AOs are the processes, which fuse given input values into a single value [48]. For aggregating the complicated information structures of various fuzzy sets, researchers have put forward various AOs. The Heronian mean (HM) operator [49], an excellent and useful AO, is capable of processing the complicated interrelationships among input values, which are common in the MCDM contexts. The HM operators can be divided into two categories: arithmetic HM (AHM) and geometric HM (GHM) operators, which are mathematically defined as follows.

Definition 8 (see [49]). Let $o_i\,(i = 1, 2, \ldots, n)$ be a series of nonnegative real values; the parameters γ, $\eta \geq 0$; then, the AHM operator can aggregate the nonnegative real values as

$$\mathrm{HM}^{\gamma,\eta}(o_1, o_2, \ldots, o_n) = \left(\frac{2}{n(n+1)}\sum_{i=1}^{n}\sum_{j=i}^{n} o_i^{\gamma} o_j^{\eta}\right)^{(1/(\gamma+\eta))}. \tag{5}$$

Definition 9 (see [49]). Let $o_i\,(i = 1, 2, \ldots, n)$ be a series of nonnegative real values; the parameters γ, $\eta \geq 0$; then, the GHM operator can aggregate the nonnegative real values as

$$\mathrm{GHM}^{\gamma,\eta}(o_1, o_2, \ldots, o_n) = \frac{1}{\gamma+\eta}\prod_{i=1}^{n}\prod_{j=i}^{n}\left(\gamma o_i + \eta o_j\right)^{(2/n(n+1))}. \tag{6}$$

For the AHM operator, its aggregated values are greatly influenced by extreme values [50]. The GHM operator is capable of balancing the big differences among input values [51]. Therefore, the GHM operator performs better than the AHM operator in some cases.

2.5. MULTIMOORA. To obtain more robust decision results, the full multiplicative form (FMF) was applied by Brauers and Zavadskas [32] to extend the initial MOORA (multiobjective optimization on the basis of ratio analysis) method. Thus, the MULTIMOORA method has three components: ratio system (RS) component, reference point (RP) component, and FMF component, respectively [52]. These three components derive the decision results independently. For the purpose of determining the final decision result, the decision results obtained from these three components are processed by the dominance theory [32]. In the following part, the process for implementing the MULTIMOORA method is listed as follows.

Let us suppose that there exists an MCDM problem consisting of m alternatives $\{x_1, x_2, \ldots, x_m\}$ and n criteria $\{a_1, a_2, \ldots, a_n\}$. The weight vector of criteria is denoted as $[\omega_1, \omega_2, \ldots, \omega_n]$, where $\sum_{j=1}^{n}\omega_j = 1$ and $0 \leq \omega_j \leq 1$. The decision matrix (DM) $R = (o_{ij})_{m\times n}$ corresponding to the MCDM problem contains the evaluation information from experts. The element o_{ij} represents the evaluation information of alternative x_i with respect to criterion a_j.

The evaluation information of alternatives across multiple criteria usually shows different dimensions, so the evaluation information in the DM $R = (o_{ij})_{m\times n}$ is suggested to be normalized as

$$\widetilde{o}_{ij} = \frac{o_{ij}}{\sqrt{\sum_{i=1}^{m}\left(o_{ij}\right)^2}}. \tag{7}$$

After that, the normalized DM $\widetilde{R} = (\widetilde{o}_{ij})_{m\times n}$ can be derived.

2.5.1. RS Component. In this component, the criteria should be divided into two categories: benefit-type (BT) criteria and cost-type (CT) criteria. For BT criteria, the larger the evaluation information of alternative, the better the alternative. For CT criteria, the larger the evaluation information of alternative, the worse the alternative. The weighted arithmetic aggregation operator (AAO) is used to calculate the ranking value Y_i of alternative x_i as

$$Y_i = \sum_{j=1}^{k} \omega_j \widetilde{o}_{ij} - \sum_{j=k+1}^{n} \omega_j \widetilde{o}_{ij}, \quad (8)$$

where k represents the number of benefit-type criteria and $n-k$ means the number of cost-type criteria. From the above equation, it is noted that the alternative in the RS component having the maximum ranking value is considered as the best one. Therefore, the alternatives can be ranked based on the descending order of their ranking values.

2.5.2. RP Component. For the RP component, the worst criterion value of each alternative that is farthest from the reference point of the corresponding criterion should be first derived, and then, the alternative with the smallest worst criterion value is considered as the optimal one.

In this component, the reference point of each criterion is first determined as

$$o_j = \left\{ \max_i \widetilde{o}_{ij}, j \leq k; \min_i \widetilde{o}_{ij}, j > k \right\}, \quad (9)$$

where o_j denotes the reference point of alternatives with respect to criterion a_j.

Then, the weighted distance between the normalized evaluation information of the alternative x_i with respect to each criterion and the reference point of the same criterion is computed as $d_{ij} = \omega_j |o_j - \widetilde{o}_{ij}|$.

Finally, the ranking value D_i of alternative x_i is computed as $D_i = \max_j d_{ij}$.

According to the RP component, the optimal alternative should have the smallest ranking value. Thus, the alternatives can be ranked based on the ascending order of their ranking values.

2.5.3. FMF Component. The design idea of FMF component is the same as that of RS component. In the FMF component, the better alternative should have higher values for benefit-type criteria and lower values for cost-type criteria. The weighted geometric aggregation operator (GGO) is used to determine the ranking value U_i of alternative x_i as $U_i = \prod_{j=1}^{k} (\widetilde{o}_{ij})^{\omega_j} / \prod_{j=k+1}^{n} (\widetilde{o}_{ij})^{\omega_j}$.

According to the design idea, the alternative having the largest ranking value should be considered as the best one in the FMF component. Hence, the alternatives can be ranked based on the descending order of their ranking values.

To aggregate the ranking orders of alternatives obtained from these three components, the dominance theory was suggested by Brauers and Zavadskas [32] to be used for deriving the final decision results.

3. q-Rung Orthopair Fuzzy Dombi Power Heronian Mean Operators

In this section, we use the PA operator, Dombi operational laws for q-ROFNs, and arithmetic HM operator to propose q-rung orthopair fuzzy Dombi power HM (q-ROFDPHM) operator and its weighted form. Then, the features are discussed.

Definition 10. Given a set of q-ROFNs $o_i = (\mu_i, \nu_i)\,(i = 1, 2, \ldots, n)$ and three parameters $\gamma, \eta \geq 0$ and $\aleph > 0$, then the q-ROFDPHM operator is defined as

$$q-\text{ROFDPHM}(o_1, o_2, \ldots, o_n) = \left(\frac{2}{n(n+1)} \underset{i=1}{\overset{n}{\oplus}} \underset{j=i}{\overset{n}{\oplus}} \left(\left(\frac{n(1+S(o_i))}{\sum_{k=1}^{n}(1+S(o_k))} o_i \right)^{\gamma} \otimes \left(\frac{n(1+S(o_j))}{\sum_{k=1}^{n}(1+S(o_k))} o_j \right)^{\eta} \right) \right)^{(1/(\gamma+\eta))}. \quad (10)$$

Based on the Dombi operational laws of q-ROFNs [36] and HM operator, the following theorems can be derived.

Theorem 1. *Given n q-ROFNs $o_i = (\mu_i, \nu_i)\,(i = 1, 2, \ldots, n)$ and the parameters $\gamma, \eta \geq 0$ and $\aleph > 0$, then the aggregated result derived from equation (10) is still an q-ROFN, which is*

$$q-\text{ROFDPHM}(o_1, o_2, \ldots, o_n) = \left(\left(\frac{1}{1 + (n(n+1)/2(\gamma+\eta))^{(1/\aleph)} \times \left(1/\left(\sum_{i=1,j=i}^{n} \left(1/\left(\gamma t_i a_i^{\aleph} + \eta e_j a_j^{\aleph} \right) \right) \right)^{(1/\aleph)} \right)} \right)^{(1/q)}, \right.$$
$$\left. \left(1 - \frac{1}{1 + (n(n+1)/2(\gamma+\eta))^{(1/\aleph)} \times \left(1/\left(\sum_{i=1,j=i}^{n} \left(1/\left(\gamma t_i b_i^{\aleph} + \eta e_j b_j^{\aleph} \right) \right) \right)^{(1/\aleph)} \right)} \right)^{(1/q)} \right), \quad (11)$$

where $\xi_i = ((1+S(o_i))/\sum_{k=1}^{n}(1+S(o_k)))$, $\psi_j = ((1+S(o_j))/\sum_{k=1}^{n}(1+S(o_k)))$, $(\mu_i^q/(1-\mu_i^q)) = (1/a_i)$, $(\mu_j^q/(1-\mu_j^q)) = (1/a_j)$, $((1-\nu_i^q)/\nu_i^q) = (1/b_i)$, $((1-\nu_j^q)/\nu_j^q) = (1/b_j)$, $(1/n\xi_i) = t_i$, *and* $(1/n\psi_j) = e_j$.

Proof. According to Definition 10, we have

$$q-\mathrm{ROFDPHM}(o_1,o_2,\ldots,o_n) = \left(\frac{2}{n(n+1)}\overset{n}{\underset{i=1}{\oplus}}\overset{n}{\underset{j=i}{\oplus}}\left(\left(\frac{n(1+S(o_i))}{\sum_{k=1}^{n}(1+S(o_k))}o_i\right)^{\gamma}\otimes\left(\frac{n(1+S(o_j))}{\sum_{k=1}^{n}(1+S(o_k))}o_j\right)^{\eta}\right)\right)^{(1/(\gamma+\eta))}. \tag{12}$$

Let $\xi_i = ((1+S(o_i))/\sum_{k=1}^{n}(1+S(o_k)))$ and $\psi_j = ((1+S(o_j))/\sum_{k=1}^{n}(1+S(o_k)))$; then, we can derive

$$q-\mathrm{ROFDPHM}(o_1,o_2,\ldots,o_n) = \left(\frac{2}{n(n+1)}\overset{n}{\underset{i=1}{\oplus}}\overset{n}{\underset{j=i}{\oplus}}\left((n\xi_i o_i)^{\gamma}\otimes(n\psi_j o_j)^{\eta}\right)\right)^{(1/(\gamma+\eta))}. \tag{13}$$

According to Definition 7, it can be derived that

$$\begin{aligned} n\xi_i o_i &= \left(\left(1-\frac{1}{1+\left(n\xi_i\left(\mu_i^q/(1-\mu_i^q)\right)^{\aleph}\right)^{(1/\aleph)}}\right)^{(1/q)},\left(\frac{1}{1+\left(n\xi_i\left((1-\nu_i^q)/\nu_i^q\right)^{\aleph}\right)^{(1/\aleph)}}\right)^{(1/q)}\right),\\ n\psi_j o_j &= \left(\left(1-\frac{1}{1+\left(n\psi_j\left(\mu_j^q/(1-\mu_j^q)\right)^{\aleph}\right)^{(1/\aleph)}}\right)^{(1/q)},\left(\frac{1}{1+\left(n\psi_j\left((1-\nu_j^q)/\nu_j^q\right)^{\aleph}\right)^{(1/\aleph)}}\right)^{(1/q)}\right). \end{aligned} \tag{14}$$

Let $(\mu_i^q/(1-\mu_i^q)) = (1/a_i)$, $(\mu_j^q/(1-\mu_j^q)) = (1/a_j)$, $((1-\nu_i^q)/\nu_i^q) = (1/b_i)$, and $((1-\nu_j^q)/\nu_j^q) = (1/b_j)$; then, we have

$$\begin{aligned} n\xi_i o_i &= \left(\left(1-\frac{1}{1+\left(n\xi_i\left(1/a_i^{\aleph}\right)\right)^{(1/\aleph)}}\right)^{(1/q)},\left(\frac{1}{1+\left(n\xi_i\left(1/b_i^{\aleph}\right)\right)^{(1/\aleph)}}\right)^{(1/q)}\right),\\ n\psi_j o_j &= \left(\left(1-\frac{1}{1+\left(n\psi_j\left(1/a_j^{\aleph}\right)\right)^{(1/\aleph)}}\right)^{(1/q)},\left(\frac{1}{1+\left(n\psi_j\left(1/b_j^{\aleph}\right)\right)^{(1/\aleph)}}\right)^{(1/q)}\right),\\ (n\xi_i o_i)^{\gamma} &= \left(\left(\frac{1}{1+\left(\gamma(1/n\xi_i)a_i^{\aleph}\right)^{(1/\aleph)}}\right)^{(1/q)},\left(1-\frac{1}{1+\left(\gamma(1/n\xi_i)b_i^{\aleph}\right)^{(1/\aleph)}}\right)^{(1/q)}\right),\\ (n\psi_j o_j)^{\eta} &= \left(\left(\frac{1}{1+\left(\eta(1/n\psi_j)a_j^{\aleph}\right)^{(1/\aleph)}}\right)^{(1/q)},\left(1-\frac{1}{1+\left(\eta(1/n\psi_j)b_j^{\aleph}\right)^{(1/\aleph)}}\right)^{(1/q)}\right). \end{aligned} \tag{15}$$

Let $(1/n\xi_i) = t_i$ and $(1/n\psi_j) = e_j$; then, the above equations can be transformed into

$$(n\xi_i o_i)^{\gamma} = \left(\left(\frac{1}{1+\left(\gamma t_i a_i^{\aleph}\right)^{(1/\aleph)}}\right)^{(1/q)}, \left(1-\frac{1}{1+\left(\gamma t_i b_i^{\aleph}\right)^{(1/\aleph)}}\right)^{(1/q)}\right),$$
$$\left(n\psi_j o_j\right)^{\eta} = \left(\left(\frac{1}{1+\left(\eta e_j a_j^{\aleph}\right)^{(1/\aleph)}}\right)^{(1/q)}, \left(1-\frac{1}{1+\left(\eta e_j b_j^{\aleph}\right)^{(1/\aleph)}}\right)^{(1/q)}\right). \tag{16}$$

Thus, $(n\xi_i o_i)^{\gamma} \otimes (n\psi_j o_j)^{\eta} = (((1/(1+(\gamma t_i a_i^{\aleph} + \eta e_j a_j^{\aleph})^{(1/\aleph)}))^{(1/q)}, (1-(1/(1+(\gamma t_i b_i^{\aleph} + \eta e_j b_j^{\aleph})^{(1/\aleph)})))^{(1/q)})$,

$$\underset{i=1}{\overset{n}{\oplus}}\underset{j=i}{\overset{n}{\oplus}}\left(\left(n\xi_i o_i\right)^{\gamma}\otimes\left(n\psi_j o_j\right)^{\eta}\right) = \left(\left(1-\frac{1}{1+\left(\sum_{i=1,j=i}^{n}\left(1/\left(\gamma t_i a_i^{\aleph}+\eta e_j a_j^{\aleph}\right)\right)\right)^{(1/\aleph)}}\right)^{(1/q)},\right.$$
$$\left.\left(\frac{1}{1+\left(\sum_{i=1,j=i}^{n}\left(1/\left(\gamma t_i b_i^{\aleph}+\eta e_j b_j^{\aleph}\right)\right)\right)^{(1/\aleph)}}\right)^{(1/q)}\right),$$
$$\frac{2}{n(n+1)}\underset{i=1}{\overset{n}{\oplus}}\underset{j=i}{\overset{n}{\oplus}}\left(\left(n\xi_i o_i\right)^{\gamma}\otimes\left(n\psi_j o_j\right)^{\eta}\right) = \left(\left(1-\frac{1}{1+\left((2/n(n+1))\sum_{i=1,j=i}^{n}\left(1/\left(\gamma t_i a_i^{\aleph}+\eta e_j a_j^{\aleph}\right)\right)\right)^{(1/\aleph)}}\right)^{(1/q)},\right.$$
$$\left.\left(\frac{1}{1+\left((2/n(n+1))\sum_{i=1,j=i}^{n}\left(1/\left(\gamma t_i b_i^{\aleph}+\eta e_j b_j^{\aleph}\right)\right)\right)^{(1/\aleph)}}\right)^{(1/q)}\right),$$
$$\left(\frac{2}{n(n+1)}\underset{i=1}{\overset{n}{\oplus}}\underset{j=i}{\overset{n}{\oplus}}\left(\left(n\xi_i o_i\right)^{\gamma}\otimes\left(n\psi_j o_j\right)^{\eta}\right)\right)^{(1/(\gamma+\eta))} = \begin{pmatrix} \left(\frac{1}{1+\left((1/(\gamma+\eta))\left(1/(2/n(n+1))\sum_{i=1,j=i}^{n}\left(1/\left(\gamma t_i a_i^{\aleph}+\eta e_j a_j^{\aleph}\right)\right)\right)\right)^{(1/\aleph)}}\right)^{(1/q)}, \\ \left(1-\frac{1}{1+\left(((1/(\gamma+\eta))\left(1/(2/n(n+1))\sum_{i=1,j=i}^{n}\left(1/\left(\gamma t_i b_i^{\aleph}+\eta e_j b_j^{\aleph}\right)\right)\right)\right)^{(1/\aleph)}}\right)^{(1/q)} \end{pmatrix}. \tag{17}$$

Then, the final result can be determined as

$$\left(\frac{2}{n(n+1)}\underset{i=1}{\overset{n}{\oplus}}\underset{j=i}{\overset{n}{\oplus}}\left(\left(n\xi_i o_i\right)^{\gamma}\otimes\left(n\psi_j o_j\right)^{\eta}\right)\right)^{(1/(\gamma+\eta))} = \begin{pmatrix} \left(\frac{1}{1+(n(n+1)/2(\gamma+\eta))^{(1/\aleph)}\times\left(1/\left(\sum_{i=1,j=i}^{n}\left(1/\left(\gamma t_i a_i^{\aleph}+\eta e_j a_j^{\aleph}\right)\right)\right)^{(1/\aleph)}\right)}\right)^{(1/q)}, \\ \left(1-\frac{1}{1+(n(n+1)/2(\gamma+\eta))^{(1/\aleph)}\times\left(1/\left(\sum_{i=1,j=i}^{n}\left(1/\left(\gamma t_i b_i^{\aleph}+\eta e_j b_j^{\aleph}\right)\right)\right)^{(1/\aleph)}\right)}\right)^{(1/q)} \end{pmatrix}. \tag{18}$$

Then, we need to prove that the aggregated result from the q-ROFDPHM operator is still a q-ROFN.

Let $\hat{\mu} = ((1/(1+(n(n+1)/2(\gamma+\eta))^{(1/\aleph)} \times (1/(\sum_{i=1,j=i}^{n}(1/(\gamma t_i a_i^{\aleph}+\eta e_j a_j^{\aleph})))^{(1/\aleph)}))))^{(1/q)}$ and $\hat{\nu} = (1-(1/(1+(n(n+1)/2(\gamma+\eta))^{(1/\aleph)} \times (1/(\sum_{i=1,j=i}^{n}(1/(\gamma t_i b_i^{\aleph}+\eta e_j b_j^{\aleph})))^{(1/\aleph)}))))^{(1/q)}$; then, we need to prove that (1) $0 \leq \hat{\mu}^q \leq 1$ and $0 \leq \hat{\nu}^q \leq 1$ and (2) $0 \leq \hat{\mu}^q + \hat{\nu}^q \leq 1$.

Since $(n(n+1)/2(\gamma+\eta))^{(1/\aleph)} \geq 0$ and $(\sum_{i=1,j=i}^{n}(1/(\gamma t_i a_i^{\aleph}+\eta e_j a_j^{\aleph})))^{(1/\aleph)} > 0$, then $(n(n+1)/2(\gamma+\eta))^{(1/\aleph)} \times (1/(\sum_{i=1,j=i}^{n}(1/(\gamma t_i a_i^{\aleph}+\eta e_j a_j^{\aleph})))^{(1/\aleph)}) \geq 0$.

Then, we can have

$$1+\left(\frac{n(n+1)}{2(\gamma+\eta)}\right)^{(1/\aleph)} \times \frac{1}{\left(\sum_{i=1,j=i}^{n}\left(1/\left(\gamma t_i a_i^{\aleph}+\eta e_j a_j^{\aleph}\right)\right)\right)^{(1/\aleph)}} \geq 1 \Longrightarrow 0 \leq \frac{1}{1+(n(n+1)/2(\gamma+\eta))^{(1/\aleph)} \times \left(1/\left(\sum_{i=1,j=i}^{n}\left(1/\left(\gamma t_i a_i^{\aleph}+\eta e_j a_j^{\aleph}\right)\right)\right)^{(1/\aleph)}\right)} \leq 1. \tag{19}$$

Thus, $0 \leq \hat{\mu}^q \leq 1$. Similarly, it can be proven that $0 \leq \hat{\nu}^q \leq 1$. It can be derived that $0 \leq \hat{\mu}^q + \hat{\nu}^q$.

Because $\mu_i^q + \nu_i^q \leq 1$ and $\mu_j^q + \nu_j^q \leq 1$, then $\mu_i^q \leq 1-\nu_i^q$ and $\mu_j^q \leq 1-\nu_j^q$. Thus, $((1-\mu_i^q)/(\mu_i^q)) \geq (\nu_i^q/(1-\nu_i^q))$ and $((1-\mu_j^q)/(\mu_j^q)) \geq (\nu_j^q/(1-\nu_j^q))$. It can be derived that $a_i \geq b_i$ and $a_j \geq b_j$. Then, we have

$$\begin{aligned}
&\left(\sum_{i=1,j=i}^{n}\frac{1}{\gamma t_i a_i^{\aleph}+\eta e_j a_j^{\aleph}}\right)^{(1/\aleph)} \leq \left(\sum_{i=1,j=i}^{n}\frac{1}{\gamma t_i b_i^{\aleph}+\eta e_j b_j^{\aleph}}\right)^{(1/\aleph)} \Longrightarrow \frac{1}{\left(\sum_{i=1,j=i}^{n}\left(1/\left(\gamma t_i a_i^{\aleph}+\eta e_j a_j^{\aleph}\right)\right)\right)^{(1/\aleph)}} \\
&\geq \frac{1}{\left(\sum_{i=1,j=i}^{n}\left(1/\left(\gamma t_i b_i^{\aleph}+\eta e_j b_j^{\aleph}\right)\right)\right)^{(1/\aleph)}} \\
&\Longrightarrow 1+\left(\frac{n(n+1)}{2(\gamma+\eta)}\right)^{(1/\aleph)} \times \frac{1}{\left(\sum_{i=1,j=i}^{n}\left(1/\left(\gamma t_i a_i^{\aleph}+\eta e_j a_j^{\aleph}\right)\right)\right)^{(1/\aleph)}} \\
&\geq 1+\left(\frac{n(n+1)}{2(\gamma+\eta)}\right)^{(1/\aleph)} \times \frac{1}{\left(\sum_{i=1,j=i}^{n}\left(1/\left(\gamma t_i b_i^{\aleph}+\eta e_j b_j^{\aleph}\right)\right)\right)^{(1/\aleph)}}.
\end{aligned} \tag{20}$$

Thus,

$$\frac{1}{1+(n(n+1)/2(\gamma+\eta))^{(1/\aleph)} \times \left(1/\left(\sum_{i=1,j=i}^{n}\left(1/\left(\gamma t_i a_i^{\aleph}+\eta e_j a_j^{\aleph}\right)\right)\right)^{(1/\aleph)}\right)} \leq \frac{1}{1+(n(n+1)/2(\gamma+\eta))^{(1/\aleph)} \times \left(1/\left(\sum_{i=1,j=i}^{n}\left(1/\left(\gamma t_i b_i^{\aleph}+\eta e_j b_j^{\aleph}\right)\right)\right)^{(1/\aleph)}\right)}. \tag{21}$$

Then, we can have

$$
\begin{aligned}
\hat{\mu}^{q}+\hat{\nu}^{q} &= \left(\frac{1}{1+(n(n+1)/2(\gamma+\eta))^{(1/\aleph)}\times\left(1/\left(\sum_{i=1,j=i}^{n}\left(1/\left(\gamma t_i a_i^{\aleph}+\eta e_j a_j^{\aleph}\right)\right)\right)^{(1/\aleph)}\right)}\right)^{(1/q)\times q}\\
&\quad+\left(1-\frac{1}{1+(n(n+1)/2(\gamma+\eta))^{(1/\aleph)}\times\left(1/\left(\sum_{i=1,j=i}^{n}\left(1/\left(\gamma t_i b_i^{\aleph}+\eta e_j b_j^{\aleph}\right)\right)\right)^{(1/\aleph)}\right)}\right)^{(1/q)\times q}\\
&= 1+\frac{1}{1+(n(n+1)/2(\gamma+\eta))^{(1/\aleph)}\times\left(1/\left(\sum_{i=1,j=i}^{n}\left(1/\left(\gamma t_i a_i^{\aleph}+\eta e_j a_j^{\aleph}\right)\right)\right)^{(1/\aleph)}\right)}\\
&\quad-\frac{1}{1+(n(n+1)/2(\gamma+\eta))^{(1/\aleph)}\times\left(1/\left(\sum_{i=1,j=i}^{n}\left(1/\left(\gamma t_i b_i^{\aleph}+\eta e_j b_j^{\aleph}\right)\right)\right)^{(1/\aleph)}\right)}\le 1,
\end{aligned}
\tag{22}
$$

which completes the proof of Theorem 1. □

Theorem 2 (idempotency). *Suppose that there are a group of q-ROFNs $o_i=(\mu_i,\nu_i)\,(i=1,2,\ldots,n)$ and the parameters γ, $\eta\ge 0$ and $\aleph>0$. If $o_i=o_j=o=(\mu,\nu)$, for $i,j=1,2,\ldots,n$, then we have*

$$
\begin{aligned}
q-\mathrm{ROFDPHM}(o_1,o_2,\ldots,o_n) &= \begin{pmatrix}\left(\dfrac{1}{1+(n(n+1)/2(\gamma+\eta))^{(1/\aleph)}\times\left(1/\left(\sum_{i=1,j=i}^{n}\left(1/\left(\gamma t_i a_i^{\aleph}+\eta e_j a_j^{\aleph}\right)\right)\right)^{(1/\aleph)}\right)}\right)^{(1/q)},\\[2ex] \left(1-\dfrac{1}{1+(n(n+1)/2(\gamma+\eta))^{(1/\aleph)}\times\left(1/\left(\sum_{i=1,j=i}^{n}\left(1/\left(\gamma t_i b_i^{\aleph}+\eta e_j b_j^{\aleph}\right)\right)\right)^{(1/\aleph)}\right)}\right)^{(1/q)}\end{pmatrix}\\
&= (\mu,\nu)=o,
\end{aligned}
\tag{23}
$$

where $\xi_i=((1+S(o_i))/\sum_{k=1}^{n}(1+S(o_k)))$, $\psi_j=((1+S(o_j))/\sum_{k=1}^{n}(1+S(o_k)))$, $(\mu_i^q/(1-\mu_i^q))=(1/a_i)$, $(\mu_j^q/(1-\mu_j^q))=(1/a_j)$, $((1-\nu_i^q)/\nu_i^q)=(1/b_i)$, $((1-\nu_j^q)/\nu_j^q)=(1/b_j)$, $(1/n\xi_i)=t_i$, *and* $(1/n\psi_j)=e_j$.

Proof. Since $o_i=o_j=o=(\mu,\nu)$, for $i,j=1,2,\ldots,n$, then $\mathrm{Sup}(o_i,o_j)=1$.

Thus, we have

$$
\begin{aligned}
\xi_i &= \frac{(1+S(o_i))}{\sum_{k=1}^{n}(1+S(o_k))}=\psi_j=\frac{(1+S(o_j))}{\sum_{k=1}^{n}(1+S(o_k))}=\frac{1}{n},\\
t_i &= e_j=1,\\
a_i^{\aleph} &= a_j^{\aleph}=\left(\frac{1-\mu_i^q}{\mu_i^q}\right)^{\aleph}=\left(\frac{1-\mu_j^q}{\mu_j^q}\right)^{\aleph}=\left(\frac{1-\mu^q}{\mu^q}\right)^{\aleph}.
\end{aligned}
\tag{24}
$$

Then, it can be derived that

$$\left(\sum_{i=1,j=i}^{n}\frac{1}{\gamma t_i a_i^{\aleph}+\eta e_j a_j^{\aleph}}\right)^{(1/\aleph)}=\left(\sum_{i=1,j=i}^{n}\frac{1}{\gamma\left(\left(1-\mu^q\right)/\mu^q\right)^{\aleph}+\eta\left(\left(1-\mu^q\right)/\mu^q\right)^{\aleph}}\right)^{(1/\aleph)}=\left(\sum_{i=1,j=i}^{n}\frac{1}{(\gamma+\eta)\times\left(\left(1-\mu^q\right)/\mu^q\right)^{\aleph}}\right)^{(1/\aleph)}$$

$$=\left(\frac{1}{(\gamma+\eta)}\times\frac{n(n+1)}{2}\times\left(\frac{\mu^q}{1-\mu^q}\right)^{\aleph}\right)^{(1/\aleph)}\Rightarrow\frac{1}{\left(\sum_{i=1,j=i}^{n}\left(1/\left(\gamma t_i a_i^{\aleph}+\eta e_j a_j^{\aleph}\right)\right)\right)^{(1/\aleph)}}$$

$$=\frac{1}{\left((1/(\gamma+\eta))\times(n(n+1)/2)\times\left(\mu^q/\left(1-\mu^q\right)\right)^{\aleph}\right)^{(1/\aleph)}}$$

$$=\frac{1}{\left((n(n+1)/2(\gamma+\eta))\times\left(\mu^q/\left(1-\mu^q\right)\right)^{\aleph}\right)^{(1/\aleph)}}=\left(\frac{2(\gamma+\eta)}{n(n+1)}\times\left(\frac{1-\mu^q}{\mu^q}\right)^{\aleph}\right)^{(1/\aleph)}$$

$$\Rightarrow\left(\frac{1}{1+(n(n+1)/2(\gamma+\eta))^{(1/\aleph)}\times\left(1/\left(\sum_{i=1,j=i}^{n}\left(1/\left(\gamma t_i a_i^{\aleph}+\eta e_j a_j^{\aleph}\right)\right)\right)^{(1/\aleph)}\right)}\right)^{(1/q)}$$

$$=\left(\frac{1}{1+(n(n+1)/2(\gamma+\eta))^{(1/\aleph)}\times\left(2(\gamma+\eta)/n(n+1)\times\left(\left(1-\mu^q\right)/\mu^q\right)^{\aleph}\right)^{(1/\aleph)}}\right)^{(1/q)}$$

$$=\left(\frac{1}{1+\left(\left(1-\mu^q\right)/\mu^q\right)}\right)^{(1/q)}=\mu. \tag{25}$$

Similarly, $(1/b_i)=(1/b_j)=\left(\left(1-\nu_i^q\right)/\nu_i^q\right)=\left(\left(1-\nu_j^q\right)/\nu_j^q\right)=\left(\left(1-\nu^q\right)/\nu^q\right)$. Then, the NMD value of the q-ROFDPHM operator can be derived as

$$\left(1-\frac{1}{1+(n(n+1)/2(\gamma+\eta))^{(1/\aleph)}\times\left(1/\left(\sum_{i=1,j=i}^{n}\left(1/\left(\gamma t_i b_i^{\aleph}+\eta e_j b_j^{\aleph}\right)\right)\right)^{(1/\aleph)}\right)}\right)^{(1/q)}$$

$$=\left(1-\frac{1}{1+(n(n+1)/2(\gamma+\eta))^{(1/\aleph)}\times\left(1/\left(\sum_{i=1,j=i}^{n}\left(1/(\gamma+\eta)\left(\nu^q/\left(1-\nu^q\right)\right)^{\aleph}\right)\right)^{(1/\aleph)}\right)}\right)^{(1/q)}$$

$$= \left(1 - \frac{1}{1 + (n(n+1)/2(\gamma+\eta))^{(1/\aleph)} \times \left(1/\left((n(n+1)/2(\gamma+\eta))((1-\nu^q)/\nu^q)^{\aleph}\right)^{(1/\aleph)}\right)}\right)^{(1/q)}$$
$$= \left(1 - \frac{1}{1 + (\nu^q/(1-\nu^q))}\right)^{(1/q)} = \nu. \tag{26}$$

Thus, we have $q - \mathrm{ROFDPHM}(o_1, o_2, \ldots, o_n) = (\mu, \nu) = o$, which completes the proof of Theorem 2. □

Theorem 3 (boundedness). *Suppose that there are a group of q-ROFNs $o_i = (\mu_i, \nu_i)\,(i = 1, 2, \ldots, n)$ and the parameters γ, $\eta \geq 0$ and $\aleph > 0$. If $o_l = \min(o_1, o_2, \ldots, o_n) = (\mu_l, \nu_l)$ and $o_h = \max(o_1, o_2, \ldots, o_n) = (\mu_h, \nu_h)$, then we have*

$$o_l \leq q - \mathrm{ROFDPHM}(o_1, o_2, \ldots, o_n) \leq o_h, \tag{27}$$

where

$$o_l = \left(\begin{array}{c} \left(\dfrac{1}{1 + (n(n+1)/2(\gamma+\eta))^{(1/\aleph)} \times \left(1/\left(\sum_{i=1,j=i}^{n}\left(1/\left(\gamma t_i a_i^{\aleph} + \eta e_j a_j^{\aleph}\right)\right)\right)^{(1/\aleph)}\right)}\right)^{(1/q)}, \\ \left(1 - \dfrac{1}{1 + (n(n+1)/2(\gamma+\eta))^{(1/\aleph)} \times \left(1/\left(\sum_{i=1,j=i}^{n}\left(1/\left(\gamma t_i b_i^{\aleph} + \eta e_j b_j^{\aleph}\right)\right)\right)^{(1/\aleph)}\right)}\right)^{(1/q)} \end{array} \right),$$
$$o_h = \left(\begin{array}{c} \left(\dfrac{1}{1 + (n(n+1)/2(\gamma+\eta))^{(1/\aleph)} \times \left(1/\left(\sum_{i=1,j=i}^{n}\left(1/\left(\gamma t_i a_i^{\aleph} + \eta e_j a_j^{\aleph}\right)\right)\right)^{(1/\aleph)}\right)}\right)^{(1/q)}, \\ \left(1 - \dfrac{1}{1 + (n(n+1)/2(\gamma+\eta))^{(1/\aleph)} \times \left(1/\left(\sum_{i=1,j=i}^{n}\left(1/\left(\gamma t_i b_i^{\aleph} + \eta e_j b_j^{\aleph}\right)\right)\right)^{(1/\aleph)}\right)}\right)^{(1/q)} \end{array} \right), \tag{28}$$

$$\frac{1}{n\xi_i} = t_i,$$
$$\frac{1}{n\psi_j} = e_j,$$
$$\xi_i = \frac{(1 + S(o_i))}{\sum_{k=1}^{n}(1 + S(o_k))},$$
$$\psi_j = \frac{(1 + S(o_j))}{\sum_{k=1}^{n}(1 + S(o_k))},$$
$$\frac{\mu_i^q}{1 - \mu_i^q} = \frac{1}{a_i},$$
$$\frac{1 - \nu_i^q}{\nu_i^q} = \frac{1}{b_i}.$$

Proof. According to Definition 7, we have

$$n\xi_i o_i = \left(\left(1-\frac{1}{1+\left(n\xi_i\left(\mu_i^q/\left(1-\mu_i^q\right)\right)^{\aleph}\right)^{(1/\aleph)}}\right)^{(1/q)},\left(\frac{1}{1+\left(n\xi_i\left(\left(1-\nu_i^q\right)/\nu_i^q\right)^{\aleph}\right)^{(1/\aleph)}}\right)^{(1/q)}\right),$$
$$n\psi_j o_j = \left(\left(1-\frac{1}{1+\left(n\psi_j\left(\mu_j^q/\left(1-\mu_j^q\right)\right)^{\aleph}\right)^{(1/\aleph)}}\right)^{(1/q)},\left(\frac{1}{1+\left(n\psi_j\left(\left(1-\nu_i^q\right)/\nu_i^q\right)^{\aleph}\right)^{(1/\aleph)}}\right)^{(1/q)}\right). \tag{29}$$

Since $o_l \le o_i$, then we have $\mu_i \ge \mu_l$ and $\nu_i \le \nu_l$. Thus, it can be derived that

$$\mu_i^q \ge \mu_l^q \Longrightarrow \frac{1}{1-\mu_i^q} \ge \frac{1}{1-\mu_l^q} \Longrightarrow \frac{\mu_i^q}{1-\mu_i^q} \ge \frac{\mu_l^q}{1-\mu_l^q} \Longrightarrow \frac{1}{a_i} \ge \frac{1}{a_l} \Longrightarrow a_i \le a_l,$$
$$\nu_i \le \nu_l \Longrightarrow 1-\nu_i^q \ge 1-\nu_l^q,\ \frac{1}{\nu_i^q} \ge \frac{1}{\nu_l^q} \Longrightarrow \frac{1}{b_i} \ge \frac{1}{b_l} \Longrightarrow b_i \le b_l. \tag{30}$$

Then, we can have

$$n\xi_i o_i = \left(\left(1-\frac{1}{1+\left(n\xi_i\left(1/a_i^{\aleph}\right)\right)^{(1/\aleph)}}\right)^{(1/q)},\left(\frac{1}{1+\left(n\xi_i\left(1/b_i^{\aleph}\right)\right)^{(1/\aleph)}}\right)^{(1/q)}\right)$$
$$\ge \left(\left(1-\frac{1}{1+\left(n\xi_i\left(1/a_l^{\aleph}\right)\right)^{(1/\aleph)}}\right)^{(1/q)},\left(\frac{1}{1+\left(n\xi_i\left(1/b_l^{\aleph}\right)\right)^{(1/\aleph)}}\right)^{(1/q)}\right)$$
$$\Longrightarrow \left(n\xi_i o_i\right)^{\gamma} = \left(\left(\frac{1}{1+\left(\gamma\left(1/n\xi_i\right)a_i^{\aleph}\right)^{(1/\aleph)}}\right)^{(1/q)},\left(1-\frac{1}{1+\left(\gamma\left(1/n\xi_i\right)b_i^{\aleph}\right)^{(1/\aleph)}}\right)^{(1/q)}\right)$$
$$\ge \left(\left(\frac{1}{1+\left(\gamma\left(1/n\xi_i\right)a_l^{\aleph}\right)^{(1/\aleph)}}\right)^{(1/q)},\left(1-\frac{1}{1+\left(\gamma\left(1/n\xi_i\right)b_l^{\aleph}\right)^{(1/\aleph)}}\right)^{(1/q)}\right). \tag{31}$$

Similarly, we have

$$\left(n\psi_j o_j\right)^{\eta} = \left(\left(\frac{1}{1+\left(\eta\left(1/n\psi_j\right)a_j^{\aleph}\right)^{(1/\aleph)}}\right)^{(1/q)},\left(1-\frac{1}{1+\left(\eta\left(1/n\psi_j\right)b_j^{\aleph}\right)^{(1/\aleph)}}\right)^{(1/q)}\right)$$
$$\ge \left(\left(\frac{1}{1+\left(\eta\left(1/n\psi_j\right)a_l^{\aleph}\right)^{(1/\aleph)}}\right)^{(1/q)},\left(1-\frac{1}{1+\left(\eta\left(1/n\psi_j\right)b_l^{\aleph}\right)^{(1/\aleph)}}\right)^{(1/q)}\right). \tag{32}$$

Since $(1/n\xi_i) = t_i$ and $(1/n\psi_j) = e_j$, then we have

$$
\begin{aligned}
(n\xi_i o_i)^\gamma &= \left(\left(\frac{1}{1+\left(\gamma t_i a_i^{\aleph}\right)^{(1/\aleph)}}\right)^{(1/q)}, \left(1-\frac{1}{1+\left(\gamma t_i b_i^{\aleph}\right)^{1/\aleph}}\right)^{(1/q)}\right) \\
&\geq \left(\left(\frac{1}{1+\left(\gamma t_i a_l^{\aleph}\right)^{1/\aleph}}\right)^{(1/q)}, \left(1-\frac{1}{1+\left(\gamma t_i b_l^{\aleph}\right)^{1/\aleph}}\right)^{(1/q)}\right) \\
\Longrightarrow \left(n\psi_j o_j\right)^\eta &= \left(\left(\frac{1}{1+\left(\eta e_j a_j^{\aleph}\right)^{(1/\aleph)}}\right)^{(1/q)}, \left(1-\frac{1}{1+\left(\eta e_j b_j^{\aleph}\right)^{(1/\aleph)}}\right)^{(1/q)}\right) \\
&\geq \left(\left(\frac{1}{1+\left(\eta e_j a_l^{\aleph}\right)^{(1/\aleph)}}\right)^{(1/q)}, \left(1-\frac{1}{1+\left(\eta e_j b_l^{\aleph}\right)^{(1/\aleph)}}\right)^{(1/q)}\right), \\
(n\xi_i o_i)^\gamma \otimes \left(n\psi_j o_j\right)^\eta &= \left(\left(\frac{1}{1+\left(\gamma t_i a_i^{\aleph} + \eta e_j a_j^{\aleph}\right)^{(1/\aleph)}}\right)^{(1/q)}, \left(1-\frac{1}{1+\left(\gamma t_i b_i^{\aleph} + \eta e_j b_j^{\aleph}\right)^{(1/\aleph)}}\right)^{(1/q)}\right) \\
&\geq \left(\left(\frac{1}{1+\left(\gamma t_i a_l^{\aleph} + \eta e_j a_l^{\aleph}\right)^{(1/\aleph)}}\right)^{(1/q)}, \left(1-\frac{1}{1+\left(\gamma t_i b_l^{\aleph} + \eta e_j b_l^{\aleph}\right)^{(1/\aleph)}}\right)^{(1/q)}\right), \\
\bigoplus_{i=1}^{n}\bigoplus_{j=i}^{n}\left((n\xi_i o_i)^\gamma \otimes \left(n\psi_j o_j\right)^\eta\right) &= \begin{pmatrix} \left(1-\dfrac{1}{1+\left(\sum_{i=1,j=i}^{n}\left(1/\left(\gamma t_i a_i^{\aleph} + \eta e_j a_j^{\aleph}\right)\right)\right)^{(1/\aleph)}}\right)^{(1/q)}, \\ \left(\dfrac{1}{1+\left(\sum_{i=1,j=i}^{n}\left(1/\left(\gamma t_i b_i^{\aleph} + \eta e_j b_j^{\aleph}\right)\right)\right)^{(1/\aleph)}}\right)^{(1/q)} \end{pmatrix} \\
&\geq \begin{pmatrix} \left(1-\dfrac{1}{1+\left(\sum_{i=1,j=i}^{n}\left(1/\left(\gamma t_i a_i^{\aleph} + \eta e_j a_l^{\aleph}\right)\right)\right)^{(1/\aleph)}}\right)^{(1/q)}, \\ \left(\dfrac{1}{1+\left(\sum_{i=1,j=i}^{n}\left(1/\left(\gamma t_i b_i^{\aleph} + \eta e_j b_l^{\aleph}\right)\right)\right)^{(1/\aleph)}}\right)^{(1/q)} \end{pmatrix}, \\
\frac{2}{n(n+1)}\bigoplus_{i=1}^{n}\bigoplus_{j=i}^{n}\left((n\xi_i o_i)^\gamma \otimes \left(n\psi_j o_j\right)^\eta\right) &= \begin{pmatrix} \left(1-\dfrac{1}{1+\left((2/n(n+1))\sum_{i=1,j=i}^{n}\left(1/\left(\gamma t_i a_i^{\aleph} + \eta e_j a_j^{\aleph}\right)\right)\right)^{(1/\aleph)}}\right)^{(1/q)}, \\ \left(\dfrac{1}{1+\left((2/n(n+1))\sum_{i=1,j=i}^{n}\left(1/\left(\gamma t_i b_i^{\aleph} + \eta e_j b_j^{\aleph}\right)\right)\right)^{(1/\aleph)}}\right)^{(1/q)} \end{pmatrix}
\end{aligned}
$$

$$\geq\left(\begin{array}{c}\left(1-\dfrac{1}{1+\left((2/n(n+1))\sum_{i=1,j=i}^{n}\left(1/\left(\gamma t_i a_i^{\aleph}+\eta e_j a_l^{\aleph}\right)\right)\right)^{(1/\aleph)}}\right)^{(1/q)},\\ \left(\dfrac{1}{1+\left((2/n(n+1))\sum_{i=1,j=i}^{n}\left(1/\left(\gamma t_i b_i^{\aleph}+\eta e_j b_l^{\aleph}\right)\right)\right)^{(1/\aleph)}}\right)^{(1/q)}\end{array}\right),$$

$$\left(\frac{2}{n(n+1)}\mathop{\oplus}_{i=1}^{n}\mathop{\oplus}_{j=i}^{n}\left(\left(n\xi_i o_i\right)^{\gamma}\otimes\left(n\psi_j o_j\right)^{\eta}\right)\right)^{(1/(\gamma+\eta))}$$

$$=\left(\begin{array}{c}\left(\dfrac{1}{1+\left((1/(\gamma+\eta))\left(1/(2/n(n+1))\sum_{i=1,j=i}^{n}\left(1/\left(\gamma t_i a_i^{\aleph}+\eta e_j a_j^{\aleph}\right)\right)\right)\right)^{(1/\aleph)}}\right)^{(1/q)},\\ \left(1-\dfrac{1}{1+\left((1/(\gamma+\eta))\left(1/(2/n(n+1))\sum_{i=1,j=i}^{n}\left(1/\left(\gamma t_i b_i^{\aleph}+\eta e_j b_j^{\aleph}\right)\right)\right)\right)^{(1/\aleph)}}\right)^{(1/q)}\end{array}\right) \quad (33)$$

$$\geq\left(\begin{array}{c}\left(\dfrac{1}{1+\left((1/(\gamma+\eta))\left(1/(2/n(n+1))\sum_{i=1,j=i}^{n}\left(1/\left(\gamma t_i a_l^{\aleph}+\eta e_j a_l^{\aleph}\right)\right)\right)\right)^{(1/\aleph)}}\right)^{(1/q)},\\ \left(1-\dfrac{1}{1+\left((1/(\gamma+\eta))\left(1/(2/n(n+1))\sum_{i=1,j=i}^{n}\left(1/\left(\gamma t_i b_l^{\aleph}+\eta e_j b_l^{\aleph}\right)\right)\right)\right)^{(1/\aleph)}}\right)^{(1/q)}\end{array}\right)=o_l.$$

Similarly, it can be proven that $q-\text{ROFDPHM}(o_1,o_2,\ldots,o_n)\leq o_h$ in the same way, which completes the proof of Theorem 3.

It can be noted that the proposed q-ROFDPHM operator uses the PA operator and Dombi operational laws to optimize the HM operator. Its significance can be listed as follows. (1) It can alleviate negative influences of extreme input values on the calculation results. (2) It shows strong flexibility for computing input values. (3) It is capable of capturing the complex interrelationships among criteria values. (4) It can process the complex information structure of q-ROFSs. Nevertheless, during the aggregation processes, it does not consider the weight values of criteria, which is very important in the MCDM contexts. To tackle this deficiency, a novel q-rung orthopair fuzzy weighted Dombi power Heronian mean (q-ROFWDPHM) operator is put forward in the following part. □

Definition 11. Given a set of q-ROFNs $o_i=(\mu_i,\nu_i)\,(i=1,2,\ldots,n)$, three parameters $\gamma,\eta\geq 0$ and $\aleph>0$, and the weight values $[\omega_1,\omega_2,\ldots,\omega_n]$ of q-ROFNs, then the q-ROFWDPHM operator is defined as

$$q-\text{ROFWDPHM}(o_1,o_2,\ldots,o_n)=\left(\frac{2}{n(n+1)}\mathop{\oplus}_{i=1}^{n}\mathop{\oplus}_{j=i}^{n}\left(\frac{n\omega_i\left(1+S(o_i)\right)}{\sum_{k=1}^{n}\omega_k\left(1+S(o_k)\right)}o_i\right)^{\gamma}\otimes\left(\frac{n\omega_j\left(1+S(o_j)\right)}{\sum_{k=1}^{n}\omega_k\left(1+S(o_k)\right)}o_j\right)^{\eta}\right)^{(1/(\gamma+\eta))}. \quad (34)$$

Theorem 4. *Given a set of q-ROFNs $o_i = (\mu_i, \nu_i)\,(i = 1, 2, \ldots, n)$, three parameters $\gamma, \eta \geq 0$ and $\aleph > 0$, and the weight values $[\omega_1, \omega_2, \ldots, \omega_n]$ of q-ROFNs, then the aggregated result obtained from the q-ROFWDPHM operator is still a q-ROFN, which is*

$$q-\mathrm{ROFWDPHM}(o_1, o_2, \ldots, o_n) = \left(\begin{array}{c} \left(\dfrac{1}{1 + (n(n+1)/2(\gamma+\eta))^{(1/\aleph)} \times \left(1/\left(\sum_{i=1, j=i}^{n} \left(1/\left(\gamma t_i a_i^{\aleph} + \eta e_j a_j^{\aleph} \right) \right) \right)^{(1/\aleph)} \right)} \right)^{(1/q)}, \\ \left(1 - \dfrac{1}{1 + (n(n+1)/2(\gamma+\eta))^{(1/\aleph)} \times \left(1/\left(\sum_{i=1, j=i}^{n} \left(1/\left(\gamma t_i b_i^{\aleph} + \eta e_j b_j^{\aleph} \right) \right) \right)^{(1/\aleph)} \right)} \right)^{(1/q)} \end{array} \right), \tag{35}$$

where $\xi_i = ((1 + S(o_i))/\sum_{k=1}^{n} \omega_k (1 + S(o_k)))$, $\psi_j = ((1 + S(o_j))/\sum_{k=1}^{n} \omega_k (1 + S(o_k)))$, $(\mu_i^q/(1 - \mu_i^q)) = (1/a_i)$, $(\mu_j^q/1 - \mu_j^q) = (1/a_j)$, $((1 - \nu_i^q)/\nu_i^q) = (1/b_i)$, $((1 - \nu_j^q)/\nu_j^q) = (1/b_j)$, $t_i = (1/n\omega_i\xi_i)$, and $e_j = (1/n\omega_j\psi_j)$.

Proof. Let $\xi_i = ((1 + S(o_i))/\sum_{k=1}^{n} \omega_k (1 + S(o_k)))$ and $\psi_j = ((1 + S(o_j))/\sum_{k=1}^{n} \omega_k (1 + S(o_k)))$; then, equation (34) can be transformed into

$$q-\mathrm{ROFWDPHM}(o_1, o_2, \ldots, o_n) = \left(\frac{2}{n(n+1)} \mathop{\oplus}_{i=1}^{n} \mathop{\oplus}_{j=i}^{n} (n\omega_i\xi_i o_i)^{\gamma} \otimes \left(n\omega_j\psi_j o_j \right)^{\eta} \right)^{(1/(\gamma+\eta))}. \tag{36}$$

According to Definition 7, we have

$$\begin{aligned} n\omega_i\xi_i o_i &= \left(\left(1 - \frac{1}{1 + \left(n\omega_i\xi_i \left(\mu_i^q/(1 - \mu_i^q) \right)^{\aleph} \right)^{(1/\aleph)}} \right)^{(1/q)}, \left(\frac{1}{1 + \left(n\omega_i\xi_i \left((1 - \nu_i^q)/\nu_i^q \right)^{\aleph} \right)^{(1/\aleph)}} \right)^{(1/q)} \right), \\ n\omega_j\psi_j o_j &= \left(\left(1 - \frac{1}{1 + \left(n\omega_j\psi_j \left(\mu_j^q/(1 - \mu_j^q) \right)^{\aleph} \right)^{(1/\aleph)}} \right)^{(1/q)}, \left(\frac{1}{1 + \left(n\omega_j\psi_j \left((1 - \nu_j^q)/\nu_j^q \right)^{\aleph} \right)^{(1/\aleph)}} \right)^{(1/q)} \right). \end{aligned} \tag{37}$$

Let $(\mu_i^q/(1 - \mu_i^q)) = (1/a_i)$, $(\mu_j^q/1 - \mu_j^q) = (1/a_j)$, $((1 - \nu_i^q)/\nu_i^q) = (1/b_i)$, and $((1 - \nu_j^q)/\nu_j^q) = (1/b_j)$; then, these equations can be transformed into

$$\begin{aligned} n\omega_i\xi_i o_i &= \left(\left(1 - \frac{1}{1 + (n\omega_i\xi_i (1/a_i^{\aleph}))^{(1/\aleph)}} \right)^{(1/q)}, \left(\frac{1}{1 + (n\omega_i\xi_i (1/b_i^{\aleph}))^{(1/\aleph)}} \right)^{(1/q)} \right), \\ n\omega_j\psi_j o_j &= \left(\left(1 - \frac{1}{1 + \left(n\omega_j\psi_j \left(1/a_j^{\aleph} \right) \right)^{(1/\aleph)}} \right)^{(1/q)}, \left(\frac{1}{1 + \left(n\omega_j\psi_j \left(1/b_j^{\aleph} \right) \right)^{(1/\aleph)}} \right)^{(1/q)} \right). \end{aligned} \tag{38}$$

According to Definition 7, then we have

$$
\begin{aligned}
\left(n\omega_i\xi_i o_i\right)^{\gamma} &= \left(\left(\frac{1}{1+\left(\gamma\left(1/n\omega_i\xi_i\right)a_i^{\aleph}\right)^{(1/\aleph)}}\right)^{(1/q)}, \left(1-\frac{1}{1+\left(\gamma\left(1/n\omega_i\xi_i\right)b_i^{\aleph}\right)^{(1/\aleph)}}\right)^{(1/q)}\right),\\
\left(n\omega_j\psi_j o_j\right)^{\eta} &= \left(\left(\frac{1}{1+\left(\eta\left(1/n\omega_j\psi_j\right)a_j^{\aleph}\right)^{(1/\aleph)}}\right)^{(1/q)}, \left(1-\frac{1}{1+\left(\eta\left(1/n\omega_j\psi_j\right)b_j^{\aleph}\right)^{(1/\aleph)}}\right)^{(1/q)}\right).
\end{aligned}
\tag{39}
$$

Let $t_i = (1/n\omega_i\xi_i)$ and $e_j = (1/n\omega_j\psi_j)$; then, the above two equations can be transformed into

$$
\begin{aligned}
\left(n\omega_i\xi_i o_i\right)^{\gamma} &= \left(\left(\frac{1}{1+\left(\gamma t_i a_i^{\aleph}\right)^{(1/\aleph)}}\right)^{(1/q)}, \left(1-\frac{1}{1+\left(\gamma t_i b_i^{\aleph}\right)^{(1/\aleph)}}\right)^{(1/q)}\right),\\
\left(n\omega_j\psi_j o_j\right)^{\eta} &= \left(\left(\frac{1}{1+\left(\eta e_j a_j^{\aleph}\right)^{(1/\aleph)}}\right)^{(1/q)}, \left(1-\frac{1}{1+\left(\eta e_j b_j^{\aleph}\right)^{(1/\aleph)}}\right)^{(1/q)}\right),\\
\left(n\omega_i\xi_i o_i\right)^{\gamma}\otimes\left(n\omega_j\psi_j o_j\right)^{\eta} &= \left(\left(\frac{1}{1+\left(\gamma t_i a_i^{\aleph}+\eta e_j a_j^{\aleph}\right)^{(1/\aleph)}}\right)^{(1/q)}, \left(1-\frac{1}{1+\left(\gamma t_i b_i^{\aleph}+\eta e_j b_j^{\aleph}\right)^{(1/\aleph)}}\right)^{(1/q)}\right),\\
\underset{i=1}{\overset{n}{\oplus}}\underset{j=i}{\overset{n}{\oplus}}\left(n\omega_i\xi_i o_i\right)^{\gamma}\otimes\left(n\omega_j\psi_j o_j\right)^{\eta} &= \left(\begin{array}{c}\left(1-\dfrac{1}{1+\left(\sum_{i=1,j=i}^{n}\left(1/\left(\gamma t_i a_i^{\aleph}+\eta e_j a_j^{\aleph}\right)\right)\right)^{(1/\aleph)}}\right)^{(1/q)},\\[2ex]
\left(\dfrac{1}{1+\left(\sum_{i=1,j=i}^{n}\left(1/\left(\gamma t_i b_i^{\aleph}+\eta e_j b_j^{\aleph}\right)\right)\right)^{(1/\aleph)}}\right)^{(1/q)}\end{array}\right),\\
\frac{2}{n(n+1)}\underset{i=1}{\overset{n}{\oplus}}\underset{j=i}{\overset{n}{\oplus}}\left(n\omega_i\xi_i o_i\right)^{\gamma}\otimes\left(n\omega_j\psi_j o_j\right)^{\eta} &= \left(\begin{array}{c}\left(1-\dfrac{1}{1+\left((2/n(n+1))\sum_{i=1,j=i}^{n}\left(1/\left(\gamma t_i a_i^{\aleph}+\eta e_j a_j^{\aleph}\right)\right)\right)^{(1/\aleph)}}\right)^{(1/q)},\\[2ex]
\left(\dfrac{1}{1+\left((2/n(n+1))\sum_{i=1,j=i}^{n}\left(1/\left(\gamma t_i b_i^{\aleph}+\eta e_j b_j^{\aleph}\right)\right)\right)^{(1/\aleph)}}\right)^{(1/q)}\end{array}\right),
\end{aligned}
$$

$$\left(\frac{2}{n(n+1)} \underset{i=1}{\overset{n}{\oplus}} \underset{j=i}{\overset{n}{\oplus}} \left(n\omega_i\xi_i o_i\right)^{\gamma} \otimes \left(n\omega_j\psi_j o_j\right)^{\eta}\right)^{(1/(\gamma+\eta))}$$

$$= \left(\begin{array}{c} \left(\dfrac{1}{1+\left((1/(\gamma+\eta))\left(1/\left((2/n(n+1))\sum_{i=1,j=i}^{n}\left(1/\left(\gamma t_i a_i^{\aleph} + \eta e_j a_j^{\aleph}\right)\right)\right)\right)\right)^{(1/\aleph)}}\right)^{(1/q)}, \\ \left(1-\dfrac{1}{1+\left((1/(\gamma+\eta))\left(1/(2/n(n+1))\sum_{i=1,j=i}^{n}\left(1/\left(\gamma t_i b_i^{\aleph} + \eta e_j b_j^{\aleph}\right)\right)\right)\right)^{(1/\aleph)}}\right)^{(1/q)} \end{array} \right),$$

$$q-\mathrm{ROFWDPHM}\left(o_1, o_2, \ldots, o_n\right) = \left(\frac{2}{n(n+1)} \underset{i=1}{\overset{n}{\oplus}} \underset{j=i}{\overset{n}{\oplus}} \left(n\omega_i\xi_i o_i\right)^{\gamma} \otimes \left(n\omega_j\psi_j o_j\right)^{\eta}\right)^{(1/(\gamma+\eta))} =$$

$$\left(\begin{array}{c} \left(\dfrac{1}{1+(n(n+1)/2(\gamma+\eta))^{(1/\aleph)} \times \left(1/\left(\sum_{i=1,j=i}^{n}\left(1/\left(\gamma t_i a_i^{\aleph} + \eta e_j a_j^{\aleph}\right)\right)\right)^{(1/\aleph)}\right)}\right)^{(1/q)}, \\ \left(1-\dfrac{1}{1+(n(n+1)/2(\gamma+\eta))^{(1/\aleph)} \times \left(1/\left(\sum_{i=1,j=i}^{n}\left(1/\left(\gamma t_i b_i^{\aleph} + \eta e_j b_j^{\aleph}\right)\right)\right)^{(1/\aleph)}\right)}\right)^{(1/q)} \end{array} \right). \tag{40}$$

The process for proving that the aggregation result of the q-ROFWDPHM operator is a q-ROFN is the same as that of Theorem 1. Thus, it is omitted here.

The proposed q-ROFWDPHM operator also owns the features of idempotency and boundedness as the proposed q-ROFDPHM operator. Their proof processes are similar to those of Theorems 2 and 3. Due to the limited space, the proof processes are omitted here. □

4. q-Rung Orthopair Fuzzy Dombi Power Geometric Heronian Mean Operators

In this section, we use the PA operator, Dombi operational laws for q-ROFNs, and geometric HM operator to develop a novel q-ROFDPGHM operator and its weighted form. Then, the features are discussed.

Definition 12. Given a set of q-ROFNs $o_i = (\mu_i, \nu_i)\,(i = 1, 2, \ldots, n)$ and three parameters $\gamma, \eta \geq 0$ and $\aleph > 0$, then the q-ROFDPGHM operator is defined as

$$q-\mathrm{ROFDPGHM}\left(o_1, o_2, \ldots, o_n\right) = \frac{1}{\gamma+\eta}\left(\underset{i=1}{\overset{n}{\otimes}} \underset{j=i}{\overset{n}{\otimes}} \left(\gamma o_i^{\left(n\left(1+S\left(o_i\right)\right)/\sum_{k=1}^{n}\left(1+S\left(o_k\right)\right)\right)} \oplus \eta o_j^{\left(n\left(1+S\left(o_j\right)\right)/\sum_{k=1}^{n}\left(1+S\left(o_k\right)\right)\right)}\right)\right)^{(2/n(n+1))}. \tag{41}$$

Based on the Dombi operational laws of q-ROFNs and GHM operator, a theorem is derived.

Theorem 5. *Given n q-ROFNs $o_i = (\mu_i, \nu_i)\,(i = 1, 2, \ldots, n)$ and the parameters $\gamma, \eta \geq 0$ and $\aleph > 0$, then the* *aggregated result derived from equation (41) is still a q-ROFN, which is*

$$q-\mathrm{ROFDPGHM}\left(o_1,o_2,\ldots,o_n\right)=\left(\begin{array}{c}\left(1-\dfrac{1}{1+\left(n(n+1)/2(\gamma+\eta)\right)^{(1/\aleph)}\times\left(1/\left(\sum_{i=1,j=i}^{n}\left(1/\gamma t_i\left(1/a_i^{\aleph}\right)+\eta e_j\left(1/a_j^{\aleph}\right)\right)\right)^{(1/\aleph)}\right)}\right)^{(1/q)},\\ \left(\dfrac{1}{1+\left(n(n+1)/2(\gamma+\eta)\right)^{(1/\aleph)}\times\left(1/\left(\sum_{i=1,j=i}^{n}\left(1/\gamma t_i\left(1/b_i^{\aleph}\right)+\eta e_j\left(1/b_j^{\aleph}\right)\right)\right)^{(1/\aleph)}\right)}\right)^{(1/q)}\end{array}\right),\tag{42}$$

where $\xi_i=\left(\left(1+S\left(o_i\right)\right)/\sum_{k=1}^{n}\left(1+S\left(o_k\right)\right)\right)$, $\psi_j=\left(\left(1+S\left(o_j\right)\right)/\sum_{k=1}^{n}\left(1+S\left(o_k\right)\right)\right)$, $a_i=\left(\left(1-\mu_i^q\right)/\mu_i^q\right)$, $a_j=\left(\left(1-\mu_j^q\right)/\mu_j^q\right)$, $b_i=\left(\nu_i^q/\left(1-\nu_i^q\right)\right)$, $b_j=\left(\nu_j^q/\left(1-\nu_j^q\right)\right)$, $t_i=\left(1/n\xi_i\right)$, *and* $e_j=\left(1/n\psi_j\right)$.

The proof process of this theorem is similar to that of Theorem 1. Thus, it is omitted here.

The proposed q-ROFDPGHM operator also owns the features of idempotency and boundedness as the proposed q-ROFDPHM operator. Their proof processes are similar to those of Theorems 2 and 3. Due to the limited space, the proof processes are omitted here.

Similar to the proposed q-ROFDPHM operator, the q-ROFDPGHM also does not consider the weight values of criteria. To tackle this deficiency, a new q-rung orthopair fuzzy weighted Dombi power geometric Heronian mean (q-ROFWDPGHM) operator is put forward in the following part.

Definition 13. Given a set of q-ROFNs $o_i=\left(\mu_i,\nu_i\right)(i=1,2,\ldots,n)$, three parameters $\gamma,\eta\geq 0$ and $\aleph>0$, and the weight values $\left[\omega_1,\omega_2,\ldots,\omega_n\right]$ of q-ROFNs, then the q-ROFWDPGHM operator is defined as

$$q-\mathrm{ROFWDPGHM}\left(o_1,o_2,\ldots,o_n\right)=\frac{1}{\gamma+\eta}\left(\bigotimes_{i=1}^{n}\bigotimes_{j=i}^{n}\left(\gamma o_i^{\left(n\omega_i\left(1+S\left(o_i\right)\right)/\sum_{k=1}^{n}\omega_k\left(1+S\left(o_k\right)\right)\right)}\oplus\eta o_j^{\left(n\omega_j\left(1+S\left(o_j\right)\right)/\sum_{k=1}^{n}\omega_k\left(1+S\left(o_k\right)\right)\right)}\right)\right)^{(2/n(n+1))}.\tag{43}$$

Based on the Dombi operational laws of q-ROFNs and GHM operator, a theorem is derived.

Theorem 6. *Given a set of q-ROFNs* $o_i=\left(\mu_i,\nu_i\right)(i=1,2,\ldots,n)$, *the parameters* γ, $\eta\geq 0$ *and* $\aleph>0$, *and the weight values* $\left[\omega_1,\omega_2,\ldots,\omega_n\right]$ *of q-ROFNs, then the aggregated result that is obtained from equation (43) is still a q-ROFN, which is*

$$q-\mathrm{ROFWDPGHM}\left(o_1,o_2,\ldots,o_n\right)=\left(\begin{array}{c}\left(1-\dfrac{1}{1+\left(n(n+1)/2(\gamma+\eta)\right)^{(1/\aleph)}\times\left(1/\left(\sum_{i=1,j=i}^{n}\left(1/\gamma t_i\left(1/a_i^{\aleph}\right)+\eta e_j\left(1/a_j^{\aleph}\right)\right)\right)^{(1/\aleph)}\right)}\right)^{(1/q)},\\ \left(\dfrac{1}{1+\left(n(n+1)/2(\gamma+\eta)\right)^{(1/\aleph)}\times\left(1/\left(\sum_{i=1,j=i}^{n}\left(1/\gamma t_i\left(1/b_i^{\aleph}\right)+\eta e_j\left(1/b_j^{\aleph}\right)\right)\right)^{(1/\aleph)}\right)}\right)^{(1/q)}\end{array}\right),\tag{44}$$

where $\xi_i = ((1+S(o_i))/\sum_{k=1}^{n}\omega_k(1+S(o_k)))$, $\psi_j = ((1+S(o_j))/\sum_{k=1}^{n}\omega_k(1+S(o_k)))$, $t_i = (1/n\omega_i\xi_i)$, $e_j = (1/n\omega_j\psi_j)$, $a_i = ((1-\mu_i^q)/\mu_i^q)$, $a_j = ((1-\mu_j^q)/\mu_j^q)$, $b_i = (\nu_i^q/(1-\nu_i^q))$, *and* $b_j = (\nu_j^q/(1-\nu_j^q))$.

Proof. The proof process is similar to that of Theorem 1. Thus, it is omitted here.

The proposed q-ROFWDPGHM operator also has the features of idempotency and boundedness as the proposed q-ROFDPHM operator. Their proof processes are similar to those of Theorems 2 and 3. Due to the limited space, the proof processes are omitted here. □

5. MULTIMOORA Method for q-Rung Orthopair Fuzzy Sets

In this section, the MULTIMOORA method is improved for processing the MCDM problems with the q-ROFS information. There usually exist the interrelationships among the criteria in the MCDM problems. Moreover, there may be extreme criteria values in the MCDM problems. To tackle these two problems, we use the proposed q-ROFWDPHM and q-ROFWDPGHM operators to modify the MULTIMOORA method.

5.1. Problem Description. Let us suppose that there exists an MCDM problem consisting of m alternatives $\{x_1, x_2, \ldots, x_m\}$ and n criteria $\{a_1, a_2, \ldots, a_n\}$. The weight values of criteria are denoted as $[\omega_1, \omega_2, \ldots, \omega_n]$, where $\sum_{j=1}^{n}\omega_j = 1$ and $0 \le \omega_j \le 1$. The decision matrix (DM) $R = (o_{ij})_{m\times n}$ corresponding to this MCDM problem consists of the evaluation information from experts. The element o_{ij} denotes the evaluation information of alternative x_i with respect to criterion a_j. In this MCDM problem, experts use the flexible q-ROFNs for expressing the evaluation information of alternative x_i with respect to criterion a_j, namely, $o_{ij} = (\mu_{ij}, \nu_{ij})$. Here, the criteria are divided into two different categories: benefit-type criteria and cost-type criteria.

Before processing DM $R = (o_{ij})_{m\times n}$, equation (45) is used to transform the values of cost-type criteria for deriving the transformed DM $\widetilde{R} = (\widetilde{o}_{ij})_{m\times n}$:

$$\widetilde{o}_{ij} = \begin{cases} (\mu_{ij}, \nu_{ij}), & \text{for benefit} - \text{type criterion}\, a, \\ (\nu_{ij}, \mu_{ij}), & \text{for cost} - \text{type criterion}\, a_j. \end{cases} \tag{45}$$

5.2. q-Rung Orthopair Fuzzy MULTIMOORA Method. According to the above problem description, we introduce the q-ROFWDPHM and q-ROFWDPGHM operators to improve the original MULTIMOORA method so as to propose a novel q-rung orthopair fuzzy MULTIMOORA (q-ROF-MULTIMOORA) method. Similar to the original MULTIMOORA method [53], the q-ROF-MULTMOORA method is also composed of three components, which are the q-rung orthopair fuzzy RS (q-ROF-RS) component, q-rung orthopair fuzzy RP (q-ROF-RP) component, and q-rung orthopair fuzzy FMF (q-ROF-FMF) component, respectively. Based on the transformed DM $\widetilde{R} = (\widetilde{o}_{ij})_{m\times n}$, these three components compute the ranking values of alternatives as follows.

5.2.1. q-ROF-RS Component. In this component, the q-ROFWDPHM operator is applied to aggregate the evaluation information of each alternative x_i with respect to its n criteria. Therefore, using (34), the aggregated criteria value of alternative x_i can be computed as

$$f_{i1} = \left(\frac{2}{n(n+1)} \bigoplus_{h=1}^{n} \bigoplus_{g=h}^{n} \left(\frac{n\omega_h(1+S(\widetilde{o}_{ih}))}{\sum_{k=1}^{n}\omega_k(1+S(\widetilde{o}_{ik}))}\widetilde{o}_{ih}\right)^{\gamma} \otimes \left(\frac{n\omega_g(1+S(\widetilde{o}_{ig}))}{\sum_{k=1}^{n}\omega_k(1+S(\widetilde{o}_{ik}))}\widetilde{o}_{ig}\right)^{\eta}\right)^{(1/\gamma+\eta)}, \tag{46}$$

where $S(\widetilde{o}_{ik}) = \sum_{l=1, l\neq k}^{n}\text{Sup}(\widetilde{o}_{ik}, \widetilde{o}_{il})$ and $\text{Sup}(\widetilde{o}_{ik}, \widetilde{o}_{il}) = 1 - d(\widetilde{o}_{ik}, \widetilde{o}_{il})$.

Since the aggregated value is a q-ROFN, then the score function in Definition 2 is used to derive the crisp ranking value of alternative x_i as

$$\begin{aligned} f_{i1} &= s(f_{i1}) = s\left(\left(\frac{2}{n(n+1)} \bigoplus_{h=1}^{n} \bigoplus_{g=h}^{n} \left(\frac{n\omega_h(1+S(\widetilde{o}_{ih}))}{\sum_{k=1}^{n}\omega_k(1+S(\widetilde{o}_{ik}))}\widetilde{o}_{ih}\right)^{\gamma} \otimes \left(\frac{n\omega_g(1+S(\widetilde{o}_{ig}))}{\sum_{k=1}^{n}\omega_k(1+S(\widetilde{o}_{ik}))}\widetilde{o}_{ig}\right)^{\eta}\right)^{(1/\gamma+\eta)}\right) \\ &= s\left(\begin{array}{c} \left(\dfrac{1}{1+(n(n+1)/2(\gamma+\eta))^{(1/\aleph)} \times \left(1/\left(\sum_{h=1,g=h}^{n}\left(1/\left(\gamma t_{ih}a_{ih}^{\aleph} + \eta e_{ig}a_{ig}^{\aleph}\right)\right)\right)\right)^{(1/\aleph)}}\right)^{(1/q)}, \\ \left(1 - \dfrac{1}{1+(n(n+1)/2(\gamma+\eta))^{(1/\aleph)} \times \left(1/\left(\sum_{h=1,g=h}^{n}\left(1/\left(\gamma t_{ih}b_{ih}^{\aleph} + \eta e_{ig}b_{ig}^{\aleph}\right)\right)\right)\right)^{(1/\aleph)}}\right)^{(1/q)} \end{array}\right), \end{aligned} \tag{47}$$

where $\xi_{ih} = ((1 + S(\widetilde{o}_{ih}))/\sum_{k=1}^{n} \omega_k (1 + S(\widetilde{o}_{ik})))$, $\psi_{ig} = ((1+ S(\widetilde{o}_{ig}))/\sum_{k=1}^{n} \omega_k (1 + S(\widetilde{o}_{ik})))$, $(\mu_{ih}^q/(1 - \mu_{ih}^q)) = (1/a_{ih})$, $(\mu_{ig}^q/1 - \mu_{ig}^q) = (1/a_{ig})$, $(1 - \nu_{ih}^q/\nu_{ih}^q) = (1/b_{ih})$, $((1 - \nu_{ig}^q)/\nu_{ig}^q) = (1/b_{ig})$, $t_{ih} = (1/n\omega_h \xi_{ih})$, and $e_{ig} = (1/n\omega_g \psi_{ig})$.

The alternative with larger ranking value is better. Hence, all the alternatives can be ranked according to the descending order of their ranking values.

5.2.2. q-ROF-RP Component. In this component, the reference point of each criterion is first derived as

$$\rho_j = \operatorname{argmax}_{i=1}^{m} s\left(\widetilde{o}_{ij}\right), \quad (j = 1, 2, \ldots, n). \tag{48}$$

In the second step, Definition 4 is applied to compute the distance between the evaluation information of alternative x_i with respect to each criterion and the reference point of the same criterion as

$$\varepsilon_{ij} = d\left(\widetilde{o}_{ij}, \rho_j\right). \tag{49}$$

It can be known that ε_{ij} is a real value and $\varepsilon_{ij} \geq 0$. Considering the interrelationships among criteria, the ranking value of alternative x_i is computed by aggregating the criteria distances of alternative x_i as

$$f_{i2} = \left(\frac{2}{n(n+1)} \sum_{h=1}^{n} \sum_{g=h}^{n} \left(\frac{n\omega_h (1 + S(\varepsilon_{ih}))}{\sum_{k=1}^{n} \omega_k (1 + S(\varepsilon_{ik}))} \varepsilon_{ih}\right)^{\gamma} \times \left(\frac{n\omega_g \left(1 + S\left(\varepsilon_{ig}\right)\right)}{\sum_{k=1}^{n} \omega_k (1 + S(\varepsilon_{ik}))} \varepsilon_{ig}\right)^{\eta}\right)^{(1/(\gamma+\eta))}, \tag{50}$$

where $S(\varepsilon_{ik}) = \sum_{l=1, l \neq k}^{n} \operatorname{Sup}(\varepsilon_{ik}, \varepsilon_{il})$ and $\operatorname{Sup}(\varepsilon_{ik}, \varepsilon_{il}) = 1- |\varepsilon_{ik} - \varepsilon_{il}|$.

In this component, the alternative with smaller ranking value is better. Thus, all the alternatives should be ranked according to the ascending order of their ranking values.

5.2.3. q-ROF-FMF Component. In this component, the proposed q-ROFWDPGHM operator is applied to aggregate the evaluation information of each alternative x_i with respect to its n criteria. Thus, using equation (43), the aggregated criteria value of alternative x_i can be computed as

$$f_{i3} = \frac{1}{\gamma + \eta} \left(\bigotimes_{h=1}^{n} \bigotimes_{g=h}^{n} \left(\gamma \widetilde{o}_{ih}^{\left(n\omega_h \left(1 + S\left(\widetilde{o}_{ih}\right)\right) / \sum_{k=1}^{n} \omega_k \left(1 + S\left(\widetilde{o}_{ik}\right)\right) \right)} \oplus \eta \widetilde{o}_{ig}^{\left(n\omega_g \left(1 + S\left(\widetilde{o}_{ig}\right)\right) / \sum_{k=1}^{n} \omega_k \left(1 + S\left(\widetilde{o}_{ik}\right)\right) \right)} \right) \right)^{(2/n(n+1))}, \tag{51}$$

where $S(\widetilde{o}_{ik}) = \sum_{l=1, l \neq k}^{n} \operatorname{Sup}(\widetilde{o}_{ik}, \widetilde{o}_{il})$ and $\operatorname{Sup}(\widetilde{o}_{ik}, \widetilde{o}_{il}) = 1- d(\widetilde{o}_{ik}, \widetilde{o}_{il})$.

Since the aggregated value is a q-ROFN, then the score function in Definition 2 is used to derive the crisp ranking value of alternative x_i as

$$f_{i3} = s\left(f_{i3}\right) = s\left(\begin{array}{c} \left(1 - \dfrac{1}{1 + (n(n+1)/2(\gamma + \eta))^{(1/\aleph)} \times \left(1/\left(\sum_{h=1, g=h}^{n} \left(1/\gamma t_{ih} \left(1/a_{ih}^{\aleph}\right) + \eta e_{ig} \left(1/a_{ig}^{\aleph}\right)\right)\right)^{(1/\aleph)}\right)}\right)^{(1/q)}, \\ \left(\dfrac{1}{1 + (n(n+1)/2(\gamma + \eta))^{(1/\aleph)} \times \left(1/\left(\sum_{h=1, g=h}^{n} \left(1/\gamma t_{ih} \left(1/b_{ih}^{\aleph}\right) + \eta e_{ig} \left(1/b_{ig}^{\aleph}\right)\right)\right)^{(1/\aleph)}\right)}\right)^{(1/q)} \end{array}\right), \tag{52}$$

where $\xi_{ih} = ((1 + S(\widetilde{o}_{ih}))/\sum_{k=1}^{n} \omega_k (1 + S(\widetilde{o}_{ik})))$, $\psi_{ig} = ((1+ S(\widetilde{o}_{ig}))/\sum_{k=1}^{n} \omega_k (1 + S(\widetilde{o}_{ik})))$, $a_{ih} = ((1 - \mu_{ih}^q)/\mu_{ih}^q)$, $a_{ig} = (1 - \mu_{ig}^q/\mu_{ig}^q)$, $b_{ih} = (\nu_{ih}^q/(1 - \nu_{ih}^q))$, $b_{ig} = (\nu_{ig}^q/(1 - \nu_{ig}^q))$, $t_{ih} = (1/n\omega_h \xi_{ih})$, and $e_{ig} = (1/n\omega_g \psi_{ig})$.

In this component, the alternative with larger ranking value is better. Hence, all the alternatives can be ranked according to the descending order of their ranking values.

After obtaining the ranking values of all the alternatives from these three components, we need to fuse them for deriving the final ranking values. In the original MULTIMOORA method, the dominance theory is usually used to aggregate three ranking orders for deriving the final ranking order. However, it is incapable of handling massive operations resulting from its cumbersome pairwise comparison processes [54]. For the purpose of overcoming the deficiency of dominancy theory, the HM operator is put forward for integrating the ranking values of alternatives obtained from three components of the proposed q-ROF-MULTIMOORA method. The HM operator owns the advantage of capturing the interrelationships hiding behind input values. Afterwards, by using the ranking values obtained from equations (47)–(52), here a new DM is constructed, where the three components of the q-ROF-MULTIMOORA method are regarded as criteria of alternatives: q-ROF-RS component (c_1), q-ROF-RP component (c_2), and q-ROF-FMF component (c_3). Hence, the new DM M is constructed as

$$M = \begin{array}{c} \\ x_1 \\ x_2 \\ \vdots \\ x_m \end{array} \begin{array}{c} \begin{array}{ccc} c_1 & c_2 & c_3 \end{array} \\ \begin{pmatrix} f_{11} & f_{12} & f_{13} \\ f_{21} & f_{22} & f_{23} \\ \vdots & \vdots & \vdots \\ f_{m1} & f_{m2} & f_{m3} \end{pmatrix} \end{array}, \tag{53}$$

where $\{x_1, x_2, \ldots, x_m\}$ denotes the set of alternatives and $\{c_1, c_2, c_3\}$ denotes the set of criteria. The element $f_{iy}\,(y = 1, 2, 3)$ in the DM M denotes the ranking value of the alternative x_i with respect to the criterion c_y. Let $\chi = \{\chi_1, \chi_2, \chi_3\}$ be the weight values of criteria $\{c_1, c_2, c_3\}$, satisfying $0 \le \chi_y \le 1$ and $\sum_{y=1}^{3} \chi_y = 1$. In general, the weight values of criteria are set to $\chi_1 = \chi_2 = \chi_3 = (1/3)$. For the DM M, the ranking values of each alternative with respect to three criteria should be aggregated for determining the final ranking values. However, the ranking values $f_{iy}\,(y = 1, 2, 3)$ show different dimensions because they are obtained from the different components. For the purpose of making them dimensionless, all the ranking values $f_{iy}\,(y = 1, 2, 3)$ are normalized as

$$\widetilde{f}_{iy} = \begin{cases} \dfrac{f_{iy} - \min_{1\le i\le m} f_{iy}}{\max_{1\le i\le m} f_{iy} - \min_{1\le i\le m} f_{iy}}, & \text{for benefit} - \text{type criterion}\, c_y, \\[2ex] \dfrac{\max_{1\le i\le m} f_{iy} - f_{iy}}{\max_{1\le i\le m} f_{iy} - \min_{1\le i\le m} f_{iy}}, & \text{for cost} - \text{type criterion}\, c_y, \end{cases} \tag{54}$$

where $1 \le i \le m$ and $1 \le y \le 3$.

Afterwards, the weighted HM operator [55] is used to aggregate the normalized ranking values $\widetilde{f}_{iy}$ of each alternative x_i with respect to three criteria for deriving the final ranking value of this alternative as

$$F_i = \left(\frac{2}{3(3+1)} \sum_{h=1}^{3} \sum_{g=h}^{3} \left(\chi_h \widetilde{f}_{ih}\right)^{\gamma} \left(\chi_g \widetilde{f}_{ig}\right)^{\eta} \right)^{(1/(\gamma+\eta))}. \tag{55}$$

The alternative with larger final ranking value is better. Hence, all the alternatives can be ranked based on the descending order of their final ranking values.

5.3. Decision-Making Procedure. Based on the discussion and results in Section 5.2, the decision-making procedure of the proposed q-ROF-MULTIMOORA method is summarized using the following 7 steps.

Step 1: all the evaluation information is collected for constructing DM $R = (o_{ij})_{m\times n} = (\mu_{ij}, \nu_{ij})_{m\times n}$. At the same time, the values of the parameters q, γ, η, and $\aleph$ should be provided.

Step 2: to transform the criteria values of each alternative with respect to cost-type criteria, (45) is used to transform DM $R = (o_{ij})_{m\times n}$ into DM $\widetilde{R} = (\widetilde{o}_{ij})_{m\times n}$.

Step 3: for the transformed DM $\widetilde{R} = (\widetilde{o}_{ij})_{m\times n}$, (47) is applied to compute the ranking value f_{i1} of each alternative x_i with respect to the q-ROF-RS component. The alternatives can be ranked according to the descending order of their ranking values.

Step 4: for the transformed DM $\widetilde{R} = (\widetilde{o}_{ij})_{m\times n}$, (50) is applied to compute the ranking value f_{i2} of each alternative x_i with respect to the q-ROF-RP component. The alternatives can be ranked according to the ascending order of their ranking values.

Step 5: for the transformed DM $\widetilde{R} = (\widetilde{o}_{ij})_{m\times n}$, (52) is applied to compute the ranking value f_{i3} of each alternative x_i with respect to the q-ROF-FMF component. The alternatives can be ranked according to the descending order of their ranking values.

Step 6: based on the ranking values of alternatives obtained from three components in Steps 3–5, a new DM $M = (f_{iy})_{m\times 3}$ is constructed. Afterwards, (54) is applied to transform DM $M = (f_{iy})_{m\times 3}$ into $\widetilde{M} = (\widetilde{f}_{iy})_{m\times 3}$.

Step 7: in the final step, (55) is used to aggregate the ranking values of alternatives with respect to three components of the q-ROF-MULTIMOORA method for deriving the final ranking values. Then, all the alternatives are ranked according to the descending order of their final ranking values.

The above steps are also shown in Figure 1.

The q-ROF-MULTIMOORA method is a combination of PA operator, Dombi operational laws, AHM, GHM, and MULTIMOORA. It shows the following advantages:

(1) It has the ability of alleviating negative influences of extreme criteria values on the decision results, which makes the decision results more stable and robust.

(2) It shows strong flexibility when computing the criteria values due to the Dombi operational laws of q-ROFNs.

(3) The HM and GHM operators are capable of capturing the complex interrelationships hiding behind the criteria values. Moreover, the MULTIMOORA method integrates the ranking values obtained from three components for deriving the final ranking values. Thus, the decision results of the q-ROF-MULTIMOORA method are more reasonable and effective.

6. Illustrative Example and Comparison Analysis

In this section, a practical case concerning the evaluation of security algorithm is shown to illustrate the decision-making procedure of the proposed q-ROF-MULTIMOORA method. Afterwards, the influences of the parameters on the decision results are analyzed. Finally, the proposed q-ROF-MULTIMOORA method is compared with the original MULTIMOORA method for processing q-ROFNs.

6.1. Decision Process Using the q-ROF-MULTIMOORA Method. In this section, a real case concerning the evaluation of security algorithms is provided to illustrate the decision procedure of the proposed q-ROF-MULTIMOORA method.

Example 1. With the quick development of Internet applications, more and more user data are stored online. Hackers frequently attack the Internet applications for obtaining the privacy data. To protect users' privacy data, various security algorithms have been designed and implemented. However, these security algorithms show different features. How to choose the suitable security algorithm is a big challenge for organizations since multiple criteria should be considered. Here, we try to formulate the process of evaluating the security algorithms and selecting a suitable one as a classical MCDM problem. Suppose organization plans to evaluate 5 candidates of security algorithms and select the suitable one by considering 6 criteria: function (c_1), reliability (c_2), usability (c_3), performance (c_4), portability (c_5), and complexity (c_6). Hence, an MCDM problem composed of 5 security algorithms $\{x_1, x_2, x_3, x_4, x_5\}$ and 6 criteria $\{c_1, c_2, c_3, c_4, c_5, c_6\}$ can be constructed. According to the real requirements for building the security system, the organization sets the weights of criteria as $\omega = (0.10, 0.15, 0.35, 0.20, 0.10, 0.10)$. The technical panel of this organization uses the q-ROFNs to evaluate these five security algorithms with respect to their criteria. All the q-ROFNs are collected to form the DM $R = (o_{ij})_{5\times 6} = (\mu_{ij}, \nu_{ij})_{5\times 6}$, as shown in Table 2.

Step 1: the values of the parameters γ, η, and $\aleph$ are set to 1 and the value of the parameter q is set to 3.

Step 2: the first five criteria are benefit-type criteria, while the maintenance cost is cost-type criteria. Hence, (45) is used to transform DM $R = (o_{ij})_{5\times 6}$ in Table 2 into DM $\widetilde{R} = (\widetilde{o}_{ij})_{5\times 6}$ as depicted in Table 3.

Step 3: for the transformed DM $\widetilde{R} = (\widetilde{o}_{ij})_{5\times 6}$, (47) is applied to compute the ranking value f_{i1} of each security algorithm x_i with respect to the q-ROF-RS component as

$$\begin{aligned} f_{11} &= 0.036, \\ f_{21} &= 0.027, \\ f_{31} &= 0.033, \\ f_{41} &= 0.111, \\ f_{51} &= 0.047. \end{aligned} \tag{56}$$

Hence, these security algorithms can be ranked as $x_4 \succ x_5 \succ x_1 \succ x_3 \succ x_2$.

Step 4: for the transformed DM $\widetilde{R} = (\widetilde{o}_{ij})_{5\times 6}$, (50) is applied to compute the ranking value f_{i2} of each security algorithm x_i with respect to the q-ROF-RP component as

$$\begin{aligned} f_{12} &= 0.179, \\ f_{22} &= 0.225, \\ f_{32} &= 0.213, \\ f_{42} &= 0.031, \\ f_{52} &= 0.229. \end{aligned} \tag{57}$$

Hence, these security algorithms can be ranked as $x_4 \succ x_1 \succ x_3 \succ x_2 \succ x_5$.

Step 5: for the transformed DM $\widetilde{R} = (\widetilde{o}_{ij})_{5\times 6}$, (52) is applied to compute the ranking value f_{i3} of each security algorithm x_i with respect to the q-ROF-FMF component as

$$\begin{aligned} f_{13} &= -0.004, \\ f_{23} &= -0.018, \\ f_{33} &= 0.007, \\ f_{43} &= -0.001, \\ f_{53} &= -0.035. \end{aligned} \tag{58}$$

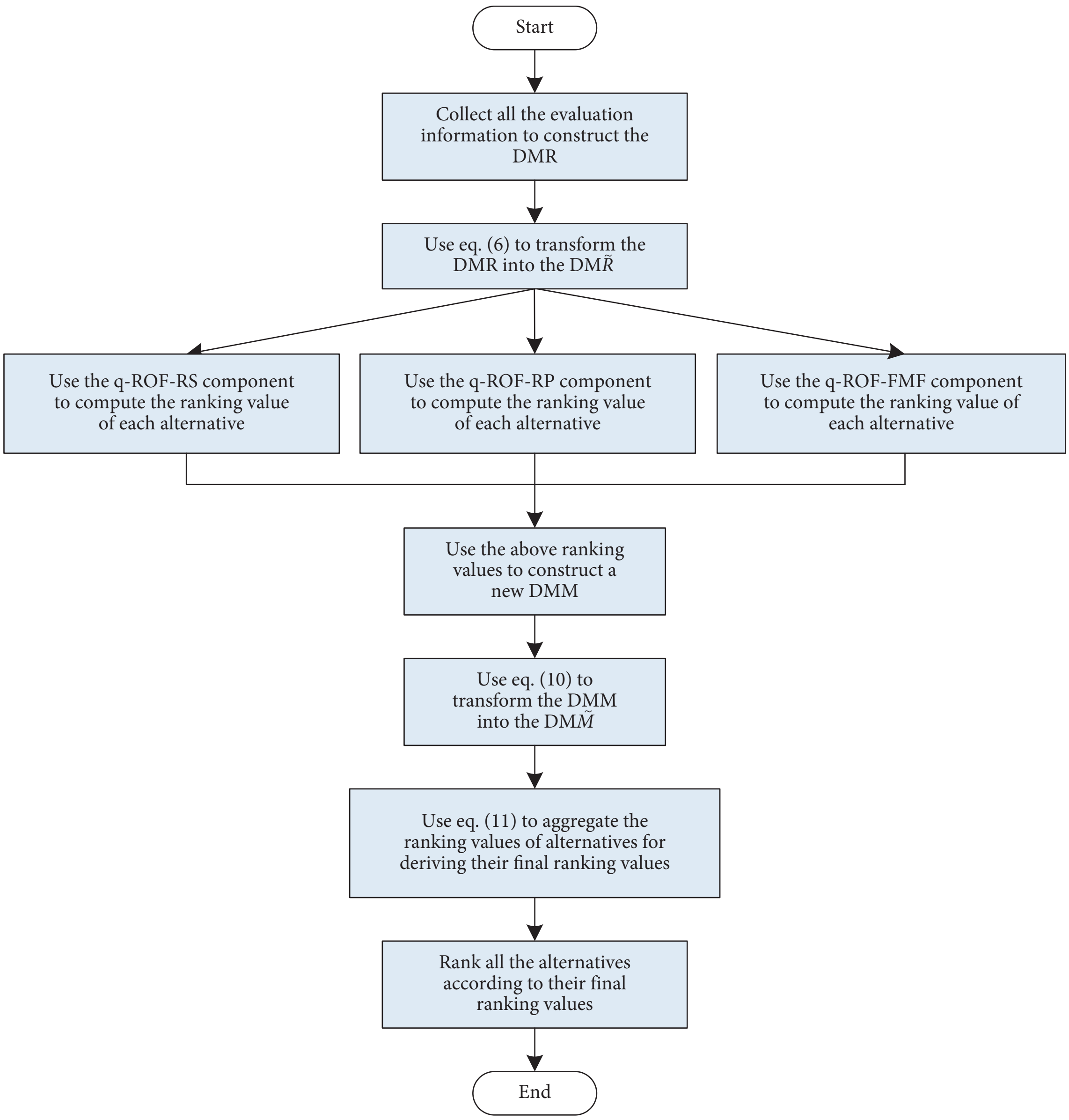

FIGURE 1: The frame diagram of the proposed method.

Hence, these security algorithms can be ranked as $x_3 \succ x_4 \succ x_1 \succ x_2 \succ x_5$.

Step 6: based on the ranking values of security algorithms obtained from three components in Steps 3–5, a new DM $M = (f_{iy})_{m\times 3}$ is formed. Afterwards, (54) is applied to transform the DM $M = (f_{iy})_{m\times 3}$ into $\widetilde{M} = (\widetilde{f}_{iy})_{m\times 3}$ as

$$\widetilde{M} = \begin{pmatrix} 0.107 & 0.253 & 0.738 \\ 0.000 & 0.020 & 0.405 \\ 0.071 & 0.081 & 1.000 \\ 1.000 & 1.000 & 0.810 \\ 0.238 & 0.000 & 0.000 \end{pmatrix}. \quad (59)$$

Step 7: in the final step, equation (55) is used to aggregate the ranking values of five security algorithms with respect to three components for deriving the final ranking values as

$$\begin{aligned} F_1 &= 0.130, \\ F_2 &= 0.057, \\ F_3 &= 0.147, \\ F_4 &= 0.313, \\ F_5 &= 0.032. \end{aligned} \quad (60)$$

Then, the final ranking order of these security algorithms is $x_4 \succ x_3 \succ x_1 \succ x_2 \succ x_5$. Thus, the security algorithm x_4 is the suitable one for the organization when building the security system.

6.2. Influences of the Parameters on the Ranking Results. In this section, the influences of the parameters on the ranking results are discussed.

6.2.1. Influence of the Parameter q on the Final Ranking Results. The influence of the parameter q on the final ranking results of the q-ROF-MULTIMOORA method is first discussed. In this case, the parameters $\gamma = \eta = \aleph = 1$. For the transformed DM $R = (o_{ij})_{5\times 6}$ in Table 2, the ranking results of security algorithms are shown in Table 4 and Figure 2 when the value of the parameter q varies.

From Table 4, it can be known that the ranking results of security algorithms are different when the value of q varies. When $q = 1$, the ranking result of security algorithms is $x_4 \succ x_1 \succ x_3 \succ x_2 \succ x_5$. When $q = 2$, the ranking result of security algorithms is $x_4 \succ x_2 \succ x_1 \succ x_3 \succ x_5$. When $q = 3$ or $q = 5$, the ranking results of security algorithms are $x_4 \succ x_3 \succ x_1 \succ x_2 \succ x_5$. Although the ranking result of security algorithms changes when the value of the parameter q varies, the most suitable security algorithm keeps unchanged, namely, x_4. When $q = 1$, then q-ROFNs reduce to IFNs. When $q = 2$, then q-ROFNs reduce to PFNs. How to determine the reasonable value of q depends on the evaluation information provided by the expert. The smallest value of the parameter q should satisfy $\mu^q + \nu^q \le 1$. For instance, if the evaluation information given by the expert is (0.9, 0.9), then the smallest value of the parameter q should be 7 so that $0.9^7 + 0.9^7 < 1$.

6.2.2. Influences of the Parameters γ and η on the Ranking Results. The influences of the parameters γ and η on the ranking results of the q-ROF-MULTIMOORA method are analyzed in this part. In this case, the parameters $\aleph = 1$ and $q = 3$. For DM $R = (o_{ij})_{5\times 6}$ in Table 2, the ranking results of security algorithms are shown in Table 5 and Figure 3 when the values of the parameters γ and η vary.

From Table 5, it can be seen that the ranking result obtained from the q-ROF-MULTIMOORA method is always $x_4 \succ x_3 \succ x_1 \succ x_2 \succ x_5$ except when $\gamma = 0$ and $\eta = 1$. Nevertheless, the most suitable security algorithm is always x_4. When $\gamma = 0$ and $\eta = 1$, the ranking result of security algorithms changes into $x_4 \succ x_1 \succ x_3 \succ x_5 \succ x_2$. Thus, the ranking result obtained from the q-ROF-MULTIMOORA method is not sensitive to the values of these two parameters. In other words, the q-ROF-MULTIMOORA method is robust and effective.

6.2.3. Influence of the Parameter $\aleph$ on the Ranking Results. The influence of the parameter $\aleph$ on the ranking results of the q-ROF-MULTIMOORA method is analyzed in this part. In this case, the parameters $\gamma = \eta = 1$ and $q = 3$. For DM $R = (o_{ij})_{5\times 6}$ in Table 2, the ranking results of security algorithms are listed in Table 6 and Figure 4 when the value of the parameter $\aleph$ varies.

Table 2: The q-rung orthopair fuzzy DM.

	c_1	c_2	c_3	c_4	c_5	c_6
x_1	(0.1,0.2)	(0.3,0.3)	(0.5,0.3)	(0.6,0.3)	(0.2,0.1)	(0.1,0.1)
x_2	(0.3,0.2)	(0.1,0.1)	(0.5,0.1)	(0.4,0.5)	(0.3,0.2)	(0.6,0.1)
x_3	(0.6,0.1)	(0.2,0.2)	(0.4,0.3)	(0.2,0.4)	(0.3,0.2)	(0.1,0.2)
x_4	(0.2,0.5)	(0.1,0.3)	(0.7,0.1)	(0.8,0.1)	(0.4,0.3)	(0.3,0.3)
x_5	(0.4,0.4)	(0.4,0.5)	(0.5,0.2)	(0.1,0.4)	(0.3,0.4)	(0.4,0.4)

Table 3: The transformed q-rung orthopair fuzzy DM.

	c_1	c_2	c_3	c_4	c_5	c_6
x_1	(0.1,.02)	(0.3,0.3)	(0.5,0.3)	(0.6,0.3)	(0.2,0.1)	(0.1,0.1)
x_2	(0.3,0.2)	(0.1,0.1)	(0.5,0.1)	(0.4,0.5)	(0.3,0.2)	(0.1,0.6)
x_3	(0.6,0.1)	(0.2,0.2)	(0.4,0.3)	(0.2,0.4)	(0.3,0.2)	(0.2,0.1)
x_4	(0.2,0.5)	(0.1,0.3)	(0.7,0.1)	(0.8,0.1)	(0.4,0.3)	(0.3,0.3)
x_5	(0.4,0.4)	(0.4,0.5)	(0.5,0.2)	(0.1,0.4)	(0.3,0.4)	(0.4,0.4)

From Table 6, it can be seen that the ranking result obtained from the q-ROF-MULTIMOORA method slightly changes when the value of the parameter $\aleph$ varies. When the value of the parameter $\aleph$ is set to $\aleph = 1$, then the ranking result of security algorithms is $x_4 \succ x_3 \succ x_1 \succ x_2 \succ x_5$. When the value of the parameter $\aleph$ is set to a value in the integer set $\{2, 3, \ldots, 10\}$, then the ranking result of security algorithms is changed into $x_4 \succ x_1 \succ x_3 \succ x_5 \succ x_2$. However, the most suitable security algorithm always keeps unchanged, namely, x_4 no matter how the value of the parameter $\aleph$ varies. Hence, the ranking result that is obtained from the q-ROF-MULTIMOORA method is relatively stable. Because of the Dombi operational laws for q-ROFNs, the q-ROF-MULTIMOORA method has high flexibility by providing the parameter $\aleph$. Experts can adjust the value of the parameter $\aleph$ according to the actual situation of MCDM problems.

6.3. Comparative Analysis. For the proposed q-ROF-MULTIMOORA method, it applies the PA operator to alleviate the negative influence of extreme values on the ranking results and integrates the AHM and GHM operators to handle the interrelationships hiding behind criteria values. For the purpose of verifying the effectiveness of the q-ROF-MULTIMOORA method, it is compared with the original MULTIMOORA method [32, 56] for handling the q-ROFNs. Different from the q-ROF-MULTIMOORA method, the original MULTIMOORA method does not contain the PA operator to solve the problem of extreme values and also does not integrate the AHM and GHM operators to handle the interrelationships among criteria values. Hence, it is a suitable way for comparing the q-ROF-MULTIMOORA method with the original MULTIMOORA method. For the purpose of conducting this comparative analysis, an example of evaluating blockchain platforms is given.

Example 2. The blockchain technology has the ability to solve the problems resulting from our increasingly connected society and tackle real-world business concerns. It has been broadly applied to many fields such as distributed

Table 4: Ranking results of the q-ROF-MULTIMOORA method when the value of q varies.

	Final ranking values of security algorithms	Ranking results
$q = 1$	$F_1 = 0.210$, $F_2 = 0.096$, $F_3 = 0.192$, $F_4 = 0.333$, and $F_5 = 0.000$	$x_4 \succ x_1 \succ x_3 \succ x_2 \succ x_5$
$q = 2$	$F_1 = 0.093$, $F_2 = 0.191$, $F_3 = 0.069$, $F_4 = 0.312$, and $F_5 = 0.043$	$x_4 \succ x_2 \succ x_1 \succ x_3 \succ x_5$
$q = 3$	$F_1 = 0.130$, $F_2 = 0.057$, $F_3 = 0.147$, $F_4 = 0.313$, and $F_5 = 0.032$	$x_4 \succ x_3 \succ x_1 \succ x_2 \succ x_5$
$q = 5$	$F_1 = 0.136$, $F_2 = 0.019$, $F_3 = 0.142$, $F_4 = 0.302$, and $F_5 = 0.014$	$x_4 \succ x_3 \succ x_1 \succ x_2 \succ x_5$

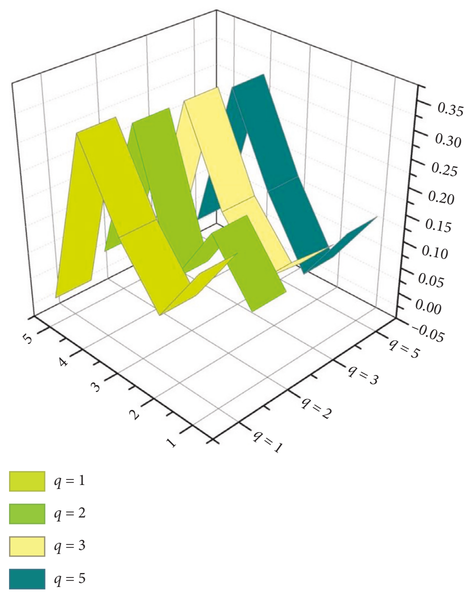

Figure 2: Ranking results of the q-ROF-MULTIMOORA method when the value of q varies.

Table 5: Ranking results of the q-ROF-MULTIMOORA method when the values of γ and η vary.

	Final ranking values of security algorithms	Ranking results
$\gamma = 1$ and $\eta = 0$	$F_1 = 0.094$, $F_2 = 0.038$, $F_3 = 0.118$, $F_4 = 0.307$, and $F_5 = 0.021$	$x_4 \succ x_3 \succ x_1 \succ x_2 \succ x_5$
$\gamma = 1$ and $\eta = 0.5$	$F_1 = 0.112$, $F_2 = 0.041$, $F_3 = 0.131$, $F_4 = 0.312$, and $F_5 = 0.024$	$x_4 \succ x_3 \succ x_1 \succ x_2 \succ x_5$
$\gamma = 1$ and $\eta = 1$	$F_1 = 0.130$, $F_2 = 0.057$, $F_3 = 0.147$, $F_4 = 0.313$, and $F_5 = 0.032$	$x_4 \succ x_3 \succ x_1 \succ x_2 \succ x_5$
$\gamma = 1$ and $\eta = 2$	$F_1 = 0.151$, $F_2 = 0.070$, $F_3 = 0.187$, $F_4 = 0.310$, and $F_5 = 0.044$	$x_4 \succ x_3 \succ x_1 \succ x_2 \succ x_5$
$\gamma = 1$ and $\eta = 3$	$F_1 = 0.174$, $F_2 = 0.082$, $F_3 = 0.215$, $F_4 = 0.312$, and $F_5 = 0.051$	$x_4 \succ x_3 \succ x_1 \succ x_2 \succ x_5$
$\gamma = 1$ and $\eta = 4$	$F_1 = 0.185$, $F_2 = 0.086$, $F_3 = 0.235$, $F_4 = 0.315$, and $F_5 = 0.055$	$x_4 \succ x_3 \succ x_1 \succ x_2 \succ x_5$
$\gamma = 0$ and $\eta = 1$	$F_1 = 0.197$, $F_2 = 0.003$, $F_3 = 0.170$, $F_4 = 0.333$, and $F_5 = 0.070$	$x_4 \succ x_1 \succ x_3 \succ x_5 \succ x_2$
$\gamma = 0.5$ and $\eta = 1$	$F_1 = 0.139$, $F_2 = 0.043$, $F_3 = 0.155$, $F_4 = 0.308$, and $F_5 = 0.024$	$x_4 \succ x_3 \succ x_1 \succ x_2 \succ x_5$
$\gamma = 2$ and $\eta = 1$	$F_1 = 0.144$, $F_2 = 0.073$, $F_3 = 0.184$, $F_4 = 0.313$, $F_5 = 0.047$	$x_4 \succ x_3 \succ x_1 \succ x_2 \succ x_5$
$\gamma = 3$ and $\eta = 1$	$F_1 = 0.162$, $F_2 = 0.093$, $F_3 = 0.213$, $F_4 = 0.317$, and $F_5 = 0.051$	$x_4 \succ x_3 \succ x_1 \succ x_2 \succ x_5$
$\gamma = 4$ and $\eta = 1$	$F_1 = 0.181$, $F_2 = 0.106$, $F_3 = 0.233$, $F_4 = 0.318$, and $F_5 = 0.054$	$x_4 \succ x_3 \succ x_1 \succ x_2 \succ x_5$

cloud storage and health care, as well as payment and transfers. To benefit from the blockchain technology, organizations across the globe try to introduce the blockchain technology for building their own decentralized systems. The blockchain platforms are a good solution, which help organizations to facilitate the development and deployment of decentralized systems. Suppose that an organization wants to evaluate five blockchain platforms with respect to five criteria: usability, performance, scalability, security, and cost. Therefore, evaluating these five blockchain platforms can be formulated as an MCDM composed of blockchain platforms $\{x_1, x_2, x_3, x_4, x_5\}$ with respect to criteria $\{c_1, c_2, c_3, c_4, c_5\}$. The weights of criteria are set to $\omega = (0.10, 0.25, 0.35, 0.2, 0.1)$. The transformed DM $R = (o_{ij})_{5\times5} = (\mu_{ij}, \nu_{ij})_{5\times5}$ is given in Table 7.

The original MULTIMOORA method and q-ROF-MULTIMOORA method are applied to process the transformed q-rung orthopair fuzzy DM in Table 7. Because of the limited space, the computation processes are omitted here and the ranking results of different methods are provided in Table 8.

In Table 8, the ranking results obtained from the q-ROF-MULTIMOORA method and original method are provided. Moreover, the ranking results obtained from the three components of q-ROF-MULTIMOORA and original method are also given. From Table 8, it can be noted that the

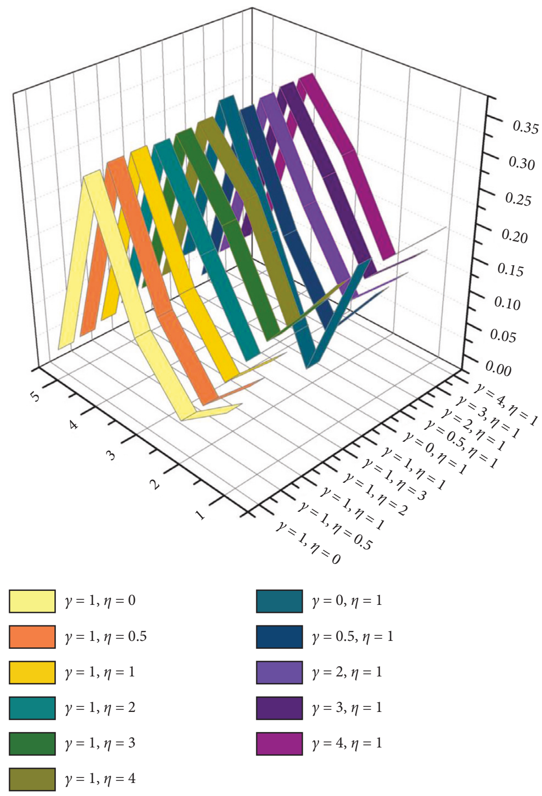

Figure 3: Ranking results of the q-ROF-MULTIMOORA method when the values of γ and η vary.

Table 6: Ranking results of the q-ROF-MULTIMOORA method when the value of $\aleph$ varies.

	Final ranking values of security algorithms	Ranking results
$\aleph = 1$	$F_1 = 0.130$, $F_2 = 0.057$, $F_3 = 0.147$, $F_4 = 0.313$, and $F_5 = 0.032$	$x_4 \succ x_3 \succ x_1 \succ x_2 \succ x_5$
$\aleph = 2$	$F_1 = 0.153$, $F_2 = 0.003$, $F_3 = 0.150$, $F_4 = 0.297$, and $F_5 = 0.027$	$x_4 \succ x_1 \succ x_3 \succ x_5 \succ x_2$
$\aleph = 3$	$F_1 = 0.170$, $F_2 = 0.003$, $F_3 = 0.154$, $F_4 = 0.296$, and $F_5 = 0.054$	$x_4 \succ x_1 \succ x_3 \succ x_5 \succ x_2$
$\aleph = 4$	$F_1 = 0.172$, $F_2 = 0.003$, $F_3 = 0.151$, $F_4 = 0.291$, and $F_5 = 0.063$	$x_4 \succ x_1 \succ x_3 \succ x_5 \succ x_2$
$\aleph = 5$	$F_1 = 0.173$, $F_2 = 0.003$, $F_3 = 0.149$, $F_4 = 0.286$, and $F_5 = 0.065$	$x_4 \succ x_1 \succ x_3 \succ x_5 \succ x_2$
$\aleph = 6$	$F_1 = 0.173$, $F_2 = 0.003$, $F_3 = 0.147$, $F_4 = 0.285$, and $F_5 = 0.067$	$x_4 \succ x_1 \succ x_3 \succ x_5 \succ x_2$
$\aleph = 7$	$F_1 = 0.173$, $F_2 = 0.003$, $F_3 = 0.145$, $F_4 = 0.283$, and $F_5 = 0.066$	$x_4 \succ x_1 \succ x_3 \succ x_5 \succ x_2$
$\aleph = 8$	$F_1 = 0.174$, $F_2 = 0.003$, $F_3 = 0.145$, $F_4 = 0.283$, and $F_5 = 0.066$	$x_4 \succ x_1 \succ x_3 \succ x_5 \succ x_2$
$\aleph = 9$	$F_1 = 0.174$, $F_2 = 0.003$, $F_3 = 0.144$, $F_4 = 0.282$, and $F_5 = 0.067$	$x_4 \succ x_1 \succ x_3 \succ x_5 \succ x_2$
$\aleph = 10$	$F_1 = 0.174$, $F_2 = 0.003$, $F_3 = 0.142$, $F_4 = 0.282$, and $F_5 = 0.067$	$x_4 \succ x_1 \succ x_3 \succ x_5 \succ x_2$

ranking results obtained from the q-ROF-MULTIMOORA method and original MULTIMOORA method are different. Moreover, the ranking result obtained from the q-ROF-RS component of the q-ROF-MULTIMOORA method is different from that obtained from the RS component of the original MULTIMOORA method, so do the ranking results of other two components in the q-ROF-MULTIMOORA method and original MULTIMOORA method. The reasons are analyzed as follows:

(1) In the process of evaluating blockchain platforms, there are the interrelationships hiding behind the criteria values. The q-ROF-MULTIMOORA method has been equipped with the AHM and GHM operators to process the interrelationships, while the original MULTIMOORA method is unable to process the hiding interrelationships.

(2) For the q-rung orthopair fuzzy DM R, there exists relatively great difference among criteria values. The q-ROF-MULTIMOORA method is integrated with the PA operator to alleviate the negative impact of extreme criteria values on the ranking results, while the original MULTIMOORA method ignores this case.

From the above analysis, it can be noted that the q-ROF-MULTIMOORA method performs better than the original MUTLIMOORA method because the q-ROF-MULTIMOORA method derives more robust and reasonable ranking results.

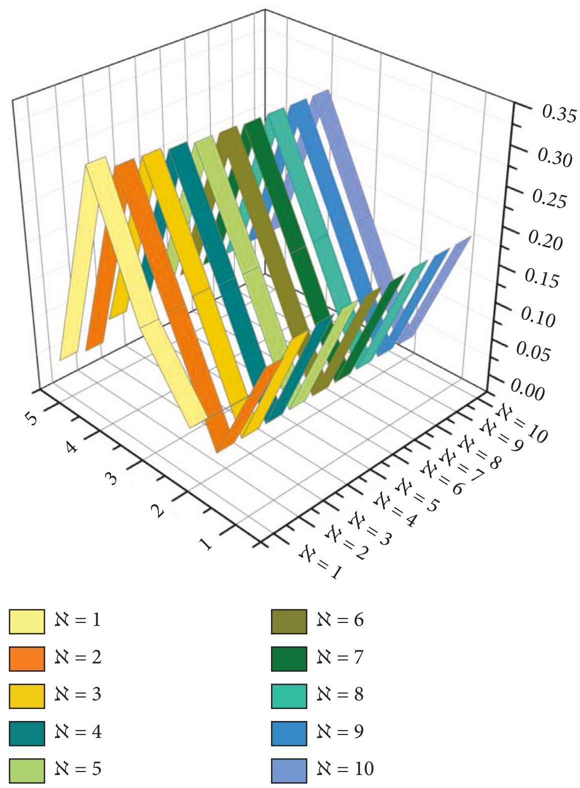

Figure 4: Ranking results of the q-ROF-MULTIMOORA method when the value of ℵ varies.

Table 7: The transformed q-rung orthopair fuzzy DM for evaluating blockchain platforms.

	c_1	c_2	c_3	c_4	c_5
x_1	(0.5,0.1)	(0.5,0.1)	(0.6,0.1)	(0.8,0.1)	(0.5,0.3)
x_2	(0.1,0.2)	(0.2,0.2)	(0.3,0.4)	(0.4,0.1)	(0.2,0.2)
x_3	(0.3,0.1)	(0.2,0.4)	(0.5,0.3)	(0.5,0.4)	(0.3,0.1)
x_4	(0.4,0.2)	(0.7,0.2)	(0.6,0.1)	(0.5,0.1)	(0.7,0.2)
x_5	(0.5,0.4)	(0.2,0.1)	(0.2,0.4)	(0.3,0.5)	(0.2,0.4)

Table 8: Ranking results of five blockchain platforms when using different methods.

	Decision method	Ranking results
1	RS component [32]	$x_1 \succ x_4 \succ x_3 \succ x_2 \succ x_5$
2	RP component [32]	$x_1 \succ x_4 \succ x_3 \succ x_2 \succ x_5$
3	FMF component [32]	$x_4 \succ x_1 \succ x_3 \succ x_2 \succ x_5$
4	The original MULTIMOORA [32]	$x_1 \succ x_4 \succ x_3 \succ x_2 \succ x_5$
5	q-ROF-RS component	$x_4 \succ x_1 \succ x_3 \succ x_5 \succ x_2$
6	q-ROF-RP component	$x_4 \succ x_1 \succ x_3 \succ x_2 \succ x_5$
7	q-ROF-FMF component	$x_1 \succ x_4 \succ x_3 \succ x_2 \succ x_5$
8	q-ROF-MULTIMOORA	$x_4 \succ x_1 \succ x_3 \succ x_2 \succ x_5$

7. Conclusions

To solve the security algorithms' evaluation problem, we propose an efficient q-ROF-MULTIMOORA method in this paper. Our contributions are listed as follows:

(1) We combine the PA operator, Dombi operational laws, and AHM and GHM operators to design the q-ROFDPHM, q-ROFWDPHM, q-ROFDPGHM, and q-ROFWDPGHM operators to aggregate q-ROFNs.

(2) The proposed q-ROFWDPHM and q-ROFWDPGHM operators are applied to modify the original MULTIMOORA method for proposing a novel q-ROF-MULTIMOORA method.

(3) A practical case of evaluating five security algorithms is given to show the decision procedure of the q-ROF-MULTIMOORA method. The influences of the parameters on the ranking results are analyzed.

(4) To validate the effectiveness of the proposed q-ROF-MULTIMOORA method, a new example of evaluating blockchain platforms is given.

The proposed methods also have some limitations:

(1) the q-ROFSs model, the uncertain information uses only three characteristic functions and does not have the characteristic function that denotes the degree of abstinence. This limitation can be removed by introducing the concept of T-spherical fuzzy sets, which was proposed by Mahmood et al. [57]. It has been studied by many scholars [58,59].

(2) The weights of attributes are directly given in this study. It ignores the objective significance. The method combining the objective weights and subjective weights should be considered in the future.

(3) In the proposed q-ROF-MULTIMOORA method, the q-ROFDPHM and q-ROFDPGHM operators do not consider the interaction between the membership degree and the nonmembership degree of q-ROFSs, which will produce unreasonable aggregated results.

The proposed q-ROF-MULTIMOORA method has some potential applications. In the future research plan, we intend to apply the proposed method into the sustainable supplier selection [60]. According to the third limitation mentioned in the above paragraph, the idea of interaction operational rules [61] will be used to improve the proposed method.

Data Availability

The data used to support the findings of this study are included within the article.

Conflicts of Interest

The authors declare that they have no conflicts of interest.

Acknowledgments

This research work was supported by the Project of Exploration and Practice of Network Engineering Major (Intelligent Internet of Things Direction) University-Enterprise Collaborative Talent Training Scheme Model Based on New Engineering and Technical Disciplines.

References

[1] L. Zhao, W. Zhao, A. Hawbani et al., "Novel online sequential learning-based adaptive routing for edge software-defined vehicular networks," *IEEE Transactions on Wireless Communications*, vol. 20, no. 5, pp. 2991–3004, 2021.

[2] M. Lin, C. Huang, Z. Xu, and R. Chen, "Evaluating IoT platforms using integrated probabilistic linguistic MCDM method," *IEEE Internet of Things Journal*, vol. 7, no. 11, pp. 11195–11208, 2020.

[3] L. Zhao, Z. Bi, M. Lin, A. Hawbani, J. Shi, and Y. Guan, "An intelligent fuzzy-based routing scheme for software-defined vehicular networks," *Computer Networks*, vol. 187, Article ID 107837, 2021.

[4] J. Liu, S. Zheng, G. Xu, and M. Lin, "Cross-domain sentiment aware word embeddings for review sentiment analysis," *International Journal of Machine Learning and Cybernetics*, vol. 12, no. 2, pp. 343–354, 2021.

[5] M. Abdel-Basset, Y. Zhou, M. Mohamed, and V. Chang, "A group decision making framework based on neutrosophic VIKOR approach for e-government website evaluation," *Journal of Intelligent and Fuzzy Systems*, vol. 34, no. 6, pp. 4213–4224, 2018.

[6] W. Wang, Z. Huang, and L. Wang, "ISAT: an intelligent web service selection approach for improving reliability via two-phase decisions," *Information Sciences*, vol. 433-434, pp. 255–273, 2018.

[7] D. N. S. Ravi Kumar and S. Barani, "Data dissemination model using epidemic and transmission-segment- based geographic routing protocol: a new perspective in vehicular ad hoc networks," *International Journal of Intelligent Computing and Cybernetics*, vol. 14, no. 2, pp. 287–301, 2021.

[8] Y. Pan, M. Lin, Z. Wu, H. Zhang, and Z. Xu, "Caching-aware garbage collection to improve performance and lifetime for NAND flash SSDs," *IEEE Transactions on Consumer Electronics*, vol. 67, no. 2, pp. 141–148, 2021.

[9] L. Zhao, H. X. Li, N. Lin, M. W. Lin, C. L. Fan, and J. L. Shi, "Intelligent content caching strategy in autonomous driving toward 6G," *IEEE Transactions on Intelligent Transportation Systems*, 2021.

[10] A. Nazir, R. N. Mir, and S. Qureshi, "Exploring compression and parallelization techniques for distribution of deep neural networks over Edge-Fog continuum - a review," *International Journal of Intelligent Computing and Cybernetics*, vol. 13, no. 3, pp. 331–364, 2020.

[11] L. Ning, Y. Ali, H. Ke, S. Nazir, and Z. Huanli, "A hybrid MCDM approach of selecting lightweight cryptographic cipher based on ISO and NIST lightweight cryptography security requirements for internet of health things," *IEEE Access*, vol. 8, pp. 220165–220187, 2020.

[12] C. Huang, M. Lin, and Z. Xu, "Pythagorean fuzzy MULTIMOORA method based on distance measure and score function: its application in multicriteria decision making process," *Knowledge and Information Systems*, vol. 62, no. 11, pp. 4373–4406, 2020.

[13] M. Lin, Z. Xu, Y. Zhai, and Z. Yao, "Multi-attribute group decision-making under probabilistic uncertain linguistic environment," *Journal of the Operational Research Society*, vol. 69, no. 2, pp. 157–170, 2018.

[14] L. A. Zadeh, "Fuzzy sets," *Information and Control*, vol. 8, no. 3, pp. 338–353, 1965.

[15] K. T. Atanassov, "Intuitionistic fuzzy sets," *Fuzzy Sets and Systems*, vol. 20, no. 1, pp. 87–96, 1986.

[16] R. R. Yager and A. M. Abbasov, "Pythagorean membership grades, complex numbers, and decision making," *International Journal of Intelligent Systems*, vol. 28, no. 5, pp. 436–452, 2013.

[17] R. R. Yager, "Generalized orthopair fuzzy sets," *IEEE Transactions on Fuzzy Systems*, vol. 25, no. 5, pp. 1222–1230, 2017.

[18] H. Wang, Y. Ju, and P. Liu, "Multi-attribute group decision-making methods based on q-rung orthopair fuzzy linguistic sets," *International Journal of Intelligent Systems*, vol. 34, no. 6, pp. 1129–1157, 2019.

[19] M. Lin, X. Li, and L. Chen, "Linguisticq-rung orthopair fuzzy sets and their interactional partitioned Heronian mean aggregation operators," *International Journal of Intelligent Systems*, vol. 35, no. 2, pp. 217–249, 2020.

[20] M. W. Lin, J. H. Wei, Z. S. Xu, and R. Q. Chen, "Multiattribute group decision-making based on linguistic Pythagorean fuzzy interaction partitioned Bonferroni mean aggregation operators," *Complexity*, vol. 2018, Article ID 9531064, 24 pages, 2018.

[21] Z. Yang, L. Zhang, and T. Li, "Group decision making with incomplete interval-valued q-rung orthopair fuzzy preference relations," *International Journal of Intelligent Systems*, vol. 36, no. 12, pp. 7274–7308, 2021.

[22] H. Z. Zhao, "Multiattribute decision-making method with intuitionistic fuzzy Archimedean Bonferroni means," *Mathematical Problems in Engineering*, vol. 2021, Article ID 5559270, 24 pages, 2021.

[23] W. Yang and Y. Pang, "New q-rung orthopair fuzzy partitioned Bonferroni mean operators and their application in multiple attribute decision making," *International Journal of Intelligent Systems*, vol. 34, no. 3, pp. 439–476, 2019.

[24] Z. Yang, M. Lin, Y. Li, W. Zhou, and B. Xu, "Assessment and selection of smart agriculture solutions using an information error-based Pythagorean fuzzy cloud algorithm," *International Journal of Intelligent Systems*, vol. 36, no. 11, pp. 6387–6418, 2021.

[25] G. Wei, C. Wei, J. Wang, H. Gao, and Y. Wei, "Some q-rung orthopair fuzzy maclaurin symmetric mean operators and their applications to potential evaluation of emerging technology commercialization," *International Journal of Intelligent Systems*, vol. 34, no. 1, pp. 50–81, 2019.

[26] P. D. Liu, S. M. Chen, and P. Wang, "Multiple-attribute group decision-making based on q-rung orthopair fuzzy power maclaurin symmetric mean operators," *IEEE Transactions on Systems, Man, and Cybernetics: Systems*, vol. 50, no. 10, pp. 3741–3756, 2020.

[27] J. Wang, G. Wei, J. Lu et al., "Some q -rung orthopair fuzzy Hamy mean operators in multiple attribute decision-making and their application to enterprise resource planning systems selection," *International Journal of Intelligent Systems*, vol. 34, no. 10, pp. 2429–2458, 2019.

[28] D. Liang, Y. Zhang, and W. Cao, "q -Rung orthopair fuzzy Choquet integral aggregation and its application in heterogeneous multicriteria two-sided matching decision making," *International Journal of Intelligent Systems*, vol. 34, no. 12, pp. 3275–3301, 2019.

[29] X. Q. Xu, J. L. Xie, N. Yue, and H. H. Wang, "Probabilistic uncertain linguistic TODIM method based on the generalized Choquet integral and its application," *International Journal of Intelligent Computing and Cybernetics*, vol. 14, no. 2, pp. 122–144, 2021.

[30] P. Liu, P. Wang, and W. Pedrycz, "Consistency- and consensus-based group decision-making method with

incomplete probabilistic linguistic preference relations," *IEEE Transactions on Fuzzy Systems*, vol. 29, no. 9, pp. 2565–2579, 2021.
[31] P. Wang, P. Liu, and F. Chiclana, "Multi-stage consistency optimization algorithm for decision making with incomplete probabilistic linguistic preference relation," *Information Sciences*, vol. 556, pp. 361–388, 2021.
[32] W. K. M. Brauers and E. K. Zavadskas, "Project management by multimoora as an instrument for transition economies/ projektų vadyba su multimoora kaip priemonė pereinamojo laikotarpio ukiams," *Technological and Economic Development of Economy*, vol. 16, no. 1, pp. 5–24, 2010.
[33] A. Hafezalkotob, A. Hafezalkotob, and M. K. Sayadi, "Extension of MULTIMOORA method with interval numbers: an application in materials selection," *Applied Mathematical Modelling*, vol. 40, no. 2, pp. 1372–1386, 2016.
[34] T. Balezentis, S. Zeng, and A. Balezentis, "Multimoora-IFN: a MCDM method based on intuitionistic fuzzy number for performance management," *Economic Computation & Economic Cybernetics Studies & Research*, vol. 48, no. 4, pp. 85–102, 2014.
[35] M. Lin, C. Huang, and Z. Xu, "MULTIMOORA based MCDM model for site selection of car sharing station under picture fuzzy environment," *Sustainable Cities and Society*, vol. 53, Article ID 101873, 2020.
[36] G. L. Xu, S. P. Wan, X. B. Li, and F. X. Feng, "An integrated method for multiattribute group decision making with probabilistic linguistic term sets," *International Journal of Intelligent Systems*, vol. 36, no. 11, pp. 6871–6912, 2021.
[37] B. Farhadinia, S. Effati, and F. Chiclana, "A family of similarity measures for q-rung orthopair fuzzy sets and their applications to multiple criteria decision making," *International Journal of Intelligent Systems*, vol. 36, no. 4, pp. 1535–1559, 2021.
[38] R. Verma, "Multiple attribute group decision-making based on order-α divergence and entropy measures under q-rung orthopair fuzzy environment," *International Journal of Intelligent Systems*, vol. 35, no. 4, pp. 718–750, 2020.
[39] Z. Ayag and F. Samanlioglu, "A hesitant fuzzy linguistic terms set-based AHP-TOPSIS approach to evaluate ERP software packages," *International Journal of Intelligent Computing and Cybernetics*, vol. 14, no. 1, pp. 54–77, 2021.
[40] P. Liu and P. Wang, "Some q-rung orthopair fuzzy aggregation operators and their applications to multiple-attribute decision making," *International Journal of Intelligent Systems*, vol. 33, no. 2, pp. 259–280, 2018.
[41] P. D. Liu, S. M. Chen, and P. Wang, "The g-rung orthopair fuzzy power maclaurin symmetric mean operators," in *Proceedings of the 2018 10th International Conference on Advanced Computational Intelligence*, Xiamen, China, March 2018.
[42] R. R. Yager, "The power average operator," *IEEE Transactions on Systems, Man, and Cybernetics—Part A: Systems and Humans*, vol. 31, no. 6, pp. 724–731, 2001.
[43] J. Dombi, "A general class of fuzzy operators, the DeMorgan class of fuzzy operators and fuzziness measures induced by fuzzy operators," *Fuzzy Sets and Systems*, vol. 8, no. 2, pp. 149–163, 1982.
[44] C. Jana, G. Muhiuddin, and M. Pal, "Some Dombi aggregation of Q -rung orthopair fuzzy numbers in multiple-attribute decision making," *International Journal of Intelligent Systems*, vol. 34, no. 12, pp. 3220–3240, 2019.
[45] M. Qiyas, S. Abdullah, and M. Naeem, "Spherical uncertain linguistic Hamacher aggregation operators and their application on achieving consistent opinion fusion in group decision making," *International Journal of Intelligent Computing and Cybernetics*, vol. 14, no. 4, pp. 550–579, 2021.
[46] M. Lin, W. Xu, Z. Lin, and R. Chen, "Determine OWA operator weights using kernel density estimation," *Economic Research-Ekonomska Istraživanja*, vol. 33, no. 1, pp. 1441–1464, 2020.
[47] M. W. Lin, X. M. Li, R. Q. Chen, H. Fujita, and J. Lin, "Picture fuzzy interactional partitioned Heronian mean aggregation operators: an application to MADM process," *Artificial Intelligence Review*, 2021.
[48] S. Zeng, Y. Hu, and X. Xie, "Q-rung orthopair fuzzy weighted induced logarithmic distance measures and their application in multiple attribute decision making," *Engineering Applications of Artificial Intelligence*, vol. 100, Article ID 104167, 2021.
[49] P. Liu, Z. Liu, and X. Zhang, "Some intuitionistic uncertain linguistic Heronian mean operators and their application to group decision making," *Applied Mathematics and Computation*, vol. 230, no. 230, pp. 570–586, 2014.
[50] P. Liu, J. Liu, and J. M. Merigó, "Partitioned Heronian means based on linguistic intuitionistic fuzzy numbers for dealing with multi-attribute group decision making," *Applied Soft Computing*, vol. 62, pp. 395–422, 2018.
[51] N. Jan, M. Aslam, K. Ullah, T. Mahmood, and J. Wang, "An approach towards decision making and shortest path problems using the concepts of interval-valued Pythagorean fuzzy information," *International Journal of Intelligent Systems*, vol. 34, no. 10, pp. 2403–2428, 2019.
[52] H. Li, L. Lv, F. Li, L. Wang, and Q. Xia, "A novel approach to emergency risk assessment using FMEA with extended MULTIMOORA method under interval-valued Pythagorean fuzzy environment," *International Journal of Intelligent Computing and Cybernetics*, vol. 13, no. 1, pp. 41–65, 2020.
[53] C. Zhang, Q. Hu, S. Zeng, and W. Su, "IOWLAD-based MCDM model for the site assessment of a household waste processing plant under a Pythagorean fuzzy environment," *Environmental Impact Assessment Review*, vol. 89, Article ID 106579, 2021.
[54] M. Afzaal, M. Usman, and A. Fong, "Tourism mobile app with aspect-based sentiment classification framework for tourist reviews," *IEEE Transactions on Consumer Electronics*, vol. 65, no. 2, pp. 233–242, 2019.
[55] K. Bai, X. Zhu, J. Wang, and R. Zhang, "Power partitioned Heronian mean operators for q -rung orthopair uncertain linguistic sets with their application to multiattribute group decision making," *International Journal of Intelligent Systems*, vol. 35, no. 1, pp. 3–37, 2020.
[56] W. K. M. Brauers and E. K. Zavadskas, "Multimoora optimization used to decide on a bank loan to buy property," *Technological and Economic Development of Economy*, vol. 17, no. 1, pp. 174–188, 2011.
[57] T. Mahmood, K. Ullah, Q. Khan, and N. Jan, "An approach toward decision-making and medical diagnosis problems using the concept of spherical fuzzy sets," *Neural Computing & Applications*, vol. 31, no. 11, pp. 7041–7053, 2019.
[58] L. Zedam, N. Jan, E. Rak, T. Mahmood, and K. Ullah, "An approach towards decision-making and shortest path problems based on T-spherical fuzzy information," *International Journal of Fuzzy Systems*, vol. 22, no. 5, pp. 1521–1534, 2020.
[59] K. Ullah, H. Garg, T. Mahmood, N. Jan, and Z. Ali, "Correlation coefficients for T-spherical fuzzy sets and their applications in clustering and multi-attribute decision making," *Soft Computing*, vol. 24, no. 3, pp. 1647–1659, 2020.

[60] Z. Ayag, "A comparison study of fuzzy-based multiple-criteria decision-making methods to evaluating green concept alternatives in a new product development environment," *International Journal of Intelligent Computing and Cybernetics*, vol. 14, no. 3, pp. 412–438, 2021.

[61] L. Wang and H. Garg, "Algorithm for multiple attribute decision-making with interactive Archimedean norm operations under Pythagorean fuzzy uncertainty," *International Journal of Computational Intelligence Systems*, vol. 14, no. 1, pp. 503–527, 2021.

Hindawi
Mathematical Problems in Engineering
Volume 2022, Article ID 6196251, 11 pages
https://doi.org/10.1155/2022/6196251

Research Article

Generalized Estimation for Two-Parameter Life Time Distributions Based on Fuzzy Life Times

Syed Habib Shah,[1] Muhammad Shafiq ,[1] and Qamruz Zaman[2]

[1]*Institute of Numerical Sciences, Kohat University of Science & Technology, Kohat, KP, Pakistan*
[2]*Department of Statistics, University of Peshawar, Peshawar, KP, Pakistan*

Correspondence should be addressed to Muhammad Shafiq; shafiq@kust.edu.pk

Received 2 November 2021; Revised 9 January 2022; Accepted 22 February 2022; Published 26 May 2022

Academic Editor: Mingwei Lin

Ongoing developments of the measurement sciences say that measurements based on continuous phenomena are no more precise observations but more or less fuzzy. Therefore, it is necessary to utilize this imprecision of observations to obtain such estimators, which are based on all the available information that is given in the form of randomness and fuzziness. Objective of this research was to get such parameter estimation procedure that utilizes all the available information for some well-known two-parameter life time distributions. Therefore, the estimators need to be generalized in such a way to cover both uncertainties. For this purpose, based on δ-cuts of the life time observations, the generalized estimators are developed in such manner to cover stochastic variation in addition to fuzziness. The proposed generalized estimators are much preferred over classical estimators for life time analysis as these are based on all the available information present in the form of fuzziness of single observations and random variation among the observations to make suitable inferences.

1. Introduction

Statistics is the science to make inference about the population from the obtained data. The obtained data are usually presented in the form of numbers, vectors, or functions, generally containing precise measurements of some phenomena. Countless techniques (stochastic models) are available to model or to draw inference from these obtained measurements.

Survival analysis or reliability analysis can generally be defined as the collection of techniques for analyzing so-called life time data.

In broad sense, one can say life time is "the time to the occurrence of a specified event."

Life time is also called survival time, event time, or failure time and is usually measured in hours, days, weeks, months, or years.

The prominence of survival analysis is to predict the probability of response, average survival time, identifying the important investigative factors associated to the life time of units, and to compare the survival distributions. Models used for survival times are usually termed as "time to event models" [1].

The analysis techniques of life time data can be traced back centuries, but the rapid development started about few decades ago, especially World War II stimulated interest in the reliability of military equipment [2].

Nowadays, life time analysis is used in almost every of field of life like biomedical sciences, industrial reliability, social sciences, and business. In the time to event modeling, the event of interest may be failure, death, recovery time, or change of address, in engineering, medical and social sciences, etc. Therefore, there are a number of reasons to say that specialized methods are required to model life time data in the best possible way [1].

Exponential, Weibull, log-logistic, and Birnbaum–Saunders distributions are considered in most applied distributions in life time analyses.

Exponential distribution has a vital role in life time analysis analogous to normal distribution in other fields. It is purely based on random failure pattern because of its "memoryless property." A two-parameter function is a more generalized form with probability density function of exponential distribution:

$$f\left(\frac{y}{\lambda,\theta}\right)=\begin{cases}\lambda e^{-\lambda(y-\theta)}, \; y\geq\theta,\\ 1, \qquad\quad y<\theta.\end{cases} \tag{1}$$

For n precise life time observations $(y_1, y_2, \ldots, y_n)$, their classical parameter estimates, i.e., maximum likelihood estimates, are given as

$$\widehat{\theta}=\min\left(y_1, y_2, \ldots, y_n\right), \tag{2}$$

and

$$\widehat{\lambda}=\frac{n}{\sum_{i=1}^{n}\left(y_i-\widehat{\theta}\right)}. \tag{3}$$

For details, see [1].

For the nonconstant hazard rate, Weibull distribution is among the top most distributions for the life time analysis. Its density is defined by

$$f(y|\tau,\eta)=\frac{\eta}{\tau}\left(\frac{y}{\tau}\right)^{\eta-1}\exp\left\{-\left(\frac{y}{\tau}\right)^{\eta}\right\} \quad \forall y>0, \tau>0, \eta>0, \tag{4}$$

τ: scale parameter (also called characteristic life time), η: shape parameter.

According to [3], let CV denote the coefficient of variation for the data defined as the ratio of standard deviation and mean, i.e., $\sigma/\overline{y}$.

For the parameter estimation of Weibull distribution, the moment method estimators are defined as

$$CV=\frac{\sqrt{\Gamma(1+2/\widehat{\eta})-\Gamma^2(1+1/\widehat{\eta})}}{\Gamma(1+1/\widehat{\eta})}. \tag{5}$$

Solve the above equation for the value of $\widehat{\eta}$ to get an estimate.

$$\widehat{\tau}=\left(\frac{\overline{y}}{\Gamma(1+1/\widehat{\eta})}\right)^{\frac{1}{\widehat{\eta}}}. \tag{6}$$

The log-logistic distribution is the extension of logistic distribution, for which it has been observed that it can be decreasing, right-skewed, or unimodal. Because of its flexibility in shapes, it is very useful to fit data from many different fields, including engineering, economics, hydrology, and survival analysis.

Its pdf is defined as

$$f(y|\alpha,\beta)=\frac{(\beta\alpha)(y\alpha)^{\beta-1}}{\left[1+(y\alpha)^{\beta}\right]^2}, \quad y>0. \tag{7}$$

For the parameter estimation, maximum likelihood estimators are obtained through the following equations:

$$\begin{aligned}\frac{n}{\beta}-n\log(\alpha)+\sum_{i=1}^{n}\log(y_i)-2\sum_{i=1}^{n}\left(\frac{y_i}{\alpha}\right)^{\beta}\log\left(\frac{y_i}{\alpha}\right)\left[1+\left(\frac{y_i}{\alpha}\right)^{\beta}\right]^{-1}&=0,\\ -\frac{n\beta}{\alpha}+\frac{2\beta}{\alpha}\sum_{i=1}^{n}\left(\frac{y_i}{\alpha}\right)^{\beta}\left[1+\left(\frac{y_i}{\alpha}\right)^{\beta}\right]^{-1}&=0.\end{aligned} \tag{8}$$

For details, see [4].

Birnbaum–Saunders life time distribution was first proposed in [5], for fatigue failures caused under cyclic loading, having the density function given below:

$$f(y|\mu,\gamma)=\frac{1}{2\sqrt{2\pi}\mu\gamma}\left[\left(\frac{\gamma}{y}\right)^{\frac{1}{2}}+\left(\frac{\gamma}{y}\right)^{\frac{3}{2}}\right]\exp\left[-\frac{1}{2\mu^2}\left(\frac{y}{\gamma}+\frac{\gamma}{y}-2\right)\right], \quad y,\mu,\gamma>0. \tag{9}$$

For n precise life time observations $(y_1, y_2, \ldots, y_n)$, the corresponding modified moment estimators are obtained as follows.

Let A and H be arithmetic mean and harmonic mean of the life times, respectively:

$$A = \frac{\sum_{i=1}^{n} y_i}{n} \text{ and } H = \frac{n}{\sum_{i=1}^{n} 1/y_i}. \tag{10}$$

Then,

$$\widehat{\mu} = \left\{2\left[\left(\frac{A}{H}\right)^{12} - 1\right]\right\}^{12}, \tag{11}$$

$$\widehat{\gamma} = (A \cdot H)^{12}. \tag{12}$$

For the proof, see [6].

For a life time random variable, Gamma distribution is defined by the density

$$f(y|\phi, \nu) = \frac{1}{\Gamma\nu\phi} y^{\nu-1} e^{\frac{-y}{\phi}} \quad \text{with } \phi > 0,\ \nu > 0. \tag{13}$$

Let $\overline{y}$ and s^2 be mean and variance of the data $y_1, y_2, \ldots, y_n$, respectively; then, the moment estimators of the parameters are defined as

$$\widehat{\nu} = \frac{\overline{y}^2}{s^2}, \tag{14}$$

$$\widehat{\phi} = \frac{s^2}{\overline{y}}. \tag{15}$$

For the proof, see [7].

The emergence of technological advancement augments the increase in life time of units. Therefore, the researchers with only few observations draw inference about the aggregate of units. Hence, it is pertinent to utilize all the available information in the best possible manner.

According to [8], in the modern science of measurements, it is not possible to get exact measurement of a continuous real variable, and stochastic models are used to model variation among the precise observations.

In addition to that, in practical situations, especially dealing with continuous variables, the measurements have two kinds of uncertainties, the first is variation among the observations and second is imprecision of single observations, called fuzziness [9].

Realizing the importance of fuzziness in the life time observations, some work has been done like ([10–18]); [19, 20]. Yet, most of the times, the information available in the form of fuzziness is ignored in the publications, which may cause misleading results.

Therefore, the very up-to-date fuzzy number approaches are more realistic and suitable for the inferences of life time observations [21].

In this research work, some the generalized estimators for well-known distributions are presented to accommodate fuzziness along with random variation.

2. Preliminary Concepts of Fuzzy Set Theory

2.1. Fuzzy Number. Let y^* denote a fuzzy number and is a special subsets of $\mathbb{R}$; it is determined by a real-valued function, so-called characterizing function (CF) $\chi(\cdot)$, with conditions:

(1) $0 \le \chi \le 1$

(2) Support of $\chi(\cdot)$ is bounded: $\text{supp}[\chi(\cdot)] := [y \in \mathbb{R}: \chi(y) > 0] \subseteq [\mathbb{R}_a, \mathbb{R}_b]$ with $-\infty < \mathbb{R}_a < \mathbb{R}_b < \infty$.

(3) The so-called δ-cut, i.e., $C_\delta(y^*) := \{y \in \mathbb{R}: \chi(y) \ge \delta\}\quad \forall \delta \in (0, 1]$, is a finite union of nonempty compact intervals, i.e., $C_\delta(y^*) = \cup_{j=1}^{J_\delta}[\underline{y}_{j,\delta}, \overline{y}_{j,\delta}] \ne \varnothing$.

In case of fuzzy number for which all the δ-cuts are closed bounded intervals, is called a fuzzy interval.

2.2. Lemma. According to [9], for a set $A \subseteq \mathbb{R}$, where $1_A(\cdot)$ is denoting the indicator function for set A, then to obtain the characterizing function for a generating fuzzy number, the given lemma holds:

$$\chi(y) = \max\left\{\delta \cdot 1_{C_\delta(y^*)}(y): \delta \in [0, 1]\right\} \quad \forall y \in \mathbb{R}. \tag{16}$$

2.3. Nested Interval. Let $I_\delta; \delta \in (0, 1]$ be a family of intervals, called nested if $I_{\delta_1} \subseteq I_{\delta_2}$ for all $\delta_1 > \delta_2$.

2.4. Remark. If $(A_\delta; \delta \in (0, 1])$ is denoting a nested family of finite unions of compact intervals, it is not necessary that all nested families are the δ-cuts of a fuzzy number. Then, the characterizing function of the generated fuzzy number is obtained by the given lemma.

2.5. Construction Lemma. According to [22], let $A_\delta = \cup_{j=1}^{J_\delta}[\underline{y}_{\delta,j}, \overline{y}_{\delta,j}]\quad \forall \delta \in (0, 1]$ be a nested family; then, the characterizing function (CF) of the generated fuzzy number is obtained by $\chi(y) = \sup\left\{\delta \cdot 1_{A_\delta}(y):\ \ \delta \in (0, 1]\right\}$ $\forall y \in \mathbb{R}$.

2.6. Extension Principle. Consider an arbitrary function $\mathscr{H}$: $\aleph \longrightarrow \mathfrak{R}$, where $\aleph$ and $\mathfrak{R}$ are two spaces.

Let m^* be a fuzzy element of $\aleph$, with corresponding membership function ψ: $\aleph \longrightarrow [0, 1]$; then, the fuzzy value $y^* = \mathscr{H}(m^*)$ is defined to be the corresponding fuzzy element in $\mathfrak{R}$ for which the membership function $\Psi(\cdot)$ is defined by

$$\Psi(y) := \begin{cases} \sup\{\psi(m)\colon m \in \aleph, \mathscr{H}(\omega) = y\} \text{ if } \exists m\colon \mathscr{H}(m) = y \\ 0 \text{ if } \nexists m\colon \mathscr{H}(m) = y \end{cases} \quad \forall y \in \Re. \tag{17}$$

For details, see [23].

2.7. Minimum and Maximum of Fuzzy Numbers. If there are n fuzzy intervals, i.e., $y_1^*, y_2^*, \ldots, y_n^*$ with corresponding characterizing functions $\chi_1(\cdot), \chi_2(\cdot), \ldots, \chi_n(\cdot)$, respectively, then its δ-cuts are denoted as $C_\delta(y_i^*) = [\underline{y}_{i,\delta}, \overline{y}_{i,\delta}] \forall \delta \in (0,1]$ and $i = 1(1)n$. Then, the minimum $y_{\min^*}$ of the fuzzy numbers is fuzzy interval, with δ-cuts $C_\delta(y_{\min^*})$. These are defined by

$$C_\delta(y_{\min^*}) := \left[\min\left\{\underline{y}_{i,\delta}\right\}, \min\left\{\overline{y}_{i,\delta}\right\}\right] \quad \forall \delta \in (0,1]. \tag{18}$$

Furthermore, the maximum $y_{\max^*}$ of the fuzzy numbers is fuzzy interval, with δ-cuts $C_\delta(y_{\max^*})$ defined by

$$C_\delta(y_{\max^*}) := \left[\max\left\{\underline{y}_{i,\delta}\right\}, \max\left\{\overline{y}_{i,\delta}\right\}\right] \quad \forall \delta \in (0,1]. \tag{19}$$

Figure 1 shows CF of minimum and maximum fuzzy observations from the above sample of fuzzy observations mentioned in Figure 2.

3. Generalized Estimation for Fuzzy Data

In Figure 3, the frame diagram explains the steps for obtaining the generalized estimators for the two-parameter life time distributions given below.

3.1. Exponential Distribution. Let $(y_1^*, y_2^*, \ldots, y_n^*)1/2$ represent fuzzy life time intervals having δ-cuts:

$$C_\delta(y_i^*) = \left[\underline{y}_{i,\delta}, \overline{y}_{i,\delta}\right], \quad i = 1,2,\ldots,n, \forall \delta \in (0,1]. \tag{20}$$

where $\underline{y}_{i,\delta} = \inf\{y \in \mathbb{R}\colon \chi(y) \geq \delta\}$ and $\overline{y}_{i,\delta} = \sup\{y \in \mathbb{R}\colon \chi(y) \geq \delta\}$ are lower and upper ends of the corresponding δ-cuts.

Based on fuzzy life times, the fuzzy (generalized) estimators of the two-parameter exponential distribution are denoted by $\widehat{\theta}^*$ and $\widehat{\lambda}^*$.

Based on lower and upper ends of the δ-cuts of fuzzy life times, the estimator presented in (2) can be generalized in the following way:

$$\widehat{\theta}^* = \min(y_1^*, y_2^*, \ldots, y_n^*). \tag{21}$$

For the fuzzy parameter estimator $\widehat{\theta}^*$, $\underline{\theta}_\delta$ and $\overline{\theta}_\delta$ are denoting lower and upper ends of the corresponding generating family of intervals, and these are obtained in the following way:

$$\underline{\theta}_\delta = \min\left[\underline{y}_{i,\delta}, i = 1(1)n\right], \quad \forall \delta \in (0,1], \tag{22}$$

and

$$\overline{\theta}_\delta = \min\left[\overline{y}_{i,\delta}, i = 1(1)n\right], \quad \forall \delta \in (0,1]. \tag{23}$$

Let $(A_\delta(\widehat{\theta}^*) = [\underline{\theta}_\delta, \overline{\theta}_\delta] \forall \delta \in (0,1])$ be the generating family of intervals; using construction lemma, the CF of the fuzzy estimate $\widehat{\theta}^*$ is obtained.

Example 1. Let us consider 12 fuzzy life time observations for two-parameter exponential distribution, i.e., $(y_1^*, y_2^*, \ldots, y_{12}^*) = ([1,2,3,4], [4,5,6,7], [8,9,10,11],$

$$\begin{gathered}[11,12,13,14], [12,13,14,15], \\ [14,15,16,17], [17,18,19,20], [19,20,21,22], [21,22,23,24].\end{gathered} \tag{24}$$

$[23,24,25,26], [24,25,26,27], [26,27,28,29]$ whose characterizing functions are given in Figure 4.

Based on the given fuzzy life time observations, the CF of the fuzzy parameter estimate obtained through (22) and (23) is depicted in Figure 5.

This parameter estimate is more suitable for realistic life time observations, as it covers both types of uncertainties.

In the same way, the fuzzy (generalized) estimator for the parameter λ is denoted by $\widehat{\lambda}^*$ having lower and upper ends $\underline{\lambda}_\delta$ and $\overline{\lambda}_\delta$ of the δ-cuts, respectively, where

$$\underline{\lambda}_\delta = \frac{n}{\sum_{i=1}^n \left(\overline{y}_{i,\delta} - \underline{\theta}_\delta\right)} \quad \forall \delta \in (0,1], \tag{25}$$

and

$$\overline{\lambda}_\delta = \frac{n}{\sum_{i=1}^n \left(\underline{y}_{i,\delta} - \overline{\theta}_\delta\right)} \quad \forall \delta \in (0,1]. \tag{26}$$

Let $(A_\delta(\widehat{\lambda}^*) = [\underline{\lambda}_\delta, \overline{\lambda}_\delta] \forall \delta \in (0,1])$ be the desired generating family of intervals; using construction lemma, the CF of the generated fuzzy estimate $\widehat{\lambda}^*$ is obtained.

In Figure 6, CF of the fuzzy estimate is obtained through (25) and (26) based on all the available information which is given in the form of fuzziness and stochastic variation; these make it more suitable in real-life applications.

3.2. Weibull Distribution. Based on (5), the fuzzy (generalized) estimates of the Weibull shape parameter can be obtained in the following way:

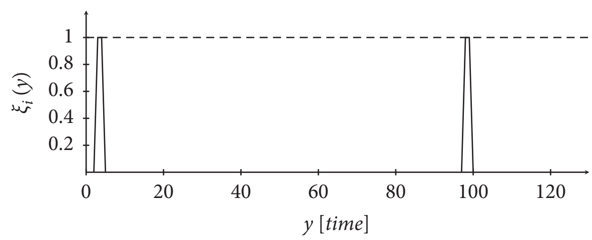

Figure 1: Minimum and maximum fuzzy observations from above sample.

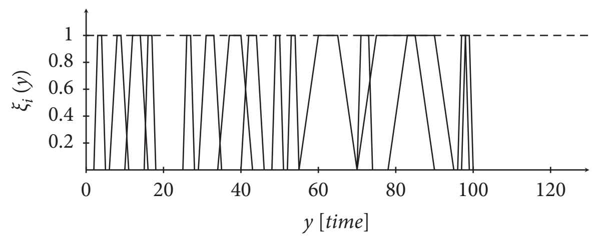

Figure 2: Sample of fuzzy observations.

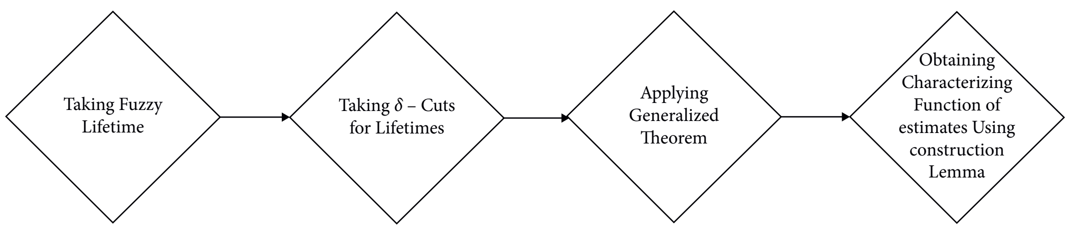

Figure 3: A frame diagram for the analysis.

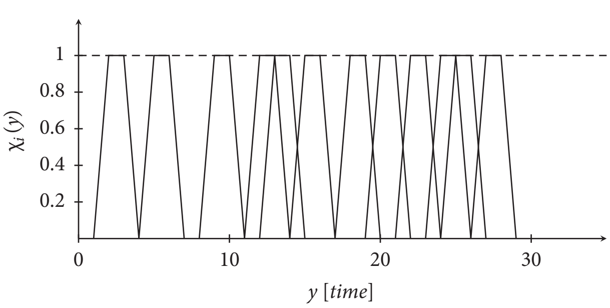

Figure 4: CF of a fuzzy sample.

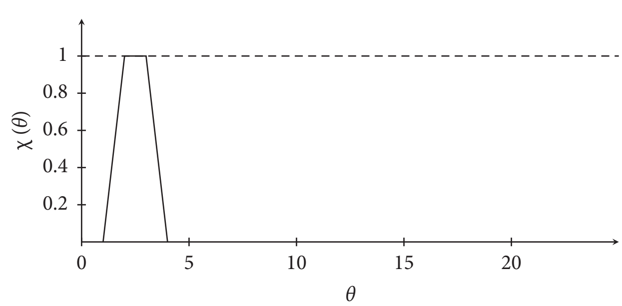

Figure 5: CF of the fuzzy estimator $\hat{\theta}^*$.

$$\underline{\eta}_\delta := \min_{\underline{y} \in \times_{i=1}^n C_\delta(y_i^*)} \left\{ CV(\underline{y}) = \frac{\sqrt{\Gamma(1 + 2/\hat{\eta}) - \Gamma^2(1 + 1/\hat{\eta})}}{\Gamma(1 + 1/\hat{\eta})} \right\} \quad \forall \delta \in (0, 1], \tag{27}$$

and

$$\overline{\eta}_\delta := \max_{\underline{y} \in \times_{i=1}^n C_\delta(y_i^*)} \left\{ CV(\underline{y}) = \frac{\sqrt{\Gamma(1 + 2/\hat{\eta}) - \Gamma^2(1 + 1/\hat{\eta})}}{\Gamma(1 + 1/\hat{\eta})} \right\} \quad \forall \delta \in (0, 1]. \tag{28}$$

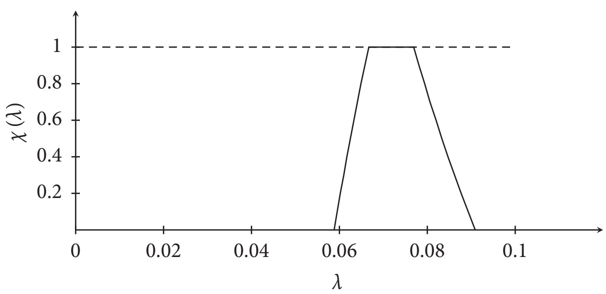

Figure 6: CF of the fuzzy estimator $\widehat{\lambda}^*$.

Similarly, based on (6), fuzzy (generalized) estimates of the Weibull scale parameter can be obtained in the following way:

$$\underline{\tau}_\delta = \left(\frac{\overline{\underline{y}}_\delta}{\Gamma\left(1 + 1/\underline{\eta}_\delta\right)}\right)^{\frac{1}{\overline{\overline{\eta}}_\delta}}, \tag{29}$$

and

$$\overline{\tau}_\delta = \left(\frac{\overline{\overline{y}}_\delta}{\Gamma\left(1 + 1/\overline{\eta}_\delta\right)}\right)^{\frac{1}{\underline{\eta}_\delta}}. \tag{30}$$

Example 2. Consider fuzzy life times $(y_1^*, y_2^*, \ldots, y_8^*) = [0,1,2,3], [1,2,3,4], [3,4,5,6], [5,6,7,8], [7,8,9,10], [9, 9.5, 10.5, 11], [10, 10.5, 11.5, 12], [11, 11.5, 12.5, 13]$ for the Weibull distribution with characterizing functions in Figure 7.

Using (27) and (28), let $(A_\delta(\widehat{\eta}^*) = [\underline{\eta}_\delta, \overline{\eta}_\delta] \quad \forall \delta \in (0,1])$ be the desired generating family of intervals; using the construction lemma, CF of the fuzzy estimate $\widehat{\eta}^*$ is obtained as shown in Figure 8.

Let $(A_\delta(\widehat{\tau}^*) = [\underline{\tau}_\delta, \overline{\tau}_\delta] \quad \forall \delta \in (0,1])$ be the desired generating family of intervals through which the CF of the fuzzy estimate $\widehat{\tau}^*$ mentioned in Figure 9 is obtained by using the construction lemma.

The above CF of the fuzzy estimate obtained through (29) and (30) is based on all the available information which is given in the form of fuzziness and stochastic variation; these kinds of additional information make it more suitable in real-life applications.

3.3. Log-Logistic Distribution. For the log-logistic distribution, the corresponding fuzzy estimators are denoted by $\widehat{\alpha}^*$ and $\widehat{\beta}^*$. Denoting $(\underline{y} = y_1, y_2, \ldots, y_n)$, the corresponding lower and upper ends of the generating family can be obtained through the following equations:

$$\underline{\alpha}_\delta := \min_{\underline{y} \in \times_{i=1}^n C_\delta(y_i^*)} \left\{ \begin{array}{c} -\dfrac{n\beta}{\alpha} + \dfrac{2\beta}{\alpha} \displaystyle\sum_{i=1}^n \left(\frac{y_i}{\alpha}\right)^\beta \left[1 + \left(\frac{y_i}{\alpha}\right)^\beta\right]^{-1} = 0, \\ \dfrac{n}{\beta} - n \log(\alpha) + \displaystyle\sum_{i=1}^n \log(y_i) \\ -2 \displaystyle\sum_{i=1}^n \left(\frac{y_i}{\alpha}\right)^\beta \log\left(\frac{y_i}{\alpha}\right) \left[1 + \left(\frac{y_i}{\alpha}\right)^\beta\right]^{-1} = 0 \end{array} \right\} \quad \forall \delta \in (0,1], \tag{31}$$

and

$$\overline{\alpha}_\delta := \max_{\underline{y} \in \times_{i=1}^n C_\delta(y_i^*)} \left\{ \begin{array}{c} -\dfrac{n\beta}{\alpha} + \dfrac{2\beta}{\alpha} \displaystyle\sum_{i=1}^n \left(\frac{y_i}{\alpha}\right)^\beta \left[1 + \left(\frac{y_i}{\alpha}\right)^\beta\right]^{-1} = 0, \\ \dfrac{n}{\beta} - n \log(\alpha) + \displaystyle\sum_{i=1}^n \log(y_i) \\ -2 \displaystyle\sum_{i=1}^n \left(\frac{y_i}{\alpha}\right)^\beta \log\left(\frac{y_i}{\alpha}\right) \left[1 + \left(\frac{y_i}{\alpha}\right)^\beta\right]^{-1} = 0 \end{array} \right\} \quad \forall \delta \in (0,1]. \tag{32}$$

Also,

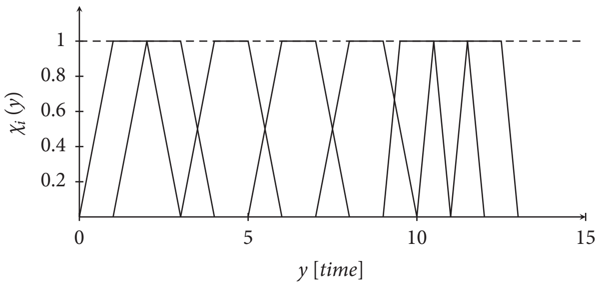

Figure 7: CF of the fuzzy life times.

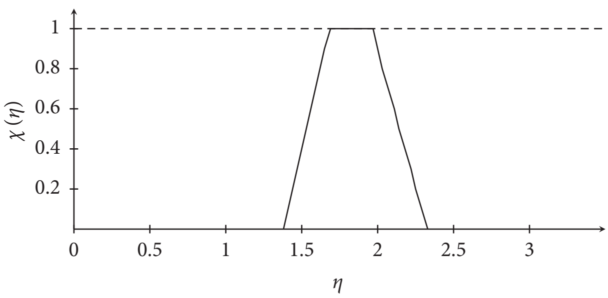

Figure 8: CF of the fuzzy estimator $\widehat{\eta}^*$.

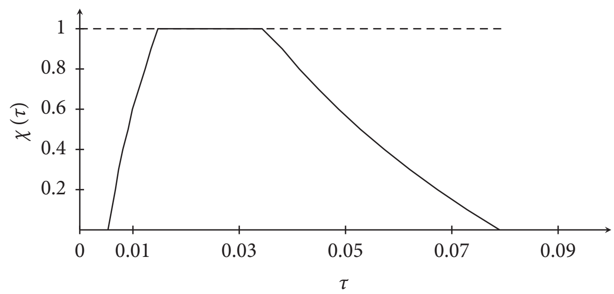

Figure 9: CF of the fuzzy estimator $\widehat{\tau}^*$.

$$\underline{\beta}_\delta := \min_{\underline{y} \in \times_{i=1}^n C_\delta(y_i^*)} \left\{ \begin{array}{c} -\dfrac{n\beta}{\alpha} + \dfrac{2\beta}{\alpha} \displaystyle\sum_{i=1}^n \left(\frac{y_i}{\alpha}\right)^\beta \left[1 + \left(\frac{y_i}{\alpha}\right)^\beta\right]^{-1} = 0, \\ \\ \dfrac{n}{\beta} - n\log(\alpha) + \displaystyle\sum_{i=1}^n \log(y_i) \\ \\ -2\displaystyle\sum_{i=1}^n \left(\frac{y_i}{\alpha}\right)^\beta \log\left(\frac{y_i}{\alpha}\right) \left[1 + \left(\frac{y_i}{\alpha}\right)^\beta\right]^{-1} = 0 \end{array} \right\} \quad \forall \delta \in (0,1], \tag{33}$$

and

$$\overline{\beta}_\delta := \max_{\underline{y} \in \times_{i=1}^n C_\delta(y_i^*)} \left\{ \begin{array}{c} -\dfrac{n\beta}{\alpha} + \dfrac{2\beta}{\alpha} \displaystyle\sum_{i=1}^n \left(\frac{y_i}{\alpha}\right)^\beta \left[1 + \left(\frac{y_i}{\alpha}\right)^\beta\right]^{-1} = 0, \\ \\ \dfrac{n}{\beta} - n\log(\alpha) + \displaystyle\sum_{i=1}^n \log(y_i) \\ \\ -2\displaystyle\sum_{i=1}^n \left(\frac{y_i}{\alpha}\right)^\beta \log\left(\frac{y_i}{\alpha}\right) \left[1 + \left(\frac{y_i}{\alpha}\right)^\beta\right]^{-1} = 0 \end{array} \right\} \quad \forall \delta \in (0,1]. \tag{34}$$

Let $(A_\delta(\widehat{\alpha}^*) = [\underline{\alpha}_\delta, \overline{\alpha}_\delta] \quad \forall \delta \in (0,1])$ and $(A_\delta(\widehat{\beta}^*) = [\underline{\beta}_\delta, \overline{\beta}_\delta] \quad \forall \delta \in (0,1])$ be the desired generating families of intervals of the fuzzy parameter estimators through which the CF of the fuzzy estimates $\widehat{\alpha}^*$ and $\widehat{\beta}^*$ is obtained using the construction lemma.

Example 3. Consider fuzzy life times $(y_1^*, y_2^*, \ldots, y_6^*) = [1,2,3,4], [4,5,6,7], [6,7,8,9], [8,9,10,11], [13,14,15,16], [17,18,19,20]$ for the log-logistic distribution with characterizing functions in Figure 10.

From the above fuzzy life time observations using (31) and (32), the CF of the fuzzy parameter estimate is depicted in Figure 11.

This estimate is based on both uncertainties, i.e., fuzziness and random variation, which make it more representative for the corresponding parameter.

From the above fuzzy life time observations shown in Figure 9, using (33) and (34), the CF of the fuzzy parameter estimate $\widehat{\beta}^*$ is depicted in Figure 12.

The above CF is the fuzzy estimate of the parameter β, which incorporates all the available information in the inference. The above CF for the fuzzy parameter estimates is based on fuzzy life time observations which holds both uncertainties, i.e., stochastic variation and fuzziness of the single observations, which make these more suitable in the real-life applications.

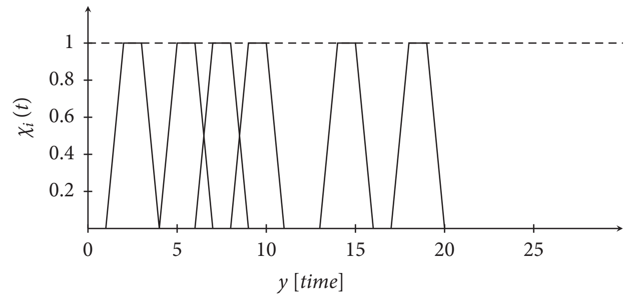

Figure 10: CF of a fuzzy sample.

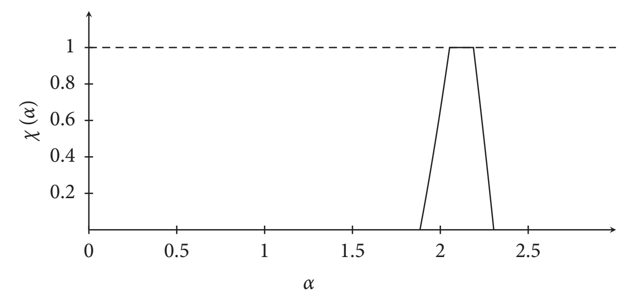

Figure 11: CF of the fuzzy estimator $\widehat{\alpha}^*$.

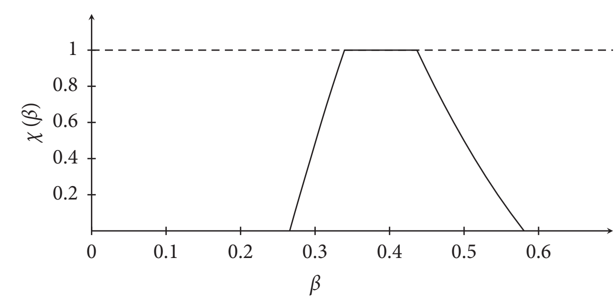

Figure 12: CF of the fuzzy estimator $\widehat{\beta}^*$.

3.4. Birnbaum–Saunders Distribution

3.4. Birnbaum–Saunders Distribution. For fuzzy life times $(y_1^*, y_2^*, \ldots, y_n^*)$, the fuzzy parameter estimators of the Birnbaum–Saunders distribution are denoted by $\widehat{\mu}^*$ and $\widehat{\gamma}^*$, having δ-cuts:

$$C_\delta(\widehat{\mu}^*) = [\underline{\mu}_\delta, \overline{\mu}_\delta] \forall \delta \in (0,1], \tag{35}$$

and

$$C_\delta(\widehat{\gamma}^*) = [\underline{\gamma}_\delta, \overline{\gamma}_\delta] \quad \forall \delta \in (0,1]. \tag{36}$$

Let A^* and H^* be fuzzy arithmetic mean and fuzzy harmonic mean, respectively, and their δ-cuts are denoted as

$$C_\delta(\widehat{A}^*) = [\underline{A}_\delta, \overline{A}_\delta] \quad \forall \delta \in (0,1], \tag{37}$$

and

$$C_\delta(\widehat{H}^*) = [\underline{H}_\delta, \overline{H}_\delta], \quad \forall \delta \in (0,1]. \tag{38}$$

Using (10), the corresponding lower and upper ends of the δ-cuts of $\widehat{A}^*$ are obtained in the following way:

$$\underline{A}_\delta = \frac{\sum_{i=1}^n \underline{y}_{i,\delta}}{n} \text{ and } \overline{A}_\delta = \frac{\sum_{i=1}^n \overline{y}_{i,\delta}}{n}, \quad \forall \delta \in (0,1]. \tag{39}$$

Example 4. Based on fuzzy life times presented in Figure 1, characterizing functions of the fuzzy estimates of the Birnbaum–Saunders distribution are given in Figures 13 and 14.

Figure 15 shows the CF of the fuzzy estimate of the arithmetic mean based on fuzzy life times. Similarly, using (10), the corresponding lower and upper ends of the δ-cuts of $\widehat{H}^*$ are obtained in the following way:

$$\underline{H}_\delta = \frac{n}{\sum_{i=1}^n 1/\underline{y}_{i,\delta}} \text{ and } \overline{H}_\delta = \frac{n}{\sum_{i=1}^n 1/\overline{y}_{i,\delta}}, \quad \forall \delta \in (0,1]. \tag{40}$$

Figure 16 shows the CF of the fuzzy estimate of the harmonic mean based on fuzzy life times. Using (11), lower and upper ends of the corresponding fuzzy parameter estimators $\widehat{\mu}^*$ are obtained in the following way:

$$\underline{\mu}_\delta = \left\{ 2\left[\left(\frac{\underline{A}_\delta}{\overline{H}_\delta}\right)^{12} - 1\right]\right\}^{12}, \quad \forall \delta \in (0,1], \tag{41}$$

and

$$\overline{\mu}_\delta = \left\{ 2\left[\left(\frac{\overline{A}_\delta}{\underline{H}_\delta}\right)^{12} - 1\right]\right\}^{12}, \quad \forall \delta \in (0,1]. \tag{42}$$

Denoting by $(A_\delta(\widehat{\mu}^*) = [\underline{\mu}_\delta, \overline{\mu}_\delta] \quad \forall \delta \in (0,1])$ the desired generating family of intervals of the fuzzy parameter estimator and using the construction lemma, the CF of the fuzzy estimator $\widehat{\mu}^*$ is obtained.

In Figure 13, the CF of the fuzzy estimate based on fuzzy life times is depicted. Using (12), lower and upper ends of the corresponding fuzzy parameter estimator $\widehat{\gamma}^*$ are obtained in the following way:

$$\underline{\gamma}_\delta = \left(\underline{A}_\delta \cdot \underline{H}_\delta\right)^{12} \text{ and } \overline{\gamma}_\delta = \left(\overline{A}_\delta \cdot \overline{H}_\delta\right)^{12}, \quad \forall\delta \in (0,1]. \tag{43}$$

Denoting by $(A_\delta(\widehat{\gamma}^*) = [\underline{\gamma}_\delta, \overline{\gamma}_\delta] \quad \forall\delta \in (0,1])$ the desired generating family of intervals of the fuzzy parameter estimator and using the construction lemma, the CF of the fuzzy estimator $\widehat{\mu}^*$ is obtained.

Figure 14 shows the CF of the fuzzy estimator of the parameter γ, which utilized all the available information in the form of fuzziness and random variation.

The fuzzy estimation of the parameter indicates that the value of γ is about 9.7 to 15.2 in the sence of the function in Figure 13. It means that it is completely possible that γ is 9.7 or 15.2. In addition, it is not possible that γ is less than 11.7 or greater than 14.11, with possibility degree of 0.8.

3.5. Gamma Distribution. Let $(y_1^*, y_2^*, \ldots, y_n^*)$ represent fuzzy life time intervals having δ-cuts:

$$C_\delta\left(y_i^*\right) = \left[\underline{y}_{i,\delta}, \overline{y}_{i,\delta}\right], \quad i = 1(1)n, \ \forall\delta \in (0,1]. \tag{44}$$

Then, the corresponding lower and upper ends of the generating family of the mean can be obtained through the following equations:

$$\underline{\overline{y}}_\delta = \frac{\sum_{i=1}^n \underline{y}_{i,\delta}}{n} \text{ and } \overline{\overline{y}}_\delta = \frac{\sum_{i=1}^n \overline{y}_{i,\delta}}{n}, \quad \forall\delta \in (0,1]. \tag{45}$$

Denoting $(\underline{y} = y_1, y_2, \ldots, y_n)$, then the corresponding lower and upper ends of the generating family of the variance can be obtained through the following equations:

$$\underline{s}_\delta^2 := \min_{\underline{y} \in \times_{i=1}^n C_\delta\left(y_i^*\right)} \left\{s^2\right\} \quad \forall\delta \in (0,1], \tag{46}$$

and

$$\overline{s}_\delta^2 := \max_{\underline{y} \in \times_{i=1}^n C_\delta\left(y_i^*\right)} \left\{s^2\right\} \quad \forall\delta \in (0,1]. \tag{47}$$

The fuzzy parameter estimators of the gamma distribution are denoted by $\widehat{\nu}^*$ and $\widehat{\phi}^*$, having δ-cuts:

$$C_\delta\left(\widehat{\nu}^*\right) = \left[\underline{\nu}_\delta, \overline{\nu}_\delta\right], \quad \forall\delta \in (0,1], \tag{48}$$

and

$$C_\delta\left(\widehat{\phi}^*\right) = \left[\underline{\phi}_\delta, \overline{\phi}_\delta\right], \quad \forall\delta \in (0,1]. \tag{49}$$

Using lower and upper ends of the generating family of the fuzzy estimates of mean and variance and (14), lower and upper ends of the corresponding fuzzy parameter estimators $\widehat{\nu}^*$ are obtained in the following way:

$$\underline{\nu}_\delta = \frac{\underline{\overline{y}}_\delta^{\,2}}{\overline{s}_\delta^2} \text{ and } \overline{\nu}_\delta = \frac{\overline{\overline{y}}_\delta^{\,2}}{\underline{s}_\delta^2}, \quad \forall\delta \in (0,1]. \tag{50}$$

In the same way, using lower and upper ends of the generating family of the fuzzy estimates of mean and variance and (15), lower and upper ends of the corresponding fuzzy parameter estimators $\widehat{\phi}^*$ are obtained in the following way:

$$\underline{\phi}_\delta = \frac{\underline{s}_\delta^2}{\overline{\overline{y}}_\delta} \text{ and } \overline{\phi}_\delta = \frac{\overline{s}_\delta^2}{\underline{\overline{y}}_\delta}, \quad \forall\delta \in (0,1]. \tag{51}$$

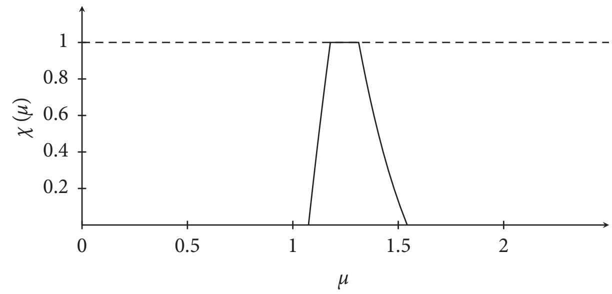

Figure 13: CF of the fuzzy estimator $\widehat{\mu}^*$.

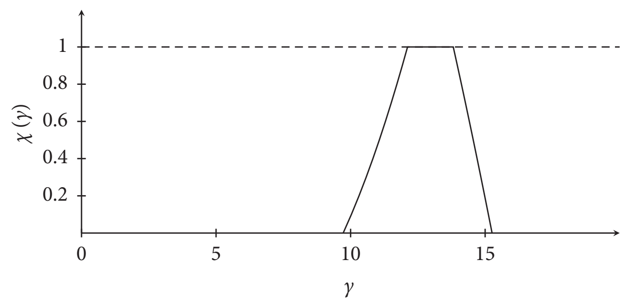

Figure 14: CF of the fuzzy estimator $\widehat{\gamma}^*$.

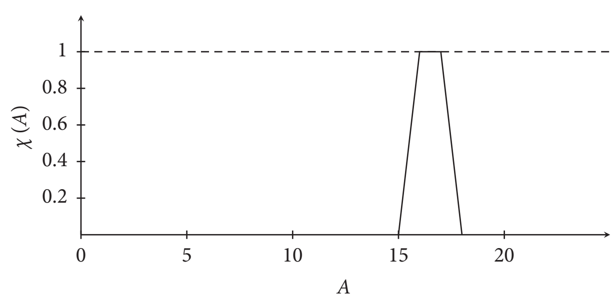

Figure 15: CF of the fuzzy estimator $\widehat{A}^*$.

Example 5. Characterizing functions of fuzzy life times $(y_1^*, y_2^*, \ldots, y_n^*)$ for the gamma distribution are given in Figure 17.

From (50), denoting by $(A_\delta(\widehat{\nu}^*) = [\underline{\nu}_\delta, \overline{\phi}_\delta] \quad \forall\delta \in (0,1])$ the desired generating family of intervals of the fuzzy parameter estimator and using the construction lemma, the CF of the fuzzy estimator $\widehat{\nu}^*$ is obtained and depicted in Figure 18.

From (51), denoting by $(A_\delta(\widehat{\phi}^*) = [\underline{\phi}_\delta, \overline{\phi}_\delta] \quad \forall\delta \in (0,1])$ the desired generating family of intervals of the fuzzy parameter estimator and using the construction lemma, the CF of the fuzzy estimator $\widehat{\phi}^*$ is obtained.

The fuzzy estimation of the parameter indicates that the value of ϕ is about 1.6 to 2.7 in the sence of the function in

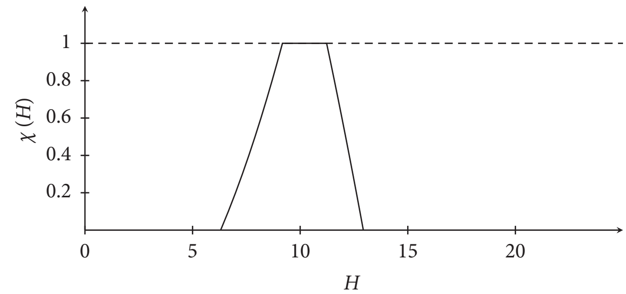

Figure 16: CF of the fuzzy estimator $\widehat{H}^*$.

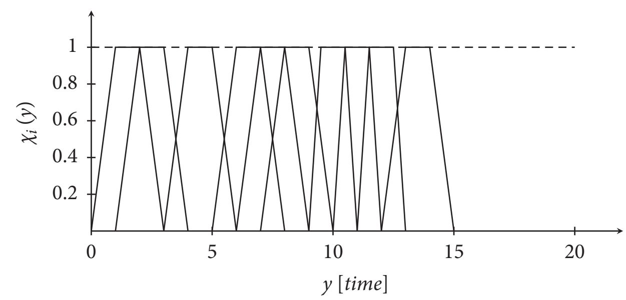

Figure 17: CF of the fuzzy life times.

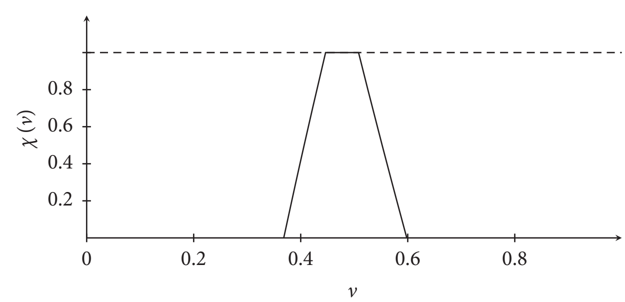

Figure 18: CF of the fuzzy estimator $\widehat{v}^*$.

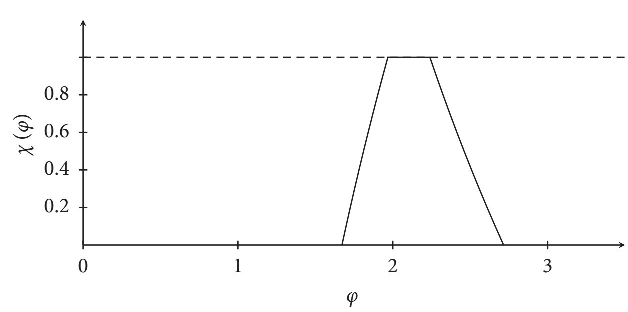

Figure 19: CF of the fuzzy estimator $\widehat{\phi}^*$.

Figure 19. It means that it is completely possible that ϕ is 1.6 or 2.7. In addition, it is not possible that ϕ is less than 1.9 or greater than 2.3, with possibility degree of 0.8.

4. Conclusion

According to recent developments of the measurement sciences, it is very easy to say that measurements based on continuous phenomena are no more precise observations but more or less fuzzy.

Life time is a continuous phenomenon, and in the development of life time distributions, it has been noted that life time observations are recorded as precise numbers. But as discussed, in real-life applications, life times are no more precise observations but fuzzy numbers.

In order to get more suitable and realistic results, this imprecision needs to be addressed; therefore, in this study, generalized estimators are proposed so that fuzziness of life time observations is integrated in the inference.

Since the proposed estimators utilize all the available information, i.e., fuzziness as well as random variation of the life time observations to cover all the available information. The proposed estimators are based on random variation like other classical approaches, but in addition to that, these estimators also utilize the fuzziness of the observations. This integration of fuzziness in the estimates make it more realistic in real-life applications. The characterizing functions for the generalized estimators are obtained and explained to cover both the uncertainties. On the other hand, the classical approaches are only based on random variations and have nothing to do with other kinds of variation.

Therefore, the results based on the proposed estimators are more suitable and realistic to real-life applications.

5. Limitation and Future Work of the Study

The study is limited to the complete observations, and this can be extended to the censored observation; in addition to that, this can be further extended to Pythagorean fuzzy uncertainty mentioned in [24].

Data Availability

The data used to support the findings of this study are available from the corresponding author upon request.

Conflicts of Interest

The authors declare that they have no conflicts of interest.

References

[1] E. T. Lee and J. W. Wang, *Statistical Methods for Survival Data Analysis*, Wiley, New Jersey, USA, 2013.

[2] R. Miller, *Survival Analysis*, Wiley, New York, USA, 2011.

[3] M. A. Al-Fawzan, *Methods for Estimating the Parameters of the Weibull Distribution*, King Abdulaziz City for Science and Technology, Saudi Arabia, 2000.

[4] J. Reath, "Improved parameter estimation of the log-logistic distribution with applications," *Open Access Master's Report*, Michigan Technological University, Houghton, USA, 2016.

[5] Z. W. Birnbaum and S. C. Saunders, "A new family of life distributions," *Journal of Applied Probability*, vol. 6, no. 2, pp. 319–327, 1969.

[6] H. K. T. Ng, D. Kundu, and N. Balakrishnan, "Modified moment estimation for the two-parameter Birnbaum-Saunders distribution," *Computational Statistics & Data Analysis*, vol. 43, no. 3, pp. 283–298, 2003.

[7] M. M. S. Amrir, "Comparing different estimators for parameters of two gamma parameters using simulation," *International Journal of Computer Science and Network Security*, vol. 14, no. 11, pp. 111–117, 2014.
[8] G. Barbato, A. Germak, G. Genta, and A. Barbato, *Measurements for Decision Making. Measurements and Basic Statistics*, Esculapio, Bologna, Italy, 2013.
[9] R. Viertl, *Statistical Methods for Fuzzy Data*, Wiley, Chichester, UK, 2011.
[10] H.-C. Wu, "Fuzzy Bayesian estimation on lifetime data," *Computational Statistics*, vol. 19, no. 4, pp. 613–633, 2004.
[11] H.-Z. Huang, M. J. Zuo, and Z.-Q. Sun, "Bayesian reliability analysis for fuzzy lifetime data," *Fuzzy Sets and Systems*, vol. 157, no. 12, pp. 1674–1686, 2006.
[12] R. Viertl, "On reliability estimation based on fuzzy lifetime data," *Journal of Statistical Planning and Inference*, vol. 139, no. 5, pp. 1750–1755, 2009.
[13] H.-C. Wu, "Statistical confidence intervals for fuzzy data," *Expert Systems with Applications*, vol. 36, no. 2, pp. 2670–2676, 2009.
[14] A. Pak, G. A. Parham, and M. Saraj, "Reliability estimation in Rayleigh distribution based on fuzzy lifetime data," *International Journal of System Assurance Engineering and Management*, vol. 5, no. 4, pp. 487–494, 2013.
[15] M. Shafiq and R. Viertl, "Empirical reliability functions based on fuzzy life time data," *Journal of Intelligent and Fuzzy Systems*, vol. 28, no. 2, pp. 707–711, 2015.
[16] M. Shafiq, Alamgir, and M. Atif, "On the estimation of three parameters lognormal distribution based on fuzzy life time data," *Sains Malaysiana*, vol. 45, no. 11, pp. 1773–1777, 2016.
[17] M. Shafiq and R. Viertl, "On the estimation of parameters, survival functions, and hazard rates based on fuzzy life time data," *Communications in Statistics - Theory and Methods*, vol. 46, no. 10, pp. 5035–5055, 2017.
[18] S. M. Taheri, G. Hesamian, and R. Viertl, "Contingency tables with fuzzy information," *Communications in Statistics - Theory and Methods*, vol. 45, no. 20, pp. 5906–5917, 2016.
[19] T. Rahimi, M. Farhadi, K. H. Loo, and J. Pou, "Fuzzy Lifetime Analysis of a Fault-Tolerant Two-phase Interleaved Converter," in *Proceedings of the 2021 IEEE 13th International Symposium on Diagnostics for Electrical Machines, Power Electronics and Drives (SDEMPED)*, Texas, USA, August, 2021.
[20] S. Lata, S. Mehfuz, S. Urooj, and F. Alrowais, "Fuzzy clustering algorithm for enhancing reliability and network lifetime of wireless sensor networks," *IEEE Access*, vol. 8, Article ID 66013, 2020.
[21] H. Bandemer, *Mathematics of uncertainty: ideas, methods, application problems*, Springer, vol. 189, 2006.
[22] R. Viertl and D. Hareter, *Beschreibung und Analyse unscharfer Information: Statistische Methoden für unscharfe Daten*, Springer, Wien, Austria, 2006.
[23] G. J. Klir and B. Yuan, *Fuzzy Sets and Fuzzy Logic: Theory and Applications*, Prentice-Hall, New Jersey, USA, 1995.
[24] L. Wang and H. Garg, "Algorithm for multiple attribute decision-making with interactive archimedean norm operations under pythagorean fuzzy uncertainty," *International Journal of Computational Intelligence Systems*, vol. 14, no. 1, pp. 503–527, 2020.

Hindawi
Mathematical Problems in Engineering
Volume 2022, Article ID 1007133, 19 pages
https://doi.org/10.1155/2022/1007133

Research Article

Spherical Fuzzy Soft Topology and Its Application in Group Decision-Making Problems

Harish Garg,[1] **Fathima Perveen P A**,[2] **Sunil Jacob John**,[2] **and Luis Perez-Dominguez**[3]

[1]*School of Mathematics, Thapar Institute of Engineering and Technology, Deemed University, Patiala 147004, Punjab, India*
[2]*Department of Mathematics, National Institute of Technology Calicut, Calicut-673 601, Kerala, India*
[3]*Departamento de Ingenieria Industrial y Manufactura, Universidad Autonoma de Ciudad Juarez, Juarez, Mexico*

Correspondence should be addressed to Harish Garg; harishg58iitr@gmail.com

Received 2 November 2021; Revised 26 December 2021; Accepted 11 March 2022; Published 26 April 2022

Academic Editor: Adiel T. de Almeida-Filho

The spherical fuzzy soft set is a generalized soft set model, which is more realistic, practical, and accurate. It is an extended version of existing fuzzy soft set models that can be used to describe imprecise data in real-world scenarios. The paper seeks to introduce the new concept of spherical fuzzy soft topology defined on spherical fuzzy soft sets. In this work, we define some basic concepts including spherical fuzzy soft basis, spherical fuzzy soft subspace, spherical fuzzy soft interior, spherical fuzzy soft closure, and spherical fuzzy soft boundary. The properties of these defined set are also discussed and explained with an appropriate examples. Also, we establish certain important results and introduce spherical fuzzy soft separation axioms, spherical fuzzy soft regular space, and spherical fuzzy soft normal space. Furthermore, as an application, a group decision-making algorithm is presented based on the TOPSIS (Technique of Order Preference by Similarity to an Ideal Solution) method for solving the decision-making problems. The applicability of the proposed method is demonstrated through a numerical example. The comprehensive advantages of the proposed work have been stated over the existing methods.

1. Introduction

The human life with all of its complexities, is currently in flux due to the exponential growth of innovation and changing technologies that constantly redefine, reshape, and redesign the way the world is perceived and experienced, and the tools once used to solve problems become obsolete and inappropriate. This is no exception to any discipline of knowledge. Thus, The strategies commonly adopted in classical mathematics are not effective all the time due to the uncertainty and ambiguity it entails. Techniques such as fuzzy set theory [1], vague set theory [2], and interval mathematics [3] are viewed as mathematical models for coping with uncertainty and variability. However, these theories suffer from their own shortcomings and inadequacies to deal with the task at hand more objectively. Zadeh's fuzzy set theory was extensively used in the beginning for many applications. Fuzzy sets are thought to be an extended version of classical sets, where each element has a membership grade. The definition of intuitionistic fuzzy sets was developed by Atanassov [4] to circumvent some limitations of fuzzy sets. Many other fuzzy set extensions have been proposed, including interval-valued intuitionistic fuzzy sets [5], Pythagorean fuzzy sets [6], picture fuzzy sets [7], and so on. These sets were effectively applied in several areas of science and engineering, economics, medical science, and environmental science. Recently, as a generalization of fuzzy set, intuitionistic fuzzy set, and picture fuzzy set, certain authors have developed the concept of spherical fuzzy sets [8] and T-spherical fuzzy sets [9] to enlarge the picture fuzzy sets as it has their restrictions. To address decision-making problems, Ashraf et al. [10] proposed the spherical fuzzy aggregation operators. Akram et al. [11] introduced the complex spherical fuzzy model that excels at expressing ambiguous information in two dimensions. The applications of these sets to solve decision-making problems are prevalent in a variety of fields [12–17].

In 1999, Molodtsov [18] proposed a new type of set, called soft set, to deal with uncertainty and vagueness. The challenge of determining the membership function in fuzzy set theory does not occur in soft set theory, making the theory applicable to multiple fields of game theory, operations research, Riemann integration, etc. Later, Maji et al. [19] studied more on soft sets and used Pawlak's rough mathematics [20] to propose a decision-making problem as an application of soft sets. Also, Maji et al. [21] developed a hybrid structure of soft sets and fuzzy sets, known as fuzzy soft sets, which is a more powerful mathematical model for handling different kinds of real-life situations. Many researchers were interested in this concept and various fuzzy set generalizations such as generalized fuzzy soft sets [22], group generalized fuzzy soft sets [23], intuitionistic fuzzy soft sets [24], Pythagorean fuzzy soft sets [25], interval-valued picture fuzzy soft sets [26] were put forward. In the recent times, Perveen et al. [27] created a spherical fuzzy soft set (SFSS), which is a more advanced form of fuzzy soft set. This newly evolved set is arguably the more realistic, practical and accurate. SFSSs are a new variation of the picture fuzzy soft set that was developed by merging soft sets and spherical fuzzy sets, where the membership degrees satisfy the condition $0 \leq \mu^2_{\aleph(\varpi)}(\varsigma) + \eta^2_{\aleph(\varpi)}(\varsigma) + \vartheta^2_{\aleph(\varpi)}(\varsigma) \leq 1$ rather than $0 \leq \mu_{\aleph(\varpi)}(\varsigma) + \eta_{\aleph(\varpi)}(\varsigma) + \vartheta_{\aleph(\varpi)}(\varsigma) \leq 1$ as in picture fuzzy soft sets. SFSS has more capability in modeling vagueness and uncertainty while dealing with decision-making problems that occur in real-life circumstances. The authors [28] also developed similarity measures of SFSS and applied the proposed spherical fuzzy soft similarity measure in the field of medical science.

These theories have applications in topology and many other fields of mathematics. Chang [29] suggested the concept of a fuzzy topological space in 1968. He extended many basic concepts like continuity, compactness, open set, and closed set in general topology to the fuzzy topological spaces. Again, Lowen [30] conducted an elaborated study of the structure of fuzzy topological spaces. Çoker [31] invented the idea of an intuitionistic fuzzy topological space in 1995. Many other results including continuity, compactness, and connectedness of intuitionistic fuzzy topological spaces were proposed by Coker et al. [32, 33]. The notion of Pythagorean fuzzy topological space was presented by Olgun et al. [34]. Kiruthika and Thangavelu [35] discussed the link between topology and soft topology. Recently, by using elementary operations over a universal set with a set of parameters, Taskopru and Altintas [36] established the elementary soft topology. Tanay and Kandemir [37] defined the idea of fuzzy soft topology. They also introduced fuzzy soft neighbourhood, fuzzy soft basis, fuzzy soft interior, and fuzzy soft subspace topology. Several related works on fuzzy soft topology can be seen in [38–40]. Osmanoglu and Tokat [41] proposed the subspace, compactness, connectedness, and separation axioms of intuitionistic fuzzy soft topological spaces. Also, intuitionistic fuzzy soft topological spaces were examined by Bayramov and Gunduz [42]. They studied intuitionistic fuzzy soft continuous mapping and related properties. Riaz et al. [43] proposed the concept of Pythagorean fuzzy soft topology defined on Pythagorean fuzzy soft sets, and provided an application of Pythagorean fuzzy soft topology in medical diagnosis by making use of TOPSIS method.

Hwang and Yoon [44] developed Technique for order of Preference by Similarity to ideal solution (TOPSIS) as a multi-criteria decision analysis and further studied by Chen et al. [45, 46]. Boran et al. [47] invented the TOPSIS approach based on intuitionistic fuzzy sets for multi-criteria decision-making problems. Chen et al. [48] developed a proportional interval T2 hesitant fuzzy TOPSIS approach based on the Hamacher aggregation operators and the andness optimization models. Further, the fuzzy soft TOPSIS method presented briefly as a multi-criteria decision-making technique by Selim and Karaaslan [49]. They proposed a group decision-making process in a fuzzy soft environment based on the TOPSIS method. Also, many researchers in [50–54] have looked at the TOPSIS approach for solving decision-making problems under the different fuzzy environment.

Topological structures on fuzzy soft sets have application in several areas including medical diagnosis, decision-making, pattern recognition, and image processing. Since SFSS is one of the most generalized versions of the fuzzy soft set, introducing topology on SFSS is highly essential in both theoretical and practical scenarios. There are some basic operations of SFSSs in the literature, more functional operations of SFSSs are derived day by day. The development of topology on SFSSs can be considered as an important contribution to fill the gap in the literature on the theory of SFSS. The aim of this paper is to introduce the notion of spherical fuzzy soft topology (SFS-topology) on SFSS, and to discuss some basic concepts such as SFS-subspace, SFS-point, SFS-nbd, SFS-basis, SFS-interior, SFS-closure, SFS-boundary, SFS-exterior and SFS-separation axioms. Also, through this paper, we use the SFS-topology in group decision-making method based on TOPSIS under spherical fuzzy soft environment.

The rest of the paper is ordered as follows. In Section 2, some fundamental concepts of fuzzy sets, spherical fuzzy sets, soft sets, fuzzy soft sets, and spherical fuzzy soft sets are recalled, and definitions of spherical fuzzy subset, spherical fuzzy union and spherical fuzzy intersection are modified. In Section 3, the concept of SFS-topology is defined on SFSS including some basic definitions. In Section 4, by using the ideas of SFS-points, SFS-open set, and SFS-closed set, SFS-separation axioms are proposed. In Section 5, an algorithm is presented besed on group decision-making method and extension of TOPSIS approach accompanied by a numerical example. This theory will have implications in the discipline of Human resource management, organizational behavior and assessing the rationale of consumer choice. In Section 6, a comparative study is conducted with an already existing algorithm to show the effectiveness of the proposed algorithm. Finally, Section 7 ends with a conclusion and recommendations for future work.

2. Preliminaries

In this section, we recall certain fundamental ideas associated with various kinds of sets including fuzzy sets, spherical fuzzy sets, soft sets, fuzzy soft sets, and spherical fuzzy soft sets. We redefine the definitions of spherical fuzzy subset, spherical fuzzy union, and spherical fuzzy intersection, also propose the notions of null SFSS and absolute SFSS. Let Σ be the initial universal set of discourse and $\mathscr{K}$ be the attribute (or parameter) set in connection with the objects in Σ, and $\mathscr{L} \subseteq \mathscr{K}$.

Definition 1 (see [1]). A fuzzy set $\aleph$ on a universe Σ is an object of the form

$$\aleph = \{(\varsigma, \mu_{\aleph}(\varsigma)) | \varsigma \in \Sigma\}, \quad (1)$$

where $\mu_{\aleph}\colon \Sigma \longrightarrow [0, 1]$ is the membership function of $\aleph$, the value $\mu_{\aleph}(\varsigma)$ is the grade of membership of ς in $\aleph$.

Definition 2 (see [9]). A spherical fuzzy set (SFS) $\mathscr{S}$ over the universal set Σ can be written as

$$\mathscr{S} = \{(\varsigma, \mu_{\mathscr{S}}(\varsigma), \eta_{\mathscr{S}}(\varsigma), \vartheta_{\mathscr{S}}(\varsigma)) | \varsigma \in \Sigma\}, \quad (2)$$

where $\mu_{\mathscr{S}}(\varsigma)$, $\eta_{\mathscr{S}}(\varsigma)$ and $\vartheta_{\mathscr{S}}(\varsigma)$ are the membership functions defined from Σ to [0, 1], indicate the positive, neutral, and negative membership degrees of $\varsigma \in \Sigma$ respectively, with the condition, $0 \le \mu^2_{\mathscr{S}}(\varsigma) + \eta^2_{\mathscr{S}}(\varsigma) + \vartheta^2_{\mathscr{S}}(\varsigma) \le 1$, $\forall \varsigma \in \Sigma$.

Definition 3 (see [9]). Let $\aleph = \{(\varsigma, \mu_{\aleph}(\varsigma), \eta_{\aleph}(\varsigma), \vartheta_{\aleph}(\varsigma)) | \varsigma \in \Sigma\}$ and $\Omega = \{(\varsigma, \mu_{\Omega}(\varsigma), \eta_{\Omega}(\varsigma), \vartheta_{\Omega}(\varsigma)) | \varsigma \in \Sigma\}$ be two SFSs over Σ. Then

(1) $\aleph \subseteq \Omega$ if $\mu_{\aleph}(\varsigma) \le \mu_{\Omega}(\varsigma)$, $\eta_{\aleph}(\varsigma) \le \eta_{\Omega}(\varsigma)$, and $\vartheta_{\aleph}(\varsigma) \ge \vartheta_{\Omega}(\varsigma)$

(2) $\aleph = \Omega$ if and only if $\aleph \subseteq \Omega$ and $\aleph \supseteq \Omega$

(3) $\aleph \cup \Omega = \{(\varsigma, \mu_{\aleph}(\varsigma) \vee \mu_{\Omega}(\varsigma), \eta_{\aleph}(\varsigma) \wedge \eta_{\Omega}(\varsigma), \vartheta_{\aleph}(\varsigma) \wedge \vartheta_{\Omega}(\varsigma)) | \varsigma \in \Sigma\}$

(4) $\aleph \cap \Omega = \{(\varsigma, \mu_{\aleph}(\varsigma) \wedge \mu_{\Omega}(\varsigma), \eta_{\aleph}(\varsigma) \wedge \eta_{\Omega}(\varsigma), \vartheta_{\aleph}(\varsigma) \vee \vartheta_{\Omega}(\varsigma)) | \varsigma \in \Sigma\}$

Where the symbols "$\vee$" and "$\wedge$" represent the maximum and minimum operations respectively.

Definition 4 (see [10]). Let Σ be the initial universal set.

(1) An SFS is said to be an absolute SFS over the universe Σ, denoted by 1^{Σ}, if $\forall \varsigma \in \Sigma$,

$$\mu_{1^{\Sigma}}(\varsigma) = 1, \eta_{1^{\Sigma}}(\varsigma) = 0, \text{and } \vartheta_{1^{\Sigma}}(\varsigma) = 0. \quad (3)$$

(2) An SFS is said to be a null SFS over the universe Σ, denoted by 1_{Σ}, if $\forall \varsigma \in \Sigma$,

$$\mu_{1_{\Sigma}}(\varsigma) = 0, \eta_{1_{\Sigma}}(\varsigma) = 0, \text{and } \vartheta_{1_{\Sigma}}(\varsigma) = 1. \quad (4)$$

Example 1. Let $\Sigma = \{\varsigma_1, \varsigma_2\}$ be the universal set. Let $\aleph$ and Ω be two SFSs over Σ given by,

$$\aleph = \{(\varsigma_1, 0.3, 0.4, 0.5), (\varsigma_2, 0.5, 0.2, 0.4)\}, \quad (5)$$

$$\Omega = \{(\varsigma_1, 0.4, 0.5, 0.2), (\varsigma_2, 0.6, 0.3, 0.3)\}. \quad (6)$$

Then it is clear that $\aleph \subseteq \Omega$, and $\aleph \cup \Omega = \{(\varsigma_1, 0.4, 0.4, 0.2), (\varsigma_2, 0.6, 0.2, 0.3)\}$.

Further, $1^{\Sigma} = \{(\varsigma_1, 1.0, 0.0, 0.0), (\varsigma_2, 1.0, 0.0, 0.1)\}$ and $1_{\Sigma} = \{(\varsigma_1, 0.0, 0.0, 0.0), (\varsigma_2, 0.0, 0.0, 0.1)\}$. Then $\aleph \cup 1_{\Sigma} = \{(\varsigma_1, 0.3, 0.0, 0.5), (\varsigma_2, 0.5, 0.0, 0.4)\}$ and $\aleph \cap 1^{\Sigma} = \{(\varsigma_1, 0.3, 0.0, 0.5), (\varsigma_2, 0.5, 0.0, 0.4)\}$.

From the above example, It can be showed that the following results are not true generally in spherical fuzzy set theory.

(1) $\aleph \subseteq 1^{\Sigma}$

(2) $\aleph \cup 1_{\Sigma} = \aleph$

(3) $\aleph \cap 1^{\Sigma} = \aleph$

(4) If $\aleph \subseteq \Omega$, then $\aleph \cup \Omega = \Omega$

To overcome this difficulty, we modified the definitions of spherical fuzzy subset, spherical fuzzy union, and spherical fuzzy intersection as follows.

Definition 5. Let $\aleph$ and Ω be two spherical fuzzy sets over the universe Σ, where $\aleph = \{(\varsigma, \mu_{\aleph}(\varsigma), \eta_{\aleph}(\varsigma), \vartheta_{\aleph}(\varsigma)) | \varsigma \in \Sigma\}$ and $\Omega = \{(\varsigma, \mu_{\Omega}(\varsigma), \eta_{\Omega}(\varsigma), \vartheta_{\Omega}(\varsigma)) | \varsigma \in \Sigma\}$. Then $\aleph$ is said to be a spherical fuzzy subset (modified) of Ω, denoted by $\aleph \,\widehat{\subseteq}\, \Omega$, if $\forall \varsigma \in \Sigma$

$$\begin{cases} \mu_{\aleph}(\varsigma) \le \mu_{\Omega}(\varsigma), \eta_{\aleph}(\varsigma) \le \eta_{\Omega}(\varsigma), \vartheta_{\aleph}(\varsigma) \ge \vartheta_{\Omega}(\varsigma)\,; \text{ if } \mu_{\Omega}(\varsigma) \ne 1 \\ \mu_{\aleph}(\varsigma) \le \mu_{\Omega}(\varsigma), \eta_{\aleph}(\varsigma) \ge \eta_{\Omega}(\varsigma), \vartheta_{\aleph}(\varsigma) \ge \vartheta_{\Omega}(\varsigma)\,; \text{ otherwise} \end{cases} \quad (7)$$

Definition 6. Let $\aleph = \{(\varsigma, \mu_{\aleph}(\varsigma), \eta_{\aleph}(\varsigma), \vartheta_{\aleph}(\varsigma)) | \varsigma \in \Sigma\}$ and $\Omega = \{(\varsigma, \mu_{\Omega}(\varsigma), \eta_{\Omega}(\varsigma), \vartheta_{\Omega}(\varsigma)) | \varsigma \in \Sigma\}$ be two spherical fuzzy sets over Σ. Then the spherical fuzzy union (modified), denoted by $\aleph \,\widehat{\cup}\, \Omega$, and the spherical fuzzy intersection (modified), denoted by $\aleph \,\widehat{\cap}\, \Omega$, are defined as follows:

(1) $\Lambda = \aleph \,\widehat{\cup}\, \Omega = \{(\varsigma, \mu_{\Lambda}(\varsigma), \eta_{\Lambda}(\varsigma), \vartheta_{\Lambda}(\varsigma)) | \varsigma \in \Sigma\}$, where

$\mu_{\Lambda}(\varsigma) = \mu_{\aleph}(\varsigma) \vee \mu_{\Omega}(\varsigma)$

$\eta_{\Lambda}(\varsigma) = \{\eta_{\aleph}(\varsigma) \vee \eta_{\Omega}(\varsigma)\,;$ if $(\mu_{\aleph}(\varsigma) \vee \mu_{\Omega}(\varsigma))^2 + (\eta_{\aleph}(\varsigma) \vee \eta_{\Omega}(\varsigma))^2 + (\vartheta_{\aleph}(\varsigma) \wedge \vartheta_{\Omega}(\varsigma))^2 \le 1 \eta_{\aleph}(\varsigma) \wedge \eta_{\Omega}(\varsigma)\,;$ otherwise

$\vartheta_{\Lambda}(\varsigma) = \vartheta_{\aleph}(\varsigma) \wedge \vartheta_{\Omega}(\varsigma)$

(2) $\Pi = \aleph \,\widehat{\cap}\, \Omega = \{(\varsigma, \mu_{\Pi}(\varsigma), \eta_{\Pi}(\varsigma), \vartheta_{\Pi}(\varsigma)) | \varsigma \in \Sigma\}$, where

$\mu_{\Pi}(\varsigma) = \mu_{\aleph}(\varsigma) \wedge \mu_{\Omega}(\varsigma)$

$$\eta_{\Pi}(\varsigma) = \begin{cases} \eta_{\aleph}(\varsigma) \vee \eta_{\Omega}(\varsigma)\,; \text{ if } (\mu_{\aleph}(\varsigma) \text{or} \mu_{\Omega}(\varsigma)) = 1 \\ \eta_{\aleph}(\varsigma) \wedge \eta_{\Omega}(\varsigma)\,; \text{ otherwise} \end{cases}$$

$\vartheta_{\Pi}(\varsigma) = \vartheta_{\aleph}(\varsigma) \vee \vartheta_{\Omega}(\varsigma)$

Definition 7 (see [18]). Let $P(\Sigma)$ denote the power set of the universal set Σ and $\mathscr{K}$ be the set of attributes. A soft set over

Σ is a pair $\langle \aleph, \mathscr{L} \rangle$, where $\aleph$ is a function from $\mathscr{L}$ to $P(\Sigma)$, and $\mathscr{L} \subseteq \mathscr{K}$.

Definition 8 (see [21]). Let $FS(\Sigma)$ denote the collection of all fuzzy subsets over the universal set Σ. A fuzzy soft set (FSS) is a pair $\langle \aleph, \mathscr{L} \rangle$, where $\aleph$ is a mapping given by $\aleph\colon \mathscr{L} \longrightarrow FS(\Sigma)$ and $\mathscr{L} \subseteq \mathscr{K}$.

Definition 9 (see [27]). Let $SFS(\Sigma)$ be the set of all spherical fuzzy sets over Σ. A spherical fuzzy soft set (SFSS) is a pair $\langle \aleph, \mathscr{L} \rangle$, where $\aleph$ is a mapping from $\mathscr{L}$ to $SFS(\Sigma)$ and $\mathscr{L} \subseteq \mathscr{K}$.

For each $\varpi \in \mathscr{L}$, $\aleph(\varpi)$ is a spherical fuzzy set such that $\aleph(\varpi) = \left\{(\varsigma, \mu_{\aleph(\varpi)}(\varsigma), \eta_{\aleph(\varpi)}(\varsigma), \vartheta_{\aleph(\varpi)}(\varsigma))\, \varsigma \in \Sigma\right\}$, where $\mu_{\aleph(\varpi)}(\varsigma), \eta_{\aleph(\varpi)}(\varsigma)$, $\vartheta_{\aleph(\varpi)}(\varsigma) \in [0, 1]$ are the membership degrees which are explained in Definition 2, with the same condition.

Definition 10 (see [27]). Let $\langle \aleph, \mathscr{L} \rangle$ and $\langle \Omega, \mathscr{M} \rangle$ be two SFSSs over Σ, and $\mathscr{L}, \mathscr{M} \subseteq \mathscr{K}$. Then $\langle \aleph, \mathscr{L} \rangle$ is said to be a SFS-subset of $\langle \Omega, \mathscr{M} \rangle$, if

(1) $\mathscr{L} \subseteq \mathscr{M}$

(2) $\forall \varpi \in \mathscr{L}$, $\aleph(\varpi) \widehat{\subseteq} \Omega(\varpi)$

Definition 11 (see [27]). Let $\langle \aleph, \mathscr{L} \rangle$ be a SFSS over the universal set Σ. Then the SFS-complement of $\langle \aleph, \mathscr{L} \rangle$, denoted by $\langle \aleph, \mathscr{L} \rangle^c$, is defined by $\langle \aleph, \mathscr{L} \rangle^c = \langle \aleph^c, \mathscr{L} \rangle$, where $\aleph^c\colon \mathscr{L} \longrightarrow SFS(\Sigma, \mathscr{K})$ is a mapping given by $\aleph^c(\varpi) = \left\{(\varsigma, \vartheta_{\aleph(\varpi)}(\varsigma), \eta_{\aleph(\varpi)}(\varsigma), \mu_{\aleph(\varpi)}(\varsigma))\, \varsigma \in \Sigma\right\}$ for every $\varpi \in \mathscr{L}$.

Definition 12 (see [27]). Let $\langle \aleph, \mathscr{L} \rangle$ and $\langle \Omega, \mathscr{M} \rangle$ be two SFSSs over Σ, and $\mathscr{L}, \mathscr{M} \subseteq \mathscr{K}$. then the SFS-union of $\langle \aleph, \mathscr{L} \rangle$ and $\langle \Omega, \mathscr{M} \rangle$, denoted by $\langle \aleph, \mathscr{L} \rangle \widehat{\cup} \langle \Omega, \mathscr{M} \rangle$, is a SFSS $\langle \Gamma, \mathscr{N} \rangle$, where $\mathscr{N} = \mathscr{L} \cup \mathscr{M}$ and $\forall \varpi \in \mathscr{N}$

$$\Gamma(e) = \begin{cases} \aleph(\varpi), & \text{if} \varpi \in \mathscr{L} - \mathscr{M} \\ \Omega(\varpi), & \text{if} \varpi \in \mathscr{M} - \mathscr{L} \\ \aleph(\varpi) \widehat{\cup} \Omega(\varpi), \text{if} \varpi \in \mathscr{L} \cap \mathscr{M}, \end{cases} \tag{8}$$

Now, we propose the definitions of spherical fuzzy soft restricted intersection, null spherical fuzzy soft, and absolute spherical fuzzy soft, which are essential for further discussions.

Definition 13. Let $\langle \aleph, \mathscr{L} \rangle$ and $\langle \Omega, \mathscr{M} \rangle$ be two SFSSs over Σ, $\mathscr{L}, \mathscr{M} \subseteq \mathscr{K}$. then the SFS-restricted intersection of $\langle \aleph, \mathscr{L} \rangle$ and $\langle \Omega, \mathscr{M} \rangle$, denoted by $\langle \aleph, \mathscr{L} \rangle \widehat{\cap} \langle \Omega, \mathscr{M} \rangle$, is a SFSS $\langle \Gamma, \mathscr{N} \rangle$, where $\mathscr{N} = \mathscr{L} \cap \mathscr{M}$ and $\forall \varpi \in \mathscr{N}$, $\Gamma(\varpi) = \aleph(\varpi) \widehat{\cap} \Omega(\varpi)$

Definition 14. Let $\langle \aleph, \mathscr{K} \rangle$ be a SFSS defined over Σ. $\langle \aleph, \mathscr{K} \rangle$ is said to be a null spherical fuzzy soft set, if for every $\varpi \in \mathscr{K}$, $\aleph(\varpi) = \{(\varsigma, 0, 0, 1) | \varsigma \in \Sigma\}$. That is, $\forall \varsigma \in \Sigma$ and $\varpi \in \mathscr{K}$, $\mu_{\aleph(\varpi)}(\varsigma) = 0$, $\eta_{\aleph(\varpi)}(\varsigma) = 0$ and $\vartheta_{\aleph(\varpi)}(\varsigma) = 1$. It is denoted by $\varnothing_{\mathscr{K}}$.

Definition 15. A SFSS $\langle \aleph, \mathscr{K} \rangle$ over Σ is said to be an absolute spherical fuzzy soft set, if for every $\varpi \in \mathscr{K}$, $\aleph(\varpi) = \{(\varsigma, 1, 0, 0) | \varsigma \in \Sigma\}$. That is, $\forall \varsigma \in \Sigma$ and $\varpi \in \mathscr{K}$, $\mu_{\aleph(\varpi)}(\varsigma) = 1$, $\eta_{\aleph(\varpi)}(\varsigma) = 0$ and $\vartheta_{\aleph(\varpi)}(\varsigma) = 0$. It is denoted by $\Sigma_{\mathscr{K}}$.

3. Spherical Fuzzy Soft Topology

In this section, we define the notion of spherical fuzzy soft topological space (SFS-topological space) so as to differentiate the concept from the existing fuzzy models and to mark the boundaries and deliberate the basic properties thereof. Further, we define SFS-subspace, SFS-point, SFS-nbd, SFS-basis, SFS-interior, SFS-closure, SFS-boundary and SFS-exterior with the support of befitting numerical illustrations.

Definition 16. Let $SFSS(\Sigma, \mathscr{K})$ be the collection of all spherical fuzzy soft sets over the universal set Σ and the parameter set $\mathscr{K}$. Let $\mathscr{L}, \mathscr{M} \widehat{\subseteq} \mathscr{K}$. Then a sub-collection $\mathscr{T}$ of $SFSS(\Sigma, \mathscr{K})$ is said to be a spherical fuzzy soft topology (SFS-topology) on Σ, if

(1) $\varnothing_{\mathscr{K}}, \Sigma_{\mathscr{K}} \in \mathscr{T}$

(2) If $\langle \aleph_1, \mathscr{L} \rangle$, $\langle \aleph_2, \mathscr{M} \rangle \in \mathscr{T}$, then $\langle \aleph_1, \mathscr{L} \rangle \widehat{\cap} \langle \aleph_2, \mathscr{M} \rangle \in \mathscr{T}$

(3) If $\langle \aleph_i, \mathscr{L}_i \rangle \in \mathscr{T}\ \forall i \in I$, an index set, then $\widehat{\cup}_{i \in I} \langle \aleph_i, \mathscr{L}_i \rangle \in \mathscr{T}$

The binary $(\Sigma_{\mathscr{K}}, \mathscr{T})$ is known as a spherical fuzzy soft topological space over Σ. Each member of $\mathscr{T}$ is considered as spherical fuzzy soft open sets and their complements are considered as spherical fuzzy soft closed sets.

Example 2. Let $\Sigma = \{\varsigma_1, \varsigma_2, \varsigma_3\}$ be the universal set with the attribute set $\mathscr{K} = \{\varpi_1, \varpi_2, \varpi_3, \varpi_4\}$. Let $\mathscr{L}, \mathscr{M} \subseteq \mathscr{K}$, where $\mathscr{L} = \{\varpi_1, \varpi_2\}$ and $\mathscr{M} = \{\varpi_1, \varpi_2, \varpi_3\}$. Consider the following SFSSs

$$
\begin{aligned}
\langle \aleph_1, \mathcal{L}\rangle &= \begin{array}{c c} & \begin{array}{cc} \varpi_1 & \varpi_2 \end{array} \\ \begin{array}{c} \varsigma_1 \\ \varsigma_2 \\ \varsigma_3 \end{array} & \begin{pmatrix} (0.5, 0.2, 0.4) & (0.7, 0.2, 0.3) \\ (0.6, 0.3, 0.5) & (0.4, 0.2, 0.6) \\ (0.9, 0.2, 0.5) & (0.9, 0.1, 0.1) \end{pmatrix} \end{array} \\
\langle \aleph_2, \mathcal{M}\rangle &= \begin{array}{c c} & \begin{array}{ccc} \varpi_1 & \varpi_2 & \varpi_3 \end{array} \\ \begin{array}{c} \varsigma_1 \\ \varsigma_2 \\ \varsigma_3 \end{array} & \begin{pmatrix} (0.6, 0.3, 0.2) & (0.8, 0.3, 0.1) & (0.1, 0.2, 0.9) \\ (0.8, 0.3, 0.4) & (0.6, 0.2, 0.5) & (0.3, 0.1, 0.7) \\ (1.0, 0.0, 0.0) & (0.9, 0.2, 0.1) & (0.5, 0.2, 0.3) \end{pmatrix} \end{array}
\end{aligned} \tag{9}
$$

Then $\mathcal{T} = \{\sigma_{\mathcal{K}}, \varnothing_{\mathcal{K}}, \langle \aleph_1, \mathcal{L}\rangle, \langle \aleph_2, \mathcal{M}\rangle\}$ is a SFS-topology on Σ.

Definition 17. Let $(\Sigma_{\mathcal{K}}, \mathcal{T})$ be a SFS-topology on Σ and let $Z \subseteq \Sigma$ and $\mathcal{L} \subseteq \mathcal{K}$. Then $\mathcal{T}_Z = \{\langle \Omega, \mathcal{L}\rangle : \langle \Omega, \mathcal{L}\rangle = \langle \aleph, \mathcal{L}\rangle \mathbin{\widehat{\cap}} Z_{\mathcal{K}}, \langle \aleph, \mathcal{L}\rangle \in \mathcal{T}\}$ is called the SFS-subspace topology of $\mathcal{T}$, where $Z_{\mathcal{K}}$ is the absolute SFSS on Z. The doublet $(Z_{\mathcal{K}}, \mathcal{T}_Z)$ is known as the SFS-subspace of the SFS-topological space $(\Sigma_{\mathcal{K}}, \mathcal{T})$.

Example 3. Consider Example 2. Suppose $Z = \{\varsigma_1, \varsigma_3\} \widehat{\subseteq} \Sigma$. Now,

$$
\begin{aligned}
Z_{\mathcal{K}} &= \begin{array}{c c} & \begin{array}{cccc} \varpi_1 & \varpi_2 & \varpi_3 & \varpi_4 \end{array} \\ \begin{array}{c} \varsigma_1 \\ \varsigma_3 \end{array} & \begin{pmatrix} (1.0, 0.0, 0.0) & (1.0, 0.0, 0.0) & (1.0, 0.0, 0.0) & (1.0, 0.0, 0.0) \\ (1.0, 0.0, 0.0) & (1.0, 0.0, 0.0) & (1.0, 0.0, 0.0) & (1.0, 0.0, 0.0) \end{pmatrix} \end{array} \\
\langle \Omega_1, \mathcal{L}\rangle &= \langle \aleph_1, \mathcal{L}\rangle \mathbin{\widehat{\cap}} Z_{\mathcal{K}} = \begin{array}{c c} & \begin{array}{cc} \varpi_1 & \varpi_2 \end{array} \\ \begin{array}{c} \varsigma_1 \\ \varsigma_3 \end{array} & \begin{pmatrix} (0.5, 0.2, 0.4) & (0.7, 0.2, 0.3) \\ (0.9, 0.2, 0.5) & (0.9, 0.1, 0.1) \end{pmatrix} \end{array} \\
\langle \Omega_2, \mathcal{M}\rangle &= \langle \aleph_2, \mathcal{M}\rangle \mathbin{\widehat{\cap}} Z_{\mathcal{K}} = \begin{array}{c c} & \begin{array}{ccc} \varpi_1 & \varpi_2 & \varpi_3 \end{array} \\ \begin{array}{c} \varsigma_1 \\ \varsigma_3 \end{array} & \begin{pmatrix} (0.6, 0.3, 0.2) & (0.8, 0.3, 0.1) & (0.1, 0.2, 0.9) \\ (1.0, 0.0, 0.0) & (0.9, 0.2, 0.1) & (0.5, 0.2, 0.3) \end{pmatrix} \end{array}
\end{aligned} \tag{10}
$$

Then $\mathcal{T}_Z = \{Z_{\mathcal{K}}, \varnothing_{\mathcal{K}}, \langle \Omega_1, \mathcal{L}\rangle, \langle \Omega_2, \mathcal{M}\rangle\}$ is a SFS-subspace topology of $\mathcal{T}$.

Definition 18. Let $(K_{\mathcal{K}}, \mathcal{T})$ be a SFS-topological space with $\mathcal{T} = \{\varnothing_{\mathcal{K}}, \Sigma_{\mathcal{K}}\}$, then $\mathcal{T}$ is said to be the indiscrete SFS-topology on Σ and $(\Sigma_{\mathcal{K}}, \mathcal{T})$ is called the indiscrete SFS-topological space. The indiscrete SFS-topology is the smallest SFS-topology on Σ.

Definition 19. Let $(\Sigma_{\mathcal{K}}, \mathcal{T})$ be a SFS-topological space with $\mathcal{T} = SFS(\Sigma, \mathcal{K})$, then $\mathcal{T}$ is called the discrete SFS-topology on Σ and $(\Sigma_{\mathcal{K}}, \mathcal{T})$ is said to be the discrete SFS-topological space. The discrete SFS-topology is the largest SFS-topology on Σ.

Example 4. Let Σ be the universal set and $\mathcal{K}$ be the parameter set, where $\Sigma = \{\varsigma_1, \varsigma_2\}$ and $\mathcal{K} = \{\varpi_1, \varpi_2, \varpi_3, \varpi_4\}$. Let $\mathcal{L}_1, \mathcal{L}_2, \mathcal{M}_1, \mathcal{M}_2 \subseteq \mathcal{K}$ with $\mathcal{L}_1 = \mathcal{M}_2 = \{\varpi_1, \varpi_2\}$, $\mathcal{L}_2 = \{\varpi_1\}$, $\mathcal{M}_1 = \{\varpi_1, \varpi_2, \varpi_3\}$. Consider the following SFSSs;

$$
\begin{aligned}
\langle \aleph_1, \mathcal{L}_1\rangle &= \begin{array}{c c} & \begin{array}{cc} \varpi_1 & \varpi_2 \end{array} \\ \begin{array}{c} \varsigma_1 \\ \varsigma_2 \end{array} & \begin{pmatrix} (0.9, 0.2, 0.1) & (0.6, 0.2, 0.2) \\ (0.7, 0.1, 0.3) & (0.4, 0.3, 0.1) \end{pmatrix} \end{array} \\
\langle \aleph_2, \mathcal{L}_2\rangle &= \begin{array}{c c} & \varpi_1 \\ \begin{array}{c} \varsigma_1 \\ \varsigma_2 \end{array} & \begin{pmatrix} (0.7, 0.2, 0.2) \\ (0.5, 0.1, 0.6) \end{pmatrix} \end{array} \\
\langle \Omega_1, \mathcal{M}_1\rangle &= \begin{array}{c c} & \begin{array}{ccc} \varpi_1 & \varpi_2 & \varpi_3 \end{array} \\ \begin{array}{c} \varsigma_1 \\ \varsigma_2 \end{array} & \begin{pmatrix} (0.7, 0.2, 0.3) & (0.8, 0.2, 0.2) & (0.5, 0.3, 0.6) \\ (0.2, 0.1, 0.9) & (0.5, 0.2, 0.3) & (0.8, 0.2, 0.1) \end{pmatrix} \end{array} \\
\langle \Omega_2, \mathcal{M}_2\rangle &= \begin{array}{c c} & \begin{array}{cc} \varpi_1 & \varpi_2 \end{array} \\ \begin{array}{c} \varsigma_1 \\ \varsigma_2 \end{array} & \begin{pmatrix} (0.6, 0.1, 0.4) & (0.8, 0.0, 0.3) \\ (0.1, 0.0, 0.9) & (0.4, 0.1, 0.7) \end{pmatrix} \end{array}
\end{aligned} \tag{11}
$$

Then $\mathcal{T}_1 = \{\varnothing_{\mathcal{K}}, \Sigma_{\mathcal{K}}, \langle \aleph_1, \mathcal{L}_1\rangle, \langle \aleph_2, \mathcal{L}_2\rangle\}$ and $\mathcal{T}_2 = \{\varnothing_{\mathcal{K}}, \Sigma_{\mathcal{K}}, \langle \Omega_1, \mathcal{M}_1\rangle, \langle \Omega_2, \mathcal{M}_2\rangle\}$ are two SFS-topologies. Consider $\mathcal{T}_1 \cup \mathcal{T}_2 = \{\varnothing_{\mathcal{K}}, \Sigma_{\mathcal{K}}, \langle \aleph_1, \mathcal{L}_1\rangle, \langle \aleph_2, \mathcal{L}_2\rangle, \langle \Omega_1, \mathcal{M}_1\rangle, \langle \Omega_2, \mathcal{M}_2\rangle\}$. Now.

$$\langle \aleph_1, \mathcal{L}_1\rangle \mathbin{\widehat{\cap}} \langle \Omega_1, \mathcal{M}_1\rangle = \begin{array}{c} \\ \varsigma_1 \\ \varsigma_3 \end{array} \begin{array}{c} \begin{array}{cc} \varpi_1 & \varpi_2 \end{array} \\ \begin{pmatrix} (0.7, 0.2, 0.3) & (0.6, 0.2, 0.2) \\ (0.2, 0.1, 0.9) & (0.4, 0.2, 0.3) \end{pmatrix} \end{array} \tag{12}$$

Thus, $\langle \aleph_1, \mathcal{L}_1\rangle, \langle \Omega_1, \mathcal{M}_1\rangle \in \mathcal{T}_1 \cup \mathcal{T}_2$, but $\langle \aleph_1, \mathcal{L}_1\rangle \mathbin{\widehat{\cap}} \langle \Omega_1, \mathcal{M}_1\rangle \notin \mathcal{T}_1 \cup \mathcal{T}_2$. Therefore, $\mathcal{T}_1 \cup \mathcal{T}_2$ is not a SFS-topology on Σ.

Theorem 1. *Suppose $\mathcal{T}_1$ and $\mathcal{T}_2$ are two SFS-topologies on Σ, then $\mathcal{T}_1 \cap \mathcal{T}_2$ is also a SFS-topology on Σ. But, $\mathcal{T}_1 \cup \mathcal{T}_2$ need not be a SFS-topology on Σ.*

Proof. Suppose that, $\mathcal{T}_1$ and $\mathcal{T}_2$ are two SFS-topologies on Σ.

Since $\varnothing_{\mathcal{K}}, \Sigma_{\mathcal{K}} \in \mathcal{T}_1$ and $\varnothing_{\mathcal{K}}, \Sigma_{\mathcal{K}} \in \mathcal{T}_2$, then $\varnothing_{\mathcal{K}}, \Sigma_{\mathcal{K}} \in \mathcal{T}_1 \cap \mathcal{T}$.

Let $\langle \aleph, \mathcal{L}\rangle, \langle \Omega, \mathcal{M}\rangle \in \mathcal{T}_1 \cap \mathcal{T}_2 \Rightarrow \langle \aleph, \mathcal{L}\rangle, \langle \Omega, \mathcal{M}\rangle \in \mathcal{T}_1$ and $\langle \aleph, \mathcal{L}\rangle, \langle \Omega, \mathcal{M}\rangle \in \mathcal{T}_2 \Rightarrow \langle \aleph, \mathcal{L}\rangle \mathbin{\widehat{\cap}} \langle \Omega, \mathcal{M}\rangle \in \mathcal{T}_1$ and $\langle \aleph, \mathcal{L}\rangle \mathbin{\widehat{\cap}} \langle \Omega, \mathcal{M}\rangle \in \mathcal{T}_2 \Rightarrow \langle \aleph, \mathcal{L}\rangle \mathbin{\widehat{\cap}} \langle \Omega, \mathcal{M}\rangle \in \mathcal{T}_1 \cap \mathcal{T}_2$.

Let $\langle \aleph_i, \mathcal{L}_i\rangle \in \mathcal{T}_1 \cap \mathcal{T}_2$, $i \in I$, an index set.

$\Rightarrow \langle \aleph_i, \mathcal{L}_i\rangle \in \mathcal{T}_1$ and $\langle \aleph_i, \mathcal{L}_i\rangle \in \mathcal{T}_2$, $\forall i \in I \Rightarrow \widehat{\bigcup}_{i\in I} \langle \aleph_i, \mathcal{L}_i\rangle \in \mathcal{T}_1$ and $\widehat{\bigcup}_{i\in I} \langle \aleph_i, \mathcal{L}_i\rangle \in \mathcal{T}_2 \widehat{\bigcup}_{i\in I} \langle \aleph_i, \mathcal{L}_i\rangle \in \mathcal{T}_1 \cap \mathcal{T}_2$

Thus $\mathcal{T}_1 \cap \mathcal{T}_2$ satisfies all requirements of SFS-topology on Σ. □

Definition 20. Consider the two SFS-topologies $\mathcal{T}_1$ and $\mathcal{T}_2$ on Σ. $\mathcal{T}_1$ is called weaker or coarser than $\mathcal{T}_2$ or $\mathcal{T}_2$ is called finer or stronger than $\mathcal{T}_1$ if and only if $\mathcal{T}_1 \subseteq \mathcal{T}_2$.

Remark 3.1. If either $\mathcal{T}_1 \subseteq \mathcal{T}_2$ or $\mathcal{T}_2 \subseteq \mathcal{T}_1$, then $\mathcal{T}_1$ and $\mathcal{T}_2$ are comparable. Otherwise $\mathcal{T}_1$ and $\mathcal{T}_2$ are not comparable.

Example 5. Consider $\Sigma = \{\varsigma_1, \varsigma_2\}$ as the universal set with the attribute set $\mathcal{K} = \{\varpi_1, \varpi_2, \varpi_3, \varpi_4\}$. Let $\mathcal{L}_1, \mathcal{L}_2, \mathcal{L}_1 \subseteq \mathcal{K}$, where $\mathcal{L}_1 = \{\varpi_1, \varpi_2, \varpi_3\}$, $\mathcal{L}_2 = \{\varpi_1, \varpi_2\}$ and $\mathcal{L}_3 = \{\varpi_1\}$. The SFSSs $\langle \aleph_1, \mathcal{L}_1\rangle, \langle \aleph_2, \mathcal{L}_2\rangle, \langle \aleph_3, \mathcal{L}_3\rangle$ are given as follows:

$$\begin{aligned}
\langle \aleph_1, \mathcal{L}_1\rangle &= \begin{array}{c} \\ \varsigma_1 \\ \varsigma_2 \end{array} \begin{array}{c} \begin{array}{ccc} \varpi_1 & \varpi_2 & \varpi_3 \end{array} \\ \begin{pmatrix} (0.3, 0.1, 0.7) & (0.4, 0.2, 0.3) & (0.7, 0.1, 0.3) \\ (0.8, 0.2, 0.3) & (0.9, 0.1, 0.1) & (0.6, 0.2, 0.4) \end{pmatrix} \end{array} \\
\langle \aleph_2, \mathcal{L}_2\rangle &= \begin{array}{c} \\ \varsigma_1 \\ \varsigma_2 \end{array} \begin{array}{c} \begin{array}{cc} \varpi_1 & \varpi_2 \end{array} \\ \begin{pmatrix} (0.2, 0.1, 0.8) & (0.2, 0.1, 0.4) \\ (0.7, 0.1, 0.4) & (0.7, 0.1, 0.3) \end{pmatrix} \end{array} \\
\langle \aleph_3, \mathcal{L}_3\rangle &= \begin{array}{c} \\ \varsigma_1 \\ \varsigma_2 \end{array} \begin{array}{c} \varpi_1 \\ \begin{pmatrix} (0.1, 0.1, 0.9) \\ (0.6, 0.0, 0.5) \end{pmatrix} \end{array}
\end{aligned} \tag{13}$$

Here, $\mathcal{T}_1 = \{\varnothing_{\mathcal{K}}, \Sigma_{\mathcal{K}}, \langle \aleph_1, \mathcal{L}_1\rangle, \langle \aleph_2, \mathcal{L}_2\rangle, \langle \aleph_3, \mathcal{L}_3\rangle\}$ and $\mathcal{T}_2 = \{\varnothing_{\mathcal{K}}, \Sigma_{\mathcal{K}}, \langle \aleph_1, \mathcal{L}_1\rangle\}$ are two SFS-topologies on Σ. It is clear that $\mathcal{T}_2 \subseteq \mathcal{T}_1$. Thus $\mathcal{T}_1$ is finer than $\mathcal{T}_2$ or $\mathcal{T}_2$ is weaker than $\mathcal{T}_1$.

Definition 21. A SFSS $\langle \aleph, \mathcal{L}\rangle$ is said to be a spherical fuzzy soft point (SFS-point), denoted by $\varpi(\aleph)$, if for every $\varpi \in \mathcal{L}$, $\aleph(\varpi) \neq \{(\varsigma, 0, 0, 1) | \varsigma \in \Sigma\}$ and $\aleph(\widehat{\varpi}) = \{(\varsigma, 0, 0, 1) | \varsigma \in \Sigma\}$, $\forall \widehat{\varpi} \in \mathcal{L} - \{\varpi\}$. Note that, any SFS-point $\varpi(\aleph)$ (say) is also considered as a singleton SFS-subset of the SFSS $\langle \aleph, \mathcal{L}\rangle$.

Definition 22. A SFS-point $\varpi(\aleph)$ is said to be in the SFSS $\langle \Omega, \mathcal{L}\rangle$, that is, $\varpi(\aleph) \in \langle \Omega, \mathcal{L}\rangle$, if $\aleph(\varpi) \mathbin{\widehat{\subseteq}} \Omega(\varpi)$, for every $\varpi \in \mathcal{L}$.

Example 6. Suppose that $\Sigma = \{\varsigma_1, \varsigma_2, \varsigma_3\}$ and $\mathcal{L} = \{\varpi_1, \varpi_2, \varpi_3\} \subseteq \mathcal{K} = \{\varpi_1, \varpi_2, \varpi_3, \varpi_4\}$. Consider the SFSS

$$\langle \aleph, \mathcal{L}\rangle = \begin{array}{c} \\ \varsigma_1 \\ \varsigma_2 \\ \varsigma_3 \end{array} \begin{array}{c} \begin{array}{ccc} \varpi_1 & \varpi_2 & \varpi_3 \end{array} \\ \begin{pmatrix} (0.0, 0.0, 1.0) & (0.0, 0.0, 1.0) & (0.5, 0.2, 0.8) \\ (0.0, 0.0, 1.0) & (0.0, 0.0, 1.0) & (0.9, 0.1, 0.1) \\ (0.0, 0.0, 1.0) & (0.0, 0.0, 1.0) & (0.4, 0.2, 0.6) \end{pmatrix} \end{array} \tag{14}$$

Here, $\varpi_3 \in \mathscr{L}$ and $\aleph(\varpi_3) \neq \{(\varsigma, 0, 0, 1) | \varsigma \in \Sigma\}$. But, for $\mathscr{L} - \{\varpi_3\} = \{\varpi_1, \varpi_2\}$, $\aleph(\varpi_1) = \aleph(\varpi_2) = \{(\varsigma, 0, 0, 1) | \varsigma \in \Sigma\}$. Thus, $\langle \aleph, \mathscr{L} \rangle$ is a SFS-point in Σ and denoted by $\varpi_3(\aleph)$.

Let

$$\langle \Omega, \mathcal{L} \rangle = \begin{array}{c} \\ \varsigma_1 \\ \varsigma_2 \\ \varsigma_3 \end{array} \begin{array}{c} \begin{array}{ccc} \varpi_1 & \varpi_2 & \varpi_3 \end{array} \\ \begin{pmatrix} (0.1, 0.2, 0.8) & (0.0, 0.0, 1.0) & (0.6, 0.3, 0.4) \\ (0.3, 0.1, 0.4) & (0.0, 0.0, 1.0) & (0.9, 0.1, 0.1) \\ (0.9, 0.1, 0.1) & (0.0, 0.0, 1.0) & (0.7, 0.2, 0.3) \end{pmatrix} \end{array} \quad (15)$$

Here, $\aleph(\varpi_3) \widehat{\subseteq} \Omega(\varpi_3)$. Thus, we can say that $\varpi_3(\aleph) \in \langle \Omega, \mathscr{L} \rangle$.

Definition 23. Let $\langle \Gamma, \mathscr{L} \rangle$ be a SFSS over Σ. $\langle \Gamma, \mathscr{L} \rangle$ is said to be a spherical fuzzy soft neighbourhood (SFS-nbd) of the SFS-point $\varpi(\aleph)$ over Σ, if there exist a SFS-open set $\langle \Omega, \mathscr{M} \rangle$ such that $\varpi(\aleph) \in \langle \Omega, \mathscr{M} \rangle \widehat{\subseteq} \langle \Gamma, \mathscr{L} \rangle$.

Definition 24. Let $\langle \Gamma, \mathscr{L} \rangle$ be a SFSS over Σ. $\langle \Gamma, \mathscr{L} \rangle$ is said to be a spherical fuzzy soft neighbourhood (SFS-nbd) of the SFSS $\langle \aleph, \mathscr{M} \rangle$, if there exist a SFS-open set $\langle \Omega, \mathscr{N} \rangle$ such that $\langle \aleph, \mathscr{M} \rangle \widehat{\subseteq} \langle \Omega, \mathscr{N} \rangle \widehat{\subseteq} \langle \Gamma, \mathscr{L} \rangle$.

Theorem 2. *Let $(\Sigma_{\mathscr{K}}, \mathscr{T})$ be a SFS-topological space. A SFSS $\langle \aleph, \mathscr{L} \rangle$ is open if and only if for each SFSS $\langle \Omega, \mathscr{M} \rangle$ such that $\langle \Omega, \mathscr{M} \rangle \widehat{\subseteq} \langle \aleph, \mathscr{L} \rangle$, $\langle \aleph, \mathscr{L} \rangle$ is a SFS-nbd of $\langle \Omega, \mathscr{M} \rangle$.*

Proof. Suppose that the SFSS $\langle \aleph, \mathscr{L} \rangle$ is SFS-open. That is, $\langle \aleph, \mathscr{L} \rangle \in \mathscr{T}$.

Thus for each $\langle \Omega, \mathscr{M} \rangle \widehat{\subseteq} \langle \aleph, \mathscr{L} \rangle$, $\langle \aleph, \mathscr{L} \rangle$ is a SFS-nbd of $\langle \Omega, \mathscr{M} \rangle$.

Conversely, suppose that, for each $\langle \Omega, \mathscr{M} \rangle \widehat{\subseteq} \langle \aleph, \mathscr{L} \rangle$, $\langle \aleph, \mathscr{L} \rangle$ is A SFS-nbd of $\langle \Omega, \mathscr{M} \rangle$.

Since $\langle \aleph, \mathscr{L} \rangle \widehat{\subseteq} \langle \aleph, \mathscr{L} \rangle$, $\langle \aleph, \mathscr{L} \rangle$ is a SFS-nbd of $\langle \aleph, \mathscr{L} \rangle$ itself.

Therefore, there exist an open set $\langle \Gamma, \mathscr{N} \rangle$ such that $\langle \aleph, \mathscr{L} \rangle \widehat{\subseteq} \langle \Gamma, \mathscr{N} \rangle \widehat{\subseteq} \langle \aleph, \mathscr{L} \rangle \Rightarrow \langle \aleph, \mathscr{L} \rangle = \langle \Gamma, \mathscr{N} \rangle \Rightarrow \langle \aleph, \mathscr{L} \rangle$ is open. □

Definition 25. Let $(\Sigma_{\mathscr{K}}, \mathscr{T})$ be a SFS-topological space. A sub-collection $\mathscr{B}$ of the SFS-topology $\mathscr{T}$ is referred as a spherical fuzzy soft basis (SFS-basis) for $\mathscr{T}$, if for each $\langle \aleph, \mathscr{L} \rangle \in \mathscr{T}$, $\exists B \in \mathscr{B}$ such that (Tex translation failed).

Example 7. Let $\Sigma = \{\varsigma_1, \varsigma_2\}$ and $\mathscr{K} = \{\varpi_1, \varpi_2, \varpi_3\}$. Let $\mathscr{L}_i \subseteq \mathscr{K}$ $i = 1$ to 11 with $\mathscr{L}_1 = \mathscr{L}_2 = \mathscr{L}_3 = \mathscr{L}_4 = \mathscr{L}_5 = \mathscr{L}_6 = \mathscr{L}_7 = \mathscr{K}$, $\mathscr{L}_8 = \mathscr{L}_9 = \{\varpi_1, \varpi_2\}$, and $\mathscr{L}_{10} = \mathscr{L}_{11} = \{\varpi_1\}$. Consider the following SFSSs;

$$
\begin{gathered}
\langle \aleph_1, \mathcal{L}_1 \rangle = \begin{array}{cc} & \begin{array}{ccc} \varpi_1 & \varpi_2 & \varpi_3 \end{array} \\ \begin{array}{c} \varsigma_1 \\ \varsigma_2 \end{array} & \begin{pmatrix} (1.0, 0.0, 0.0) & (0.6, 0.2, 0.4) & (1.0, 0.0, 0.0) \\ (0.6, 0.3, 0.2) & (1.0, 0.0, 0.0) & (0.7, 0.3, 0.2) \end{pmatrix} \end{array} \\
\langle \aleph_2, \mathcal{L}_2 \rangle = \begin{array}{cc} & \begin{array}{ccc} \varpi_1 & \varpi_2 & \varpi_3 \end{array} \\ \begin{array}{c} \varsigma_1 \\ \varsigma_2 \end{array} & \begin{pmatrix} (0.9, 0.1, 0.2) & (0.6, 0.2, 0.4) & (0.3, 0.4, 0.5) \\ (0.6, 0.3, 0.2) & (0.8, 0.2, 0.1) & (0.7, 0.3, 0.2) \end{pmatrix} \end{array} \\
\langle \aleph_3, \mathcal{L}_3 \rangle = \begin{array}{cc} & \begin{array}{ccc} \varpi_1 & \varpi_2 & \varpi_3 \end{array} \\ \begin{array}{c} \varsigma_1 \\ \varsigma_2 \end{array} & \begin{pmatrix} (0.9, 0.1, 0.2) & (1.0, 0.0, 0.0) & (0.3, 0.4, 0.5) \\ (1.0, 0.0, 0.0) & (0.8, 0.2, 0.1) & (1.0, 0.0, 0.0) \end{pmatrix} \end{array} \\
\langle \aleph_4, \mathcal{L}_4 \rangle = \begin{array}{cc} & \begin{array}{ccc} \varpi_1 & \varpi_2 & \varpi_3 \end{array} \\ \begin{array}{c} \varsigma_1 \\ \varsigma_2 \end{array} & \begin{pmatrix} (1.0, 0.0, 0.0) & (0.6, 0.2, 0.4) & (1.0, 0.0, 0.0) \\ (0.6, 0.3, 0.2) & (1.0, 0.0, 0.0) & (1.0, 0.0, 0.0) \end{pmatrix} \end{array} \\
\langle \aleph_5, \mathcal{L}_5 \rangle = \begin{array}{cc} & \begin{array}{ccc} \varpi_1 & \varpi_2 & \varpi_3 \end{array} \\ \begin{array}{c} \varsigma_1 \\ \varsigma_2 \end{array} & \begin{pmatrix} (0.9, 0.1, 0.2) & (1.0, 0.0, 0.0) & (0.3, 0.4, 0.5) \\ (1.0, 0.0, 0.0) & (0.8, 0.2, 0.1) & (0.7, 0.3, 0.2) \end{pmatrix} \end{array} \\
\langle \aleph_6, \mathcal{L}_6 \rangle = \begin{array}{cc} & \begin{array}{ccc} \varpi_1 & \varpi_2 & \varpi_3 \end{array} \\ \begin{array}{c} \varsigma_1 \\ \varsigma_2 \end{array} & \begin{pmatrix} (1.0, 0.0, 0.0) & (1.0, 0.0, 0.0) & (1.0, 0.0, 0.0) \\ (1.0, 0.0, 0.0) & (1.0, 0.0, 0.0) & (0.7, 0.3, 0.2) \end{pmatrix} \end{array} \\
\langle \aleph_7, \mathcal{L}_7 \rangle = \begin{array}{cc} & \begin{array}{ccc} \varpi_1 & \varpi_2 & \varpi_3 \end{array} \\ \begin{array}{c} \varsigma_1 \\ \varsigma_2 \end{array} & \begin{pmatrix} (0.9, 0.1, 0.2) & (0.6, 0.2, 0.4) & (0.3, 0.4, 0.5) \\ (0.6, 0.3, 0.2) & (0.8, 0.2, 0.1) & (1.0, 0.0, 0.0) \end{pmatrix} \end{array} \\
\langle \aleph_8, \mathcal{L}_8 \rangle = \begin{array}{cc} & \begin{array}{cc} \varpi_1 & \varpi_2 \end{array} \\ \begin{array}{c} \varsigma_1 \\ \varsigma_2 \end{array} & \begin{pmatrix} (0.9, 0.1, 0.2) & (1.0, 0.0, 0.0) \\ (1.0, 0.0, 0.0) & (0.8, 0.2, 0.1) \end{pmatrix} \end{array} \\
\langle \aleph_9, \mathcal{L}_9 \rangle = \begin{array}{cc} & \begin{array}{cc} \varpi_1 & \varpi_2 \end{array} \\ \begin{array}{c} \varsigma_1 \\ \varsigma_2 \end{array} & \begin{pmatrix} (0.9, 0.1, 0.2) & (0.6, 0.2, 0.4) \\ (0.6, 0.3, 0.2) & (0.8, 0.2, 0.1) \end{pmatrix} \end{array} \\
\langle \aleph_{10}, \mathcal{L}_{10} \rangle = \begin{array}{cc} & \varpi_1 \\ \begin{array}{c} \varsigma_1 \\ \varsigma_2 \end{array} & \begin{pmatrix} (0.3, 0.4, 0.5) \\ (1.0, 0.0, 0.0) \end{pmatrix} \end{array} \\
\langle \aleph_{11}, \mathcal{L}_{11} \rangle = \begin{array}{cc} & \varpi_1 \\ \begin{array}{c} \varsigma_1 \\ \varsigma_2 \end{array} & \begin{pmatrix} (0.3, 0.4, 0.5) \\ (0.7, 0.3, 0.2) \end{pmatrix} \end{array}
\end{gathered} \tag{16}
$$

Then the sub-collection

$$\mathcal{B} = \{B_1 = \langle \aleph_1, \mathcal{L}_1, \rangle, B_2 = \langle \aleph_2, \mathcal{L}_2 \rangle, B_3 = \langle \aleph_8, \mathcal{L}_8 \rangle, B_4 = \langle \aleph_9, \mathcal{L}_9 \rangle, B_5 = \langle \aleph_{10}, \mathcal{L}_{10} \rangle, B_6 = \langle \aleph_{11}, \mathcal{L}_{11} \rangle\}$$

is a SFS-basis for the SFS-topology $\mathcal{T} = \{\varnothing_{\mathcal{K}}, \Sigma_{\mathcal{K}}, \langle \aleph_i, \mathcal{L}_i \rangle, i = 1 \text{ to } 11\}$.

Theorem 3. *Let $\mathcal{B}$ be a SFS-basis for a SFS-topology $\mathcal{T}$, then for each $\varpi \in \mathcal{L}, \mathcal{L} \subseteq \mathcal{K}$, $\mathcal{B}_\varpi = \{\aleph(\varpi) \colon \langle \aleph, \mathcal{L} \rangle \in \mathcal{B}\}$ acts as a spherical fuzzy basis for the spherical fuzzy topology $\mathcal{T}(\varpi) = \{\aleph(\varpi) \colon \langle \aleph, \mathcal{L} \rangle \in \mathcal{T}\}$.*

Proof. Suppose that $\aleph(\varpi) \in \mathcal{T}(\varpi)$ for some $\varpi \in \mathcal{L}$
$\Rightarrow \langle \aleph, \mathcal{L} \rangle \in \mathcal{T}$

Since $\mathcal{B}$ is a SFS-basis for the SFS-topology $\mathcal{T}$, $\exists B' \widehat{\subseteq} B$ such that $\langle \aleph, \mathcal{L} \rangle = \widehat{\cup} B \Rightarrow \aleph(\varpi) = \widehat{\cup} B_\varpi$, where $B_\varpi = \left\{ \aleph(\varpi) \colon \langle \aleph, \mathcal{L} \rangle \in B \right\} \widehat{\subseteq} \mathcal{B}_\varpi \; \aleph(\varpi) = \widehat{\cup} \mathcal{B}_\varpi \Rightarrow \mathcal{B}_\varpi$ is a spherical fuzzy basis for the spherical fuzzy topology $\mathcal{T}(\varpi)$. □

Theorem 4. *Let $(\Sigma_E, \mathcal{T})$ be a SFS-topological space. Let $\mathcal{B} = \{\langle \aleph_i, \mathcal{L}_i \rangle : i \in I\}$ be a sub-collection of SFS-topology $\mathcal{T}$. $\mathcal{B}$ is a SFS-basis for $\mathcal{T}$ if and only if for any SFS-open set $\langle \Omega, \mathcal{M} \rangle$ and a SFS-point $\varpi(\Gamma) \in \langle \Omega, \mathcal{M} \rangle$, there exist a $\langle \aleph_i, \mathcal{L}_i \rangle \in \mathcal{B}$ for some $i \in I$, such that $\varpi(\Gamma) \in \langle \aleph_i, \mathcal{L}_i \rangle \widehat{\subseteq} \langle \Omega, \mathcal{M} \rangle$.*

Proof. Suppose that, $\mathscr{B} = \{\langle \aleph_i, \mathscr{L}_i \rangle : i \in I\} \subseteq \mathscr{T}$ is a SFS-basis for the SFS-topology $\mathscr{T}$.

For any SFS-open set $\langle \Omega, \mathscr{M} \rangle$, there exists SFSSs $\langle \aleph_j, \mathscr{L}_j \rangle$, $j \in J \subseteq I$, where (Tex translation failed)

Thus, for any SFS-point $\varpi(\Gamma) \in \langle \Omega, \mathscr{M} \rangle$, there exist a $\langle \aleph_j, \mathscr{L}_j \rangle \in \mathscr{B}$ such that $\varpi(\Gamma) \in \langle \aleph_j, \mathscr{L}_j \rangle \widehat{\subseteq} \langle \Omega, \mathscr{M} \rangle$.

Conversely, suppose for any SFS-open set $\langle \Omega, \mathscr{M} \rangle$ and a SFS-point $\varpi(\Gamma) \in \langle \Omega, \mathscr{M} \rangle$, there exist a $\langle \aleph_i, \mathscr{L}_i \rangle \in \mathscr{B}$ such that $\varpi(\Gamma) \in \langle \aleph_i, \mathscr{L}_i \rangle \widehat{\subseteq} \langle \Omega, \mathscr{M} \rangle$

Thus, $\langle \Omega, \mathscr{M} \rangle \widehat{\subseteq} \widehat{\bigcup}_{\varpi(\Gamma) \in \langle \Omega, \mathscr{M} \rangle} \langle \aleph_i, \mathscr{L}_i \rangle \widehat{\subseteq} \langle \Omega, \mathscr{M} \rangle \langle \Omega, \mathscr{M} \rangle \widehat{\bigcup}_{\varpi(\Gamma) \in \langle \Omega, \mathscr{M} \rangle} \langle \aleph_i, \mathscr{L}_i \rangle$

Since $\langle \aleph_i, \mathscr{L}_i \rangle \in \mathscr{B}$, $\mathscr{B}$ is a SFS-basis for the SFS-topology $\mathscr{T}$. □

Definition 26. Suppose $(\Sigma_{\mathscr{K}}, \mathscr{T})$ is a SFS-topological space and $\langle \aleph, \mathscr{L} \rangle$ is a SFSS over Σ, where $\mathscr{L} \subseteq \mathscr{K}$. Then

(1) The SFS-union of all SFS-open subsets of $\langle \aleph, \mathscr{L} \rangle$ is known as spherical fuzzy soft interior (SFS-interior) of $\langle \aleph, \mathscr{L} \rangle$, symbolized by $\langle \aleph, \mathscr{L} \rangle$. It is the largest SFS-open set contained in $\langle \aleph, \mathscr{L} \rangle$. That is, $\langle \aleph, \mathscr{L} \rangle^{\circ} \widehat{\subseteq} \langle \aleph, \mathscr{L} \rangle$.

(2) The SFS-intersection of all SFS-closed supersets of $\langle \aleph, \mathscr{L} \rangle$ is known as spherical fuzzy soft closure (SFS-closure) of $\langle \aleph, \mathscr{L} \rangle$, symbolized by $\overline{\langle \aleph, \mathscr{L} \rangle}$. It is the smallest SFS-closed set containing $\langle \aleph, \mathscr{L} \rangle$. That is, $\langle \aleph, \mathscr{L} \rangle \widehat{\subseteq} \overline{\langle \aleph, \mathscr{L} \rangle}$.

(3) The spherical fuzzy soft boundary (SFS-boundary) of $\langle \aleph, \mathscr{L} \rangle$, denoted by $\partial \langle \aleph, \mathscr{L} \rangle$, is defined as follows: $\partial \langle \aleph, \mathscr{L} \rangle = \overline{\langle \aleph, \mathscr{L} \rangle} \,\widehat{\cap}\, \overline{\langle \aleph, \mathscr{L} \rangle^{c}}$

(4) The spherical fuzzy soft exterior (SFS-exterior) of $\langle \aleph, \mathscr{L} \rangle$, denoted by $Ext\langle \aleph, \mathscr{L} \rangle$, is defined as follows: $Ext\langle \aleph, \mathscr{L} \rangle = (\langle \aleph, \mathscr{L} \rangle^{c})^{\circ}$

Example 8. Suppose that $\Sigma = \{\varsigma_1, \varsigma_2\}$ is the universal set with the attribute set $\mathscr{K} = \{\varpi_1, \varpi_2, \varpi_3\}$. Consider the SFS-topology $\mathscr{T} = \{\varnothing_{\mathscr{K}}, \Sigma_{\mathscr{K}}, \langle \aleph_1, \mathscr{K} \rangle, \langle \aleph_2, \mathscr{K} \rangle, \langle \aleph_3, \mathscr{K} \rangle\}$, where

$$
\begin{aligned}
\langle \aleph_1, \mathcal{K} \rangle &= \begin{array}{c} \\ \varsigma_1 \\ \varsigma_2 \end{array} \begin{array}{c} \begin{array}{ccc} \qquad\varpi_1\qquad & \qquad\varpi_2\qquad & \qquad\varpi_3\qquad \end{array} \\ \begin{pmatrix} (0.8, 0.2, 0.3) & (0.6, 0.3, 0.4) & (0.7, 0.2, 0.4) \\ (0.4, 0.1, 0.5) & (0.5, 0.1, 0.5) & (0.3, 0.2, 0.4) \end{pmatrix} \end{array} \\
\langle \aleph_2, \mathcal{K} \rangle &= \begin{array}{c} \\ \varsigma_1 \\ \varsigma_2 \end{array} \begin{array}{c} \begin{array}{ccc} \qquad\varpi_1\qquad & \qquad\varpi_2\qquad & \qquad\varpi_3\qquad \end{array} \\ \begin{pmatrix} (0.7, 0.1, 0.4) & (0.5, 0.2, 0.5) & (0.7, 0.1, 0.5) \\ (0.3, 0.1, 0.6) & (0.4, 0.0, 0.6) & (0.2, 0.1, 0.8) \end{pmatrix} \end{array} \\
\langle \aleph_3, \mathcal{K} \rangle &= \begin{array}{c} \\ \varsigma_1 \\ \varsigma_2 \end{array} \begin{array}{c} \begin{array}{ccc} \qquad\varpi_1\qquad & \qquad\varpi_2\qquad & \qquad\varpi_3\qquad \end{array} \\ \begin{pmatrix} (0.5, 0.0, 0.6) & (0.4, 0.2, 0.6) & (0.6, 0.1, 0.7) \\ (0.1, 0.1, 0.9) & (0.2, 0.0, 0.8) & (0.1, 0.0, 0.9) \end{pmatrix} \end{array}
\end{aligned}
\tag{17}
$$

Clearly, the members of $\mathscr{T}$ are the SFS-open sets. Now, the corresponding closed sets are given as follows: $(\varnothing_{\mathscr{K}})^{c} = \Sigma_{\mathscr{K}}$ $(\Sigma_{\mathscr{K}})^{c} = \varnothing_{\mathscr{K}}$

$$
\begin{aligned}
(\emptyset_{\mathcal{K}})^{c} &= \Sigma_{\mathcal{K}} \\
(\Sigma_{\mathcal{K}})^{c} &= \emptyset_{\mathcal{K}} \\
\langle \aleph_1, \mathcal{K} \rangle^{c} &= \begin{array}{c} \\ \varsigma_1 \\ \varsigma_2 \end{array} \begin{array}{c} \begin{array}{ccc} \qquad\varpi_1\qquad & \qquad\varpi_2\qquad & \qquad\varpi_3\qquad \end{array} \\ \begin{pmatrix} (0.3, 0.2, 0.8) & (0.4, 0.3, 0.6) & (0.4, 0.2, 0.7) \\ (0.5, 0.1, 0.4) & (0.5, 0.1, 0.5) & (0.4, 0.2, 0.3) \end{pmatrix} \end{array} \\
\langle \aleph_2, \mathcal{K} \rangle^{c} &= \begin{array}{c} \\ \varsigma_1 \\ \varsigma_2 \end{array} \begin{array}{c} \begin{array}{ccc} \qquad\varpi_1\qquad & \qquad\varpi_2\qquad & \qquad\varpi_3\qquad \end{array} \\ \begin{pmatrix} (0.4, 0.1, 0.7) & (0.5, 0.2, 0.5) & (0.5, 0.1, 0.7) \\ (0.6, 0.1, 0.3) & (0.6, 0.0, 0.4) & (0.8, 0.1, 0.2) \end{pmatrix} \end{array} \\
\langle \aleph_3, \mathcal{K} \rangle^{c} &= \begin{array}{c} \\ \varsigma_1 \\ \varsigma_2 \end{array} \begin{array}{c} \begin{array}{ccc} \qquad\varpi_1\qquad & \qquad\varpi_2\qquad & \qquad\varpi_3\qquad \end{array} \\ \begin{pmatrix} (0.6, 0.0, 0.5) & (0.6, 0.2, 0.4) & (0.7, 0.1, 0.6) \\ (0.9, 0.1, 0.1) & (0.8, 0.0, 0.2) & (0.9, 0.0, 0.1) \end{pmatrix} \end{array}
\end{aligned}
\tag{18}
$$

Consider the following SFSS.

$$
\langle \aleph, \mathcal{K} \rangle = \begin{array}{c} \\ \varsigma_1 \\ \varsigma_2 \end{array} \begin{array}{c} \begin{array}{ccc} \qquad\varpi_1\qquad & \qquad\varpi_2\qquad & \qquad\varpi_3\qquad \end{array} \\ \begin{pmatrix} (0.7, 0.1, 0.3) & (0.6, 0.2, 0.4) & (0.7, 0.1, 0.5) \\ (0.3, 0.1, 0.7) & (0.4, 0.1, 0.5) & (0.2, 0.2, 0.6) \end{pmatrix} \end{array}
\tag{19}
$$

Thus.

$$\langle \aleph, \mathcal{K}\rangle^{c} = \begin{array}{cc} & \begin{array}{ccc} \varpi_1 & \varpi_2 & \varpi_3 \end{array} \\ \begin{array}{c} \varsigma_1 \\ \varsigma_2 \end{array} & \begin{pmatrix} (0.3, 0.1, 0.7) & (0.4, 0.2, 0.6) & (0.5, 0.1, 0.7) \\ (0.7, 0.1, 0.3) & (0.5, 0.1, 0.4) & (0.6, 0.2, 0.2) \end{pmatrix} \end{array} \tag{20}$$

Then, the SFS-interior of $\langle \aleph, \mathscr{K}\rangle$,

$$\langle \aleph, \mathcal{K}\rangle^{\circ} = \emptyset_{\mathcal{K}} \mathbin{\widehat{\cup}} \langle \aleph_2, \mathcal{K}\rangle \mathbin{\widehat{\cup}} \langle \aleph_3, \mathcal{K}\rangle = \langle \aleph_2, \mathcal{K}\rangle$$

4

The SFS-closure of $\langle \aleph, \mathscr{K}\rangle$, $\overline{\langle \aleph, \mathscr{K}\rangle} = \Sigma_{\mathscr{K}}$

$$\begin{aligned} \overline{\langle \aleph, \mathcal{K}\rangle^{c}} &= \Sigma_{\mathcal{K}} \mathbin{\widehat{\cap}} \langle \aleph_2, \mathcal{K}\rangle^{c} \mathbin{\widehat{\cap}} \langle \aleph_3, \mathcal{K}\rangle^{c} \\ &= \begin{array}{cc} & \begin{array}{ccc} \varpi_1 & \varpi_2 & \varpi_3 \end{array} \\ \begin{array}{c} \varsigma_1 \\ \varsigma_2 \end{array} & \begin{pmatrix} (0.4, 0.0, 0.7) & (0.5, 0.2, 0.5) & (0.5, 0.1, 0.7) \\ (0.6, 0.1, 0.3) & (0.6, 0.0, 0.4) & (0.8, 0.0, 0.2) \end{pmatrix} \end{array} \end{aligned} \tag{21}$$

So that the SFS-boundary of $\langle \aleph, \mathscr{K}\rangle$,

$$\begin{aligned} \partial\langle \aleph, \mathcal{K}\rangle &= \overline{\langle \aleph, \mathcal{K}\rangle} \mathbin{\widehat{\cap}} \overline{\langle \aleph, \mathcal{K}\rangle^{c}} \\ &= \begin{array}{cc} & \begin{array}{ccc} \varpi_1 & \varpi_2 & \varpi_3 \end{array} \\ \begin{array}{c} \varsigma_1 \\ \varsigma_2 \end{array} & \begin{pmatrix} (0.4, 0.0, 0.7) & (0.5, 0.2, 0.5) & (0.5, 0.1, 0.7) \\ (0.6, 0.1, 0.3) & (0.6, 0.0, 0.4) & (0.8, 0.0, 0.2) \end{pmatrix} \end{array} \end{aligned} \tag{22}$$

The SFS-exterior of $\langle \aleph, \mathscr{K}\rangle$, $Ext\langle \aleph, \mathscr{K}\rangle = (\langle \aleph, \mathscr{K}\rangle^{c})^{\circ} = \varnothing_{\mathscr{K}}$.

Theorem 5. *Suppose that $(\Sigma_{\mathscr{K}}, \mathscr{T})$ is a SFS-topological space and $\langle \aleph, \mathscr{L}\rangle$ is a spherical fuzzy soft set over Σ, where $\mathscr{L} \subseteq \mathscr{K}$. Then we have*

(1) $(\langle \aleph, \mathscr{L}\rangle^{\circ})^{c} = \overline{\langle \aleph, \mathscr{L}\rangle^{c}}$

(2) $\overline{\langle \aleph, \mathscr{L}\rangle}^{c} = (\langle \aleph, \mathscr{L}\rangle^{c})^{\circ}$

Proof. Proof is direct □

Theorem 6. *Suppose that $(\Sigma_{\mathscr{K}}, \mathscr{T})$ is a SFS-topological space and $\langle \aleph, \mathscr{L}\rangle$ is a spherical fuzzy soft set over Σ, where $\mathscr{L} \subseteq \mathscr{K}$. Then $\partial\langle \aleph, \mathscr{K}\rangle = \partial\langle \aleph, \mathscr{K}\rangle^{c}$*

Proof. Proof is direct. □

Definition 27. Let $\varpi(\Xi)$ and $\varpi(\Psi)$ be two SFS-points. $\varpi(\Xi)$ and $\varpi(\Psi)$ are said to be distinct, denoted by $\varpi(\Xi) \neq \varpi(\Psi)$, if their corresponding SFSSs $\langle \Xi, \mathscr{L}\rangle$ and $\langle \Psi, \mathscr{M}\rangle$ are disjoint. That is, $\langle \Xi, \mathscr{L}\rangle \mathbin{\widehat{\cap}} \langle \Psi, \mathscr{M}\rangle = \varnothing_{\mathscr{L}\cap\mathscr{M}}$.

4. Spherical Fuzzy Soft Separation Axioms

In this section, we define SFS-separation axioms by using the concepts SFS-point, SFS-open sets and SFS-closed sets.

Definition 28. Let $(\Sigma_{\mathscr{K}}, \mathscr{T})$ be a SFS-topological space and let $\varpi(\Xi)$ and $\varpi(\Psi)$ be any two distinct SFS-points over Σ. If there exist SFS-open sets $\langle \aleph, \mathscr{L}\rangle$ and $\langle \Omega, \mathscr{M}\rangle$ such that $\varpi(\Xi) \in \langle \aleph, \mathscr{L}\rangle$ and $\varpi(\Psi) \notin \langle \aleph, \mathscr{L}\rangle$ or $\varpi(\Psi) \in \langle \Omega, \mathscr{M}\rangle$ and $\varpi(\Xi) \notin \langle \Omega, \mathscr{M}\rangle$, then $(\Sigma_{\mathscr{K}}, \mathscr{T})$ is known as SFS T_0-space.

Example 9. All discrete SFS-topological spaces are SFS T_0-spaces. Because, for any two distinct SFS-points $\varpi(\Xi)$ and $\varpi(\Psi)$ over Σ, there exist a SFS-open set $\{\varpi(\Xi)\}$, such that $\varpi(\Xi) \in \{\varpi(\Xi)\}$ and $\varpi(\Psi) \notin \{\varpi(\Xi)\}$.

Definition 29. Let $(\Sigma_{\mathscr{K}}, \mathscr{T})$ be a SFS-topological space and let $\varpi(\Xi), \varpi(\Psi)$ be two SFS-points over Σ with $\varpi(\Xi) \neq \varpi(\Psi)$. If there exist two SFS-open sets $\langle \aleph, \mathscr{L}\rangle$ and $\langle \Omega, \mathscr{M}\rangle$ such that $\varpi(\Xi) \in \langle \aleph, \mathscr{L}\rangle$, $\varpi(\Psi) \notin \langle \aleph, \mathscr{L}\rangle$ and $\varpi(\Psi) \in \langle \Omega, \mathscr{M}\rangle$, $\varpi(\Xi) \notin \langle \Omega, \mathscr{M}\rangle$, then $(\Sigma_{\mathscr{K}}, \mathscr{T})$ is known as SFS T_1-space.

Example 10. Every discrete SFS-topological space is a SFS T_1-space. Because, for any two distinct SFS -points $\varpi(\Xi)$ and

$\varpi(\Psi)$ over Σ, there exist SFS-open sets $\{\varpi(\Xi)\}$ and $\{\varpi(\Psi)\}$, such that $\varpi(\Xi) \in \{\varpi(\Xi)\}$, $\varpi(\Psi) \notin \{\varpi(\Xi)\}$ and $\varpi(\Xi) \notin \{\varpi(\Psi)\}$, $\varpi(\Psi) \in \{\varpi(\Psi)\}$.

Definition 30. Let $(\Sigma_{\mathscr{K}}, \mathscr{T})$ be a SFS-topological space and let $\varpi(\Xi)$ and $\varpi(\Psi)$ be any two distinct SFS-points over Σ. If there exist two SFS-open sets $\langle \aleph, \mathscr{L}\rangle$ and $\langle \aleph, \mathscr{L}\rangle$ such that $\varpi(\Xi) \in \langle \aleph, \mathscr{L}\rangle$ and $\varpi(\Psi) \in \langle \Omega, \mathscr{M}\rangle$, and $\langle \aleph, \mathscr{L}\rangle \widehat{\cap} \langle \Omega, \mathscr{M}\rangle = \varnothing_{\mathscr{L}\cap\mathscr{M}}$, then $(\Sigma_{\mathscr{K}}, \mathscr{T})$ is said to be SFS T_2-space or SFS-Hausdorff space.

Example 11. Suppose that $(\Sigma_{\mathscr{K}}, \mathscr{T})$ is a discrete SFS-topological space. If $\varpi(\Xi)$ and $\varpi(\Psi)$ are any two distinct SFS-points over Σ. Then there exists distinct SFS-open sets $\{\varpi(\Xi)\}$ and $\{\varpi(\Psi)\}$ such that $\varpi(\Xi) \in \{\varpi(\Xi)\}$ and $\varpi(\Psi) \in \{\varpi(\Psi)\}$. Therefore, $(\Sigma_{\mathscr{K}}, \mathscr{T})$ is a SFS-Hausdorff space.

Theorem 7. *Let $(\Sigma_{\mathscr{K}}, \mathscr{T})$ be a SFS-topological space with attribute set $\mathscr{K}$. $(\Sigma_{\mathscr{K}}, \mathscr{T})$ is a SFS-Hausdorff space if and only if for any two distinct SFS-points $\varpi(\Xi)$ and $\varpi(\Psi)$, there exist SFS-closed sets $\langle \Omega_1, \mathscr{K}\rangle$ and $\langle \Omega_2, \mathscr{K}\rangle$ such that $\varpi(\Xi) \in \langle \Omega_1, \mathscr{K}\rangle$, $\varpi(\Psi) \notin \langle \Omega_1, \mathscr{K}\rangle$ and $\varpi(\Xi) \notin \langle \Omega_2, \mathscr{K}\rangle$, $\varpi(\Psi) \in \langle \Omega_2, \mathscr{K}\rangle$, and also $\langle \Omega_1, \mathscr{K}\rangle \widehat{\cup} \langle \Omega_2, \mathscr{K}\rangle = \Sigma_{\mathscr{K}}$.*

Proof. Suppose that $(\Sigma_{\mathscr{K}}, \mathscr{T})$ is a SFS-Hausdorff space, $\varpi(\Xi)$ and $\varpi(\Psi)$ are any two distinct SFS-points over Σ. That is, $\varpi(\Xi) \widehat{\cap} \varpi(\Psi) = \varnothing_{\mathscr{K}}$.

Since $(\Sigma_{\mathscr{K}}, \mathscr{T})$ is SFS-Hausdorff space, there exist two SFS-open sets $\langle \aleph_1, \mathscr{K}\rangle$ and $\langle \aleph_2, \mathscr{K}\rangle$ such that $\varpi(\Xi) \in \langle \aleph_1, \mathscr{K}\rangle$, $\varpi(\Psi) \notin \langle \aleph_1, \mathscr{K}\rangle$ and $\varpi(\Xi) \notin \langle \aleph_2, \mathscr{K}\rangle$, $\varpi(\Psi) \in \langle \aleph_2, \mathscr{K}\rangle$. And also $\langle \aleph_1, \mathscr{K}\rangle \widehat{\cap} \langle \aleph_1, \mathscr{K}\rangle = \varnothing_{\mathscr{K}} \Rightarrow \langle \aleph_1, \mathscr{K}\rangle^c \widehat{\cup} \langle \aleph_1, \mathscr{K}\rangle^c = \Sigma_{\mathscr{K}}$ and also both $\langle \aleph_1, \mathscr{K}\rangle^c$ and $\langle \aleph_2, \mathscr{K}\rangle^c$ are SFS-closed sets.

Let $\langle \aleph_1, \mathscr{K}\rangle^c = \langle \Omega_1, \mathscr{K}\rangle$ and $\langle \aleph_2, \mathscr{K}\rangle^c = \langle \Omega_2, \mathscr{K}\rangle$

Then, $\varpi(\Xi) \notin \langle \Omega_1, \mathscr{K}\rangle, \varpi(\Psi) \in \langle \Omega_1, \mathscr{K}\rangle$ and $\varpi(\Xi) \notin \langle \Omega_2, \mathscr{K}\rangle, \varpi(\Psi) \in \langle \Omega_2, \mathscr{K}\rangle$.

Conversely, suppose that for any two distinct SFS-points $\varpi(\Xi)$ and $\varpi(\Psi)$, there exist SFS-closed sets $\langle \Omega_1, \mathscr{K}\rangle$ and $\langle \Omega_2, \mathscr{K}\rangle$ such that $\varpi(\Xi) \in \langle \Omega_1, \mathscr{K}\rangle$, $\varpi(\Psi) \notin \langle \Omega_1, \mathscr{K}\rangle$ and $\varpi(\Xi) \notin \langle \Omega_2, \mathscr{K}\rangle$, $\varpi(\Psi) \in \langle \Omega_2, \mathscr{K}\rangle$, and also $\langle \Omega_1, \mathscr{K}\rangle \widehat{\cup} \langle \Omega_2, \mathscr{K}\rangle = \Sigma_{\mathscr{K}}$.

$\Rightarrow \langle \Omega_1, \mathscr{K}\rangle^c$ and $\langle \Omega_2, \mathscr{K}\rangle^c$ are SFS-open sets and $\langle \Omega_1, \mathscr{K}\rangle^c \widehat{\cap} \langle \Omega_2, \mathscr{K}\rangle^c = \varnothing_{\mathscr{K}}$

Also, $\varpi(\Xi) \notin \langle \Omega_1, \mathscr{K}\rangle^c$, $\varpi(\Psi) \in \langle \Omega_1, \mathscr{K}\rangle^c$ and $\varpi(\Xi) \in \langle \Omega_2, \mathscr{K}\rangle^c$, $\varpi(\Psi) \notin \langle \Omega_2, \mathscr{K}\rangle^c$.

Thus, $(\Sigma_{\mathscr{K}}, \mathscr{T})$ is a SFS-Hausdorff space. □ □

Definition 31. Let $(\Sigma_{\mathscr{K}}, \mathscr{T})$ be a SFS-topological space, $\langle \Omega, \mathscr{M}\rangle$ be a SFS-closed set $\varpi(\Xi)$ and $\varpi(\Psi)$, be a SFS-point over Σ such that $\varpi(\Xi) \notin \langle \Omega, \mathscr{M}\rangle$. If there is SFS-open sets $\langle \aleph_1, \mathscr{L}_1\rangle$ and $\langle \aleph_2, \mathscr{L}_2\rangle$ such that $\varpi(\Xi) \in \langle \aleph_1, \mathscr{L}_1\rangle$, $\langle \Omega, \mathscr{M}\rangle \widehat{\subseteq} \langle \aleph_2, \mathscr{L}_2\rangle$ and $\langle \aleph_1, \mathscr{L}_1\rangle \widehat{\cap} \langle \aleph_2, \mathscr{L}_2\rangle = \varnothing_{\mathscr{L}_1\cap\mathscr{L}_2}$, then $(\Sigma_{\mathscr{K}}, \mathscr{T})$ is called a SFS-regular space.

Example 12. Let $(\Sigma_{\mathscr{K}}, \mathscr{T})$ be a SFS-topological space over $\Sigma = \{\varsigma_1, \varsigma_2\}$ with SFS-topology $\mathscr{T} = \{\Sigma_{\mathscr{K}}, \varnothing_{\mathscr{K}}, \langle \aleph_1, \mathscr{K}\rangle, \langle \aleph_2, \mathscr{K}\rangle\}$, where,

$$\begin{aligned}
\langle \aleph_1, \mathcal{K}\rangle &= \begin{array}{c c} & \begin{array}{cc} \varpi_1 & \varpi_2 \end{array} \\ \begin{array}{c} \varsigma_1 \\ \varsigma_2 \end{array} & \begin{pmatrix} (0.0, 0.0, 1.0) & (1.0, 0.0, 0.0) \\ (0.0, 0.0, 1.0) & (1.0, 0.0, 0.0) \end{pmatrix} \end{array} \\
\langle \aleph_2, \mathcal{K}\rangle &= \begin{array}{c c} & \begin{array}{cc} \varpi_1 & \varpi_2 \end{array} \\ \begin{array}{c} \varsigma_1 \\ \varsigma_2 \end{array} & \begin{pmatrix} (1.0, 0.0, 0.0) & (0.0, 0.0, 1.0) \\ (1.0, 0.0, 0.0) & (0.0, 0.0, 1.0) \end{pmatrix} \end{array}
\end{aligned} \tag{23}$$

Then $(\Sigma_{\mathscr{K}}, \mathscr{T})$ is a SFS-regular space.

Definition 32. Let $(\Sigma_{\mathscr{K}}, \mathscr{T})$ be a SFS-topological space. If $(\Sigma_{\mathscr{K}}, \mathscr{T})$ is a SFS-regular T_1-space, then it is called a SFS T_3-space.

Definition 33. Let $(\Sigma_{\mathscr{K}}, \mathscr{T})$ be a SFS-topological space and let $\langle \Omega_1, \mathscr{M}_1\rangle$ and $\langle \Omega_2, \mathscr{M}_2\rangle$ be two disjoint SFS-closed sets in $(\Sigma_{\mathscr{K}}, \mathscr{T})$. If there exist SFS-open sets $\langle \aleph_1, \mathscr{L}_1\rangle$ and $\langle \aleph_2, \mathscr{L}_2\rangle$ such that $\langle \Omega_1, \mathscr{M}_1\rangle \widehat{\subseteq} \langle \aleph_1, \mathscr{L}_1\rangle$, $\langle \Omega_2, \mathscr{M}_2\rangle \widehat{\subseteq} \langle \aleph_2, \mathscr{L}_2\rangle$ and $\langle \aleph_1, \mathscr{L}_1\rangle \widehat{\cap} \langle \aleph_2, \mathscr{L}_2\rangle = \varnothing_{\mathscr{L}_1\cap\mathscr{L}_2}$, then $(\Sigma_{\mathscr{K}}, \mathscr{T})$ is called a SFS-normal space.

Example 13. Let $(\Sigma_{\mathscr{K}}, \mathscr{T})$ be a SFS-topological space over $\Sigma = \{\varsigma_1, \varsigma_2\}$ with SFS-topology

$$\mathcal{T} = \{\Sigma_{\mathcal{K}}, \emptyset_{\mathcal{K}}, \langle \aleph_1, \mathcal{K}\rangle, \langle \aleph_2, \mathcal{K}\rangle, \langle \aleph_3, \mathcal{K}\rangle, \langle \aleph_4, \mathcal{K}\rangle, \langle \aleph_5, \mathcal{K}\rangle, \langle \aleph_6, \mathcal{K}\rangle\}, \text{ where,}$$

$$
\begin{gathered}
\langle \aleph_1, \mathcal{K}\rangle = \begin{array}{cc} & \begin{array}{cc} \quad\varpi_1 & \qquad\qquad \varpi_2 \end{array} \\ \begin{array}{c} \varsigma_1 \\ \varsigma_2 \end{array} & \begin{pmatrix} (0.7, 0.3, 0.2) & (1.0, 0.0, 0.0) \\ (0.9, 0.2, 0.1) & (1.0, 0.0, 0.0) \end{pmatrix} \end{array} \\
\langle \aleph_2, \mathcal{K}\rangle = \begin{array}{cc} & \begin{array}{cc} \quad\varpi_1 & \qquad\qquad \varpi_2 \end{array} \\ \begin{array}{c} \varsigma_1 \\ \varsigma_2 \end{array} & \begin{pmatrix} (0.5, 0.3, 0.4) & (0.0, 0.0, 1.0) \\ (0.3, 0.2, 0.5) & (0.0, 0.0, 1.0) \end{pmatrix} \end{array} \\
\langle \aleph_3, \mathcal{K}\rangle = \begin{array}{cc} & \begin{array}{cc} \quad\varpi_1 & \qquad\qquad \varpi_2 \end{array} \\ \begin{array}{c} \varsigma_1 \\ \varsigma_2 \end{array} & \begin{pmatrix} (1.0, 0.0, 0.0) & (0.8, 0.4, 0.3) \\ (1.0, 0.0, 0.0) & (0.6, 0.3, 0.4) \end{pmatrix} \end{array} \\
\langle \aleph_4, \mathcal{K}\rangle = \begin{array}{cc} & \begin{array}{cc} \quad\varpi_1 & \qquad\qquad \varpi_2 \end{array} \\ \begin{array}{c} \varsigma_1 \\ \varsigma_2 \end{array} & \begin{pmatrix} (0.0, 0.0, 1.0) & (0.6, 0.4, 0.4) \\ (0.0, 0.0, 1.0) & (0.5, 0.3, 0.5) \end{pmatrix} \end{array} \\
\langle \aleph_5, \mathcal{K}\rangle = \begin{array}{cc} & \begin{array}{cc} \quad\varpi_1 & \qquad\qquad \varpi_2 \end{array} \\ \begin{array}{c} \varsigma_1 \\ \varsigma_2 \end{array} & \begin{pmatrix} (0.7, 0.3, 0.2) & (0.8, 0.4, 0.3) \\ (0.9, 0.2, 0.1) & (0.6, 0.3, 0.4) \end{pmatrix} \end{array} \\
\langle \aleph_6, \mathcal{K}\rangle = \begin{array}{cc} & \begin{array}{cc} \quad\varpi_1 & \qquad\qquad \varpi_2 \end{array} \\ \begin{array}{c} \varsigma_1 \\ \varsigma_2 \end{array} & \begin{pmatrix} (0.5, 0.3, 0.4) & (0.6, 0.4, 0.4) \\ (0.3, 0.2, 0.5) & (0.5, 0.3, 0.5) \end{pmatrix} \end{array}
\end{gathered}
\tag{24}
$$

Then $(\Sigma_{\mathscr{K}}, \mathscr{T})$ is a SFS-normal space.

Definition 34. Let $(\Sigma_{\mathscr{K}}, \mathscr{T})$ be a SFS-topological space. If $(\Sigma_{\mathscr{K}}, \mathscr{T})$ is a SFS-normal T_1-space, then it is known as SFS T_4-space.

Theorem 8. *Suppose that $(\Sigma_{\mathscr{K}}, \mathscr{T})$ is a SFS-topological space and Z is a non-empty subset of Σ.*

(1) If $(\Sigma_{\mathscr{K}}, \mathscr{T})$ is a SFS T_0-space, then $(Z_{\mathscr{K}}, \mathscr{T}_Z)$ is also a SFS T_0-space.

(2) If $(\Sigma_{\mathscr{K}}, \mathscr{T})$ is a SFS T_1-space, then $(Z_{\mathscr{K}}, \mathscr{T}_Z)$ is also a SFS T_1-space.

(3) If $(\Sigma_{\mathscr{K}}, \mathscr{T})$ is a SFS T_2-space, then $(Z_{\mathscr{K}}, \mathscr{T}_Z)$ is also a SFS T_2-space.

Proof. Here we provide the proof if (1). (2) and (3) can be proved in the similar way.

Suppose that $\varpi(\Xi)$ and $\varpi(\Psi)$ are two distinct SFS-points over Z.

Since $(\Sigma_{\mathscr{K}}, \mathscr{T})$ is a SFS T_0-space, there is SFS-open sets $\langle \aleph, \mathscr{L}\rangle$ and $\langle \Omega, \mathscr{M}\rangle$ such that $\varpi(\Xi) \in \langle \aleph, \mathscr{L}\rangle$, $\varpi(\Psi) \notin \langle \aleph, \mathscr{L}\rangle$ or $\varpi(\Psi) \in \langle \Omega, \mathscr{M}\rangle$, $\varpi(\Xi) \notin \langle \Omega, \mathscr{M}\rangle$

Thus, $\varpi(\Xi) \in \langle \aleph, \mathscr{L}\rangle \,\widehat{\cap}\, Z_{\mathscr{K}}$, $\varpi(\Psi) \notin \langle \aleph, \mathscr{L}\rangle \,\widehat{\cap}\, Z_{\mathscr{K}}$ or $\varpi(\Psi) \in \langle \Omega, \mathscr{M}\rangle \,\widehat{\cap}\, Z_{\mathscr{K}}$, $\varpi(\Xi) \notin \langle \Omega, \mathscr{M}\rangle \,\widehat{\cap}\, Z_{\mathscr{K}}$

Therefore, $(Z_{\mathscr{K}}, \mathscr{T}_Z)$ is also a SFS T_0-space. □

5. Group Decision Algorithm and Illustrative Example

In this section, we utilize the proposed SFS-topology to the group decision-making (GDM) process under the spherical fuzzy soft environment. For it, we presented the concept of TOPSIS method and embedding it into the proposed SFS-topology.

5.1. Proposed Algorithm with TOPSIS Method. Consider a GDM process which consist a certain set of alternatives $K = \{\varsigma_1, \varsigma_2, \ldots, \varsigma_m\}$. Each alternative is evaluated under the different set of attributes denoted by $\mathscr{K} = \{\varpi_1, \varpi_2, \ldots, \varpi_n\}$ by the different "p" decision-makers (or experts), say $\mathscr{DM}_1, \mathscr{DM}_2, \ldots, \mathscr{DM}_p$. Each expert has evaluated the given alternatives and provide their ratings in terms of linguistic variables such as "Excellent," "Good" etc. All the linguistic variables and their corresponding weights are considered in this work from the list which is summarized in Table 1.

Then to access the finest alternative(s) from the given alternative, we summarize the following steps of the proposed approach as below.

Step 1: Create a weighted SFS parameter matrix $A_w = [\alpha_{ij}]_{p\times m}$ by considering the linguistic terms from Table 1. That is,

$$
A_w = [\alpha_{ij}]_{p\times n} = \begin{pmatrix} \alpha_{11} & \alpha_{12} & \cdots & \alpha_{1n} \\ \alpha_{21} & \alpha_{22} & \cdots & \alpha_{2n} \\ \vdots & \vdots & \ddots & \vdots \\ \alpha_{p1} & \alpha_{p2} & \cdots & \alpha_{pn} \end{pmatrix} \tag{25}
$$

Table 1: Linguistic terms to determine the alternatives.

Linguistic terms	Weights
Excellent	0.90
Very good	0.70
Good	0.50
Bad	0.30
Very bad	0.10

where each element α_{ij} is the linguistic rating given by the decision-maker $\mathscr{DM}_i$ to the attribute ϖ_j.

Step 2: Create the weighted normalized SFS parameter matrix N_w as follows:

$$N_w = [\rho_{ij}]_{p\times n} = \begin{pmatrix} \rho_{11} & \rho_{12} & \cdots & \rho_{1n} \\ \rho_{21} & \rho_{22} & \cdots & \rho_{2n} \\ \vdots & \vdots & \ddots & \vdots \\ \rho_{p1} & \rho_{p2} & \cdots & \rho_{pn} \end{pmatrix} \tag{26}$$

where, $\rho_{ij} = \alpha_{ij}/\sqrt{\sum_{i=1}^{p} (\alpha_{ij})^2}$

Step 3: Compute the weight vector $\Theta = \{\theta_1, \theta_2, \ldots, \theta_n\}$, where θ_i's are obtained as

$$\theta_i = \frac{w_i}{\sum\limits_{q=1}^{n} w_q} \quad ; \quad w_j = \frac{\sum\limits_{i=1}^{p} \rho_{ij}}{p} \tag{27}$$

Step 4: Construct a SFS-topology by aggregating the SFSSs $\langle \mathscr{DM}_i, \mathscr{K} \rangle$, $i = 1, 2, \ldots, p$, accorded by each decision-makers in the matrix form as their evaluation value. The matrix corresponding to the SFSS $\langle \mathscr{DM}_i, \mathscr{K} \rangle$ is denoted by $\mathbb{DM}_i$ for all $i = 1, 2, \ldots, p$ and it is called the SFS-decision matrix, where the rows and columns of each $\mathbb{DM}_i$ represents the alternatives and the attributes respectively.

Step 5: Compute the aggregated SFS matrix $\mathbb{DM}_{Agg}$ given as follows:

$$\mathbb{DM}_{Agg} = \frac{\mathbb{DM}_1 + \mathbb{DM}_2 + \ldots + \mathbb{DM}_p}{p} = [d_{pq}]_{m\times n} \tag{28}$$

Step 6: Construct the weighted SFS-decision matrix

$$B = [\beta_{pq}]_{m\times n} = \begin{pmatrix} \beta_{11} & \beta_{12} & \cdots & \beta_{1n} \\ \beta_{21} & \beta_{22} & \cdots & \beta_{2n} \\ \vdots & \vdots & \ddots & \vdots \\ \beta_{m1} & \beta_{m2} & \cdots & \beta_{mn} \end{pmatrix} \tag{29}$$

where $\beta_{pq} = \theta_q \times d_{pq}$ and each $\beta_{pq} = (\mu_{\varpi_q}(\varsigma_p), \eta_{\varpi_q}(\varsigma_p), \vartheta_{\varpi_q}(\varsigma_p))$, $p = 1, 2, \ldots, m$ and $q = 1, 2, \ldots, n$.

Step 7: Obtain SFS-valued positive ideal solution ($SFSV^+$) and SFS-valued negative ideal solution ($SFSV^-$), where

$$\begin{aligned} SFSV^{+} &= \{\beta_1^{+}, \beta_2^{+}, ..., \beta_n^{+}\} \\ &= \{(\max_p \mu_{\varpi_q}(\varsigma_p), \min_p \eta_{\varpi_q}(\varsigma_p), \min_p \vartheta_{\varpi_q}(\varsigma_p)); q = 1, 2, ..., n\} \\ &= \{(\mu_q^{+}, \eta_q^{+}, \vartheta_q^{+}); q = 1, 2, ..., n\} \end{aligned} \tag{30}$$

$$\begin{aligned} SFSV^{-} &= \{\beta_1^{-}, \beta_2^{-}, ..., \beta_n^{-}\} \\ &= \{(\min_p \mu_{\varpi_q}(\varsigma_p), \min_p \eta_{\varpi_q}(\varsigma_p), \max_p \vartheta_{\varpi_q}(\varsigma_p)); q = 1, 2, ..., n\} \\ &= \{(\mu_q^{-}, \eta_q^{-}, \vartheta_q^{-}); q = 1, 2, ..., n\} \end{aligned} \tag{31}$$

Step 8: Compute the SFS-separation measurements Ed_p^{+} and Ed_p^{-}, $\forall\, p = 1, 2, \ldots, m$, defined as follows:

$$Ed_p^{+} = \sqrt{\sum_{q=1}^{n} \left\{ \left(\mu_{\varpi_q}(\varsigma_p) - \mu_q^{+}\right)^2 + \left(\eta_{\varpi_q}(\varsigma_p) - \eta_q^{+}\right)^2 + \left(\vartheta_{\varpi_q}(\varsigma_p) - \vartheta_q^{+}\right)^2 \right.}, \tag{32}$$

$$Ed_p^{-} - = \sqrt{\sum_{q=1}^{n} \left\{ \left(\mu_{\varpi_q}(\varsigma_p) - \mu_q^{-}\right)^2 + \left(\eta_{\varpi_q}(\varsigma_p) - \eta_q^{+}\right)^2 + \left(\vartheta_{\varpi_q}(\varsigma_p) - \vartheta_q^{-}\right)^2 \right.}. \tag{33}$$

Step 9: Obtain the SFS-closeness coefficient $\widehat{\mathbf{C}_p}$ of each alternatives. Where

$$\widehat{\mathbf{C}_p} = \frac{Ed_p^{-}}{Ed_p^{+} + Ed_p^{-}} \in [0, 1]. \tag{34}$$

provided $Ed_p^{+} \neq 0$.

Step 10: Based on the SFS-closeness coefficient, rank the alternatives in decreasing (or increasing) order and choose the optimal object from the alternatives.

5.2. Illustrative Example. An international company conducted a campus recruitment in a college and shortlisted four students $\Sigma = \{\varsigma_1, \varsigma_2, \varsigma_3, \varsigma_4\}$ through the first round of recruitment. There is only one vacancy and they have to select one student as their candidate out of these five students. Suppose there are six decision-makers $\mathscr{DM} = \{\mathscr{DM}_1, \mathscr{DM}_2, \mathscr{DM}_3, \mathscr{DM}_4, \mathscr{DM}_5, \mathscr{DM}_6\}$ for the final round and they must have select the candidate based on the parameter set $\mathscr{K} = \{\varpi_1, \varpi_2, \varpi_3, \varpi_4, \varpi_5\}$. For $i = 1, 2, 3, 4, 5$, the parameters ϖ_j stand for "educational discipline," "English speaking," "writing skill," "technical discipline," and "general knowledge" respectively. Then the steps of the proposed approach have been executed to find the best alternative(s) as follows.

Step 1: The weighted SFS parameter matrix A_w is formulated on the basis of equation (25) as follows:

$$A_w = \begin{pmatrix} 0.70 & 0.90 & 0.50 & 0.70 & 0.30 \\ 0.30 & 0.10 & 0.70 & 0.90 & 0.90 \\ 0.90 & 0.70 & 0.30 & 0.50 & 0.30 \\ 0.50 & 0.30 & 0.70 & 0.90 & 0.50 \\ 0.90 & 0.70 & 0.10 & 0.30 & 0.90 \\ 0.10 & 0.90 & 0.30 & 0.50 & 0.70 \end{pmatrix} \tag{35}$$

Step 2: The weighted normalized SFS parameter matrix N_w is computed by using equation (26).

$$N_w = \begin{pmatrix} 0.45 & 0.55 & 0.41 & 0.43 & 0.18 \\ 0.19 & 0.06 & 0.59 & 0.55 & 0.56 \\ 0.57 & 0.43 & 0.25 & 0.30 & 0.18 \\ 0.32 & 0.18 & 0.59 & 0.55 & 0.31 \\ 0.57 & 0.43 & 0.08 & 0.18 & 0.56 \\ 0.06 & 0.55 & 0.25 & 0.30 & 0.44 \end{pmatrix} \quad (36)$$

Step 3: By using equation (27), the weight vector of the given attributes are computed as

$$\Theta = \{0.195, 0.200, 0.195, 0.210, 0.200\} \quad (37)$$

Step 4: For each decision-maker $\mathbb{DM}_i, i = 1 \text{ to } 6$ and their corresponding SFS-decision matrices, we get a SFS-topology on Σ as

$$\begin{gathered}
\langle \mathcal{DM}_1, \mathcal{K} \rangle = \mathbb{DM}_1 = \begin{array}{c} \\ \varsigma_1 \\ \varsigma_2 \\ \varsigma_3 \\ \varsigma_4 \end{array} \begin{array}{c} \begin{array}{ccccc} \varpi_1 & \varpi_2 & \varpi_3 & \varpi_4 & \varpi_5 \end{array} \\ \begin{pmatrix} (0.4, 0.1, 0.5) & (0.5, 0.2, 0.1) & (0.9, 0.1, 0.2) & (0.8, 0.1, 0.3) & (0.9, 0.2, 0.2) \\ (0.8, 0.1, 0.2) & (0.7, 0.2, 0.3) & (0.6, 0.2, 0.4) & (0.7, 0.2, 0.2) & (0.3, 0.1, 0.8) \\ (0.7, 0.1, 0.3) & (0.2, 0.1, 0.5) & (0.3, 0.2, 0.7) & (0.6, 0.3, 0.4) & (0.7, 0.2, 0.5) \\ (0.6, 0.2, 0.4) & (0.4, 0.2, 0.8) & (0.5, 0.3, 0.6) & (0.5, 0.2, 0.6) & (0.4, 0.3, 0.5) \end{pmatrix} \end{array} \\
\langle \mathcal{DM}_2, \mathcal{K} \rangle = \mathbb{DM}_2 = \begin{array}{c} \\ \varsigma_1 \\ \varsigma_2 \\ \varsigma_3 \\ \varsigma_4 \end{array} \begin{array}{c} \begin{array}{ccccc} \varpi_1 & \varpi_2 & \varpi_3 & \varpi_4 & \varpi_5 \end{array} \\ \begin{pmatrix} (1.0, 0.0, 0.0) & (1.0, 0.0, 0.0) & (1.0, 0.0, 0.0) & (1.0, 0.0, 0.0) & (1.0, 0.0, 0.0) \\ (1.0, 0.0, 0.0) & (1.0, 0.0, 0.0) & (1.0, 0.0, 0.0) & (1.0, 0.0, 0.0) & (1.0, 0.0, 0.0) \\ (1.0, 0.0, 0.0) & (1.0, 0.0, 0.0) & (1.0, 0.0, 0.0) & (1.0, 0.0, 0.0) & (1.0, 0.0, 0.0) \\ (1.0, 0.0, 0.0) & (1.0, 0.0, 0.0) & (1.0, 0.0, 0.0) & (1.0, 0.0, 0.0) & (1.0, 0.0, 0.0) \end{pmatrix} \end{array} \\
\langle \mathcal{DM}_3, \mathcal{K} \rangle = \mathbb{DM}_3 = \begin{array}{c} \\ \varsigma_1 \\ \varsigma_2 \\ \varsigma_3 \\ \varsigma_4 \end{array} \begin{array}{c} \begin{array}{ccccc} \varpi_1 & \varpi_2 & \varpi_3 & \varpi_4 & \varpi_5 \end{array} \\ \begin{pmatrix} (0.5, 0.2, 0.6) & (0.7, 0.1, 0.2) & (0.3, 0.2, 0.2) & (0.2, 0.1, 0.9) & (0.9, 0.0, 0.0) \\ (0.9, 0.0, 0.3) & (0.8, 0.3, 0.4) & (0.5, 0.2, 0.7) & (0.6, 0.2, 0.4) & (1.0, 0.0, 0.0) \\ (0.4, 0.2, 0.5) & (0.7, 0.1, 0.5) & (0.9, 0.1, 0.1) & (0.8, 0.3, 0.2) & (0.2, 0.1, 0.8) \\ (0.6, 0.3, 0.5) & (0.4, 0.1, 0.7) & (0.7, 0.3, 0.1) & (0.1, 0.1, 0.4) & (0.6, 0.3, 0.4) \end{pmatrix} \end{array} \\
\langle \mathcal{DM}_4, \mathcal{K} \rangle = \mathbb{DM}_4 = \begin{array}{c} \\ \varsigma_1 \\ \varsigma_2 \\ \varsigma_3 \\ \varsigma_4 \end{array} \begin{array}{c} \begin{array}{ccccc} \varpi_1 & \varpi_2 & \varpi_3 & \varpi_4 & \varpi_5 \end{array} \\ \begin{pmatrix} (0.5, 0.2, 0.5) & (0.7, 0.2, 0.1) & (0.9, 0.2, 0.2) & (0.8, 0.1, 0.3) & (0.9, 0.2, 0.0) \\ (0.9, 0.1, 0.2) & (0.8, 0.3, 0.3) & (0.6, 0.2, 0.4) & (0.7, 0.2, 0.2) & (1.0, 0.0, 0.0) \\ (0.7, 0.2, 0.3) & (0.7, 0.1, 0.5) & (0.9, 0.2, 0.1) & (0.8, 0.3, 0.2) & (0.7, 0.2, 0.5) \\ (0.6, 0.3, 0.4) & (0.4, 0.2, 0.7) & (0.7, 0.3, 0.1) & (0.5, 0.2, 0.4) & (0.6, 0.3, 0.4) \end{pmatrix} \end{array} \\
\langle \mathcal{DM}_5, \mathcal{K} \rangle = \mathbb{DM}_5 = \begin{array}{c} \\ \varsigma_1 \\ \varsigma_2 \\ \varsigma_3 \\ \varsigma_4 \end{array} \begin{array}{c} \begin{array}{ccccc} \varpi_1 & \varpi_2 & \varpi_3 & \varpi_4 & \varpi_5 \end{array} \\ \begin{pmatrix} (0.0, 0.0, 0.1) & (0.0, 0.0, 0.1) & (0.0, 0.0, 0.1) & (0.0, 0.0, 0.1) & (0.0, 0.0, 0.1) \\ (0.0, 0.0, 0.1) & (0.0, 0.0, 0.1) & (0.0, 0.0, 0.1) & (0.0, 0.0, 0.1) & (0.0, 0.0, 0.1) \\ (0.0, 0.0, 0.1) & (0.0, 0.0, 0.1) & (0.0, 0.0, 0.1) & (0.0, 0.0, 0.1) & (0.0, 0.0, 0.1) \\ (0.0, 0.0, 0.1) & (0.0, 0.0, 0.1) & (0.0, 0.0, 0.1) & (0.0, 0.0, 0.1) & (0.0, 0.0, 0.1) \end{pmatrix} \end{array} \\
\langle \mathcal{DM}_6, \mathcal{K} \rangle = \mathbb{DM}_6 = \begin{array}{c} \\ \varsigma_1 \\ \varsigma_2 \\ \varsigma_3 \\ \varsigma_4 \end{array} \begin{array}{c} \begin{array}{ccccc} \varpi_1 & \varpi_2 & \varpi_3 & \varpi_4 & \varpi_5 \end{array} \\ \begin{pmatrix} (0.4, 0.1, 0.6) & (0.5, 0.1, 0.2) & (0.3, 0.1, 0.2) & (0.2, 0.1, 0.9) & (0.9, 0.0, 0.2) \\ (0.8, 0.0, 0.3) & (0.7, 0.2, 0.4) & (0.5, 0.2, 0.7) & (0.6, 0.2, 0.4) & (0.3, 0.1, 0.8) \\ (0.4, 0.1, 0.5) & (0.2, 0.1, 0.5) & (0.3, 0.1, 0.7) & (0.6, 0.3, 0.4) & (0.2, 0.1, 0.8) \\ (0.6, 0.2, 0.5) & (0.4, 0.1, 0.8) & (0.5, 0.3, 0.6) & (0.1, 0.1, 0.6) & (0.4, 0.3, 0.5) \end{pmatrix} \end{array}
\end{gathered} \quad (38)$$

Thus, the collection $\{\mathbb{DM}_1, \mathbb{DM}_2, \mathbb{DM}_3, \mathbb{DM}_4, \mathbb{DM}_5, \mathbb{DM}_6\}$ gives a SFS-topology on Σ.

Step 5: The aggregated SFS matrix $\mathbb{DM}_{Agg}$ is obtained by using equation (28) and summarized as

$$\mathbb{DM}_{Agg} = \begin{array}{c} \\ \varsigma_1 \\ \varsigma_2 \\ \varsigma_3 \\ \varsigma_4 \end{array} \begin{array}{c} \begin{array}{ccccc} \quad\varpi_1\quad & \quad\varpi_2\quad & \quad\varpi_3\quad & \quad\varpi_4\quad & \quad\varpi_5\quad \end{array} \\ \begin{pmatrix} (0.47, 0.10, 0.53) & (0.57, 0.10, 0.27) & (0.57, 0.10, 0.30) & (0.50, 0.07, 0.57) & (0.77, 0.07, 0.23) \\ (0.73, 0.03, 0.33) & (0.67, 0.17, 0.40) & (0.53, 0.13, 0.53) & (0.60, 0.13, 0.37) & (0.60, 0.03, 0.43) \\ (0.53, 0.10, 0.43) & (0.47, 0.07, 0.50) & (0.57, 0.10, 0.43) & (0.63, 0.20, 0.37) & (0.47, 0.10, 0.60) \\ (0.57, 0.17, 0.47) & (0.43, 0.10, 0.67) & (0.57, 0.20, 0.40) & (0.37, 0.10, 0.50) & (0.50, 0.20, 0.47) \end{pmatrix} \end{array} \quad (39)$$

Step 6: The weighted SFS-decision matrix B is obtained by using equation (29) and written as

$$B = \begin{array}{c} \\ \varsigma_1 \\ \varsigma_2 \\ \varsigma_3 \\ \varsigma_4 \end{array} \begin{array}{c} \begin{array}{ccccc} \quad\varpi_1\quad & \quad\varpi_2\quad & \quad\varpi_3\quad & \quad\varpi_4\quad & \quad\varpi_5\quad \end{array} \\ \begin{pmatrix} (0.091, 0.019, 0.103) & (0.114, 0.020, 0.054) & (0.111, 0.019, 0.059) & (0.105, 0.015, 0.120) & (0.154, 0.014, 0.046) \\ (0.142, 0.005, 0.064) & (0.134, 0.034, 0.080) & (0.103, 0.025, 0.103) & (0.126, 0.027, 0.018) & (0.120, 0.006, 0.086) \\ (0.103, 0.019, 0.084) & (0.094, 0.014, 0.100) & (0.111, 0.019, 0.084) & (0.132, 0.042, 0.078) & (0.094, 0.020, 0.120) \\ (0.111, 0.033, 0.091) & (0.086, 0.020, 0.134) & (0.111, 0.039, 0.078) & (0.078, 0.021, 0.105) & (0.100, 0.040, 0.094) \end{pmatrix} \end{array} \quad (40)$$

Step 7: From the weighted matrix B and utilizing equations (30), (31), we obtain ideal solutions $SFSV^+$ and $SFSV^-$ are

$$\begin{aligned} SFSV^+ &= \left\{ \begin{array}{c} (0.142, 0.005, 0.064), (0.134, 0.014, 0.054), (0.111, 0.019, 0.059), \\ (0.132, 0.015, 0.078), (0.154, 0.006, 0.046) \end{array} \right\} \\ SFSV^- &= \left\{ \begin{array}{c} (0.091, 0.005, 0.103), (0.086, 0.014, 0.134), (0.103, 0.019, 0.103), \\ (0.078, 0.015, 0.120), (0.094, 0.006, 0.120) \end{array} \right\} \end{aligned} \quad (41)$$

Step 8: For each $p = 1, 2, 3, 4$, the SFS-separation measurements Ed_p^+ and Ed_p^- are calculated by using equations (32), (33) as

$$\begin{array}{ccccccc} Ed_1^+ = 0.0855 & ; & Ed_2^+ = 0.0982 & ; & Ed_3^+ = 0.1283 & ; & Ed_4^+ = 0.1484 \\ Ed_1^- = 0.1389 & ; & Ed_2^- = 0.1564 & ; & Ed_3^- = 0.0892 & ; & Ed_4^- = 0.0677 \end{array} \quad (42)$$

Step 9: Using equation (34), compute the SFS-closeness coefficients $\widehat{\mathbf{C}}_p$, for each $p = 1, 2, 3, 4$ and get

$$\hat{\mathbf{C}}_1 = 0.6190 \quad ; \quad \hat{\mathbf{C}}_2 = 0.6142 \quad ; \quad \hat{\mathbf{C}}_3 = 0.4101 \quad ; \quad \hat{\mathbf{C}}_4 = 0.3132 \quad (43)$$

Step 10: Based on the ratings of $\widehat{\mathbf{C}}_p$'s, we can obtain the ordering of the given alternatives as

$$\hat{\mathbf{C}}_1 > \hat{\mathbf{C}}_2 > \hat{\mathbf{C}}_3 > \hat{\mathbf{C}}_4 \quad (44)$$

Which corresponds to the alternatives ratings as $\varsigma_1 > \varsigma_2 > \varsigma_3 > \varsigma_4$. This, we conclude that the international company should select the student ς_1 as their candidate.

6. Comparison Analysis

In this section, the proposed algorithm is compared to the existing algorithm (Algorithm 1: Decision making based on adjustable soft discernibility matrix) [27]. Since the optimal solution of the study discussed in Section 5.2 using Algorithm 1 is also "ς_1," it can be seen that the proposed algorithm based on the group decision-making method and the extension of TOPSIS approach is comparable to previously known method, which validates the reliability and dependability of the proposed algorithm.

The advantages of the work drawn in earlier sections can be summarized as follows:

(i) Topological structures on fuzzy soft sets are used in a variety of applications, including medical diagnosis, decision-making, pattern recognition, image processing, and so on.

(ii) SFSS is one of the most generalized version of fuzzy soft set and it is arguably the more realistic, practical and accurate.

(iii) Introducing topology on SFSS is seem to be highly important in both theoretical and practical scenarios.

(iv) While dealing with group decision-making problems of SFSS, the proposed algorithm is more reliable and expressive.

7. Conclusions

The spherical fuzzy soft set is the most generalized version of all other existing fuzzy soft set models. This newest concept is more precise, accurate, and sensible and the models are thus capable of solving myriad problems more deftly and practically. In this paper, we probed into certain basic aspects of spherical fuzzy soft topological space. SFS-topology is developed by using the notions of SFS-union and SFS-intersection. The paper has also provided certain fundamental definitions pertaining to the SFS-topology including SFS-subspace, SFS-point, SFS-nbd, SFS-basis, SFS-interior, SFS-closure, SFS-boundary, and SFS-exterior and on the basis of the said definitions mooted, we have proven a few theorems. Further, SFS-separation axioms are presented by using the concepts of SFS-point, SFS-closed sets, and SFS-open sets on the basis of which an algorithm is also proposed as an application with vivid implications in group decision-making method. The model is presented as an extension of TOPSIS approach as well. A numerical example is used to illustrate the efficiency of the proposed algorithm.

In the future, we will explore algebraicproperties of SFSSs and investigate their applications in decision making, medical diagnosis, clustering analysis, pattern recognition, and information science. Also relationship between SFSSs and T-SFSSs, and the algebraic and topological structures of T-SFSSs can be studied as future work.

Data Availability

No data were used to support this study.

Ethical Approval

This article does not contain any studies with human participants or animals performed by any of the authors.

Conflicts of Interest

The authors declare that they have no conflicts of interest.

Acknowledgments

The first author is grateful to DST-FIST grant SR/FST/MS-1/2017/13 for providing technical support. Also, the second author gratefully acknowledges the financial assistance provided by the University Grants Commission (UGC) of India, and the third author would like to thank the DST, Government of India, for providing support to carry out this work under the scheme "FIST" (No. SR/FST/MS-I/2019/40).

References

[1] L. A. Zadeh, "Fuzzy sets," *Information and Control*, vol. 8, no. 3, pp. 338–353, 1965.

[2] W.-L. Gau and D. J. Buehrer, "Vague sets," *IEEE Transactions on Systems, Man, and Cybernetics*, vol. 23, no. 2, pp. 610–614, 1993.

[3] K. T. Atanassov, "Operators over interval valued intuitionistic fuzzy sets," *Fuzzy Sets and Systems*, vol. 64, no. 2, pp. 159–174, 1994.

[4] K. T. Atanassov, "Intuitionistic fuzzy sets," *Fuzzy Sets and Systems*, vol. 20, no. 1, pp. 87–96, 1986.

[5] K. Atanassov and G. Gargov, "Interval valued intuitionistic fuzzy sets," *Fuzzy Sets and Systems*, vol. 31, no. 3, pp. 343–349, 1989.

[6] R. R. Yager, "Pythagorean fuzzy subsets," *2013 Joint IFSA World Congress and NAFIPS Annual Meeting (IFSA/NAFIPS)*, pp. 57–61, IEEE, 2013.

[7] B. C. Cuong and V. Kreinovich, "Picture fuzzy sets-a new concept for computational intelligence problems," *Proceedings of 2013 Third World Congress on Information and Communication Technologies (WICT 2013)*, , pp. 1–6, IEEE, 2013.

[8] F. Kutlu Gundogdu and C. Kahraman, "Spherical fuzzy sets and spherical fuzzy TOPSIS method," *Journal of Intelligent and Fuzzy Systems*, vol. 36, no. 1, pp. 337–352, 2019.

[9] T. Mahmood, K. Ullah, Q. Khan, and N. Jan, "An approach toward decision-making and medical diagnosis problems using the concept of spherical fuzzy sets," *Neural Computing & Applications*, vol. 31, no. 11, pp. 7041–7053, 2019.

[10] S. Ashraf, S. Abdullah, T. Mahmood, F. Ghani, and T. Mahmood, "Spherical fuzzy sets and their applications in multi-attribute decision making problems," *Journal of Intelligent and Fuzzy Systems*, vol. 36, no. 3, pp. 2829–2844, 2019.

[11] M. Akram, C. Kahraman, and K. Zahid, "Group decision-making based on complex spherical fuzzy VIKOR approach," *Knowledge-Based Systems*, vol. 216, p. 106793, 2021.

[12] M. Akram, A. Khan, and F. Karaaslan, "Complex spherical dombi fuzzy aggregation operators for decision-making," *Journal of Multiple-Valued Logic and Soft Computing*, vol. 37, pp. 503–531, 2021.

[13] P. A. Ejegwa and J. M. Agbetayo, "Similarity-distance decision-making technique and its applications via intuitionistic

fuzzy pairs," *Journal of Computational and Cognitive Engineering*, 2022.
[14] M. Akram and M. Shabir, "Complex T-spherical fuzzy N-soft sets," *Intelligent and Fuzzy Techniques for Emerging Conditions and Digital Transformation*, Springer, vol. 308, pp. 819–834, , Cham, 2021.
[15] M. Akram, "Spherical fuzzy K-algebras," *Journal of Algebraic Hyperstructures and Logical Algebras*, vol. 2, no. 3, pp. 85–98, 2021.
[16] R. Khan, K. Ullah, D. Pamucar, and M. Bari, "Performance measure using a multi-attribute decision making approach based on Complex T-spherical fuzzy power aggregation operators," *Journal of Computational and Cognitive Engineering*, 2022.
[17] T. Mahmood and Z. Ali, "Prioritized Muirhead mean aggregation operators under the complex single-valued neutrosophic settings and their application in multi-attribute decision making," *Journal of Computational and Cognitive Engineering*, https://doi.org/10.47852/bonviewJCCE2022010104, 2021.
[18] D. Molodtsov, "Soft set theory-first results," *Computers & Mathematics with Applications*, vol. 37, no. 4-5, pp. 19–31, 1999.
[19] P. K. Maji, R. Biswas, and A. R. Roy, "An application of soft sets in a decision making problem," *Computers & Mathematics With Applications*, vol. 44, no. 8-9, pp. 1077–1083, 2002.
[20] Z. a. Pawlak, "Rough sets," *International Journal of Computer & Information Sciences*, vol. 11, no. 5, pp. 341–356, 1982.
[21] P. K. Maji, R. Biswas, and A. R. Roy, "Fuzzy soft sets," *Journal of Fuzzy Mathematics*, vol. 9, no. 3, pp. 589–602, 2001.
[22] P. Majumdar and S. K. Samanta, "Generalised fuzzy soft sets," *Computers & Mathematics with Applications*, vol. 59, no. 4, pp. 1425–1432, 2010.
[23] H. Garg and R. Arora, "Generalized and group-based generalized intuitionistic fuzzy soft sets with applications in decision-making," *Applied Intelligence*, vol. 48, no. 2, pp. 343–356, 2018.
[24] P. K. Maji, R. Biswas, and A. R. Roy, "Intuitionistic fuzzy soft sets," *Journal of Fuzzy Mathematics*, vol. 9, no. 3, pp. 677–692, 2001.
[25] X. Peng, Y. Yang, J. Song, and Y. Jiang, "Pythagorean fuzzy soft set and its application," *Computer Engineering*, vol. 41, no. 7, pp. 224–229, 2015.
[26] A. M. Khalil, S.-G. Li, H. Garg, H. Li, and S. Ma, "New operations on interval-valued picture fuzzy set, interval-valued picture fuzzy soft set and their applications," *IEEE Access*, vol. 7, pp. 51236–51253, 2019.
[27] F. Perveen, J. J. Sunil, K. V. Babitha, and H. Garg, "Spherical fuzzy soft sets and its applications in decision-making problems," *Journal of Intelligent and Fuzzy Systems*, vol. 37, no. 6, pp. 8237–8250, 2019.
[28] P. A. Perveen and J. J. Sunil, "A similarity measure of spherical fuzzy soft sets and its application," *AIP Publishing LLC*, vol. 2336, no. 1, 2021.
[29] C. L. Chang, "Fuzzy topological spaces," *Journal of Mathematical Analysis and Applications*, vol. 24, no. 1, pp. 182–190, 1968.
[30] R. Lowen, "Fuzzy topological spaces and fuzzy compactness," *Journal of Mathematical Analysis and Applications*, vol. 56, no. 3, pp. 621–633, 1976.
[31] D. Çoker, "An introduction to intuitionistic fuzzy topological spaces," *Fuzzy Sets and Systems*, vol. 88, no. 1, pp. 81–89, 1997.
[32] D. Coker and A. Haydar Es, "On fuzzy compactness in intuitionistic fuzzy topological spaces," *Journal of Fuzzy Mathematics*, vol. 3, pp. 899–910, 1995.
[33] D. Coker and N. Turanli, "Fuzzy connectedness in intuitionistic fuzzy topological spaces," *Fuzzy Sets and Systems*, vol. 116, no. 3, pp. 369–375, 2000.
[34] M. Olgun, M. Ünver, and Ş. Yardımcı, "Pythagorean fuzzy topological spaces," *Complex & Intelligent Systems*, vol. 5, no. 2, pp. 177–183, 2019.
[35] M. Kiruthika and P. Thangavelu, "A link between topology and soft topology," *Hacettepe Journal of Mathematics and Statistics*, vol. 48, no. 3, pp. 800–804, 2019.
[36] K. Taskopru and I. Altintas, "A new approach for soft topology and soft function via soft element," *Mathematical Methods in the Applied Sciences*, vol. 44, no. 9, pp. 7556–7570, 2021.
[37] B. Tanay and M. B. Kandemir, "Topological structure of fuzzy soft sets," *Computers & Mathematics with Applications*, vol. 61, no. 10, pp. 2952–2957, 2011.
[38] C. Gunduz and S. Bayramov, "Some results on fuzzy soft topological spaces," *Mathematical Problems in Engineering*, vol. 2013, Article ID 835308, 2013.
[39] A. Aygunoglu, V. Cetkin, and H. Aygn, "An introduction to fuzzy soft topological spaces," *Hacettepe Journal of Math. and Stat*, vol. 43, no. 2, pp. 193–204, 2014.
[40] T. Simsekler and S. Yuksel, "Fuzzy soft topological spaces," *Annals of Fuzzy Mathematics and informatics*, vol. 5, no. 1, pp. 87–96, 2013.
[41] I. Osmanoglu and D. Tokat, "On intuitionistic Fuzzy soft topology," *General Mathematics Notes*, vol. 19, no. 2, pp. 59–70, 2013.
[42] S. Bayramov and C. Gunduz, "On intuitionistic fuzzy soft topological spaces," *TWMS Journal of Pure and Applied Mathematics*, vol. 5, no. 1, pp. 66–79, 2014.
[43] M. Riaz, K. Naeem, M. Aslam, D. Afzal, F. A. A. Almahdi, and S. S. Jamal, "Multi-criteria group decision making with Pythagorean fuzzy soft topology," *Journal of Intelligent and Fuzzy Systems*, vol. 39, no. 5, pp. 6703–6720, 2020.
[44] C. L. Hwang and K. S. Yoon, *Multiple Attribute Decision Methods and Applications*", Springer, Berlin, Germany, 1981.
[45] C.-T. Chen, C.-T. Lin, and S.-F. Huang, "A fuzzy approach for supplier evaluation and selection in supply chain management," *International Journal of Production Economics*, vol. 102, no. 2, pp. 289–301, 2006.
[46] Z.-S. Chen, M. Li, W.-T. Kong, and K.-S. Chin, "Evaluation and selection of HazMat transportation alternatives: a phflts- and TOPSIS-integrated multi-perspective approach," *International Journal of Environmental Research and Public Health*, vol. 16, no. 21, p. 4116, 2019.
[47] F. E. Boran, S. Genç, M. Kurt, and D. Akay, "A multi-criteria intuitionistic fuzzy group decision making for supplier selection with TOPSIS method," *Expert Systems with Applications*, vol. 36, no. 8, pp. 11363–11368, 2009.
[48] Z.-S. Chen, Y. Yang, X.-J. Wang, K.-S. Chin, and K.-L. Tsui, "Fostering linguistic decision-making under uncertainty: a proportional interval type-2 hesitant fuzzy TOPSIS approach based on Hamacher aggregation operators and andness optimization models," "*Information Sciences*, vol. 500, pp. 229–258, 2019.
[49] E. Selim and F. Karaaslan, "A group decision making method based on TOPSIS under fuzzy soft environment," *Journal of New Theory*, vol. 3, pp. 30–40, 2015.

[50] A. Adeel, M. Akram, and A. N. A. Koam, “Group decision-making based on m-polar fuzzy linguistic TOPSIS method,” *Symmetry Plus*, vol. 11, no. 735, pp. 1–20, 2019.
[51] A. Keikha, H. Garg, and H. Mishmast Nehi, “An approach based on combining Choquet integral and TOPSIS methods to uncertain MAGDM problems,” *Soft Computing*, vol. 25, no. 10, pp. 7181–7195, 2021.
[52] H. Garg, R. Arora, and R. Arora, “TOPSIS method based on correlation coefficient for solving decision-making problems with intuitionistic fuzzy soft set information,” *AIMS Mathematics*, vol. 5, no. 4, pp. 2944–2966, 2020.
[53] Z. Xu and X. Zhang, “Hesitant fuzzy multi-attribute decision making based on TOPSIS with incomplete weight information,” *Knowledge-Based Systems*, vol. 52, pp. 53–64, 2013.
[54] J. Zhan, M. I. Ali, and N. Mehmood, “On a novel uncertain soft set model: Z -soft fuzzy rough set model and corresponding decision making methods,” *Applied Soft Computing*, vol. 56, pp. 446–457, 2017.

Hindawi
Mathematical Problems in Engineering
Volume 2022, Article ID 2766254, 11 pages
https://doi.org/10.1155/2022/2766254

Research Article

A New Approach to Study h-Hemiregular Hemirings in terms of Bipolar Fuzzy h-Ideals

Shahida Bashir ,[1] Ahmad N. Al-Kenani,[2] Rabia Mazhar,[1] and Zunaira Pervaiz[1]

[1]*Department of Mathematics, University of Gujrat, Gujrat 50700, Pakistan*
[2]*Department of Mathematics, Faculty of Science, King Abdulaziz University, P.O. Box 80219, Jeddah 21589, Saudi Arabia*

Correspondence should be addressed to Shahida Bashir; shahida.bashir@uog.edu.pk

Received 6 January 2022; Revised 7 February 2022; Accepted 2 March 2022; Published 15 April 2022

Academic Editor: Mingwei Lin

This paper provides a generalized form of ideals, that is, h-ideals of hemirings with the combination of a bipolar fuzzy set (BFS). The BFS is an extension of the fuzzy set (FS), which deals with complex and vague problems in both positive and negative aspects. The basic purpose of this paper is to introduce the idea of $(\alpha,\beta)-$bipolar fuzzy h-subhemirings (h-BFSHs), $(\alpha,\beta)-$bipolar fuzzy h-ideals (h-BFIs), and $(\alpha,\beta)-$bipolar fuzzy h-bi-ideals (h-BFbIs) in hemirings by applying the definitions of belongingness $(\in)$ and quasicoincidence (q) of the bipolar fuzzy point. We will also focus on upper and lower parts of the h-product of bipolar fuzzy subsets (BFSSs) of hemirings. In the end, we have characterized the h-hemiregular and h-intrahemiregular hemirings in terms of the $(\in,\in\vee q)-$h-BFIs and $(\in,\in\vee q)-$h-BFbIs.

1. Introduction and Motivation

In 1994, Zhang [1] introduced bipolar fuzzy set theory which is an inflation of fuzzy set theory. Bipolarity is an important idea that is mostly used in our daily life. In a lot of disciplines such as decision making, algebraic structures, graph theory, and medical science, bipolar valued fuzzy sets have become a significant research work. In real life, it is noticed that people may have a different response at a time for the same qualities of an item or a plan. One may have a positive response, and the other one may have a negative response; for example, \$100 is a big amount for a needy person, but at the same time, this amount may have less value for a rich man. Similarly, sweetness and sourness of a food, effects and side effects of medicines, good and bad human behavior, happiness and sadness, thin and thick fluid, and honesty and dishonesty all are two-sided aspects of an object or situation. See [2–10] for examples and results which are relevant to bipolar fuzzy sets.

In 1965, Zadeh [11] introduced the concept of fuzzy set theory which deals with the uncertain and complex problems in decision-making theory, medical science, engineering, automata theory, and graph theory [12–16]. The right place of entries to fuzzy set is indicated by a membership degree. In [0, 1] interval, perimeter point 0 shows no fuzzy set acceptability and 1 shows the fuzzy set acceptance. Also, (0, 1) defines the fuzzy collection to be partially belonging. If the membership degree is any property, then 1 describes that the element satisfies the property and 0 describes that the element does not satisfy the property. Interval (0, 1) shows the midway condition. But, there was a difficulty to deliberate the irrelevancy of data to the fuzzy set. The FS is extended to BFS to tackle such situations.

In 1934, Vandiver [17] firstly familiarized the theory of semiring. In 1935, Von Neumann introduced the idea of regularity in rings and showed that for any nonempty set R, if the semigroup $(R,\cdot)$ is regular, then the ring $(R,+,\cdot)$ is also regular [18]. In 1951, Bourne showed if for all $r\in R$ there exist $x,y\in R$ such that $r+rxr=ryr$, then semiring $(R,+,\cdot)$ is also regular [19]. Hemirings (semirings with zero and commutative addition) are studied in the theory of automata and formal languages [20–22]. Algebraic patterns are very important in mathematics. Hemiring is also a useful algebraic structure. It is very useful in functional analysis, physics, computation, coding, topological space, automata theory, formal language theory, mathematical modelling, and graph theory.

In the structure theory of semirings, ideals play a vital role [23]. Henriksen gave in [24] a restricted class of ideals in semirings, which is k-ideals. Another more restricted class of ideals which is h-ideals has been given in hemirings by Iizuka [25]. However, in an additively commutative semiring, ideals of a semiring coincide with "ideals" of a ring, provided that the semiring is a hemiring [26, 27]. For more applications of h-ideals, see [28, 29].

Ahsan et al. [30] presented applications of fuzzy semirings in automata theory. Since the bipolar fuzzy theory is a development of fuzzy theory, one may expect that bipolar fuzzy semirings will be useful in studying bipolar fuzzy automata theory and bipolar fuzzy languages.

1.1. Related Works. Zadeh's fuzzy set is a much innovative, crucial, and useful set due to its significance in multiple research dimensions. Fuzzy set addresses the ill-defined situations by which we are often encountered. From these ill-defined situations, we can evaluate results by using a degree of membership of the fuzzy set but the bipolar fuzzy set is a much better set to manage uncertainty, vagueness, and impreciseness than the fuzzy set. A bipolar fuzzy set is much valuable due to its degree of membership [−1,1]. Latorre [31] discussed the properties of h-ideals of hemirings and presented some suitable results with respect to hemirings. Zhan and Dudek [28] proposed a model of fuzzy h-ideals with their useful properties. They presented some algebraic properties of prime fuzzy h-hemiregular hemirings. Kumaran et al. [32] discussed some basic properties of (α, β)-level subsets of bipolar valued fuzzy subsemiring of a hemiring and their related results. We extended this useful model and introduced h-hemiregular hemiring in terms of bipolar fuzzy h-ideals.

1.2. Historical Background. The bipolar fuzzy set describes the main idea which lies in the existence of bipolarity (positivity and negativity). In fact, human decision-making consists of double sides on the positive and negative aspects, for example, competition and cooperation, effect and side effect, and hostility and friendship. In traditional Chinese medicine, "Yin" is a negative side of a system and "Yang" is a positive side of a system. The equilibrium and coexistence of the two sides are keys for prosperity and stability of a social system [33].

1.3. Motivation. Bipolarity fuzzy sets have potential impacts on many fields, including information science, neural science, computer science, artificial intelligence, decision science, economics, cognitive science, and medical science [33]. Recently, the bipolarity fuzzy set has been studied in terms of a hemiring a bit increasingly and a bit enthusiastically. That is why we have been encouraged and motivated to introduce and study h-hemiregular hemiring in terms of a bipolar fuzzy set.

1.4. Innovative Contribution. In fuzzy sets, the degree of membership was restricted to [0,1]. In our realistic life, someone may have a negative response and another one may have a positive response at the same time for the same characteristic of an object. In this regard, bipolarity is a very useful concept that is commonly used in our real-world problems. Recently, Shabir et al. presented $(\in, \in\vee q)$-fuzzy h-subhemirings and their related properties [34]. Bhakat and Das [35] firstly introduced the idea of (α, β)−fuzzy subgroups. Dudek et al. [36] worked on (α, β)−fuzzy ideals of hemirings. The idea of finite state machine on bipolar fuzzy theory is given by Jun and Kavikumar in [2]. Lee [37] introduced bipolar valued fuzzy ideals. Ibrar et al. [38] used (α, β)−bipolar fuzzy generalized bi-ideal for characterizations of regular ordered semigroups. In 2019, Shabir et al. [39] used (α, β)−bipolar fuzzy ideals and (α, β)−bipolar fuzzy bi-ideals for the characterizations of the regular and intraregular semiring. Recently, Anjum et al. [27] studied ordered h-ideals in regular semiring. Here, we have extended the study in [39] for (α, β)−h-BFSHs and (α, β)−h-BFIs of hemirings.

1.5. Organization of the Paper. In Section 1, we have familiarized ourselves with the background of bipolar fuzzy hemiring and its characterizations towards regular and intraregular hemiring. Section 2 describes the literature review of h-BFSHs, h-BFIs, and some new important definitions which is used as the basic concept for the major works. In Section 3, the concepts of (α, β)−h-BFSHs and (α, β)−h-BFIs of hemirings are discussed. In Section 4, we have worked on the upper and lower parts of BFSH by h-product. In Section 5, the description of theorems of h-hemi-regular and h-intrahemiregular hemirings in terms of the $(\in, \in\vee q)$−h-BFIs and $(\in, \in\vee q)$−h-BFbIs is given. In Section 6, the comparative study is given, and the last section consists of the conclusions and future plans.

The list of acronyms used here is given in Table 1.

2. Preliminaries

A semiring is an algebraic system $(M, +, \cdot)$ consisting of a nonempty set M together with two binary operations addition and multiplication such that $(M, +)$ and $(M, \cdot)$ are semigroups satisfying for all $u, v, w \in M$, the following distributive laws $u(v + w) = uv + uw$ and $(u + v)w = uw + vw$. By zero, we mean an element $0 \in M$ such that $0 \cdot u = u \cdot 0 = 0$ and $0 + u = u + 0 = u$ for all $u \in M$. A semiring with zero and a commutative semigroup $(M, +)$ is known as hemiring.

A nonempty subset N of a semiring M is called a subhemiring of M if N is a hemiring under the induced operations of addition and multiplication of M. A nonempty subset "N" of a hemiring M is called a left (right) ideal of M if N is closed under "+" and $mr \in N\,(rm \in N)$ for all $m \in M$ and $r \in N$, and N is called a two-sided ideal or simply an ideal of M if it is both a left and a right ideal of M.

A hemiring M is said to be h-hemiregular if, for each $x \in M$, there exist $a_1, a_2, z \in M$ such that

$x + xa_1x + z = xa_2x + z$, and M is said to be h-intra-hemiregular if, for each $x \in M$, there exist $a_i, a'_j, b_i, b'_j, z \in R$ such that $x + \sum_{i=1}^{m} a_i x^2 b_i + z = \sum_{j=1}^{n} a'_j x^2 b'_j + z$ [29]. Throughout the paper, M is hemiring unless otherwise identified.

Lemma 1 (see [29]). *If M is h-intrahemiregular iff for any left h-ideal L and right h-ideal N, $L \cap N \subseteq \overline{LN}$.*

Lemma 2 (see [29]). *If M is h-hemiregular iff for any right h-ideal L and any left h-ideal N, we have $\overline{LN} = L \cap N$.*

Definition 1 (see [1]). Let $\eta = (M, \eta_n, \eta_p)$ and $\zeta = (M, \zeta_n, \zeta_p)$ be two BFSSs of M. Then, h-product $\eta \circ_h \zeta = (M, \eta_n \circ_h \zeta_n, \eta_p \circ_h \zeta_p)$ is defined as follows:

$$\begin{aligned}
(\eta_n \circ_h \zeta_n)(u) &= \bigwedge_{u+\sum_{i=1}^{m} c_i d_i + v = \sum_{j=1}^{n} c'_j d'_j + v} \left\{\eta_n(c_i) \vee \eta_n(c'_j) \vee \zeta_n(d_i) \vee \zeta_n(d'_j)\right\},\\
(\eta_p \circ_h \zeta_p)(u) &= \bigvee_{u+\sum_{i=1}^{m} c_i d_i + v = \sum_{j=1}^{n} c'_j d'_j + v} \left\{\eta_p(c_i) \wedge \eta_p(c'_j) \wedge \zeta_p(d_i) \wedge \zeta_p(d'_j)\right\},\\
(\eta_n \circ_h \zeta_n)(u) &= 0,\\
(\eta_p \circ_h \zeta_p)(u) &= 0 \text{ if } u \text{ is not representable as } u + \sum_{i=1}^{m} c_i d_i + v = \sum_{j=1}^{n} c'_j d'_j + v.
\end{aligned} \tag{1}$$

Definition 2 (see [1]). If H is an h-subset of M. Then, the bipolar fuzzy characteristic function on H is denoted by $\chi_H = (M; \chi_{nH}, \chi_{pH})$ and is defined by $\chi_{nH}(u) = \begin{cases} -1 \text{ if } u \in H \\ 0 \text{ if } u \notin H \end{cases}$, $\chi_{pH}(u) = \begin{cases} 1 \text{ if } u \in H \\ 0 \text{ if } u \notin H \end{cases}$ for all $u \in M$. If $H = M$, then we have BFSS $M = (M; M_n, M_p)$ defined as $\widetilde{M}_n(u) = -1$ and $\widetilde{M}_p(u) = 1$ for all $u \in M$.

Definition 3 (see [1]). A BFSS $\eta = (M, \eta_n, \eta_p)$ of M is called h-BFSH of M if it satisfies the following:

(a) $\eta_n(0) \leq \eta_n(u)$ and $\eta_p(0) \geq \eta_p(u)$
(b) $\eta_n(u+v) \leq \max\{\eta_n(u), \eta_n(v)\}$ and $\eta_p(u+v) \geq \min\{\eta_p(u), \eta_p(v)\}$
(c) $\eta_n(uv) \leq \max\{\eta_n(u), \eta_n(v)\}$ and $\eta_p(uv) \geq \min\{\eta_p(u), \eta_p(v)\}$
(d) If $u + c + v = d + v$, then $\eta_n(u) \leq \max\{\eta_n(c), \eta_n(d)\}$ and $\eta_p(u) \geq \min\{\eta_p(c), \eta_p(d)\}$ for all $c, d, u, v \in M$

Definition 4. A BFSS $\eta = (M, \eta_n, \eta_p)$ of M is said to be an h-$\mathrm{BFI_L}$ (resp., h-$\mathrm{BFI_R}$) of M, if it satisfies the following:

(a) $\eta_n(u+v) \leq \max\{\eta_n(u), \eta_n(v)\}$ and $\eta_p(u+v) \geq \min\{\eta_p(u), \eta_p(v)\}$
(b) $\eta_n(uv) \leq \eta_n(v)$ and $\eta_p(uv) \geq \eta_p(v)$ (resp., $\eta_n(uv) \leq \eta_n(u)$ and $\eta_p(uv) \geq \eta_p(u)$)
(c) If $u + c + v = d + v$, then $\eta_n(u) \leq \max\{\eta_n(c), \eta_n(d)\}$ and $\eta_p(u) \geq \min\{\eta_p(c), \eta_p(d)\}$ for all $c, d, u, v \in M$

Example 1. Consider a BFSS η of a hemiring $M = \{0, 1, 2, 3, \ldots\}$ as $\eta_n(u) = \begin{cases} 0 \text{ if } u = 0 \\ -0.5 \text{ otherwise} \end{cases}$ and $\eta_p(u) = \begin{cases} 0 \text{ if } u = 0 \\ 0.5 \text{ otherwise} \end{cases}$.

Then, η is a BFI but not a h-BFI of M because if we take $x = 0, a = 1, b = 1$ and $z = 5$, then for $0 + 1 + 5 = 1 + 5$, $\eta_n(0) = 0 \geq -0.5 = \max\{\eta_n(1), \eta_n(5)\}$ and $\eta_p(0) = 0 \leq 0.5 = \min\{\eta_p(1), \eta_p(5)\}$.

Example 2. Consider a hemiring $M = \{0, a, b, c\}$ under the operations as in Tables 2 and 3.

Define a BFSS $\eta = (M, \eta_n, \eta_p)$ on M as shown in Table 4. Then, it is easy to check that η is a h-BFI of M.

Definition 5. A BFSS $\eta = (M, \eta_n, \eta_p)$ of M is called an h-BFbI of M, if is satisfies the following:

(a) $\eta_n(0) \leq \eta_n(u)$ and $\eta_p(0) \geq \eta_p(u)$
(b) $\eta_n(u+v) \leq \max\{\eta_n(u), \eta_n(v)\}$ and $\eta_p(u+v) \geq \min\{\eta_p(u), \eta_p(v)\}$
(c) $\eta_n(uv) \leq \max\{\eta_n(u), \eta_n(v)\}$ and $\eta_p(uv) \geq \min\{\eta_p(u), \eta_p(v)\}$
(d) $\eta_n(uvw) \leq \max\{\eta_n(u), \eta_n(w)\}$ and $\eta_p(uvw) \geq \min\{\eta_p(u), \eta_p(w)\}$
(e) If $u + c + v = d + v$, then $\eta_n(u) \leq \max\{\eta_n(c), \eta_n(d)\}$ and $\eta_p(u) \geq \min\{\eta_p(c), \eta_p(d)\}$ for all $c, d, u, v, w \in M$

Table 1: List of acronyms.

Acronyms	Representation
FS	Fuzzy set
BFS	Bipolar fuzzy set
BFSS	Bipolar fuzzy subset
h-BFSH	Bipolar fuzzy h-subhemiring
h-BFI	Bipolar fuzzy h-ideal
h-BFIL	Bipolar fuzzy left h-ideal
h-BFIR	Bipolar fuzzy right h-ideal
h-BFbI	Bipolar fuzzy h-bi-ideal
Iff	If and only if

Table 2: Binary addition.

+	0	a	b	c
0	0	a	b	c
a	a	a	b	c
b	b	b	b	c
c	c	c	c	b

Table 3: Binary multiplication.

.	0	a	b	c
0	0	0	0	0
a	0	b	b	b
b	0	b	b	b
c	0	b	b	b

Table 4: Values of BFSS on M.

M	0	a	b	c
η_p	0.5	0.5	0.5	0.2
η_n	−0.5	−0.5	−0.5	−0.1

Lemma 3. *If H is a left h-ideal (resp., right) of M, then $\chi_H = (M;\chi_{nH},\chi_{pH})$ is an h-BFI$_L$ (resp., h-BFI$_R$) of M.*

Proof. We have to prove the following three inequalities for left h-ideal:

(a) $\chi_{nH}(u+v) \le \max\{\chi_{nH}(u), \chi_{nH}(v)\}$ and $\chi_{pH}(u+v) \ge \min\{\chi_{pH}(u), \chi_{pH}(v)\}$
(b) $\chi_{nH}(uv) \le \chi_{nH}(v)$ and $\chi_{pH}(uv) \ge \chi_{pH}(v)$
(c) If $u+c+v = d+v$, then $\chi_{nH}(u) \le \max\{\chi_{nH}(c), \chi_{nH}(d)\}$ and $\chi_{pH}(u) \ge \min\{\chi_{pH}(c), \chi_{pH}(d)\}$ for all $c, d, u, v \in H$

For the proof of parts (a) and (b), see [2]. Here, we just prove part (c). For this, we discuss cases for all $c, d, u, v \in H, u+c+v = d+v$. □

Case 1. If $u, c, d \in H$, then $\chi_{nH}(u) = -1 = \chi_{nH}(v) = \chi_{nH}(c) = \chi_{nH}(d)$ and $\chi_{pH}(u) = 1 = \chi_{pH}(v) = \chi_{pH}(c) = \chi_{pH}(d)$.

Then, $\chi_{nH}(u) = -1 \le \max\{\chi_{nH}(c), \chi_{nH}(d)\}$ and $\chi_{pH}(u) = 1 \ge \min\{\chi_{pH}(c), \chi_{pH}(d)\}$.

Case 2. If $u, c, d \notin H$, then $\chi_{nH}(u) = 0 = \chi_{nH}(v) = \chi_{nH}(c) = \chi_{nH}(d)$ and $\chi_{pH}(u) = 0 = \chi_{pH}(v) = \chi_{pH}(c) = \chi_{pH}(d)$.

Then, $\chi_{nH}(u) = 0 \le \max\{\chi_{nH}(c), \chi_{nH}(d)\}$ and $\chi_{pH}(u) = 0 \ge \min\{\chi_{pH}(c), \chi_{pH}(d)\}$.

Case 3. If one of $u, c,$ and d does not belong to H, say $c \notin H$, then $\chi_{nH}(c) = 0 = \chi_{pH}(c)$, $\chi_{nH}(u) = -1 = \chi_{nH}(v) = \chi_{nH}(d)$, and $\chi_{pH}(u) = 1 = \chi_{pH}(v) = \chi_{pH}(d)$. This implies that $\chi_{nH}(u) = -1 \le 0 = \max\{\chi_{nH}(c), \chi_{nH}(d)\}$ and $\chi_{pH}(u) = 1 \ge 0 = \min\{\chi_{pH}(c), \chi_{pH}(d)\}$.

Case 4. If any two of $u, c,$ and d do not belong to H, say $u, c \notin H$, then $\chi_{nH}(u) = 0 = \chi_{nH}(c)$, $\chi_{pH}(u) = 0 = \chi_{pH}(c)$, $\chi_{nH}(d) = -1$, and $\chi_{pH}(d) = 1$. This implies that $\chi_{nH}(u) = 0 \le \max\{\chi_{nH}(c), \chi_{nH}(d)\}$ and $\chi_{pH}(u) = 0 \ge \min\{\chi_{pH}(c), \chi_{pH}(d)\}$.

Hence, $\chi_H = (M;\chi_{nH},\chi_{pH})$ is an h-BFI$_L$ of M.

3. (α,β) – Bipolar Fuzzy h-Ideals

In this section, we will introduce the concept of (α,β)−h-BFSHs, (α,β)−h-BFIs, and (α,β)−h-BFbIs of hemiring and properties of such kinds of ideals are discussed.

Definition 6 (see [2]). Let $(c,d) \in [-1,0) \times t(0,1]$; then, $t/(c,d)$ is called bipolar fuzzy point in M with BFSS $\eta = (M,\eta_n,\eta_p)$ of M if $\eta_p(u) = \begin{cases} d \text{ if } u = t \\ 0 \text{ if } u \ne t \end{cases}$ and $\eta_n(u) = \begin{cases} c \text{ if } u = t \\ 0 \text{ if } u \ne t \end{cases}$ for all $u, t \in M$.

Definition 7 (see [2]). A bipolar fuzzy point $t/(c,d)$ belongs to (resp., quasicoincident to) a BFSS $\eta = (M,\eta_n,\eta_p)$ as follows:

(a) $t/(c,d) \in \eta$ if $\eta_n(t) \le c$ and $\eta_p(t) \ge d$
(b) $t/(c,d) q\eta$ if $\eta_n(t) + c < -1$ and $\eta_p(t) + d > 1$
(c) $t/(c,d) \in\vee q\eta$ if $t/(c,d) \in \eta$ or $t/(c,d) q\eta$
(d) $t/(c,d) \in\wedge q\eta$ if $t/(c,d) \in \eta$ and $t/(c,d) q\eta$

In this paper, we consider $\alpha, \beta \in \{\in, q, \in\vee q, \in\wedge q\}$ and $\alpha \ne \in\wedge q$. Consider a BFSS $\eta = (R,\eta_n,\eta_p)$ such that $\eta_n(t) \ge -0.5$ and $\eta_p(t) \ge 0.5$ for all $t \in R$ and $t/(c,d) \in\wedge q\eta$. Then, $\eta_n(t) \le c$, $\eta_p(u) \ge d$, $\eta_n(t) + c < -1$, and $\eta_p(u) + d > 1$. It follows that $-1 > \eta_n(t) + c \ge \eta_n(t) + \eta_n(t) = 2\eta_n(t)$ which implies that $\eta_n(t) \le -0.5$, thus a contradiction. So, $t/(c,d)\overline{\in\wedge q}\eta$, and hence, $\alpha \ne \in\wedge q$.

Definition 8. A BFSS $\eta = (M,\eta_n,\eta_p)$ of M is said to be an (α,β)−h-BFSH of M if for all $t, u \in M$ and $(c_1,d_1), (c_2,d_2) \in [-1,0) \times t(0,1]$, it satisfies the following:

(a) $t/(c_1,d_1)\alpha\eta$ and $u/(c_2,d_2)\alpha\eta \longrightarrow t+u/(c_1 \vee c_2, d_1 \wedge d_2)\beta\eta$
(b) $t/(c_1,d_1)\alpha\eta$ and $u/(c_2,d_2)\alpha\eta \longrightarrow tu/(c_1 \vee c_2, d_1 \wedge d_2)\beta\eta$
(c) If $c, d, t, u \in M$ such that $t+c+u = d+u$, then $c/(c_1,d_1)\alpha\eta$ and $d/(c_2,d_2)\alpha\eta \longrightarrow t/(c_1 \vee c_2, d_1 \wedge d_2)\beta\eta$; here, $\alpha \ne \in\wedge q$

Definition 9. A BFSS $\eta = (M, \eta_n, \eta_p)$ of M is known as an (α,β)–h-BFI$_L$ (resp., (α,β)–h-BFI$_R$) of M if for all $t, u \in M$ and $(c_1, d_1), (c_2, d_2) \in [-1, 0) \times t(0, 1]$, it satisfies the following:

(a) $t/(c_1, d_1)\alpha\eta$ and $u/(c_2, d_2)\alpha\eta \longrightarrow t + u/(c_1 \vee c_2, d_1 \wedge d_2)\beta\eta$
(b) $t/(c_1, d_1)\alpha\eta$ and $u \in M \longrightarrow ut/(c_1, d_1)\beta\eta$ (rep. $(tu/(c_1, d_1)\beta\eta)$)
(c) If $c, d, t, u \in M$ such that $t + c + u = d + u$, then $c/(c_1, d_1)\alpha\eta$ and $d/(c_2, d_2)\alpha\eta \longrightarrow t/(c_1 \vee c_2, d_1 \wedge d_2)\beta\eta$; here, $\alpha \neq \in\wedge q$

Definition 10. A BFSS $\eta = (M, \eta_n, \eta_p)$ of M is known as an (α,β)–h-BFbI of M if for all $t, u, y \in M$ and $(c_1, d_1), (c_2, d_2) \in [-1, 0) \times t(0, 1]$, it satisfies the following:

(a) $t/(c_1, d_1)\alpha\eta$ and $u/(c_2, d_2)\alpha\eta \longrightarrow t + u/(c_1 \vee c_2, d_1 \wedge d_2)\beta\eta$
(b) $t/(c_1, d_1)\alpha\eta$ and $u/(c_2, d_2)\alpha\eta \longrightarrow tu/(c_1 \vee c_2, d_1 \wedge d_2)\beta\eta$
(c) $t/(c_1, d_1)\alpha\eta$ and $u/(c_2, d_2)\alpha\eta \longrightarrow tyu/(c_1 \vee c_2, d_1 \wedge d_2)\beta\eta$
(d) If $c, d, t, u \in M$ such that $t + c + u = d + u$, then $c/(c_1, d_1)\alpha\eta$ and $d/(c_2, d_2)\alpha\eta \longrightarrow t/(c_1 \vee c_2, d_1 \wedge d_2)\beta\eta$; here, $\alpha \neq \in\wedge q$

Throughout this paper, our main focus will be on $(\in, \in\vee q)$–h-BFSHs, $(\in, \in\vee q)$–h-BFIs, and $(\in, \in\vee q)$–h-BFBIs of M.

Lemma 4. *For a BFSS $\eta = (M, \eta_n, \eta_p)$ of M, if $c, d, t, u \in M$ such that $t + c + u = d + u$, then $c/(c_1, d_1)\alpha\eta$ and $d/(c_2, d_2)\alpha\eta \longrightarrow t/(c_1 \vee c_2, d_1 \wedge d_2)\beta\eta$; then, $\eta_n(t) \le \max\{\eta_n(c), \eta_n(d), -0.5\}$ and $\eta_p(t) \ge \min\{\eta_p(c), \eta_p(d), 0.5\}$.*

Proof. Let $c, d, t, u \in M$; then, we have the following four cases:

(i) $\max\{\eta_n(c), \eta_n(d)\} \le -0.5$ and $\min\{\eta_p(c), \eta_p(d)\} \ge 0.5$
(ii) $\max\{\eta_n(c), \eta_n(d)\} \le -0.5$ and $\min\{\eta_p(c), \eta_p(d)\} < 0.5$
(iii) $\max\{\eta_n(c), \eta_n(d)\} > -0.5$ and $\min\{\eta_p(c), \eta_p(d)\} \ge 0.5$
(iv) $\max\{\eta_n(c), \eta_n(d)\} > -0.5$ and $\min\{\eta_p(c), \eta_p(d)\} < 0.5$

Contrarily assume for $c, d \in M$, $\eta_n(t) > \max\{\eta_n(c), \eta_n(d), -0.5\}$ or $\eta_p(t) < \min\{\eta_p(c), \eta_p(d), 0.5\}$.

For case-(i): $\eta_n(t) > -0.5$ or $\eta_p(t) < 0.5$; this implies $t/(-0.5, 0.5)\overline{\in}\,\eta$. Now, consider $\max\{\eta_n(c), \eta_n(d)\} \le -0.5$ and $\min\{\eta_p(c), \eta_p(d)\} \ge 0.5$ and then $c/(-0.5, 0.5) \in \eta$ and $d/(-0.5, 0.5) \in \eta$ but for $t \in M, t/(-0.5, 0.5)\overline{\in}\,\eta$. In the same way, $t/(-0.5, 0.5)\overline{q}\eta$ because $\eta_n(t) - 0.5 > -1$ or $\eta_p(t) + 0.5 < 1$. So, $t/(-0.5, 0.5)\overline{\in\vee q}\eta$ which is a contradiction.

For case-(ii): $\eta_n(t) > -0.5$ or $\eta_p(t) < \min\{\eta_p(c), \eta_p(d)\}$; so for $s \in (0, 0.5)$, $\eta_p(t) < s = \min\{\eta_p(c), \eta_p(d)\}$ implies $t/(-0.5, s)\overline{\in}\,\eta$. Now, consider again $\max\{\eta_n(c), \eta_n(d)\} \le -0.5$ and $\min\{\eta_p(c), \eta_p(d)\} = s$ and then $c/(-0.5, s) \in \eta$ and $d/(-0.5, s) \in \eta$ but for $t \in M, t/(-0.5, s)\overline{\in}\,\eta$. In the same way, $t/(-0.5, s)\overline{q}\eta$ because $\eta_n(t) - 0.5 > -1$ or $\eta_p(t) + s < 1$. So, $t/(-0.5, s)\overline{\in\vee q}\eta$, and it contradicts our supposition.

For case-(iii): $\eta_n(t) > \max\{\eta_n(c), \eta_n(d)\}$ or $\eta_p(t) < 0.5$. So, for $r \in (-0.5, 0)$, $\eta_n(t) > r = \max\{\eta_n(c), \eta_n(d)\}$ implies $t/(r, 0.5)\overline{\in}\,\eta$. Also, $\max\{\eta_n(c), \eta_n(d)\} = r$ and $\min\{\eta_p(c), \eta_p(d)\} \ge 0.5$ and then we obtain $c/(r, 0.5) \in \eta$ and $d/(r, 0.5) \in \eta$ but for $t \in M, t/(r, 0.5)\overline{\in}\,\eta$. Similarly, $t/(r, 0.5)\overline{q}\eta$ because $\eta_n(t) + r > -1$ or $\eta_p(t) + 0.5 < 1$. Therefore, $t/(r, 0.5)\overline{\in\vee q}\eta$, which is a contradiction.

For case-(iv): $\eta_n(t) > \max\{\eta_n(c), \eta_n(d)\}$ or $\eta_p(t) < \min\{\eta_p(c), \eta_p(d)\}$. For $r \in (-0.5, 0)$ and $s \in (0, 0.5)$, $\eta_n(t) > r = \max\{\eta_n(c), \eta_n(d)\}$ and $\eta_p(t) < s = \min\{\eta_p(c), \eta_p(d)\}$ and then $t/(r, s)\overline{\in}\,\eta$. Also, $\max\{\eta_n(c), \eta_n(d)\} = r$ and $\min\{\eta_p(c), \eta_p(d)\} = s$; then, we obtain $c/(r, s) \in \eta$ and $d/(r, s) \in \eta$ but for $t \in M, t/(r, s)\overline{\in}\,\eta$. Similarly, $t/(r, s)\overline{q}\eta$ because $\eta_n(t) + r > -1$ or $\eta_p(t) + s < 1$. Therefore, $t/(r, s)\overline{\in\vee q}\eta$, which is a contradiction.

Therefore, $\eta_n(t) \le \max\{\eta_n(c), \eta_n(d), -0.5\}$ and $\eta_p(t) \ge \min\{\eta_p(c), \eta_p(d), 0.5\}$. The reverse of this theorem does not hold in general, shown by the following example. □

Example 3. Consider a BFSS η in Example 2; for $t + c + u = d + u$, η satisfies $\eta_n(t) \le \max\{\eta_n(c), \eta_n(d), -0.5\}$ and $\eta_p(t) \ge \min\{\eta_p(c), \eta_p(d), 0.5\}$. But if $c/(c_1, d_1) \in \eta$ and $d/(c_2, d_2) \in \eta$, then $t/(c_1 \vee c_2, d_1 \wedge d_2) \in\vee q\eta$ does not hold. Because for $b + 0 + c = a + c$, $0/(-0.5, 0.5) \in \eta$ and $a/(-0.5, 0.5) \in \eta$, but $b/(-0.5, 0.5)\overline{\in\vee q}\eta$ as $\eta_p(b) = 0.2 < 0.5$ and $\eta_n(b) = -0.1 > -0.5$. Also, $\eta_p(b) + 0.5 = 0.2 + 0.5 < 1$ and $\eta_n(b) + (-0.5) = -0.1 + (-0.5) > -1$ implies $b/(-0.5, 0.5)\overline{q}\eta$. So, $b/(-0.5, 0.5)\overline{\in\vee q}\eta$.

Theorem 1. *If a BFSS $\eta = (M, \eta_n, \eta_p)$ of M is an $(\in, \in\vee q)$ -h-BFSH of M, then it fulfills the following conditions for each $c, d, t, u \in M$:*

(a) $\eta_n(c + d) \le \max\{\eta_n(c), \eta_n(d), -0.5\}$ and $\eta_p(c + d) \ge \min\{\eta_p(c), \eta_p(d), 0.5\}$
(b) $\eta_n(c\ d) \le \max\{\eta_n(c), \eta_n(d), -0.5\}$ and $\eta_p(c\ d) \ge \min\{\eta_p(c), \eta_p(d), 0.5\}$
(c) For $t + c + u = d + u$, $\eta_n(t) \le \max\{\eta_n(c), \eta_n(d), -0.5\}$ and $\eta_p(t) \ge \min\{\eta_p(c), \eta_p(d), 0.5\}$

Proof. Follows from Lemma 4 and [2]. □

Theorem 2. *If a BFSS $\eta = (M, \eta_n, \eta_p)$ of M is an $(\in, \in\vee q)$ -h-BFI$_L$ (resp., $(\in, \in\vee q)$ -h-BFI$_R$) of M, then it fulfills the following conditions for each $c, d, t, u \in M$:*

(a) $\eta_n(c+d) \leq \max\{\eta_n(c), \eta_n(d), -0.5\}$ *and* $\eta_p(c+d) \geq \min\{\eta_p(c), \eta_p(d), 0.5\}$
(b) $\eta_n(c\ d) \leq \max\{\eta_n(d), -0.5\}$ *and* $\eta_p(c\ d) \geq \min\{\eta_p(d), 0.5\}$ *(resp.,* $\eta_n(c\ d) \leq \max\{\eta_n(c), -0.5\}$ *and* $\eta_p(c\ d) \geq \min\{\eta_p(c), 0.5\}$*)*
(c) *For* $t+c+u=d+u$, $\eta_n(t) \leq \max\{\eta_n(c), \eta_n(d), -0.5\}$ *and* $\eta_p(t) \geq \min\{\eta_p(c), \eta_p(d), 0.5\}$

Proof: Follows from Lemma 4 and [2]. □

Theorem 3. *If a BFSS* $\eta = (M, \eta_n, \eta_p)$ *of* M *is an* $(\in, \in\vee q)$*-h-BFbI of* M*, then it fulfills the following conditions for each* $c, d, t, u \in M$*:*

(a) $\eta_n(c+d) \leq \max\{\eta_n(c), \eta_n(d), -0.5\}$ *and* $\eta_p(c+d) \geq \min\{\eta_p(c), \eta_p(d), 0.5\}$
(b) $\eta_n(c\ d) \leq \max\{\eta_n(c), \eta_n(d), -0.5\}$ *and* $\eta_p(c\ d) \geq \min\{\eta_p(c), \eta_p(d), 0.5\}$
(c) $\eta_n(cb\ d) \leq \max\{\eta_n(c), \eta_n(d), -0.5\}$ *and* $\eta_p(cb\ d) \geq \min\{\eta_p(c), \eta_p(d), 0.5\}$
(d) *For* $t+c+u=d+u$, $\eta_n(t) \leq \max\{\eta_n(c), \eta_n(d), -0.5\}$ *and* $\eta_p(t) \geq \min\{\eta_p(c), \eta_p(d), 0.5\}$

Proof: Follows from Lemma 4 and [2]. □

4. Upper and Lower Parts of a Bipolar Fuzzy Set

In the following segment, we have offered the definitions and several stimulating outcomes regarding the upper parts and lower parts of h-BFSS.

Definition 11. (see [2]). If $\eta = (M, \eta_n, \eta_p)$ is a bipolar fuzzy h-set in M, then the upper part $\eta^+ = (M, \eta_n^+, \eta_p^+)$ of η is written as $(\eta_n^+)(t) = (\eta_n)(t) \wedge -0.5$ and $(\eta_p^+)(t) = (\eta_p)(t) \vee 0.5$. The lower part of η is denoted by $\eta^- = (M, \eta_n^-, \eta_p^-)$ and is defined as $(\eta_n^-)(t) = (\eta_n)(t) \vee -0.5$ and $(\eta_p^-)(t) = (\eta_p)(t) \wedge 0.5$ for all $t \in M$.

Lemma 5. *Let* $\eta = (M, \eta_n, \eta_p)$ *and* $\zeta = (M, \zeta_n, \zeta_p)$ *be two BFSHs in M. Then, the following equations hold:*

(a) $(\eta \wedge \zeta)^- = \eta^- \wedge \zeta^-$
(b) $(\eta \vee \zeta)^- = \eta^- \vee \zeta^-$
(c) $(\eta \circ_h \zeta)^- = \eta^- \circ_h \zeta^-$

Proof: Straightforward. □

Lemma 6. *Let* $\eta = (M, \eta_n, \eta_p)$ *and* $\zeta = (M, \zeta_n, \zeta_p)$ *be two BFSHs in M. Then, the following equations hold:*

(a) $(\eta \wedge \zeta)^+ = \eta^+ \wedge \zeta^+$
(b) $(\eta \vee \zeta)^+ = \eta^+ \vee \zeta^+$
(c) $(\eta \circ_h \zeta)^+ = \eta^+ \circ_h \zeta^+$

Proof: Straightforward. □

Lemma 7. *For an* $(\in, \in\vee q)$*–h-BFI*$_R$ $\eta = (M, \eta_n, \eta_p)$ *and* $(\in, \in\vee q)$*–h-BFI*$_L$ $\zeta = (M, \zeta_n, \zeta_p)$*, then we have* $(\eta \circ_h \zeta)^- \leq (\eta \wedge \zeta)^-$.

Proof: Let $t \in M$ if $(\eta \circ_h \zeta)(t) = 0$, that is, $(\eta_n \circ_h \zeta_n)(t) = 0$, and then $(\eta_n \circ_h \zeta_n)^-(t) = 0 \vee -0.5 = 0 \geq (\eta_n \vee \zeta_n)^-(t)$ and $(\eta_p \circ_h \zeta_p)(t) = 0$ indicates $(\eta_p \circ_h \zeta_p)^-(t) = 0 \wedge 0.5 = 0 \leq (\eta_p \wedge \zeta_p)^-(t)$. Otherwise,

$$
\begin{aligned}
(\eta_n \circ_h \zeta_n)^-(t) &= (\eta_n \circ_h \zeta_n)(t) \vee -0.5 \\
&= \bigwedge_{t+\sum_{i=1}^{m} a_i b_i + v = \sum_{j=1}^{n} c_j d_j + v} \left\{ \left\{ \bigvee_{i=1}^{m} \eta_n(a_i) \right\} \vee \left\{ \bigvee_{i=1}^{m} \zeta_n(b_i) \right\} \vee \left\{ \bigvee_{j=1}^{n} \eta_n(c_j) \right\} \vee \left\{ \bigvee_{j=1}^{n} \zeta_n(d_j) \right\} \right\} \vee -0.5 \\
&= \bigwedge_{t+\sum_{i=1}^{m} a_i b_i + v = \sum_{j=1}^{n} c_j d_j + v} \left\{ \begin{array}{l} \left\{ \bigvee_{i=1}^{m} (\eta_n(a_i) \vee -0.5) \right\} \vee \left\{ \bigvee_{i=1}^{m} (\zeta_n(b_i) \vee -0.5) \right\} \vee \\ \left\{ \bigvee_{j=1}^{n} (\eta_n(c_j) \vee -0.5) \right\} \vee \left\{ \bigvee_{j=1}^{n} (\zeta_n(d_j) \vee -0.5) \right\} \end{array} \right\} \vee -0.5 \\
&\geq \bigwedge_{t+\sum_{i=1}^{m} a_i b_i + v = \sum_{j=1}^{n} c_j d_j + v} \left\{ \begin{array}{l} \left\{ \bigvee_{i=1}^{m} \eta_n(a_i b_i) \right\} \vee \left\{ \bigvee_{i=1}^{m} \zeta_n(a_i b_i) \right\} \vee \\ \left\{ \bigvee_{j=1}^{n} \eta_n(c_j d_j) \right\} \vee \left\{ \bigvee_{j=1}^{n} \zeta_n(c_j d_j) \right\} \end{array} \right\} \vee -0.5
\end{aligned}
$$

$$
\begin{aligned}
&= \bigwedge_{t+\sum_{i=1}^{m} a_i b_i + v = \sum_{j=1}^{n} c_j d_j + v} \left\{ \begin{array}{l} \left\{ \bigvee_{i=1}^{m} \left(\eta_n (a_i b_i) \vee -0.5\right) \right\} \vee \left\{ \bigvee_{i=1}^{m} \left(\zeta_n (a_i b_i) \vee -0.5\right) \right\} \vee \\ \left\{ \bigvee_{j=1}^{n} \left(\eta_n \left(c_j d_j\right) \vee -0.5\right) \right\} \vee \left\{ \bigvee_{j=1}^{n} \left(\zeta_n \left(c_j d_j\right) \vee -0.5\right) \right\} \end{array} \right\} \vee -0.5 \\
&\geq \bigwedge_{t+\sum_{i=1}^{m} a_i b_i + v = \sum_{j=1}^{n} c_j d_j + v} \left\{ \begin{array}{l} \eta_n \left(\sum_{i=1}^{m} a_i b_i \right) \vee \zeta_n \left(\sum_{i=1}^{m} a_i b_i \right) \vee \\ \eta_n \left(\sum_{j=1}^{n} c_j d_j \right) \vee \zeta_n \left(\sum_{j=1}^{n} c_j d_j \right) \end{array} \right\} \vee -0.5 \\
&= \left(\eta_n \vee \zeta_n\right)(t) \vee -0.5.
\end{aligned}
\tag{2}
$$

This implies $\left(\eta_n \circ_h \zeta_n\right)^{-}(t) \geq \left(\eta_n \vee \zeta_n\right)^{-}(t)$.

Similarly, $\left(\eta_p \circ_h \zeta_p\right)^{-}(t) \leq \left(\eta_p \wedge \zeta_p\right)^{-}(t)$.

Hence, $\left(\eta \circ_h \zeta\right)^{-} \leq \left(\eta \wedge \zeta\right)^{-}$. □

Definition 12. If H is an h-subset of M, the upper part $\chi_H^{+} = \left(M; \chi_{nH}^{+}, \chi_{pH}^{+}\right)$ of the bipolar fuzzy characteristic function $\chi_H = \left(M; \chi_{nH}, \chi_{pH}\right)$ of H is defined by the following:

$$
\begin{aligned}
\chi_{nH}^{+}(t) &= \begin{cases} -1 \text{ if } t \in H, \\ -0.5 \text{ if } t \notin H, \end{cases} \\
\chi_{pH}^{+}(t) &= \begin{cases} 1 \text{ if } t \in H, \\ 0.5 \text{ if } t \notin H. \end{cases}
\end{aligned}
\tag{3}
$$

Similarly, the lower part $\chi_H^{-} = \left(M; \chi_{nH}^{-}, \chi_{pH}^{-}\right)$ of the bipolar fuzzy characteristic function $\chi_H = \left(M; \chi_{nH}, \chi_{pH}\right)$ of H is defined by the following:

$$
\begin{aligned}
\chi_{nH}^{-}(t) &= \begin{cases} -0.5 \text{ if } t \in H, \\ 0 \text{ if } t \notin H, \end{cases} \\
\chi_{pH}^{-}(t) &= \begin{cases} 0.5 \text{ if } t \in H, \\ 0 \text{ if } t \notin H. \end{cases}
\end{aligned}
\tag{4}
$$

For all $t \in M$, if $H = M$, then we have BFSS $M = \left(M; M_n, M_p\right)$ defined as $\widetilde{M}_n(t) = -1$ and $\widetilde{M}_p(t) = 1$ for all $t \in M$.

Lemma 8. *Let E and F be two nonempty h-subsets of M. Then, the following results hold:*

(a) $\left(\chi_E \wedge \chi_F\right)^{-} = \chi_{E \cap F}^{-}$

(b) $\left(\chi_E \vee \chi_F\right)^{-} = \chi_{E \cup F}^{-}$

(c) $\left(\chi_E \circ_h \chi_F\right)^{-} = \chi_{\overline{EF}}^{-}$

Proof: Proofs of (a) and (b) are straightforward. Here is just a proof of (c).

Suppose $t \in M$ and $t \in \overline{EF}$. Then, $\chi_{n\overline{EF}}(t) = -0.5$ and $\chi_{p\overline{EF}}(t) = 0.5$. For $t \in \overline{EF}$, $t + \sum_{i=1}^{m} a_i b_i + v = \sum_{j=1}^{n} c_j d_j + v$ where $a_i, c_j \in E$ and $b_i, d_j \in F$.; then, we have $\chi_{nE}(a_i) = -1$, $\chi_{pE}(c_j) = 1$, $\chi_{nF}(b_i) = -1$, and $\chi_{pF}(d_j) = 1$.

Consider the following:

$$
\begin{aligned}
\left(\chi_{nE} \circ_h \chi_{nF}\right)^{-}(t) &= \bigwedge_{t+\sum_{i=1}^{m} a_i b_i + v = \sum_{j=1}^{n} c_j d_j + v} \left\{ \begin{array}{l} \left(\bigvee_{i=1}^{m} \chi_{nE}(a_i) \right) \vee \left(\bigvee_{i=1}^{m} \chi_{nF}(b_i) \right) \\ \vee \left(\bigvee_{j=1}^{n} \chi_{nE}(c_j) \right) \vee \left(\bigvee_{j=1}^{n} \chi_{nF}(d_j) \right) \end{array} \right\} \vee -0.5 \\
&= \{(-1) \vee (-1) \vee (-1) \vee (-1)\} \vee -0.5 = -0.5 \\
&= \chi_{n\overline{EF}}^{-}(t).
\end{aligned}
\tag{5}
$$

Now,

$$\left(\chi_{pE}\circ_{h}\chi_{pF}\right)^{-}(t)=\bigvee_{t+\sum_{i=1}^{m}a_ib_i+v=\sum_{j=1}^{n}c_jd_j+v}\left\{\begin{array}{c}\left(\bigwedge_{i=1}^{m}\chi_{nE}(a_i)\right)\wedge\left(\bigwedge_{i=1}^{m}\chi_{nF}(b_i)\right)\\ \wedge\left(\bigwedge_{j=1}^{n}\chi_{nE}(c_j)\right)\wedge\left(\bigwedge_{j=1}^{n}\chi_{nF}(d_j)\right)\end{array}\right\}\wedge 0.5$$
$$=\{(1)\wedge(1)\wedge(1)\wedge(1)\}\wedge 0.5=0.5$$
$$=\chi_{p\overline{EF}}^{-}(t). \tag{6}$$

Hence, $(\chi_E\circ_h\chi_F)^{-}=\chi_{\overline{EF}}^{-}$.

If $t\notin\overline{EF}$, then $\chi_{n\overline{EF}}(t)=0$ and also $\chi_{p\overline{EF}}(t)=0$.

Then, $(\chi_{nE}\circ_h\chi_{nF})^{-}(t)=(\chi_{nE}\circ_h\chi_{nF})(t)\vee-0.5=0\vee-0.5=0=\chi_{n\overline{EF}}^{-}(t)$.

And, $(\chi_{pE}\circ_h\chi_{pF})^{-}(t)=(\chi_{pE}\circ_h\chi_{pF})(t)\wedge 0.5=0\wedge 0.5=0=\chi_{p\overline{EF}}^{-}(t)$.

That is, $(\chi_E\circ_h\chi_F)^{-}=\chi_{\overline{EF}}^{-}$. □

Lemma 9. *If H is left (resp., right) h-ideal of M, then $\chi_H^{-}=(M;\chi_{nH}^{-},\chi_{pH}^{-})$ is $(\in,\in\vee q)$–h-BFI$_L$ (resp., $(\in,\in\vee q)$–h-BFI$_R$) of M.*

Proof: Straightforward. □

Lemma 10. *If H is h-bi-ideal of M, then $\chi_H^{-}=(M;\chi_{nH}^{-},\chi_{pH}^{-})$ is $(\in,\in\vee q)$–h-BFbI of M.*

Proof: Straightforward. □

5. h-Hemiregular and h-Intrahemiregular Hemirings

In this section, by using the h-BFIs, theorems on hemiregular and intrahemiregular hemirings are presented.

Theorem 4. *Suppose M is a hemiring, then the following subsequent conditions are identical:*

(a) M is h-hemiregular

(b) $(\eta\wedge\zeta)^{-}=(\eta\circ_h\zeta)^{-}$ for all $(\in,\in\vee q)$–h-BFI$_R$ $\eta=(M,\eta_n,\eta_p)$ and $(\in,\in\vee q)$–h-BFI$_L$ $\zeta=(M,\zeta_n,\zeta_p)$ of M

Proof: Let M be an h-hemi-regular hemiring. For each $t\in M$, there exist $x_1,x_2,y\in M$ such that $t+tx_1t+y=tx_2t+y$; then,

$$\left(\eta_n\circ_h\zeta_n\right)^{-}(t)=\bigwedge_{t+\sum_{i=1}^{m}a_ib_i+v=\sum_{j=1}^{n}c_jd_j+v}\left\{\begin{array}{c}\left(\bigvee_{i=1}^{m}\eta_n(a_i)\right)\vee\left(\bigvee_{i=1}^{m}\zeta_n(b_i)\right)\\ \vee\left(\bigvee_{j=1}^{n}\eta_n(c_j)\right)\vee\left(\bigvee_{j=1}^{n}\zeta_n(d_j)\right)\end{array}\right\}\vee-0.5$$
$$\leq\{\eta_n(tx_1)\vee\zeta_n(t)\vee\eta_n(tx_2)\vee\zeta_n(t)\}\vee-0.5$$
$$\leq\{(\eta_n(t)\vee-0.5)\vee\zeta_n(t)\vee(\eta_n(t)\vee-0.5)\vee\zeta_n(t)\}\vee-0.5$$
$$=\{(\eta_n(t)\vee\zeta_n(t)\}\vee-0.5$$
$$=(\eta_n\vee\zeta_n)^{-}(t). \tag{7}$$

In the same way, $(\eta_p\circ_h\zeta_p)^{-}(t)\geq(\eta_p\wedge\zeta_p)^{-}(t)$.

Thus, $(\eta\wedge\zeta)^{-}\leq(\eta\circ_h\zeta)^{-}$. But, we have $(\eta\circ_h\zeta)^{-}\leq(\eta\wedge\zeta)^{-}$ by Lemma 7. Hence, $(\eta\wedge\zeta)^{-}=(\eta\circ_h\zeta)^{-}$.

Conversely, $(\eta\wedge\zeta)^{-}=(\eta\circ_h\zeta)^{-}$ for all $(\in,\in\vee q)$–h-BFI$_R$ $\eta=(M,\eta_n,\eta_p)$ and $(\in,\in\vee q)$–h-BFI$_L$ $\zeta=(M,\zeta_n,\zeta_p)$ of M. Let E and F be right h-ideal and left h-ideal of M correspondingly. Formerly, the lower parts of the bipolar fuzzy characteristic function $\chi_E^{-}=(M;\chi_{nE},\chi_{pE})$ are an $(\in,\in\vee q)$–h-BFI$_R$ and $\chi_F^{-}=(M;\chi_{nF},\chi_{pF})$ are an $(\in,\in\vee q)$–h-BFI$_L$ of M. Therefore, by our supposition, $(\chi_E\wedge\chi_F)^{-}=(\chi_E\circ\chi_F)^{-}$. This indicates that $\chi_{E\cap F}^{-}=\chi_{\overline{EF}}$ implies $E\cap F=\overline{EF}$. Therefore, by Lemma 2, M is h-hemiregular. □

Theorem 5. *For a hemiring M, the following subsequent conditions are identical:*

(a) M is h-hemiregular

(b) $(\eta\wedge\zeta\wedge\upsilon)^{-}\leq(\eta\circ_h\zeta\circ_h\upsilon)^{-}$ for each $(\in,\in\vee q)$–h-BFI$_R$ $\eta=(M,\eta_n,\eta_p)$, for all $(\in,\in\vee q)$–h-BFI $\zeta=(M,\zeta_n,\zeta_p)$ and for all $(\in,\in\vee q)$–h-BFI$_L$ $\upsilon=(M,\upsilon_n,\upsilon_p)$ of M

Proof: Same as Theorem 4. □

Theorem 6. *Suppose M is hemiring, then the following conditions are equivalent:*

(a) M is h-hemiregular

(b) $(\eta \wedge \zeta)^- \leq (\eta \circ_h \zeta)^-$ for all $(\in, \in \vee q)$–h-BFbI $\eta = (M, \eta_n, \eta_p)$ and for all $(\in, \in \vee q)$–h-BFI$_L$ $\zeta = (M, \zeta_n, \zeta_p)$ of M

(c) $(\eta \wedge \zeta)^- \leq (\eta \circ_h \zeta)^-$ for all $(\in, \in \vee q)$–h-BFI$_R$ $\eta = (M, \eta_n, \eta_p)$ and for all $(\in, \in \vee q)$–h-BFbI $\zeta = (M, \zeta_n, \zeta_p)$ of M

Proof: (a) ⟶ (b): Let M be an h-hemiregular. For each $t \in M$, there exists $x_1, x_2, y \in M$ such that $t + t x_1 t + y = t x_2 t + y$; then,

$$\begin{aligned}
(\eta_n \circ_h \zeta_n)^-(t) &= \bigwedge_{t + \sum_{i=1}^m a_i b_i + v = \sum_{j=1}^n c_j d_j + v} \left\{ \begin{array}{c} \left(\bigvee_{i=1}^m \eta_n(a_i) \right) \vee \left(\bigvee_{i=1}^m \zeta_n(b_i) \right) \\ \vee \left(\bigvee_{j=1}^n \eta_n(c_j) \right) \vee \left(\bigvee_{j=1}^n \zeta_n(d_j) \right) \end{array} \right\} \vee -0.5 \\
&\leq \{\eta_n(t) \vee \zeta_n(x_1 t) \vee \eta_n(t) \vee \zeta_n(x_2 t)\} \vee -0.5 \\
&\leq \{\eta_n(t) \vee (\zeta_n(t) \vee -0.5) \vee \eta_n(t) \vee (\zeta_n(t) \vee -0.5)\} \vee -0.5 \\
&= \{(\eta_n(t) \vee \zeta_n(t)\} \vee -0.5 \\
&= (\eta_n \vee \zeta_n)^-(t).
\end{aligned} \tag{8}$$

In the same way, $(\eta_p \circ_h \zeta_p)^-(t) \geq (\eta_p \wedge \zeta_p)^-(t)$. Thus, $(\eta \wedge \zeta)^- \leq (\eta \circ_h \zeta)^-$.

(b) ⟶ (a): Let $\eta = (M, \eta_n, \eta_p)$ be a $(\in, \in \vee q)$–h-BFI$_R$ and $\zeta = (M, \zeta_n, \zeta_p)$ be a $(\in, \in \vee q)$–h-BFI$_L$ of M. Since each $(\in, \in \vee q)$–h-BFI$_R$ is $(\in, \in \vee q)$–h-BFbI of M, by (a), we obtain $(\eta \wedge \zeta)^- \leq (\eta \circ_h \zeta)^-$ but by Lemma 7, $(\eta \circ_h \zeta)^- \leq (\eta \wedge \zeta)^-$. Hence, $(\eta \wedge \zeta)^- = (\eta \circ_h \zeta)^-$, and by Theorem 4, M is h-hemiregular. Similarly, we can prove (a) ⟶ (c) and (c) ⟶ (a). □

Theorem 7. *For a hemiring M, the following subsequent conditions are equivalent:*

(a) M is h-intrahemiregular

(b) $(\eta \wedge \zeta)^- \leq (\eta \circ_h \zeta)^-$ for all $(\in, \in \vee q)$–h-BFI$_L$ $\eta = (M, \eta_n, \eta_p)$ and for all $(\in, \in \vee q)$–h-BFI$_R$ $\zeta = (M, \zeta_n, \zeta_p)$ of M

Proof: Assume M is h-intrahemiregular hemiring. For every $t \in M$, there exists $x_i, z_i, x'_j, z'_j, y \in M$ such that $t + \sum_{i=1}^n x_i t^2 z_i + v = \sum_{j=1}^m x'_j t^2 z'_j + v$.

$$\begin{aligned}
(\eta_n \circ_h \zeta_n)^-(t) &= \bigwedge_{t + \sum_{i=1}^m a_i b_i + v = \sum_{j=1}^n c_j d_j + v} \left\{ \begin{array}{c} \left(\bigvee_{i=1}^m \eta_n(a_i) \right) \vee \left(\bigvee_{i=1}^m \zeta_n(b_i) \right) \\ \vee \left(\bigvee_{j=1}^n \eta_n(c_j) \right) \vee \left(\bigvee_{j=1}^n \zeta_n(d_j) \right) \end{array} \right\} \vee -0.5 \\
&\leq \left\{ \eta_n(x_i t) \vee \zeta_n(t z_i) \vee \eta_n\left(x_j t\right) \vee \zeta_n\left(t z_j\right) \right\} \vee -0.5 \\
&\leq \{(\eta_n(t) \vee -0.5) \vee (\zeta_n(t) \vee -0.5) \vee (\eta_n(t) \vee -0.5) \vee (\zeta_n(t) \vee -0.5)\} \vee -0.5 \\
&= \{(\eta_n(t) \vee \zeta_n(t)\} \vee -0.5 \\
&= (\eta_n \vee \zeta_n)^-(t).
\end{aligned} \tag{9}$$

In the same way, $(\eta_p \circ_h \zeta_p)^-(t) \geq (\eta_p \wedge \zeta_p)^-(t)$.

Thus, $(\eta \wedge \zeta)^- \leq (\eta \circ_h \zeta)^-$.

Conversely, assume E and F are left and right h-ideal of M, respectively. The lower parts of the bipolar fuzzy characteristic function of E and F, $\chi_E^- = (M, \chi_{nE}^-, \chi_{pE}^-)$ and $\chi_F^- = (M, \chi_{nF}^-, \chi_{pF}^-)$, are $(\in, \in \vee q)$–h-BFI$_L$ and $(\in, \in \vee q)$–h-BFI$_R$ of M, respectively. Now, from our supposition, $(\chi_E \wedge \chi_F)^- \leq (\chi_E \circ_h \chi_F)^-$. Also, $\chi_{E \cap F}^- = (\chi_E \wedge \chi_F)^- \leq (\chi_E \circ_h \chi_F)^- = \chi_{\overline{EF}}^-$ which suggests that $E \cap F \subseteq \overline{EF}$. From Lemma 1, M is h-intrahemiregular. □

6. Comparative Study and Discussion

In [2], Shabir et al. used regular and intraregular semirings with the help of (α, β)−BFIs. We extended the work of [2] to hemirings with the help of (α, β)−h-BFIs. Semiring with zero and commutative addition is hemiring. We have characterized h-hemiregular and h-intrahemiregular hemirings by using (α, β)−h-BFIs. As h-ideal is a more restricted form of ideal, our extension is more applicable than the approach discussed in [2].

7. Conclusion

BFS is a dominant tool of mathematics to resolve the uncertainty in positive as well as a negative aspect of the data. In this paper, basic concepts, operations, and related properties with respect to (α, β)−h-BFIs are proposed. Generally, we have proved with an example that if a BFSS η of M is an $(\in, \in\vee q)$−h-BFI of M, then it satisfies three particular conditions, but the reverse may not hold. Also, we have studied the lower and upper parts of $(\in, \in\vee q)$−h-BFI of hemirings. We have characterized h-hemiregular and h-intrahemiregular hemirings by using (α, β)−h-BFIs.

The bipolar fuzzy set has membership degree ranges from −1 to 1, but we often face such critical situations in real life which cannot be handled by bipolar fuzzy sets due to their membership degree [−1,1]. To control these critical situations, Pythagorean fuzzy sets are more useful because of the sum of its membership degree and nonmembership degree which can be greater than 1.

In the future, we will extend this work for hyperstructures, LA-semigroups, near-rings, etc. We will utilize this proposed bipolar fuzzy model to enhance these studies such as fuzzy stochastic data envelopment analysis model, intuitionistic fuzzy linear regression model, bounded linear programs with trapezoidal fuzzy numbers, interval-valued trapezoidal fuzzy number, fuzzy arc waves based on artificial bee colony algorithm, and fuzzy efficiency measures in data envelopment analysis. In addition, we will study its real-life applications in medical science, computer science, management science, and many other fields.

Data Availability

No data were used to support the study.

Conflicts of Interest

The authors declare that they have no conflicts of interest.

Authors' Contributions

Conceptualization was performed by S. B. and R. M. Methodology was prepared by Zu. Software was implemented by S. B. Validation was done by A. N. A. -K. Formal analysis was carried out by Zu. Investigation and data curation were done by R. M. Resources were obtained by A. N. A. -K. Original draft preparation was performed by Zu. Review and editing were conducted by S. B. and R. M. Visualization was done by R. M. Supervision was done by S. B. Project administration was performed by Zu. Funding acquisition was done by A. N. A. -K. All authors have read and agreed to the published version of the manuscript.

References

[1] W. R. Zhang, "Bipolar fuzzy sets and relations: a computational framework for cognitive modeling and multiagent decision analysis," in *Proceedings of the Fuzzy Information Processing Society Biannual Conference, 1994. Industrial Fuzzy Control and Intelligent Systems Conference, and the NASA Joint Technology Workshop on Neural Networks and Fuzzy Logic*, pp. 305–309, IEEE, San Antonio, TX, USA, 1994, December.

[2] Y. B. Jun and J. Kavikumar, "Bipolar fuzzy finite state machines," *Bull. Malays. Math. Sci. Soc*, vol. 34, no. 1, pp. 181–188, 2011.

[3] M. Zhou and S. Li, "Application of bipolar fuzzy sets in semirings," *Journal of Mathematical Research with Applications*, vol. 34, no. 1, pp. 61–72, 2014.

[4] M. Shabir, T. Abbas, S. Bashir, and R. Mazhar, "Bipolar fuzzy hyperideals in regular and intra-regular semihypergroups," *Computational and Applied Mathematics*, vol. 40, no. 6, pp. 1–20, 2021.

[5] S. Bashir, R. Mazhar, H. Abbas, and M. Shabir, "Regular ternary semirings in terms of bipolar fuzzy ideals," *Computational and Applied Mathematics*, vol. 39, no. 4, pp. 1–18, 2020.

[6] M. A. Mehmood, M. Akram, M. G. Alharbi, and S. Bashir, "Optimization of-type fully bipolar fuzzy linear programming problems," *Mathematical Problems in Engineering*, vol. 2021, Article ID 1199336, 36 pages, 2021.

[7] M. A. Mehmood, M. Akram, M. G. Alharbi, and S. Bashir, "Solution of fully bipolar fuzzy linear programming models," *Mathematical Problems in Engineering*, vol. 2021, Article ID 9961891, 31 pages, 2021.

[8] M. Saqib, M. Akram, and S. Bashir, "Certain efficient iterative methods for bipolar fuzzy system of linear equations," *Journal of Intelligent and Fuzzy Systems*, vol. 39, pp. 1–15, 2020, Preprint.

[9] M. Saqib, M. Akram, S. Bashir, and T. Allahviranloo, "Numerical solution of bipolar fuzzy initial value problem," *Journal of Intelligent and Fuzzy Systems*, vol. 40, pp. 1–32, 2021, Preprint.

[10] M. Saqib, M. Akram, S. Bashir, and T. Allahviranloo, "A Runge–Kutta numerical method to approximate the solution of bipolar fuzzy initial value problems," *Computational and Applied Mathematics*, vol. 40, no. 4, pp. 1–43, 2021.

[11] L. A. Zadeh, "Fuzzy sets," *Information and Control*, vol. 8, no. 3, pp. 338–353, 1965.

[12] M. Lin, Q. Zhan, and Z. Xu, "Decision making with probabilistic hesitant fuzzy information based on multiplicative consistency," *International Journal of Intelligent Systems*, vol. 35, no. 8, pp. 1233–1261, 2020.

[13] M. Lin, C. Huang, R. Chen, H. Fujita, and X. Wang, "Directional correlation coefficient measures for Pythagorean fuzzy sets: their applications to medical diagnosis and cluster analysis," *Complex & Intelligent Systems*, vol. 7, no. 2, pp. 1025–1043, 2021.

[14] M. Lin, X. Li, R. Chen, H. Fujita, and J. Lin, "Picture fuzzy interactional partitioned Heronian mean aggregation operators: an application to MADM process," *Artificial Intelligence Review*, vol. 55, pp. 1–38, 2021.

[15] M. Lin, Z. Chen, R. Chen, and H. Fujita, "Evaluation of startup companies using multicriteria decision making based on hesitant fuzzy linguistic information envelopment analysis models," *International Journal of Intelligent Systems*, vol. 36, no. 5, pp. 2292–2322, 2021.

[16] Z. Yang, M. Lin, Y. Li, W. Zhou, and B. Xu, "Assessment and selection of smart agriculture solutions using an information error based Pythagorean fuzzy cloud algorithm," *International Journal of Intelligent Systems*, vol. 36, no. 11, pp. 6387–6418, 2021.

[17] H. S. Vandiver, "Note on a simple type of algebra in which the cancellation law of addition does not hold," *Bulletin of the American Mathematical Society*, vol. 40, no. 12, pp. 914–920, 1934.

[18] J. Von Neumann, "On regular rings," *Proceedings of the National Academy of Sciences of the United States of America*, vol. 22, 1935.

[19] S. Bourne, "The Jacobson radical of a semiring," *Proceedings of the National Academy of Sciences of the United States of America*, vol. 37, 1951.

[20] A. W. Aho and J. D. Ullman, *Intutionistic to Automata Theory, Languages and Computation,* Addison-Wesley, Massachusetts, MA, USA, 1979.

[21] J. S. Golan, *Semirings and Their Applications*, Kluwer Academic Publishers, Netherlands, 1999.

[22] I. Simon, *The Nondeterministic Complexity of Finite Automaton*, In: Notes Hermes, Paris, 1990.

[23] J. S. Golan, *Semirings and Affine Equations over Them: Theory and Applications*, Springer Science Business Media, Berlin, Germany, 2013.

[24] M. Henriksen, "Ideals in semirings with commutative addition," *Amer. Math. Soc. Notices*, vol. 6, p. 321, 1958.

[25] K. Iizuka, "On the Jacobson radical of a semiring," *Tohuku Math. J.,* vol. 11, no. 2, pp. 409–421, 1959.

[26] X. Ma, Y. Yin, and J. Zhan, "Characterizations of h-intra-and h-quasi-hemiregular hemirings," *Computers & Mathematics with Applications*, vol. 63, no. 4, pp. 783–793, 2012.

[27] R. Anjum, S. Ullah, Y. M. Chu, M. Munir, N. Kausar, and S. Kadry, "Characterizations of ordered h-regular semirings by ordered h-ideals," *AIMS Mathematics*, vol. 5, no. 6, pp. 5768–5790, 2020.

[28] J. Zhan and W. A. Dudek, "Fuzzy h-ideals of hemirings," *Information Sciences*, vol. 177, no. 3, pp. 876–886, 2007.

[29] Y. Yin and H. Li, "The characterizations of h-hemiregular hemirings and h-intra-hemiregular hemirings," *Information Sciences*, vol. 178, no. 17, pp. 3451–3464, 2008.

[30] J. Ahsan, J. N. Mordeson, and M. Shabir, "Fuzzy ideals of semirings," in *Fuzzy Semirings with Applications to Automata Theory*vol. 278, Berlin, Germany, Springer, 2012.

[31] N. Kumaran, K. Arjunan, and B. Ananth, "Level subsets of bipolar valued fuzzy subhemiring of a hemiring," *Malaya Journal of Matematik*, vol. 6, no. 1, pp. 230–235, 2018.

[32] D. R. Latorre, "On h-ideals and k-ideals in hemirings," *Publicationes Mathematicae*, vol. 12, p. 219, 1965.

[33] J. Chen, S. Li, S. Ma, and X. Wang, "M-polar fuzzy sets: an extension of bipolar fuzzy sets," *The Scientific World Journal*, Hindawi Publishing Corporation, vol. 2014, Article ID 416530, 8 pages, 2014.

[34] M. Shabir, Y. Nawaz, and T. Mahmood, "Characterizations of hemirings by $\in$, $\in \vee q$)-fuzzy ideals," *East Asian Mathematical Journal*, vol. 31, pp. 1–18, 2015.

[35] S. K. Bhakat and P. Das, "On the definition of a fuzzy subgroup," *Fuzzy Sets and Systems*, vol. 51, no. 2, pp. 235–241, 1992.

[36] W. A. Dudek, M. Shabir, and M. I. Ali, "(α, β)-fuzzy ideals of hemirings," *Computers & Mathematics with Applications*, vol. 58, no. 2, pp. 310–321, 2009.

[37] K. M. Lee, "Bipolar-valued fuzzy sets and their operations," in *Proceedings of the International Conference on Intelligent Technologies*, pp. 307–312, Bangkok, Thailand, 2000.

[38] M. Ibrar, A. Khan, and B. Davvaz, "Characterizations of regular ordered semigroups in terms of (α, β)-bipolar fuzzy generalized bi-ideals," *Journal of Intelligent and Fuzzy Systems*, vol. 33, no. 1, pp. 365–376, 2017.

[39] M. Shabir, S. Liaquat, and S. Bashir, "Regular and intra-regular semirings in terms of bipolar fuzzy ideals," *Computational and Applied Mathematics*, vol. 38, no. 4, 2019.

Hindawi
Mathematical Problems in Engineering
Volume 2023, Article ID 9851279, 1 page
https://doi.org/10.1155/2023/9851279

Retraction

Retracted: Method for Fuzzy Number Intuitionistic Fuzzy Multiple Attribute Decision Making and Its Application to Blended Classroom Teaching Reform Effect Evaluation

Mathematical Problems in Engineering

Received 26 September 2023; Accepted 26 September 2023; Published 27 September 2023

This article has been retracted by Hindawi following an investigation undertaken by the publisher [1]. This investigation has uncovered evidence of one or more of the following indicators of systematic manipulation of the publication process:

(1) Discrepancies in scope
(2) Discrepancies in the description of the research reported
(3) Discrepancies between the availability of data and the research described
(4) Inappropriate citations
(5) Incoherent, meaningless and/or irrelevant content included in the article
(6) Peer-review manipulation

The presence of these indicators undermines our confidence in the integrity of the article's content and we cannot, therefore, vouch for its reliability. Please note that this notice is intended solely to alert readers that the content of this article is unreliable. We have not investigated whether authors were aware of or involved in the systematic manipulation of the publication process.

Wiley and Hindawi regrets that the usual quality checks did not identify these issues before publication and have since put additional measures in place to safeguard research integrity.

We wish to credit our own Research Integrity and Research Publishing teams and anonymous and named external researchers and research integrity experts for contributing to this investigation.

The corresponding author, as the representative of all authors, has been given the opportunity to register their agreement or disagreement to this retraction. We have kept a record of any response received.

References

[1] X. Sun, "Method for Fuzzy Number Intuitionistic Fuzzy Multiple Attribute Decision Making and Its Application to Blended Classroom Teaching Reform Effect Evaluation," *Mathematical Problems in Engineering*, vol. 2022, Article ID 3907871, 14 pages, 2022.

Hindawi
Mathematical Problems in Engineering
Volume 2022, Article ID 3907871, 14 pages
https://doi.org/10.1155/2022/3907871

Research Article

Method for Fuzzy Number Intuitionistic Fuzzy Multiple Attribute Decision Making and Its Application to Blended Classroom Teaching Reform Effect Evaluation

Xia Sun

Department of Internet, Jiaxing Vocational & Technical College, Jiaxing 314000, Zhejiang, China

Correspondence should be addressed to Xia Sun; sunxia@jxvtc.edu.cn

Received 6 January 2022; Revised 21 January 2022; Accepted 12 February 2022; Published 8 March 2022

Academic Editor: Mingwei Lin

With the continuous development of mobile Internet and educational technology, the deep integration of education and Internet has a great impact on the education concept and teaching mode. The mixed teaching based on Rain Classroom is the specific application of new educational technology in the teaching of Internet plus education. Most of the students in ethnic universities come from the central and western ethnic regions. In addition, the evaluation of blended classroom teaching reform effect is looked as the classical multiple attribute decision making (MADM). We extend the dual MSM (DMSM) operator with fuzzy number intuitionistic fuzzy numbers (FNIFNs) to build the fuzzy number intuitionistic fuzzy dual MSM (FNIFDMSM) operator and fuzzy number intuitionistic fuzzy weighted DMSM (FNIFWDMSM) equation in this study. A few MADM operators are built with FNIFWDMSM operator. Finally, taking blended classroom teaching reform effect evaluation as an useful example, this paper illustrates the depicted approach.

1. Introduction

In 1965, Zadeh [1] proposed the fuzzy sets (FSs) to fuse information in the fuzzy information domain [2–6]. To extend the FSs, the intuitionistic fuzzy sets (IFSs) [7] were also proposed. Subsequently, FS and its corresponding extension are investigated in more and more decision-making analysis domains [8–15]. At the same time, more and more methods are built to solve the different MADM issues [16–22] and MAGDM issues [23–28]. Su et al. [29] proposed the interactive dynamic IF-MAGDM. Arya and Yadav [30] proposed the intuitionistic fuzzy super-efficiency measure. Tian et al. [31] defined the partial derivative and complete differential of binary intuitionistic fuzzy functions. Garg [32] proposed the cosine similarity measure under given IFSs. Tan [33] proposed the Choquet-TOPSIS tools for IF-MADM. Zhao et al. [34] defined the Interactive intuitionistic fuzzy methods for multilevel programming problems. Li [35] proposed the GOWA operators to MADM under IFSs. Buyukozkan et al. [36] selected the transportation decision schemes with the intuitionistic fuzzy Choquet method. Joshi et al. [37] proposed the given dissimilarity measure along with IFSs. De and Sana [38] solved the random demand models along with Bonferroni operator under IFSs. Li et al. [39] devised the given VIKOR-based dynamic IF-MADM. Niroomand [40] solved the multiobjective linear programming with IFSs. Yu et al. [41] defined the derivatives and differentials for multiplicative IFSs. Yu [42] proposed the prioritized geometric means under IFSs. Wu and Zhang [43] solved the IF-MADM with weighted entropy. Verma and Sharma [44] built the inaccuracy measure for IF-MADM. Furthermore, Liu and Yuan [45] proposed the fuzzy number IFSs (FNIFSs) along with the IFSs. The membership and non-membership of IFSs are [0, 1], and the sum of membership and non-membership of IFSs is less than one. Different from the IFSs, the membership and non-membership of FNIFSs are triangular fuzzy sets (TFSs). Thus, The FNIFSs could well depict the uncertainties and fuzziness during the real-life decision issues. Fan [46] built the FNIFHPWG function to make evaluation about knowledge innovation ability. Wang and Wang [47] defined the FNIFHCG operator under FNIFSs. Chen and Wang [48] defined the IFNIFHOWA operator for project performance evaluation. Wang and Yu [49] defined the FNIFHCA function to evaluate the rural landscape design projects. Lu [50] built the IFNIFHCG operator for international competitiveness assessment. Wang [51] defined some useful operational laws along with FNIFSs based on the arithmetic operators. Zhao et al. [52] defined the FNIFHPWA function for appraising the software performance. Li et al. [53] built the information entropy and similarity measure with FNIFSs. Wang [54] proposed the geometric means under FNIFSs. Li [55] expanded the generalized Maclaurin symmetric mean (GMSM) equation under FNIFNs to establish the fuzzy number intuitionistic fuzzy GMSM (FNIFGMSM) equation and fuzzy number intuitionistic fuzzy weighted GMSM (FNIFWGMSM) equation.

Nevertheless, all the given functions and useful tools proposed by these scholars do not take into account the relationship between given parameters [56–60]. To conquer these given shortcomings, the crucial purpose of such given article is to combine the FNIFSs with DMSM means [61] to propose several novel fused tools under FNIFSs. The motivations of the paper can be summarized as follows: (1) the DMSM formula is utilized to build several DMSM fused formulas with FNIFNs: FNIFDMSM operator and FNIFWDMSM operator; (2) the FNIFDMSM operator and FNIFWDMSM operator method is proposed to solve the MADM problems with FNIFNs; (3) a case study for blended classroom teaching reform effect evaluation is supplied to show the developed approach; and (4) some comparative studies are provided with the existing methods. The rest of the paper is organized as follows. Several basic concepts of FNIFSs and DMSM means are given in Section 2. The DMSM means with FNIFSs are given in Section 3. An instance about blended classroom teaching reform effect evaluation is given in Section 4. The conclusions are drawn in Section 5.

2. Preliminaries

In this section, we introduce the definition of FNIFSs [32] and the DMSM operator.

2.1. FNIFSs. Liu and Yuan [45] built the FNIFS, and the membership and non-membership are depicted under TFNs.

Definition 1 (see [45]). Suppose $E = \{e_1, e_2, \ldots, e_n\}$ is a given fixed set and B is a given FNIFS on E, and its mathematical expression is

$$B = \in \{\langle e, T_B(e), F_B(e)\rangle e \in E\}. \tag{1}$$

$T_B(e)$, $F_B(e)$ are two given TFNs between 0 and 1, and $T_B(e) = (X(e), Y(e), Z(e)), e \longrightarrow [0,1]$, $F_B(e) = (A(e), S(e), D(e)), e \longrightarrow [0,1]$, $0 \leq Z(e) + D(e) \leq 1$, $\forall e \in E$. Let $T_B(e) = (X(e), Y(e), Z(e))$, $F_B(e) = (A(e), S(e), D(e))$, so $Q(e) = \langle (X(e), Y(e), Z(e)), (A(e), S(e), D(e))\rangle$, and $Q(e)$ is viewed as a given FNIFN.

Definition 2 (see [51, 54]). $Q(e_i) = \langle (X(e_i), Y(e_i), Z(e_i)), (A(e_i), S(e_i), D(e_i))\rangle$ and $Q(e_j) = \langle (X(e_j), Y(e_j), Z(e_j)), (A(e_j), S(e_j), D(e_j))\rangle$ are two given FNIFNs; consequently,

(1) $$Q(e_i) \oplus Q(e_j) = \left\{\begin{pmatrix} X(e_i) + X(e_j) - X(e_i)X(e_j) \\ Y(e_i) + Y(e_j) - Y(e_i)Y(e_j) \\ Z(e_i) + Z(e_j) - Z(e_i)Z(e_j) \end{pmatrix}, \begin{pmatrix} A(e_i)A(e_j) \\ S(e_i)S(e_j) \\ D(e_i)D(e_j) \end{pmatrix}\right\}.$$

(2) $$Q(e_i) \otimes Q(e_j) = \left\{\left(\begin{pmatrix} X(e_i)X(e_j) \\ Y(e_i)Y(e_j) \\ Z(e_i)Z(e_j) \end{pmatrix}\right), \left(\begin{pmatrix} A(e_i) + A(e_j) - A(e_i)A(e_j) \\ S(e_i) + S(e_j) - S(e_i)S(e_j) \\ D(e_i) + D(e_j) - D(e_i)D(e_j) \end{pmatrix}\right)\right\}.$$

(3) $$\lambda Q(e_i) = \left\{\begin{pmatrix} 1 - (1 - X(e_i))^{\lambda} \\ 1 - (1 - Y(e_i))^{\lambda} \\ 1 - (1 - Z(e_i))^{\lambda} \end{pmatrix}, \begin{pmatrix} (A(e_i))^{\lambda} \\ (S(e_i))^{\lambda} \\ (D(e_i))^{\lambda} \end{pmatrix}\right\}, \lambda \geq 0.$$

(4) $$(Q(e_i))^{\lambda} = \left\{\begin{pmatrix} (X(e_i))^{\lambda} \\ (Y(e_i))^{\lambda} \\ (Z(e_i))^{\lambda} \end{pmatrix}, \begin{pmatrix} 1 - (1 - A(e_i))^{\lambda} \\ 1 - (1 - S(e_i))^{\lambda} \\ 1 - (1 - D(e_i))^{\lambda} \end{pmatrix}\right\}, \lambda \geq 0.$$

Definition 3 (see [51, 54]). Let $Q(e) = \langle (X(e), Y(e), Z(e)), (A(e), S(e), D(e))\rangle$ be a given FNIFN, and the score function of $Q(e)$ is depicted as

$$SF(Q(e)) = \frac{X(e) + 2Y(e) + Z(e)}{4} - \frac{A(e) + 2S(e) + D(e)}{4}, \quad SF(Q(e)) \in [-1, 1]. \tag{2}$$

Definition 4 (see [51, 54]). Let $Q(e) = \langle (X(e), Y(e), Z(e)), (A(e), S(e), D(e))\rangle$ be the given FNIFN, and an accuracy function of $Q(e)$ is defined as

$$AH(Q(e)) = \frac{X(e) + 2Y(e) + Z(e)}{4} + \frac{A(e) + 2S(e) + D(e)}{4}, \quad AH(Q(e)) \in [0, 1]. \tag{3}$$

Based on $SF(Q(e))$ and $AH(Q(e))$, let us look at the size comparison of the two FNIFNs.

Definition 5 (see [51, 54]). Let $Q(e_1)$ and $Q(e_2)$ be two FNIFNs; then, if $SF(Q(e_1)) < SF(Q(e_2))$, then $Q(e_1) < Q(e_2)$; if $SF(Q(e_1)) = SF(Q(e_2))$, then

(1) If $AH(Q(e_1)) = AH(Q(e_2))$, then $Q(e_1) = Q(e_2)$.

(2) If $AH(Q(e_1)) < AH(Q(e_2))$, then $Q(e_1) < Q(e_2)$.

2.2. DMSM Operators. Qin and Liu [61] proposed the dual MSM (DMSM) operator considering both the MSM and the dual operation.

Definition 6. (see [61]). Let $a_i\,(i = 1, 2, \ldots, n)$ be a couple of non-negative real numbers, and $\lambda_1, \lambda_2, \ldots, \lambda_k \geq 0$. If

$$DMSM^{(k)}(x_1, x_2, \ldots, x_n) = \frac{1}{k}\left(\prod_{1 \leq i_1 < \ldots < i_k \leq i_n}\left(\sum_{j=1}^{k} x_{i_j}\right)^{(1/C_n^k)}\right), \tag{4}$$

then we name $DM\ SM^{(k)}$ as dual MSM (DMSM) operator, where $(i_1, i_2, \ldots, i_k)$ changes all the k-tuple information combinations of $(1, 2, \ldots, n)$ and C_n^k is the mathematical binomial coefficient value.

3. FNIFDMSM and FNIFWDMSM Operators

3.1. The FNIFDMSM Operator. The DMSM is built to coalesce all given FNIFNs, and the fuzzy number intuitionistic fuzzy DMSM (FNIFDMSM) operators are built.

Definition 7. Let $Q(e_m) = \langle (X(e_m), Y(e_m), Z(e_m)), (A(e_m), S(e_m), D(e_m))\rangle, m = 1, 2, \ldots k$, be a couple of given FNIFNs. The FNIFGMSM operator could be defined as

$$FNIFDMSM^{(k)}(Q(e_1), Q(e_2), \ldots, Q(e_n)) = \frac{1}{k}\left(\underset{1 \leq i_1 < \ldots < i_k \leq i_n}{\otimes}\left(\bigoplus_{j=1}^{n} Q\left(e_{i_j}\right)\right)^{(1/C_n^k)}\right). \tag{5}$$

Theorem 1. *Let $Q(e_m) = \langle (X(e_m), Y(e_m), Z(e_m)), (A(e_m), S(e_m), D(e_m))\rangle, m = 1, 2, \ldots k$, be a set of FNIFNs. The obtained value from FNIFDMSM is still an FNIFN.*

$$\begin{aligned}
&FNIFDMSM^{(k)}(Q(e_1), Q(e_2), \ldots, Q(e_n))\\
&= \frac{1}{k}\left(\underset{1 \leq i_1 < \cdots < i_k \leq i_n}{\otimes}\left(\bigoplus_{j=1}^{n} Q\left(e_{i_j}\right)\right)^{(1/C_n^k)}\right),\\
&= \left\{\begin{pmatrix}
1 - \left(1 - \prod\limits_{1 \leq i_1 < \cdots < i_k \leq i_n}\left(1 - \prod\limits_{j=1}^{k}\left(1 - X\left(e_{i_j}\right)\right)\right)^{(1/C_n^k)}\right)^{(1/k)},\\
1 - \left(1 - \prod\limits_{1 \leq i_1 < \cdots < i_k \leq i_n}\left(1 - \prod\limits_{j=1}^{k}\left(1 - Y\left(e_{i_j}\right)\right)\right)^{(1/C_n^k)}\right)^{(1/k)},\\
1 - \left(1 - \prod\limits_{1 \leq i_1 < \ldots < i_k \leq i_n}\left(1 - \prod\limits_{j=1}^{k}\left(1 - Z\left(e_{i_j}\right)\right)\right)^{(1/C_n^k)}\right)^{(1/k)}
\end{pmatrix}, \begin{pmatrix}
\left(1 - \prod\limits_{1 \leq i_1 < \cdots < i_k \leq i_n}\left(1 - \prod\limits_{j=1}^{k}\left(A\left(e_{i_j}\right)\right)\right)^{(1/C_n^k)}\right)^{(1/k)},\\
\left(1 - \prod\limits_{1 \leq i_1 < \cdots < i_k \leq i_n}\left(1 - \prod\limits_{j=1}^{k}\left(S\left(e_{i_j}\right)\right)\right)^{(1/C_n^k)}\right)^{(1/k)},\\
\left(1 - \prod\limits_{1 \leq i_1 < \cdots < i_k \leq i_n}\left(1 - \prod\limits_{j=1}^{k}\left(D\left(e_{i_j}\right)\right)\right)^{(1/C_n^k)}\right)^{(1/k)}
\end{pmatrix}\right\}.
\end{aligned} \tag{6}$$

Proof. From Definition 2, we can derive

$$\bigoplus_{j=1}^{n} Q\left(e_{i_j}\right) = \left\{\begin{matrix}
\left(1 - \prod\limits_{j=1}^{k}\left(1 - X\left(e_{i_j}\right)\right), 1 - \prod\limits_{j=1}^{k}\left(1 - Y\left(e_{i_j}\right)\right), 1 - \prod\limits_{j=1}^{k}\left(1 - Z\left(e_{i_j}\right)\right)\right),\\
\left(\prod\limits_{j=1}^{k}\left(A\left(e_{i_j}\right)\right), \prod\limits_{j=1}^{k}\left(S\left(e_{i_j}\right)\right), \prod\limits_{j=1}^{k}\left(D\left(e_{i_j}\right)\right)\right)
\end{matrix}\right\}. \tag{7}$$

Thus,

$$\left(\bigoplus_{j=1}^{n} Q\left(e_{i_j}\right)\right)^{\left(1/C_n^k\right)} = \left\{ \begin{array}{l} \left(\left(1-\prod_{j=1}^{k}\left(1-X\left(e_{i_j}\right)\right)\right)^{\left(1/C_n^k\right)}, \left(1-\prod_{j=1}^{k}\left(1-Y\left(e_{i_j}\right)\right)\right)^{\left(1/C_n^k\right)}, \left(1-\prod_{j=1}^{k}\left(1-Z\left(e_{i_j}\right)\right)\right)^{\left(1/C_n^k\right)} \right) \\ \left(1-\left(1-\prod_{j=1}^{k}\left(A\left(e_{i_j}\right)\right)\right)^{\left(1/C_n^k\right)}, 1-\left(1-\prod_{j=1}^{k}\left(S\left(e_{i_j}\right)\right)\right)^{\left(1/C_n^k\right)}, 1-\left(1-\prod_{j=1}^{k}\left(D\left(e_{i_j}\right)\right)\right)^{\left(1/C_n^k\right)} \right) \end{array} \right\}. \tag{8}$$

Thereafter,

$$\bigotimes_{1 \le i_1 < \cdots < i_k \le i_n} \left(\bigoplus_{j=1}^{n} Q\left(e_{i_j}\right)\right)^{\left(1/C_n^k\right)} = \left\{ \left(\begin{array}{l} \prod_{1 \le i_1 < \cdots < i_k \le i_n} \left(1-\prod_{j=1}^{k}\left(1-X\left(e_{i_j}\right)\right)\right)^{\left(1/C_n^k\right)} \\ \prod_{1 \le i_1 < \cdots < i_k \le i_n} \left(1-\prod_{j=1}^{k}\left(1-Y\left(e_{i_j}\right)\right)\right)^{\left(1/C_n^k\right)} \\ \prod_{1 \le i_1 < \cdots < i_k \le i_n} \left(1-\prod_{j=1}^{k}\left(1-Z\left(e_{i_j}\right)\right)\right)^{\left(1/C_n^k\right)} \end{array} \right), \left(\begin{array}{l} 1-\prod_{1 \le i_1 < \cdots < i_k \le i_n} \left(1-\prod_{j=1}^{k}\left(A\left(e_{i_j}\right)\right)\right)^{\left(1/C_n^k\right)} \\ 1-\prod_{1 \le i_1 < \cdots < i_k \le i_n} \left(1-\prod_{j=1}^{k}\left(S\left(e_{i_j}\right)\right)\right)^{\left(1/C_n^k\right)} \\ 1-\prod_{1 \le i_1 < \cdots < i_k \le i_n} \left(1-\prod_{j=1}^{k}\left(D\left(e_{i_j}\right)\right)\right)^{\left(1/C_n^k\right)} \end{array} \right) \right\}. \tag{9}$$

Furthermore,

$$FNIFDMSM^{(k)}\left(Q\left(e_1\right), Q\left(e_2\right), \ldots, Q\left(e_n\right)\right) = \frac{1}{k}\left(\bigotimes_{1 \le i_1 < \cdots < i_k \le i_n} \left(\bigoplus_{j=1}^{n} Q\left(e_{i_j}\right)\right)^{\left(1/C_n^k\right)}\right)$$

$$= \left\{ \left(\begin{array}{l} 1-\left(1-\prod_{1 \le i_1 < \cdots < i_k \le i_n} \left(1-\prod_{j=1}^{k}\left(1-X\left(e_{i_j}\right)\right)\right)^{\left(1/C_n^k\right)}\right)^{(1/k)}, \\ 1-\left(1-\prod_{1 \le i_1 < \cdots < i_k \le i_n} \left(1-\prod_{j=1}^{k}\left(1-Y\left(e_{i_j}\right)\right)\right)^{\left(1/C_n^k\right)}\right)^{(1/k)}, \\ 1-\left(1-\prod_{1 \le i_1 < \cdots < i_k \le i_n} \left(1-\prod_{j=1}^{k}\left(1-Z\left(e_{i_j}\right)\right)\right)^{\left(1/C_n^k\right)}\right)^{(1/k)} \end{array} \right), \left(\begin{array}{l} \left(1-\prod_{1 \le i_1 < \cdots < i_k \le i_n} \left(1-\prod_{j=1}^{k}\left(A\left(e_{i_j}\right)\right)\right)^{\left(1/C_n^k\right)}\right)^{(1/k)}, \\ \left(1-\prod_{1 \le i_1 < \cdots < i_k \le i_n} \left(1-\prod_{j=1}^{k}\left(S\left(e_{i_j}\right)\right)\right)^{\left(1/C_n^k\right)}\right)^{(1/k)}, \\ \left(1-\prod_{1 \le i_1 < \cdots < i_k \le i_n} \left(1-\prod_{j=1}^{k}\left(D\left(e_{i_j}\right)\right)\right)^{\left(1/C_n^k\right)}\right)^{(1/k)} \end{array} \right) \right\} \tag{10}$$

Hence, (6) is kept.

Then, we can prove that (11) is an FNIFN. We shall check the following two conditions:

(i) $(X(e), Y(e), Z(e)) \subseteq [0,1]$, $(A(e), S(e), D(e)) \subseteq [0,1]$.

(ii) $0 \le Z(e) + D(e) \le 1$. □

Proof

(i) Since $0 \leq X(e_{i_j}) \leq 1$, we get

$$0 \leq \prod_{j=1}^{k}\left(1 - X\left(e_{i_j}\right)\right) \leq 1 \text{ and } 0 \leq 1 - \prod_{j=1}^{k}\left(1 - X\left(e_{i_j}\right)\right) \leq 1. \tag{11}$$

Then,

$$0 \leq 1 - \prod_{1 \leq i_1 < \cdots < i_k \leq i_n}\left(1 - \prod_{j=1}^{k}\left(1 - X\left(e_{i_j}\right)\right)\right)^{\left(1/C_n^k\right)} \leq 1. \tag{12}$$

Thus,

$$0 \leq 1 - \left(1 - \prod_{1 \leq i_1 < \cdots < i_k \leq i_n}\left(1 - \prod_{j=1}^{k}\left(1 - X\left(e_{i_j}\right)\right)\right)^{\left(1/C_n^k\right)}\right)^{(1/k)} \leq 1. \tag{13}$$

That means $X(e) = 1 - (1 - \prod_{1 \leq i_1 < \cdots < i_k \leq i_n}(1 - \prod_{j=1}^{k}(1 - X(e_{i_j})))^{(1/C_n^k)})^{(1/k)} \subseteq [0,1]$. Similarly, we can get $(Y(e), Z(e)) \subseteq [0,1]$, and $(A(e), S(e), D(e)) \subseteq [0,1]$, so (1) is kept.

(2) For $Z(e_{i_j}) + D(e_{i_j}) \leq 1$, then we can have $D(e_{i_j}) \leq 1 - Z(e_{i_j})$, and thus

$$\begin{aligned}
0 &\leq Z(e) + D(e) \\
&= 1 - \left(1 - \prod_{\substack{1 \leq i_1 < \ldots \\ < i_k \leq i_n}}\left(1 - \prod_{j=1}^{k}\left(1 - Z\left(e_{i_j}\right)\right)\right)^{\left(1/C_n^k\right)}\right)^{(1/k)} + \left(1 - \prod_{\substack{1 \leq i_1 < \ldots \\ < i_k \leq i_n}}\left(1 - \prod_{j=1}^{k}\left(D\left(e_{i_j}\right)\right)\right)^{\left(1/C_n^k\right)}\right)^{(1/k)} \\
&\leq 1 - \left(1 - \prod_{\substack{1 \leq i_1 < \ldots \\ < i_k \leq i_n}}\left(1 - \prod_{j=1}^{k}\left(1 - Z\left(e_{i_j}\right)\right)\right)^{\left(1/C_n^k\right)}\right)^{(1/k)} + \left(1 - \prod_{\substack{1 \leq i_1 < \ldots \\ < i_k \leq i_n}}\left(1 - \prod_{j=1}^{k}\left(1 - Z\left(e_{i_j}\right)\right)\right)^{\left(1/C_n^k\right)}\right)^{(1/k)} \\
&= 1.
\end{aligned} \tag{14}$$

□

Example 1. Let $Q(e_1) = \langle(0.1, 0.2, 0.3), (0.2, 0.5, 0.6)\rangle$, $Q(e_2) = \langle(0.2, 0.3, 0.3), (0.2, 0.5, 0.5)\rangle$, and $Q(e_3) = \langle(0.4, 0.5, 0.5), (0.3, 0.4, 0.4)\rangle$ be three FNIFNs, and suppose $k = 2$; then, according to (10), we derive

$$\begin{aligned}
&FNIFDMSM^{(k)}\left(Q(e_1), Q(e_2), \ldots, Q(e_n)\right) = \frac{1}{k}\left(\underset{1 \leq i_1 < \cdots < i_k \leq i_n}{\otimes}\left(\bigoplus_{j=1}^{n} Q\left(e_{i_j}\right)\right)^{\left(1/C_n^k\right)}\right) \\
&= \left\{\begin{array}{c}
\left(\begin{array}{l}
1 - \left(1 - ((1-(1-0.1)\times(1-0.2))\times(1-(1-0.1)\times(1-0.4))\times(1-(1-0.2)\times(1-0.4)))^{\left(1/C_3^2\right)}\right)^{(1/2)} \\
1 - \left(1 - ((1-(1-0.2)\times(1-0.3))\times(1-(1-0.2)\times(1-0.5))\times(1-(1-0.3)\times(1-0.5)))^{\left(1/C_3^2\right)}\right)^{(1/2)} \\
1 - \left(1 - ((1-(1-0.3)\times(1-0.3))\times(1-(1-0.3)\times(1-0.5))\times(1-(1-0.3)\times(1-0.5)))^{\left(1/C_3^2\right)}\right)^{(1/2)}
\end{array}\right), \\
\left(\begin{array}{l}
\left(1 - ((1-0.2\times0.2)\times(1-0.2\times0.3)\times(1-0.2\times0.3))^{\left(1/C_3^2\right)}\right)^{(1/2)} \\
\left(1 - ((1-0.5\times0.5)\times(1-0.5\times0.4)\times(1-0.5\times0.4))^{\left(1/C_3^2\right)}\right)^{(1/2)} \\
\left(1 - ((1-0.6\times0.5)\times(1-0.6\times0.4)\times(1-0.5\times0.4))^{\left(1/C_3^2\right)}\right)^{(1/2)}
\end{array}\right)
\end{array}\right\} \\
&= \langle(0.2294, 0.3335, 0.3672), (0.2311, 0.4659, 0.4978)\rangle.
\end{aligned} \tag{15}$$

Then, we discuss some better properties for FNIFDMSM.

Property 1 (idempotency). If $Q(e_i) = \langle (X(e_i), Y(e_i), Z(e_i)), (A(e_i), S(e_i), D(e_i))\rangle\, (i = 1, 2, \ldots, n)$ are same, then

$$FNIFDMSM^{(k)}(Q(e_1), Q(e_2), \ldots, Q(e_n)) = Q(e). \tag{16}$$

Property 2 (monotonicity). Let $Q(e_i) = \langle (X(e_i), Y(e_i), Z(e_i)), (A(e_i), S(e_i), D(e_i))\rangle\, (i = 1, 2, \ldots, n)$ and $Q(e_j) = \langle (X(e_j), Y(e_j), Z(e_j)), (A(e_j), S(e_j), D(e_j))\rangle\, (j = 1, 2, \ldots, n)$ be two sets of FNIFNs. If $X(e_i) \le X(e_j), Y(e_i) \le Y(e_j), Z(e_i) \le Z(e_j), A(e_i) \ge A(e_j), S(e_i) \ge S(e_j), D(e_i) \ge D(e_j)$ hold for all i, j, then

$$\begin{aligned} &FNIFDMSM^{(k)}\left(Q\left(e_{i_1}\right), Q\left(e_{i_2}\right), \ldots, Q\left(e_{i_n}\right)\right) \\ &\quad \le FNIFDMSM^{(k)}\left(Q\left(e_{j_1}\right), Q\left(e_{j_2}\right), \ldots, Q\left(e_{j_n}\right)\right). \end{aligned} \tag{17}$$

Property 3 (boundedness). Let $Q(e_i) = \langle (X(e_i), Y(e_i), Z(e_i)), (A(e_i), S(e_i), D(e_i))\rangle\, (i = 1, 2, \ldots, n)$ be a group of FNIFNs. If $Q(e)^+ = \left\{ \begin{matrix} (\max(X(e_i)), \max(Y(e_i)), \max(Z(e_i))), \\ (\min(A(e_i)), \min(S(e_i)), \min(D(e_i))) \end{matrix} \right\}$ $(i = 1, 2, \ldots, n)$ and $Q(e)^- = \left\{ \begin{matrix} (\min(X(e_i)), \min(Y(e_i)), \min(Z(e_i))), \\ (\max(A(e_i)), \end{matrix} \right.$ $\max(S(e_i)), \max(D(e_i)))\}\, (i = 1, 2, \ldots, n)$, then

$$Q(e)^- \le FNIFDMSM^{(k)}(Q(e_1), Q(e_2), \ldots, Q(e_n)) \le Q(e)^+. \tag{18}$$

Property 4 (commutativity). Let $Q(e_i)\, (i = 1, 2, \ldots, n)$ be a set of given FNIFNs, and $Q(e_i')\, (i = 1, 2, \ldots, n)$ is any permutation of $Q(e_i)\, (i = 1, 2, \ldots, n)$; then,

$$\begin{aligned} &FNIFDMSM^{(k)}(Q(e_1), Q(e_2), \ldots, Q(e_n)) \\ &\quad = FNIFDMSM^{(k)}(Q(e_1'), Q(e_2'), \ldots, Q(e_n')). \end{aligned} \tag{19}$$

3.2. The FNIFWDMSM Operator. In real-life MADM, it is very crucial to take weights into account. We shall solve the fuzzy number intuitionistic fuzzy weighted DMSM (FNIFWDMSM) mean.

Definition 8. Let $Q(e_m) = \langle (X(e_m), Y(e_m), Z(e_m)), (A(e_m), S(e_m), D(e_m))\rangle\, (m = 1, 2, \ldots, k)$ be a couple of built FNIFNs with given weight values $\xi_m = (\xi_1, \xi_2, \ldots, \xi_k)^T$, and $\xi_m \in [0, 1]$, $\sum_{m=1}^{k} \xi_m = 1$. If

$$\begin{aligned} &FNIFWDMSM_{nw}^{(k)}(Q(e_1), Q(e_2), \ldots, Q(e_n)) \\ &\quad = \frac{1}{k}\left(\underset{1 \le i_1 < \ldots < i_k \le i_n}{\otimes} \left(\bigoplus_{j=1}^{k} \left(n\xi_{i_j} \otimes Q\left(e_{i_j}\right)\right)\right)^{\left(1/C_n^k\right)}\right), \end{aligned} \tag{20}$$

then we call $FNIFWDMSM_{k\xi}^{(k, \lambda_1, \lambda_2, \ldots, \lambda_k)}$ the fuzzy number intuitionistic fuzzy weighted DMSM (FNIFWDMSM) formula.

Theorem 2. *Let $Q(e_m) = \langle (X(e_m), Y(e_m), Z(e_m)), (A(e_m), S(e_m), D(e_m))\rangle\, (i = 1, 2, \ldots, n)$ be a couple of built FNIFNs. The obtained value from FNIFWDMSM formula is still a FNIFN.*

$$\begin{aligned} &\mathrm{FNIFWDMSM}_{n\xi}^{(k)}(Q(e_1), Q(e_2), \ldots, Q(e_n)) = \frac{1}{k}\left(\underset{1 \le i_1 < \ldots < i_k \le i_n}{\otimes} \left(\bigoplus_{j=1}^{k} \left(n\xi_{i_j} \otimes Q\left(e_{i_j}\right)\right)\right)^{\left(1/C_n^k\right)}\right) \\ &= \left\{ \begin{pmatrix} 1 - \left(1 - \prod\limits_{1 \le i_1 < \cdots < i_k \le i_n} \left(1 - \prod\limits_{j=1}^{k} \left(1 - X\left(e_{i_j}\right)\right)^{n\xi_{i_j}}\right)^{\left(1/C_n^k\right)}\right)^{(1/k)} \\ 1 - \left(1 - \prod\limits_{1 \le i_1 < \cdots < i_k \le i_n} \left(1 - \prod\limits_{j=1}^{k} \left(1 - Y\left(e_{i_j}\right)\right)^{n\xi_{i_j}}\right)^{\left(1/C_n^k\right)}\right)^{(1/k)} \\ 1 - \left(1 - \prod\limits_{1 \le i_1 < \cdots < i_k \le i_n} \left(1 - \prod\limits_{j=1}^{k} \left(1 - Z\left(e_{i_j}\right)\right)^{n\xi_{i_j}}\right)^{\left(1/C_n^k\right)}\right)^{(1/k)} \end{pmatrix}, \begin{pmatrix} \left(1 - \prod\limits_{1 \le i_1 < \cdots < i_k \le i_n} \left(1 - \prod\limits_{j=1}^{k} \left(A\left(e_{i_j}\right)\right)^{n\xi_{i_j}}\right)^{\left(1/C_n^k\right)}\right)^{(1/k)} \\ \left(1 - \prod\limits_{1 \le i_1 < \cdots < i_k \le i_n} \left(1 - \prod\limits_{j=1}^{k} \left(S\left(e_{i_j}\right)\right)^{n\xi_{i_j}}\right)^{\frac{1}{C_n^k}}\right)^{(1/k)} \\ \left(1 - \prod\limits_{1 \le i_1 < \cdots < i_k \le i_n} \left(1 - \prod\limits_{j=1}^{k} \left(D\left(e_{i_j}\right)\right)^{n\xi_{i_j}}\right)^{\left(1/C_n^k\right)}\right)^{(1/k)} \end{pmatrix} \right\}. \end{aligned} \tag{21}$$

Proof. With Definition 2, we can derive

$$n\xi_{i_j}\otimes Q\left(e_{i_j}\right)=\left\{\begin{array}{c}\left(1-\left(1-X\left(e_{i_j}\right)\right)^{n\xi_{i_j}},1-\left(1-Y\left(e_{i_j}\right)\right)^{n\xi_{i_j}},1-\left(1-Z\left(e_{i_j}\right)\right)^{n\xi_{i_j}}\right),\\ \left(\left(A\left(e_{i_j}\right)\right)^{n\xi_{i_j}},\left(S\left(e_{i_j}\right)\right)^{n\xi_{i_j}},\left(D\left(e_{i_j}\right)\right)^{n\xi_{i_j}}\right)\end{array}\right\}. \tag{22}$$

Thus,

$$\begin{aligned}&\bigoplus_{j=1}^{k}\left(n\xi_{i_j}\otimes Q\left(e_{i_j}\right)\right)\\&=\left\{\begin{array}{c}\left(1-\prod_{j=1}^{k}\left(1-X\left(x_{i_j}\right)\right)^{n\xi_{i_j}},1-\prod_{j=1}^{k}\left(1-Y\left(x_{i_j}\right)\right)^{n\xi_{i_j}},1-\prod_{j=1}^{k}\left(1-Z\left(x_{i_j}\right)\right)^{n\xi_{i_j}}\right),\\ \left(\prod_{j=1}^{k}\left(A\left(e_{i_j}\right)\right)^{n\xi_{i_j}},\prod_{j=1}^{k}\left(S\left(e_{i_j}\right)\right)^{n\xi_{i_j}},\prod_{j=1}^{k}\left(D\left(e_{i_j}\right)\right)^{n\xi_{i_j}}\right)\end{array}\right\}.\end{aligned} \tag{23}$$

Thereafter,

$$\begin{aligned}&\left(\bigoplus_{j=1}^{k}\left(n\xi_{i_j}\otimes Q\left(e_{i_j}\right)\right)\right)^{\left(1/C_n^k\right)}\\&=\left\{\begin{array}{c}\left(\left(1-\prod_{j=1}^{k}\left(1-X\left(e_{i_j}\right)\right)^{n\xi_{i_j}}\right)^{\left(1/C_n^k\right)},\left(1-\prod_{j=1}^{k}\left(1-Y\left(e_{i_j}\right)\right)^{n\xi_{i_j}}\right)^{\left(1/C_n^k\right)},\left(1-\prod_{j=1}^{k}\left(1-Z\left(e_{i_j}\right)\right)^{n\xi_{i_j}}\right)^{\left(1/C_n^k\right)}\right)\\ \left(1-\left(1-\prod_{j=1}^{k}\left(A\left(e_{i_j}\right)\right)^{n\xi_{i_j}}\right)^{\left(1/C_n^k\right)},1-\left(1-\prod_{j=1}^{k}\left(S\left(e_{i_j}\right)\right)^{n\xi_{i_j}}\right)^{\left(1/C_n^k\right)},1-\left(1-\prod_{j=1}^{k}\left(D\left(e_{i_j}\right)\right)^{n\xi_{i_j}}\right)^{\left(1/C_n^k\right)}\right)\end{array}\right\}.\end{aligned} \tag{24}$$

Furthermore,

$$\begin{aligned}&\bigotimes_{1\le i_1<\ldots<i_k\le i_n}\left(\bigoplus_{j=1}^{k}\left(n\xi_{i_j}\otimes Q\left(e_{i_j}\right)\right)\right)^{\left(1/C_n^k\right)}\\&=\left\{\left(\begin{array}{c}\prod_{1\le i_1<\ldots<i_k\le i_n}\left(1-\prod_{j=1}^{k}\left(1-X\left(e_{i_j}\right)\right)^{n\xi_{i_j}}\right)^{\left(1/C_n^k\right)}\\ \prod_{1\le i_1<\ldots<i_k\le i_n}\left(1-\prod_{j=1}^{k}\left(1-Y\left(e_{i_j}\right)\right)^{n\xi_{i_j}}\right)^{\left(1/C_n^k\right)}\\ \prod_{1\le i_1<\ldots<i_k\le i_n}\left(1-\prod_{j=1}^{k}\left(1-Z\left(e_{i_j}\right)\right)^{n\xi_{i_j}}\right)^{\left(1/C_n^k\right)}\end{array}\right),\left(\begin{array}{c}1-\prod_{1\le i_1<\ldots<i_k\le i_n}\left(1-\prod_{j=1}^{k}\left(A\left(e_{i_j}\right)\right)^{n\xi_{i_j}}\right)^{\left(1/C_n^k\right)}\\ 1-\prod_{1\le i_1<\ldots<i_k\le i_n}\left(1-\prod_{j=1}^{k}\left(S\left(e_{i_j}\right)\right)^{n\xi_{i_j}}\right)^{\left(1/C_n^k\right)}\\ 1-\prod_{1\le i_1<\ldots<i_k\le i_n}\left(1-\prod_{j=1}^{k}\left(D\left(e_{i_j}\right)\right)^{n\xi_{i_j}}\right)^{\left(1/C_n^k\right)}\end{array}\right)\right\}.\end{aligned} \tag{25}$$

Therefore,

$$FNIFWDMSM_{n\xi}^{(k)}\left(Q(e_1),Q(e_2),\ldots,Q(e_n)\right)=\frac{1}{k}\left(\underset{1\le i_1<\ldots<i_k\le i_n}{\otimes}\left(\bigoplus_{j=1}^{k}\left(n\xi_{i_j}\otimes Q\left(e_{i_j}\right)\right)\right)^{\left(1/C_n^k\right)}\right)$$

$$=\left\{\begin{array}{l}\left(\begin{array}{l}1-\left(1-\prod\limits_{\substack{1\le i_1<\ldots\\<i_k\le i_n}}\left(1-\prod\limits_{j=1}^{k}\left(1-X\left(e_{i_j}\right)\right)^{n\xi_{i_j}}\right)^{\left(1/C_n^k\right)}\right)^{(1/k)}\\ 1-\left(1-\prod\limits_{\substack{1\le i_1<\ldots\\<i_k\le i_n}}\left(1-\prod\limits_{j=1}^{k}\left(1-Y\left(e_{i_j}\right)\right)^{n\xi_{i_j}}\right)^{\left(1/C_n^k\right)}\right)^{(1/k)}\\ 1-\left(1-\prod\limits_{\substack{1\le i_1<\ldots\\<i_k\le i_n}}\left(1-\prod\limits_{j=1}^{k}\left(1-Z\left(e_{i_j}\right)\right)^{n\xi_{i_j}}\right)^{\left(1/C_n^k\right)}\right)^{(1/k)}\end{array}\right),\left(\begin{array}{l}\left(1-\prod\limits_{\substack{1\le i_1<\ldots\\<i_k\le i_n}}\left(1-\prod\limits_{j=1}^{k}\left(A\left(e_{i_j}\right)\right)^{n\xi_{i_j}}\right)^{\left(1/C_n^k\right)}\right)^{(1/k)}\\ \left(1-\prod\limits_{\substack{1\le i_1<\ldots\\<i_k\le i_n}}\left(1-\prod\limits_{j=1}^{k}\left(S\left(e_{i_j}\right)\right)^{n\xi_{i_j}}\right)^{\left(1/C_n^k\right)}\right)^{(1/k)}\\ \left(1-\prod\limits_{\substack{1\le i_1<\ldots\\<i_k\le i_n}}\left(1-\prod\limits_{j=1}^{k}\left(D\left(e_{i_j}\right)\right)^{n\xi_{i_j}}\right)^{\left(1/C_n^k\right)}\right)^{(1/k)}\end{array}\right)\end{array}\right\}. \tag{26}$$

Hence, (23) is kept.

Then, we shall prove that (23) is an FNIFN. We shall check the following two conditions:

(i) $(X(e),Y(e),Z(e))\subseteq[0,1]$, $(A(e),S(e),D(e))\subseteq[0,1]$.

(ii) $0\le Z(e)+D(e)\le 1$. □

Proof. (1) Since $0\le X(e_{i_j})\le 1$, we get

$$0\le\prod_{j=1}^{k}\left(1-X\left(e_{i_j}\right)\right)^{n\xi_{i_j}}\le 1 \text{ and } 0\le 1-\prod_{j=1}^{k}\left(1-X\left(e_{i_j}\right)\right)^{n\xi_{i_j}}\le 1. \tag{27}$$

Then,

$$0\le 1-\prod_{1\le i_1<\cdots<i_k\le i_n}\left(1-\prod_{j=1}^{k}\left(1-X\left(e_{i_j}\right)\right)^{n\xi_{i_j}}\right)^{\left(1/C_n^k\right)}\le 1. \tag{28}$$

Thus,

$$0\le 1-\left(1-\prod_{1\le i_1<\cdots<i_k\le i_n}\left(1-\prod_{j=1}^{k}\left(1-X\left(e_{i_j}\right)\right)^{n\xi_{i_j}}\right)^{\left(1/C_n^k\right)}\right)^{(1/k)}\le 1. \tag{29}$$

That means $X(e) = 1-(1-\prod_{1\le i_1<\cdots<i_k\le i_n}(1-\prod_{j=1}^{k}(1-X(e_{i_j}))^{n\xi_{i_j}})^{(1/C_n^k)})^{(1/k)}\subseteq[0,1]$. Similarly, we can get $(Y(e),Z(e))\subseteq[0,1]$, and $(A(e),S(e),D(e))\subseteq[0,1]$, so (1) is maintained.

(2) For $Z(e_{i_j})+D(e_{i_j})\le 1$, then we can derive $D(e_{i_j})\le 1-Z(e_{i_j})$, and thus

$$
\begin{aligned}
0 &\le Z(e)+D(e)\\
&= 1-\left(1-\prod_{1\le i_1<\cdots<i_k\le i_n}\left(1-\prod_{j=1}^{k}\left(1-Z\left(e_{i_j}\right)\right)^{n\xi_{i_j}}\right)^{(1/C_n^k)}\right)^{(1/k)}+\left(1-\prod_{1\le i_1<\cdots<i_k\le i_n}\left(1-\prod_{j=1}^{k}\left(D\left(e_{i_j}\right)\right)^{n\xi_{i_j}}\right)^{(1/C_n^k)}\right)^{(1/k)}\\
&\le 1-\left(1-\prod_{1\le i_1<\cdots<i_k\le i_n}\left(1-\prod_{j=1}^{k}\left(1-Z\left(e_{i_j}\right)\right)^{n\xi_{i_j}}\right)^{(1/C_n^k)}\right)^{(1/k)}+\left(1-\prod_{1\le i_1<\cdots<i_k\le i_n}\left(1-\prod_{j=1}^{k}\left(1-Z\left(e_{i_j}\right)\right)^{n\xi_{i_j}}\right)^{(1/C_n^k)}\right)^{(1/k)}\\
&= 1.
\end{aligned}
\tag{30}
$$

□

Example 2. Let $Q(e_1)=\langle(0.1,0.2,0.3),(0.2,0.5,0.6)\rangle$, $Q(e_2)=\langle(0.2,0.3,0.3),(0.2,0.5,0.5)\rangle$, and $Q(e_3)=\langle(0.4,0.5,0.5),(0.3,0.4,0.4)\rangle$ be three FNIFNs, and suppose $k=2\xi=(0.2,0.3,0.5)$; then according to (21), we have

$$
\begin{aligned}
&FNIFW\ DM\ SM_{n\xi}^{(k)}\left(Q(e_1),Q(e_2),\ldots,Q(e_n)\right)\\
&=\frac{1}{k}\left(\underset{1\le i_1<\cdots<i_k\le i_n}{\otimes}\left(\bigoplus_{j=1}^{k}\left(n\xi_{i_j}\otimes Q\left(e_{i_j}\right)\right)\right)^{(1/C_n^k)}\right)\\
&=\left\{\begin{matrix}
\left(\begin{matrix}
1-\left(1-\left(\begin{matrix}\left(1-(1-0.1)^{0.6}\times(1-0.2)^{0.9}\right)\times\left(1-(1-0.1)^{0.6}\times(1-0.4)^{1.5}\right)\\ \times\left(1-(1-0.2)^{0.9}\times(1-0.4)^{1.5}\right)\end{matrix}\right)^{(1/C_3^2)}\right)^{(1/2)},\\
1-\left(1-\left(\begin{matrix}\left(1-(1-0.2)^{0.6}\times(1-0.3)^{0.9}\right)\times\left(1-(1-0.2)^{0.6}\times(1-0.5)^{1.5}\right)\\ \times\left(1-(1-0.3)^{0.9}\times(1-0.5)^{1.5}\right)\end{matrix}\right)^{(1/C_3^2)}\right)^{(1/2)}\\
1-\left(1-\left(\begin{matrix}\left(1-(1-0.3)^{0.6}\times(1-0.3)^{0.9}\right)\times\left(1-(1-0.3)^{0.6}\times(1-0.5)^{1.5}\right)\\ \times\left(1-(1-0.3)^{0.9}\times(1-0.5)^{1.5}\right)\end{matrix}\right)^{(1/C_3^2)}\right)^{(1/2)}
\end{matrix}\right)\\
\left(\begin{matrix}
\left(1-\left(\left(1-0.2^{0.6}\times0.2^{0.9}\right)\times\left(1-0.2^{0.6}\times0.3^{1.5}\right)\times\left(1-0.2^{0.9}\times0.3^{1.5}\right)\right)^{(1/C_3^2)}\right)^{(1/2)}\\
\left(1-\left(\left(1-0.5^{0.6}\times0.5^{0.9}\right)\times\left(1-0.5^{0.6}\times0.4^{1.5}\right)\times\left(1-0.5^{0.9}\times0.4^{1.5}\right)\right)^{(1/C_3^2)}\right)^{(1/2)}\\
\left(1-\left(\left(1-0.6^{0.6}\times0.5^{0.9}\right)\times\left(1-0.6^{0.6}\times0.4^{1.5}\right)\times\left(1-0.5^{0.9}\times0.4^{1.5}\right)\right)^{(1/C_3^2)}\right)^{(1/2)}
\end{matrix}\right)
\end{matrix}\right\}\\
&=\langle(0.2469,0.3463,0.3706),(0.2526,0.4744,0.4976)\rangle.
\end{aligned}
\tag{31}
$$

Then, we shall discuss some better properties for FNIFWDMSM.

Property 5 (idempotency). If $Q(e_i) = \langle (X(e_i), Y(e_i), Z(e_i)), (A(e_i), S(e_i), D(e_i))\rangle$ $(i = 1, 2, \ldots, n)$ are same, then

$$FNIFWDMSM_{n\xi}^{(k)}(Q(e_1), Q(e_2), \ldots, Q(e_n)) = Q(e). \tag{32}$$

Property 6 (monotonicity). Let $Q(e_i) = \langle (X(e_i), Y(e_i), Z(e_i)), (A(e_i), S(e_i), D(e_i))\rangle$ $(i = 1, 2, \ldots, n)$ and $Q(e_j) = \langle (X(e_j), Y(e_j), Z(e_j)), (A(e_j), S(e_j), D(e_j))\rangle$ $(j = 1, 2, \ldots, n)$ be two sets of FNIFNs. If $X(e_i) \le X(e_j), Y(e_i) \le Y(e_j), Z(e_i) \le Z(e_j), A(e_i) \ge A(e_j), S(e_i) \ge S(e_j), D(e_i) \ge D(e_j)$ hold for all i, j, then

$$\begin{aligned} &FNIFWDMSM_{n\xi}^{(k)}\left(Q\left(e_{i_1}\right), Q\left(e_{i_2}\right), \ldots, Q\left(e_{i_n}\right)\right) \\ &\quad \le FNIFWDMSM_{n\xi}^{(k)}\left(Q\left(e_{j_1}\right), Q\left(e_{j_2}\right), \ldots, Q\left(e_{j_n}\right)\right). \end{aligned} \tag{33}$$

Property 7 (boundedness). Let $Q(e_i) = \langle (X(e_i), Y(e_i), Z(e_i)), (A(e_i), S(e_i), D(e_i))\rangle$ $(i = 1, 2, \ldots, n)$ be a couple of FNIFNs. If $Q(e)^+ = \left\{\begin{matrix} (\max(X(e_i)), \max(Y(e_i)), \max(Z(e_i))) \\ (\min(A(e_i)), \min(S(e_i)), \min(D(e_i))) \end{matrix}\right\}$ $(i = 1, 2, \ldots, n)$ and $Q(e)^- = \left\{\begin{matrix} (\min(X(e_i)), \min(Y(e_i)), \min(Z(e_i))) \\ (\max(A(e_i)), \end{matrix}\right.$ $\max(S(e_i)), \max(D(e_i))\}$ $(i = 1, 2, \ldots, n)$, then

$$\begin{aligned} Q(e)^- &\le FNIFWDMSM_{n\xi}^{(k)}(Q(e_1), Q(e_2), \ldots, Q(e_n)) \\ &\le Q(e)^+. \end{aligned} \tag{34}$$

Property 8 (commutativity). Let $Q(e_i)$ $(i = 1, 2, \ldots, n)$ be a couple of FNIFNs, and $Q(e_i')$ $(i = 1, 2, \ldots, n)$ is any permutation of $Q(e_i)$ $(i = 1, 2, \ldots, n)$; then,

$$\begin{aligned} &FNIFWDMSM_{n\xi}^{(k)}(Q(e_1), Q(e_2), \ldots, Q(e_n)) \\ &\quad = FNIFWDMSM_{n\xi}^{(k)}(Q(e_1'), Q(e_2'), \ldots, Q(e_n')). \end{aligned} \tag{35}$$

4. Data Instance and Comparative Analysis

4.1. Data Instance. With the rapid development of information technology in the world and the new form of knowledge economy under "Internet +," more and more traditional industries are carrying science and technology for further development and communication. Of course, education is no exception. However, at the present stage, all kinds of schools only achieve "Internet +" rather than "Internet +" in the real sense. Most of the information-based teaching reform is just to add some network means to traditional classroom for auxiliary teaching, without truly integrating high-quality teaching content. Since the emergence of MOOC, a large-scale online network platform, in 2008, it has had a significant impact on the education of all countries in the world. Although this platform has not been introduced to China for a long time, it has been rapidly applied in the field of higher education. At the same time, flipped classroom, as a new classroom mode, overturns the traditional language teaching method, changes the role of teachers and students, and sets up the student-centered teaching concept. By selecting high-quality resources from all over the world and using flipped classroom teaching, the education in colleges and universities has taken on a new look. Vocational education, as an important branch of the education system, is rarely applied in this aspect. Especially in the accounting course, which plays an important role in secondary vocational education, students with low level of teaching informatization, low comprehensive quality of classes and teachers, and poor learning motivation lack learning motivation in the current teaching process, and the overall teaching quality has problems. Therefore, with the help of the MOOC+ rolling classroom teaching mode, the current predicament of accounting courses can be effectively alleviated, and accounting education can be effectively promoted. A point in case about the blended classroom teaching reform effect evaluation with FNIFNs would be used to illustrate the built methods. We shall give 5 possible schools H_i $(i = 1, 2, 3, 4, 5)$ to select. The experts shall select four given attributes to assess the management quality level of teacher education of these given schools: (1) J_1 represents the teaching environment and studying environment; (2) J_2 depicts curriculum design; (3) J_3 depicts the teaching practice; (4) J_4 depicts the student satisfaction degree. Several schools are depicted with FNIFNs by the given DMs with 4 given criteria (whose weighting vector $\xi = (0.25, 0.20, 0.15, 0.40)$), and the FNIFN decision values are depicted in Table 1.

Then, the FNIFWDMSM operator is used to deal with blended classroom teaching reform effect evaluation with FNIFNs.

Step 1. From Table 1, we can fuse all FNIFNs r_{ij} by FNIFWDMSM mean to calculate the FNIFNs H_i $(i = 1, 2, 3, 4, 5)$ of the given schools H_i; the obtained values are shown in Table 2 $(n = 2)$.

Step 2. The SF of schools is calculated in Table 3.

Step 3. From Table 3, the order of the schools is given in Table 4. Note that ">" depicts "preferred to." The best college school is H_1.

4.2. Argument Analysis. Table 5 describes the corresponding calculation results of different n values in FNIFWGMSM formula. From Table 5, it could be seen that the results are stable along with different parameter alteration. The best optimal alternative is still H_1.

4.3. Comparative Analysis. In this section, we will compare the technology depicted with other technologies, and the conclusions are shown in Table 6.

From above analysis, comparing the result of the proposed FNIFWDMSM operator with FNIFWA and FNIFWG formulas, these schemes rank a little differently and the

Table 1: The FNIFN DM.

	J_1	J_2
H1	$\langle(0.3, 0.4, 0.4), (0.4, 0.5, 0.5)\rangle$	$\langle(0.2, 0.2, 0.4), (0.1, 0.2, 0.2)\rangle$
H2	$\langle(0.4, 0.5, 0.5), (0.3, 0.4, 0.4)\rangle$	$\langle(0.2, 0.3, 0.3), (0.4, 0.4, 0.6)\rangle$
H3	$\langle(0.4, 0.4, 0.6), (0.2, 0.2, 0.3)\rangle$	$\langle(0.5, 0.6, 0.6), (0.2, 0.3, 0.3)\rangle$
H4	$\langle(0.5, 0.6, 0.6), (0.1, 0.2, 0.2)\rangle$	$\langle(0.6, 0.6, 0.7), (0.1, 0.1, 0.2)\rangle$
H5	$\langle(0.4, 0.6, 0.6), (0.1, 0.2, 0.3)\rangle$	$\langle(0.1, 0.4, 0.5), (0.2, 0.3, 0.4)\rangle$
	J_3	J_4
H1	$\langle(0.1, 0.1, 0.4), (0.3, 0.3, 0.4)\rangle$	$\langle(0.4, 0.5, 0.5), (0.3, 0.3, 0.4)\rangle$
H2	$\langle(0.1, 0.2, 0.3), (0.2, 0.5, 0.6)\rangle$	$\langle(0.2, 0.3, 0.3), (0.2, 0.5, 0.5)\rangle$
H3	$\langle(0.5, 0.7, 0.7), (0.1, 0.2, 0.2)\rangle$	$\langle(0.3, 0.4, 0.5), (0.1, 0.2, 0.4)\rangle$
H4	$\langle(0.4, 0.5, 0.6), (0.2, 0.3, 0.3)\rangle$	$\langle(0.6, 0.6, 0.7), (0.1, 0.1, 0.2)\rangle$
H5	$\langle(0.2, 0.2, 0.4), (0.3, 0.3, 0.4)\rangle$	$\langle(0.1, 0.3, 0.4), (0.2, 0.3, 0.5)\rangle$

Table 2: The fused values by FNIFWMSM.

Fused operator	Schools	Results
FNIFWDMSM	H_1	<(0.5167, 0.5616, 0.6303), (0.1797, 0.1963, 0.2468)>
	H_2	<(0.1791, 0.3712, 0.4633), (0.2166, 0.2952, 0.4191)>
	H_3	<(0.2552, 0.3039, 0.4154), (0.2877, 0.3451, 0.3907)>
	H_4	<(0.2229, 0.3226, 0.3411), (0.3008, 0.4649, 0.5321)>
	H_5	<(0.4002, 0.4986, 0.5769), (0.1804, 0.2509, 0.3218)>

Table 3: The SF of the schools.

	FNIFWDMSM
H_1	0.3628
H_2	0.0397
H_3	−0.0226
H_4	−0.1383
H_5	0.2426

Table 4: Order of the schools.

	Order
FNIFWDMSM	$H_1 > H_5 > H_2 > H_3 > H_4$

Table 5: Ranking results under different parameters of FNIFWMSM operator.

	SF (H_1)	SF (H_2)	SF (H_3)	SF (H_4)	SF (H_5)	Ordering
$n = 1$	0.2985	-0.0189	−0.1036	−0.1946	0.2246	$H_1 > H_5 > H_2 > H_3 > H_4$
$n = 2$	0.3628	0.0397	−0.0226	−0.1383	0.2426	$H_1 > H_5 > H_2 > H_3 > H_4$
$n = 3$	0.3999	0.0668	0.0228	−0.1134	0.2563	$H_1 > H_5 > H_2 > H_3 > H_4$
$n = 4$	0.4416	0.0866	0.0572	-0.0943	0.2745	$H_1 > H_5 > H_2 > H_3 > H_4$

Table 6: Comparative analysis.

	Order
FNIFWA operator [51]	$H_1 > H_5 > H_2 > H_3 > H_4$
FNIFWG operator [54]	$H_1 > H_5 > H_2 > H_3 > H_4$
FNIFWHM operator [62]	$H_1 > H_5 > H_2 > H_3 > H_4$
FNIFHPWG operator [46]	$H_1 > H_5 > H_3 > H_2 > H_4$
IFNIFHCA operator [63]	$H_1 > H_5 > H_2 > H_3 > H_4$
FNIFWDMSM	$H_1 > H_5 > H_2 > H_3 > H_4$

optimal alternative is not different. The FNIFWHM, FNIFHPWG, and IFNIFHCA operators only consider relationship between two given arguments. Nevertheless, the FNIFWA and FNIFWG formulas do not consider the relationship between given arguments, which cannot correctly estimate the effect of different given values of n arguments on the final ranking results. The FNIFWDMSM formula could perfectly consider the relationship between different values of n being fused.

5. Conclusion

With the progress of science and technology, the information age has come, and information technology plays an important role in many fields. The social environment of informationization promotes the development of educational information, and new educational ideas and methods are emerging, which makes the development of education informatization more indepth. The introduction of information-based means into teaching based on the blended teaching mode of flipped classroom helps to realize the concept of student-centered education, which can enrich the content of classroom teaching and effectively improve students' enthusiasm for learning. In order to solve the difficult problems faced in the current mathematics teaching in rural junior high schools, the study draws on the experience of carrying out blended teaching mode based on flipped classroom at home and abroad. After the teaching experiment, through the analysis of experimental results, it is concluded that the implementation of the blended teaching mode based on flipped classroom in rural junior high schools is conducive to improving the effect of mathematics teaching and improving students' ability of self-learning. In this paper, we deal with the MADM issues under FNIFNs and utilize the DMSM means to devise several GMSM fused means with FNIFNs: FNIFDMSM tool and FNIFWDMSM tool. The characteristic of these two built operators is also analyzed. The FNIFWDMSM tool is utilized to cope with MADM issues under FNIFNs. Finally, a point in case for blended classroom teaching reform effect evaluation is used to show the built method. In our future work, the application and expansion of the FNIFN information fused operators will be debated in another MADM research direction [64–71] and also taking into account the decision makers' risk attitude [72–74] for MAGDM with FNIFNs.

Data Availability

The data used to support the findings of this study are included within the article.

Conflicts of Interest

The author declares that there are no conflicts of interest.

Acknowledgments

This study was supported by Research on the Second Batch of Teaching Reform of Higher Education in Zhejiang Province during the 13th Five-Year Plan (Research on the reform of blended teaching mode to promote deep learning and cooperation based on SPOC (taking computer basic course as an example)) (jg20190961).

References

[1] L. A. Zadeh, "Fuzzy sets," *Information and Control*, vol. 8, no. 3, pp. 338–353, 1965.
[2] H. Garg and K. Kumar, "Group decision making approach based on possibility degree measures and the linguistic intuitionistic fuzzy aggregation operators using einstein norm operations," *Journal of Multiple-Valued Logic and Soft Computing*, vol. 31, pp. 175–209, 2018.
[3] H. Garg, "Generalized interaction aggregation operators in intuitionistic fuzzy multiplicative preference environment and their application to multicriteria decision-making," *Applied Intelligence*, vol. 48, no. 8, pp. 2120–2136, 2018.
[4] Y. Huang, R. Lin, and X. Chen, "An enhancement EDAS method based on prospect theory," *Technological and Economic Development of Economy*, vol. 27, no. 5, pp. 1019–1038, 2021.
[5] X. Zhang and Z. Xu, "Hesitant fuzzy QUALIFLEX approach with a signed distance-based comparison method for multiple criteria decision analysis," *Expert Systems with Applications*, vol. 42, no. 2, pp. 873–884, 2015.
[6] D. Zhang, Y. Su, M. Zhao, and X. Chen, "CPT-TODIM method for interval neutrosophic MAGDM and its application to third-party logistics service providers selection," *Technological and Economic Development of Economy*, vol. 28, pp. 201–219, 2022.
[7] K. T. Atanassov, "More on intuitionistic fuzzy sets," *Fuzzy Sets and Systems*, vol. 33, no. 1, pp. 37–45, 1989.
[8] G.-F. Yu, D.-F. Li, J.-M. Qiu, and Y.-F. Ye, "Application of satisfactory degree to interval-valued intuitionistic fuzzy multi-attribute decision making," *Journal of Intelligent and Fuzzy Systems*, vol. 32, no. 1, pp. 1019–1028, 2017.
[9] Y. Su, M. Zhao, G. Wei, C. Wei, and X. Chen, "Probabilistic uncertain linguistic EDAS method based on prospect theory for multiple attribute group decision-making and its application to green finance," *International Journal of Fuzzy Systems*, vol. 73, 2021.
[10] J. Lu, S. Zhang, J. Wu, and Y. Wei, "COPRAS method for multiple attribute group decision making under picture fuzzy environment and their application to green supplier selection," *Technological and Economic Development of Economy*, vol. 27, no. 2, pp. 369–385, 2021.
[11] S.-P. Wan and D.-F. Li, "Atanassov's intuitionistic fuzzy programming method for heterogeneous multiattribute group decision making with atanassov's intuitionistic fuzzy truth degrees," *IEEE Transactions on Fuzzy Systems*, vol. 22, no. 2, pp. 300–312, 2014.
[12] Y. Su, M. Zhao, C. Wei, and X. Chen, "PT-TODIM method for probabilistic linguistic MAGDM and application to industrial control system security supplier selection," *International Journal of Fuzzy Systems*, vol. 24, no. 1, pp. 202–215, 2021.
[13] S. Wang, G. Wei, J. Lu, J. Wu, C. Wei, and X. Chen, "GRP and CRITIC method for probabilistic uncertain linguistic MAGDM and its application to site selection of hospital constructions," *Soft Computing*, vol. 26, no. 1, pp. 237–251, 2022.
[14] Z. Jiang, G. Wei, and X. Chen, "EDAS method based on cumulative prospect theory for multiple attribute group decision-making under picture fuzzy environment," *Journal of*

Intelligent and Fuzzy Systems, vol. 42, no. 3, pp. 1723–1735, 2022.

[15] H. Zhang, G. Wei, and X. Chen, “SF-GRA method based on cumulative prospect theory for multiple attribute group decision making and its application to emergency supplies supplier selection,” *Engineering Applications of Artificial Intelligence*, vol. 110, p. 104679, 2022.

[16] M. Yazdani, Z. Wen, H. Liao, A. Banaitis, and Z. Turskis, “A grey combined compromise solution (CoCoSo-G) method for supplier selection in construction management,” *Journal of Civil Engineering and Management*, vol. 25, no. 8, pp. 858–874, 2019.

[17] M. Yazdani, P. Zarate, E. K. Zavadskas, and Z. Turskis, “A combined compromise solution (CoCoSo) method for multi-criteria decision-making problems,” *Management Decision*, vol. 57, pp. 2501–2519, 2018.

[18] J. Roy, H. K. Sharma, S. Kar, E. K. Zavadskas, and J. Saparauskas, “An extended COPRAS model for multi-criteria decision-making problems and its application in web-based hotel evaluation and selection,” *Economic Research-Ekonomska Istraživanja*, vol. 32, no. 1, pp. 219–253, 2019.

[19] A. Arabameri, M. Yamani, B. Pradhan, A. Melesse, K. Shirani, and D. Tien Bui, “Novel ensembles of COPRAS multi-criteria decision-making with logistic regression, boosted regression tree, and random forest for spatial prediction of gully erosion susceptibility,” *The Science of the Total Environment*, vol. 688, pp. 903–916, 2019.

[20] J.-P. Fan, R. Cheng, and M.-Q. Wu, “Extended EDAS methods for multi-criteria group decision-making based on IV-cfswaa and IV-cfswga operators with interval-valued complex fuzzy soft information,” *Ieee Access*, vol. 7, Article ID 105546, 2019.

[21] W.-Z. Liang, G.-Y. Zhao, and S.-Z. Luo, “An integrated EDAS-ELECTRE method with picture fuzzy information for cleaner production evaluation in gold mines,” *Ieee Access*, vol. 6, Article ID 65747, 2018.

[22] F. K. Gundogdu, C. Kahraman, and H. N. Civan, “A novel hesitant fuzzy EDAS method and its application to hospital selection,” *Journal of Intelligent and Fuzzy Systems*, vol. 35, pp. 6353–6365, 2018.

[23] C. Zhang, C. Chen, D. Streimikiene, and T. Balezentis, “Intuitionistic fuzzy MULTIMOORA approach for multi-criteria assessment of the energy storage technologies,” *Applied Soft Computing*, vol. 79, pp. 410–423, 2019.

[24] J. Roy, S. Das, S. Kar, and D. Pamucar, “An Extension of the CODAS Approach Using Interval-Valued Intuitionistic Fuzzy Set for Sustainable Material Selection in Construction Projects with Incomplete Weight Information,” *Symmetry-Basel*, vol. 11, 2019.

[25] Z. Jiang, G. Wei, and Y. Guo, “Picture fuzzy MABAC method based on prospect theory for multiple attribute group decision making and its application to suppliers selection,” *Journal of Intelligent & Fuzzy Systems*, 2022.

[26] T. Rashid, S. Faizi, and S. Zafar, “Outranking method for intuitionistic 2-tuple fuzzy linguistic information model in group decision making,” *Soft Computing*, vol. 23, no. 15, pp. 6145–6155, 2019.

[27] N. Liao, G. Wei, and X. Chen, “TODIM method based on cumulative prospect theory for multiple attributes group decision making under probabilistic hesitant fuzzy setting,” *International Journal of Fuzzy Systems*, vol. 24, no. 1, pp. 322–339, 2021.

[28] R. X. Liang, S. S. He, J. Q. Wang, K. Chen, and L. Li, “An extended MABAC method for multi-criteria group decision-making problems based on correlative inputs of intuitionistic fuzzy information,” *Computational and Applied Mathematics*, vol. 38, 2019.

[29] Z.-x. Su, M.-y. Chen, G.-p. Xia, and L. Wang, “An interactive method for dynamic intuitionistic fuzzy multi-attribute group decision making,” *Expert Systems with Applications*, vol. 38, no. 12, Article ID 15286, 2011.

[30] A. Arya and S. P. Yadav, “Development of intuitionistic fuzzy super-efficiency slack based measure with an application to health sector,” *Computers & Industrial Engineering*, vol. 115, pp. 368–380, 2018.

[31] F. Tian, S. Liu, Z. Xu, and Q. Lei, “Partial derivative and complete differential of binary intuitionistic fuzzy functions,” *International Journal of Fuzzy Systems*, vol. 19, no. 2, pp. 273–284, 2017.

[32] H. Garg, “An improved cosine similarity measure for intuitionistic fuzzy sets and their applications to decision-making process,” *Hacettepe Journal of Mathematics and Statistics*, vol. 47, pp. 1578–1594, 2018.

[33] C. Tan, “A multi-criteria interval-valued intuitionistic fuzzy group decision making with Choquet integral-based TOPSIS,” *Expert Systems with Applications*, vol. 38, no. 4, pp. 3023–3033, 2011.

[34] X. Zhao, Y. Zheng, and Z. Wan, “Interactive intuitionistic fuzzy methods for multilevel programming problems,” *Expert Systems with Applications*, vol. 72, pp. 258–268, 2017.

[35] D.-F. Li, “The GOWA operator based approach to multi-attribute decision making using intuitionistic fuzzy sets,” *Mathematical and Computer Modelling*, vol. 53, no. 5-6, pp. 1182–1196, 2011.

[36] G. Büyüközkan, O. Feyzioğlu, and F. Göçer, “Selection of sustainable urban transportation alternatives using an integrated intuitionistic fuzzy Choquet integral approach,” *Transportation Research Part D: Transport and Environment*, vol. 58, pp. 186–207, 2018.

[37] R. Joshi, S. Kumar, D. Gupta, and H. Kaur, “A jensen-α-norm dissimilarity measure for intuitionistic fuzzy sets and its applications in multiple attribute decision making,” *International Journal of Fuzzy Systems*, vol. 20, no. 4, pp. 1188–1202, 2018.

[38] S. K. De and S. S. Sana, “The (p, q, r, l) model for stochastic demand under Intuitionistic fuzzy aggregation with Bonferroni mean,” *Journal of Intelligent Manufacturing*, vol. 29, no. 8, pp. 1753–1771, 2018.

[39] J.-q. Li, W. Chen, Z.-l. Yang, and C.-y. Li, “A time-preference and VIKOR-based dynamic intuitionistic fuzzy decision making method,” *Filomat*, vol. 32, no. 5, pp. 1523–1533, 2018.

[40] S. Niroomand, “A multi-objective based direct solution approach for linear programming with intuitionistic fuzzy parameters,” *Journal of Intelligent and Fuzzy Systems*, vol. 35, no. 2, pp. 1923–1934, 2018.

[41] S. Yu, Z.-s. Xu, and S.-s. Liu, “Derivatives and differentials for multiplicative intuitionistic fuzzy information,” *Applied Mathematics-A Journal of Chinese Universities*, vol. 32, no. 4, pp. 443–461, 2017.

[42] D. Yu, “Group decision making based on generalized intuitionistic fuzzy prioritized geometric operator,” *International Journal of Intelligent Systems*, vol. 27, no. 7, pp. 635–661, 2012.

[43] J.-Z. Wu and Q. Zhang, “Multicriteria decision making method based on intuitionistic fuzzy weighted entropy,” *Expert Systems with Applications*, vol. 38, no. 1, pp. 916–922, 2011.

[44] R. Verma and B. D. Sharma, “A new measure of inaccuracy with its application to multi-criteria decision making under

Hindawi
Mathematical Problems in Engineering
Volume 2022, Article ID 6897221, 14 pages
https://doi.org/10.1155/2022/6897221

Research Article

Man-Machine Synergy Control for Pneumatically Powered Exoskeleton Based on Surface Electromyogram Signal

Feilong Jiang,[1] Hao Liu,[2] Qingwei Li,[3] Jian Cao,[1] Xiaoliang Yin,[1] and Rui Dong[1]

[1]*Jia Xing University, Jiaxing, China*
[2]*State Key Laboratory of Fluid Power and Mechatronic Systems, Zhejiang University, Hangzhou, China*
[3]*Yunnan University of Bussiness Management, Kunming, China*

Correspondence should be addressed to Feilong Jiang; jiangfeilong2007@163.com

Received 10 December 2021; Revised 27 December 2021; Accepted 26 January 2022; Published 22 February 2022

Academic Editor: Xindong Peng

The biceps and triceps alternatively act as agonists and antagonists to realize upper limb movement. Pneumatic artificial muscle (PAM), which is inflated and deflated with compressed air instead of water, has similar characteristics to those of human muscle. The challenge is whether an exoskeleton actuated by PAM can help biceps lift the upper limb. Accordingly, the principal aim of this research is to guarantee precise signal collection and control process and adopt the synergy control of PAM and upper limb. In this system, the biceps and triceps provide the main signals in synergy control, electrodes are pasted outside of biceps and triceps to sample their electromyogram signal (EMGs), and the mechanical structure and control system of the pneumatic exoskeleton are proposed. The relationship between duty-ratio-controlled variables and PAM contraction speed is given by experimental analysis, and the maximum duty ratio of controlled variables of input is set to 80. The feature analysis of EMGs can be various including envelope, moving average, and moving root mean square (RMS). The envelope is taken to extract muscle contraction information through upper limb muscles in a static contraction experiment. Then, the processes of biceps and triceps EMGs feature changes including rapid swing, slow swing, and discontinuous swing under various loads are analyzed during upper limb muscle dynamic contraction. The duty-ratio-controlled variables can be divided into five levels, which correspond to exertion rating from powerless to very strong in two EMG characters. These can be reflected in a scatter diagram of duty-ratio-controlled variables and average EMG characters. A nonlinear relationship can be transferred into the continuous system by the polynomial interpolation method, solving the problem of saturation. The net duty-ratio-controlled variables are adopted to control the on-off state and pulse-width modulation (PWM) duty ratio of the high-speed on-off valve. The forearm lifting up movement is unpowered and powered with various load EMGs, and elbow discontinuous swing angle overshoot is performed to analyze the coordination effect in a synergy control experiment.

1. Introduction

The exoskeleton has become one of the important research subjects in recent years, especially in gait training [1], rehabilitation [2, 3], and tremor-suppression orthoses [4]. Almost all existing actuators adopt a driven exoskeleton, including a motor [5–9], hydraulic system [10], pneumatic system [11], and wires [12, 13]. Motors possess the advantages of small volume, low weight, large force of traction, simple operation, good performance, and high safety; therefore, they have been widely used in artificial exoskeletons. The relevant research work mainly focuses on the control algorithm to reduce the error; examples of solutions include adaptive neural network fast fractional sliding mode control [7] and standard force feedback control such as interaction force feedback control and the reference generation [8], adaptive impedance control [9], or sliding mode control [11].

The above researches mainly focus on the active rehabilitation of the exoskeleton; studies on load carriage represent another research direction. Nonetheless, electromyogram signals (EMGs), which reflect muscle and joint actual condition, have been rarely considered. For example, a motor combined with EMGs was presented for upper limb rehabilitation [14]. Muscles are often in more than one state at any given time; that is, they can be in isobaric, isotonic, and isometric contraction and expansion. Pneumatic artificial muscle (PAM), which is much lighter and, at the same time, more compliant than a traditional motor, has similar properties as human muscles; therefore, it is a better choice for movement rehabilitation.

This paper proposes an exoskeleton for load carriage actuated by PAM. Its mechanical structure, the control system of the pneumatic exoskeleton, and the relationship between duty-ratio-controlled variables and PAM contraction speed are presented in Section 2. Section 3 experimentally evaluates the upper limb muscles' static contraction characteristics. Section 4 illustrates the AR model process flow and upper limb muscles dynamic contraction characteristics. In Section 5, the experimental verification of the coordination effect in synergy control is presented.

2. Mechanism and Control Principle

As can be seen in Figure 1, the pneumatic exoskeleton chiefly consists of a posterior arm, a forearm, a baffle, an angular transducer, a plate, and PAM. The posterior arm is sufficiently tightened to hold the articulatio humeri in position, in order to provide a stable point of attachment of PAM that remains relatively fixed during contraction. Forearm lift-up motion occurs as a result of PAM contraction, where a cable pulls a pulley in the elbow, and the forearm revolves around the elbow. Baffles are mounted individually onto the posterior arm and forearm, and the upper limb is fixed onto baffles by the bandage. An angular transducer is set on the elbow, which measures angle changes in the forearm. The tester wears short-sleeved shirts, and the baffle is in direct contact with the arm in actual use. A dumbbell is used for additional load in the plate, which makes it more convenient to increase and decrease the applied load.

The control principle of the proposed pneumatic exoskeleton is shown in Figure 2, where the host computer outputs pulse-width modulation (PWM) signals to a data acquisition card, and then, a single-chip microcomputer performs further processing. After the single-chip microcomputer receives signals, it will allow for the corresponding PWM signals' duty cycle and frequency to be drawn out of the amplifier, which will, in turn, control the opening and closing of a high-speed on-off valve. The sampled data of angle change in the elbow flow through the signal adjust circuit, and then, it is transmitted to the data acquisition card and host computer. The host computer also shows the collection of EMGs by electrodes, which are attached outside of the biceps and triceps [15]. The PAM is in the condition of either being deflated or inflated according to collected data of EMGs and angle changes.

The MHE2-MS1H-3/2G-QS-4-K (FESTO company) is selected as a high-speed on-off valve. The most suitable valve is found by studying the relationship between the high-speed on-off valve duty cycle and PAM contraction speed.

With the plate carrying a 3 kg weight, the duty ratio of the high-speed on-off valve is simultaneously altered, the recording time is from 3° to 60° in the elbow, and movements can be roughly divided into two types: up and down. The relationship between duty-ratio-controlled variables and contraction speed is shown in Figure 3, which can evaluate the speed of the exoskeleton according to the inverse of elapsed time.

Figure 1: Overall mechanical structure of pneumatic exoskeleton.

Figure 3 shows that when the value of duty-ratio-controlled variables is less than 80, it shows approximating linear relationships with the increase and decrease of speed. The elbow rotational speed reduces as the value of duty-ratio-controlled variables continues to increase. Moreover, it is experimentally found that the maximum permissible comfortable rotational speed in the elbow occurs when the duty-ratio-controlled variable is 80. Thus, the maximum duty-ratio-controlled variable of input is set to 80, and the problem of speed limit can be resolved, while the requirement of linear PAM contraction speed can be met.

3. Static Contraction of Upper Limb Muscles

3.1. Purpose and Experimental Design. With a constant elbow joint angle, we investigate how the EMGs of biceps and triceps change over time when different weights are loaded.

We try to imitate how the human limb works using the proposed exoskeleton, picking up and analyzing the EMGs when the exoskeleton is attached to the tester. Electrodes are laid outside of the biceps and triceps, and the posterior arm and forearm are fastened to the exoskeleton by the bandage. The posterior arm is in a vertical position, while the forearm is horizontal. Both upper limbs of the tester and the exoskeleton are lifted from the initial position to a set position, kept still for a period of 10 seconds, dropped, and returned to the initial position.

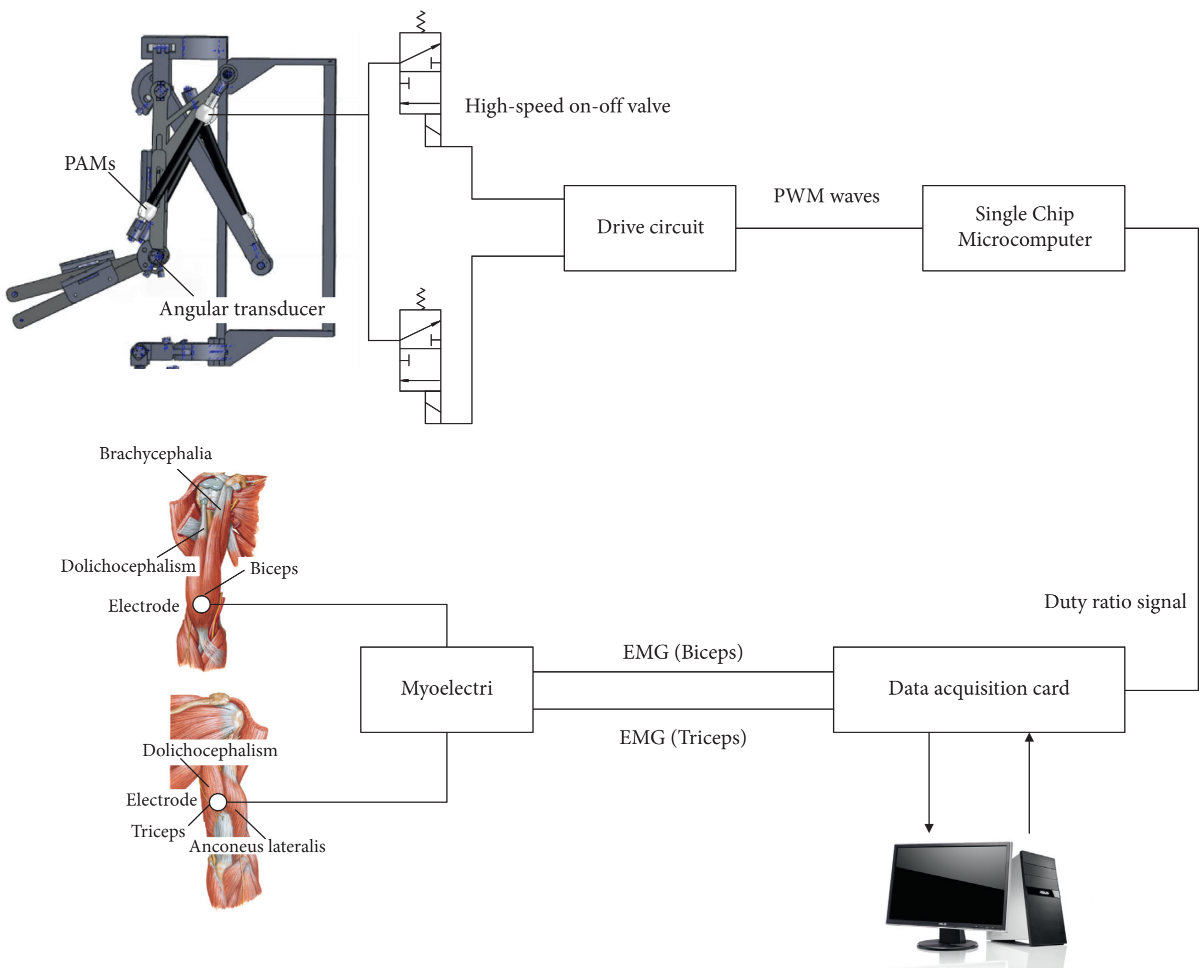

Figure 2: Control principle of the pneumatic exoskeleton.

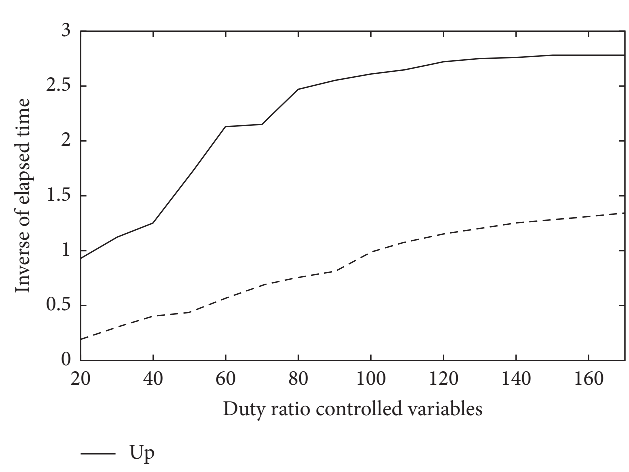

Figure 3: Relationship between duty-ratio-controlled variables and PAM contraction speed.

The load is gradually increased from 0 kg to 5 kg at an interval of 1 kg. The tester is given 30 seconds of break between the two experiments to prevent muscle fatigue.

3.2. Data Processing. Data acquisition is performed throughout holding up the forearm, recording the signals derived from interception, processing, and analysis of experimental findings, in order to characterize the upper limb muscles' static contraction features during keeping still.

The signals may contain a lot of noise and large voltage deviation, which greatly influences real data, so it is unnecessary to filter EMG signals prior to analysis. The frequency distribution of EMGs is 20–500 Hz, the frequency of main signals is 50–500 Hz, and signal interception is realized by a band-pass filter with a frequency of 50–500 Hz.

More research is needed to extract muscle contraction information after pretreatment of original EMGs. There are three methods for solving this problem: envelope, moving average, and moving RMS.

In envelope, first, full-wave rectification of the signal is performed, and then, a low band filter of two-order 2 Hz is applied, so that the local EMGs amplitude of the vibration can be briefly estimated.

With moving average, a period of time is selected that reads out the sum of signals after rectification (200 ms is taken as research object), and then, the average is found. This can often effectively reflect the amplitude of EMGs. Generally, the longer the time chosen, the more accurate amplitude can be obtained. However, if the time is too long, it will affect real-time control, and thus, 200 ms is preferred.

The difference between moving RMS and moving average is in the calculation of the square root of the average.

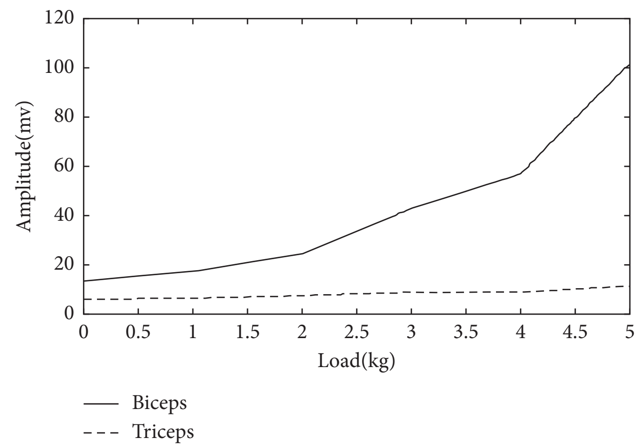

Figure 4: Biceps envelope.

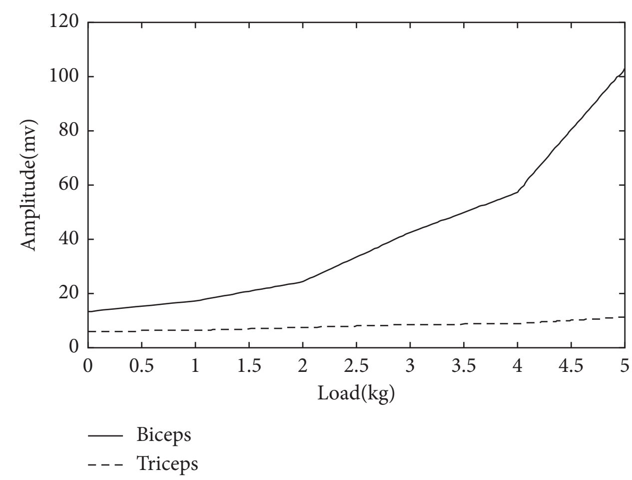

Figure 5: Biceps moving average.

3.3. Analysis of Results. The method of averaging the values of various quantities for 7 seconds is taken as the overall evaluation of feature variables, and the effects of load on the exoskeleton are investigated.

There are three methods of dissecting EMGs, as shown in Figures 4–7, and their results are approximately the same. The figures demonstrate how the characteristics obtained from biceps EMGs grow in an unlinear trend as more load is applied, which is closely corresponds to the EMGs and muscle force in human physiology. According to the characteristics obtained from triceps EMGs, the load comes to near-linear in the triceps. The difference between the biceps and the triceps is that the contraction length of the latter is much less than that of the former. The contraction length is very small, and the nonlinear EMG characteristics are close to linear.

4. Dynamic Contraction of Upper Limb Muscles

4.1. AR Model. Let $s(n)$ be a zero mean steady random signal, from which we can derive the source of white noise with known first-order and second-order statistics, where a linear system $h(k)$ is impelled by $w(n)$. The parameter $w(n)$ is zero mean white noise sequence, and its variance is σ_w^2; $h(k)$ or its transfer function $H(z)$ all comprise a linear system. If the power and system parameters of white noise excitation are known, the stochastic signal can become a model parameter, and its properties can be studied as shown in Figure 8 [16].

If $s(n)$ is only influenced by its previous value and present stimulus signals, we can obtain

$$s(n) = -\sum_{k=1}^{p} a_k s(n-k) + w(n), \qquad (1)$$

where a_k represents a model parameter, p represents order, $w(n)$ represents zero-mean-value stationary white noise, and its variance is σ^2.

The model transfer function $H(z)$ can be written as

$$\begin{aligned} H(z) &= \frac{1}{1+\sum_{k=1}^{p} a_k z^{-k}} \\ &= \frac{1}{A(z)}, \end{aligned} \qquad (2)$$

where $A(z) = 1 + \sum_{k=1}^{p} a_k z^{-k}$.

This is a p-order all-pole AR model, in which the randomness of the stochastic signal can be combined with some predictability by model parameters. Stimulus white noise reflects the randomness of signals, while the deterministic linear model reflects signal predictability.

4.2. Module Calculation. There are many methods to estimate AR module parameters, such as the correlation method

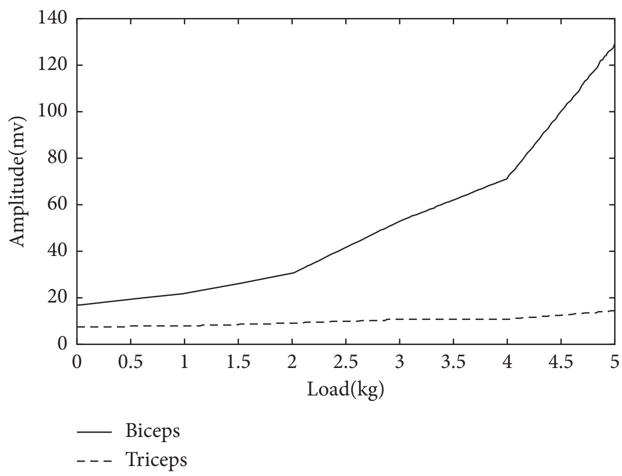

Figure 6: Biceps moving RMS.

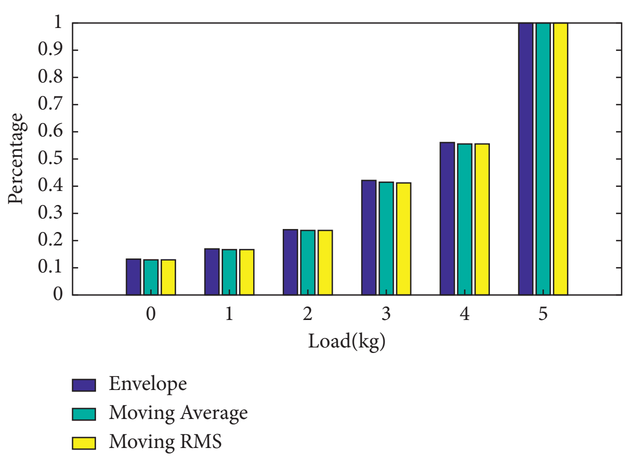

Figure 7: Comparison of biceps various treatment methods in the time domain.

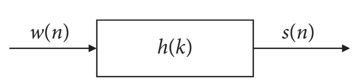

Figure 8: AR model.

and the Bury method. The relationship between AR module parameters and autocorrelation function is used in the correlation method.

For the p-order AR model, $s(n) = -\sum_{k=1}^{p} a_k s(n-k) + w(n)$; we multiply $s(n-i)\,(i>0)$ on both sides of the preceding formula at the same time and then calculate the average, which is performed because $E[w(n)s(n-i)] = 0$.

The Yule-Walker equation can also be deduced as

$$R_{ss}(i) = -\sum_{k=1}^{p} a_k R_{ss}(i-k)\; i>0 \tag{3}$$

As can be seen from (3), for signals as described by the p-order AR model, only the p autocorrelation function is independent, and the solution to the rest can be the recurrence formulas.

$$\begin{pmatrix} R_{ss}(0) & R_{ss}(-1) & \dots & R_{ss}(1-p) \\ R_{ss}(1) & R_{ss}(0) & \dots & R_{ss}(2-p) \\ \vdots & \vdots & \vdots & \vdots \\ R_{ss}(p-1) & R_{ss}(p-2) & \dots & R_{ss}(0) \end{pmatrix} \begin{pmatrix} a_1 \\ a_2 \\ \vdots \\ a_p \end{pmatrix} = -\begin{pmatrix} R_{ss}(1) \\ R_{ss}(2) \\ \vdots \\ R_{ss}(p) \end{pmatrix}. \tag{4}$$

The autocorrelation function is an even function, and the matrix is symmetric, where all diagonal elements are equal to $R_{ss}(0)$. If any elements clinodiagonal or parallel to the principal diagonal are the same, it is a Toeplitz matrix. The autocorrelation function is known, and the solution of the AR model-related coefficient is through (4).

The Burg method is the most commonly used approach for AR module parameters. It presents a method of forwarding prediction error and backward prediction error based on the least mean-square error rule, to obtain reflection coefficient *Km*, which is unexpectedly left outside of known data. The Burg method demonstrates better resolution than the correlation method on this account and is the proper solution for analyzing EMGs.

4.3. Feature Extraction. Using the copy of data analyzed in AR module parameters, we carry out the division to EMGs after filtering. The longer the segment of data, the greater meaning it contains, and the higher stability and accuracy of the AR coefficient. However, if the segment of data is too long, it is not conducive to real-time information control. To guarantee real-time control, and to avoid causing a discernible delay, the total time for data storage and data processing cannot be more than 300 ms.

There are two alternative segmentation methods, namely, overlapping window and alternating windows.

In the overlapping window method, operations are constantly performed on data, the same block of data is executed for a specified number of times, the more running code is operated, and it will be more complicated for the control system. If accelerated by computing, the data processing time can be reduced to 1 ms, and a good result for the data segment of 200 ms can be obtained. Taking all factors into consideration, alternating windows are chosen for segmentation.

As can be derived from Figures 9–11, with the increase of amplitude, the AR module coefficient enhances, and the order coefficient does not change much. If the sum of the absolute value of the AR module order is directly adopted, the other items will not adjust automatically, and it increases with load.

4.4. Forearm Rapid Swing and Slow Swing. With the forearm held up and the elbow joint rotated, the EMGs of biceps and triceps change are explored under different loads.

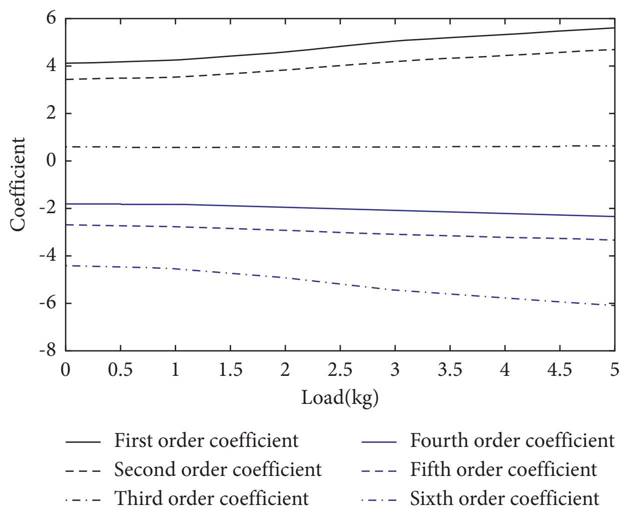

Figure 9: Change of biceps AR module coefficient.

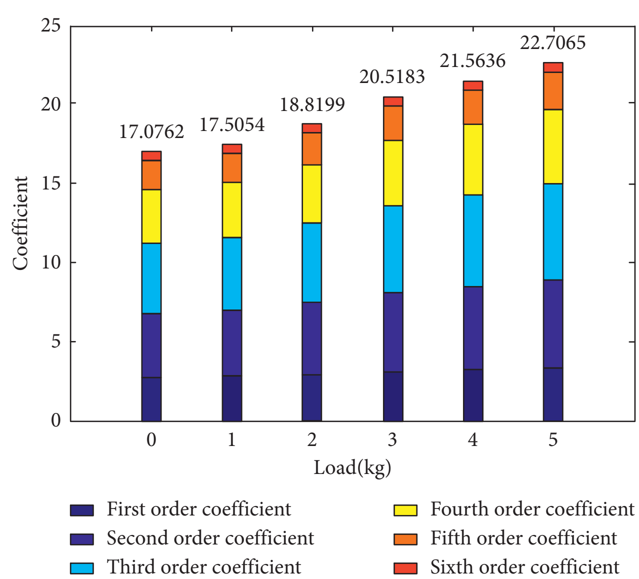

Figure 10: Absolute value sum of biceps AR module coefficient.

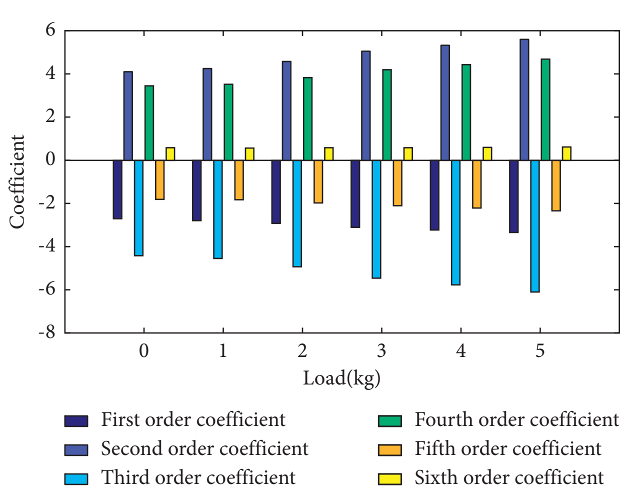

Figure 11: Biceps AR module coefficient.

The EMGs amplitude can be estimated by the methods of envelope, moving average, and moving RMS with the static contraction of upper limb muscles. However, the method of envelope provides much higher real-time amplitudes, which is of great benefit to the control system design, and is selected to obtain the upper limb muscle dynamic contraction feature variables.

The tester lifts their forearm as briskly as they can with the loaded exoskeleton in rapid swing, while it is lifted slowly in slow swing.

As shown in Figure 12, biceps EMGs are the most obvious, and the amplitude of triceps EMGs rises and falls, but at a modest rate when the forearm is held up. Biceps EMGs rapidly increase with the elbow joint angle, decay quickly as the elbow joint angle remains unchanged, and continue to fall if the angle decreases. This suggests that rapid swing occurs at the moment when the forearm outputs force when biceps EMGs gain more intensity and quickly fall back. The intensity of biceps EMGs increases slowly, and it fluctuates during the forearm slow swing. The signal intensity during rapid swing is much higher than that during slow swing.

4.5. Intermittent Forearm Swing. The movement of the upper limb is usually irregular, not always showing reciprocating action and featuring spasmodic stops in usual daily life. Therefore, the value changes of EMGs in such cases will have to be studied. Here, the exoskeleton is loaded with 3 kg weight, and the tester lifts-up their forearm freely.

As shown in Figure 13, the relationship between EMGs intensity and joint angle is nonlinear. The amplitude of EMGs does not increase when the angle is 0–50°. However, it obviously increases when the angle is 60–85°. In addition, when the angle changes abruptly, the amplitude also changes suddenly.

4.6. Comparison of Results. The large difference between dynamic contraction and static contraction is that EMGs reach the peak at one moment, and the highest value has nothing to do with joint velocity change. The change in joint velocity is fast, the muscular instantaneous contraction is violent, and EMGs are intense. The analysis of maximum EMGs can reflect the dynamic contraction of muscles.

Table 1 and Figure 14 show that there is a distinctive difference between rapid swing and slow swing in rise time and fall time, which further effectively proves that movement modes can be classified into rapid and slow swing in dynamic contraction. The amplitude of maximum EMGs increases with the load, whether rapid swing or slow swing, which is similar to static contraction. Meanwhile, it is obvious that the relationship between maximum EMGs amplitude and load is nonlinear; the growth rate is comparatively larger at the beginning and then slowly descends. Moreover, by comparing the two different swing modes, we can find that the capacity of separating the maximum EMGs is weak when the load is small, and EMGs' magnitude for fast swing is much larger than that for slow swing when the load is large.

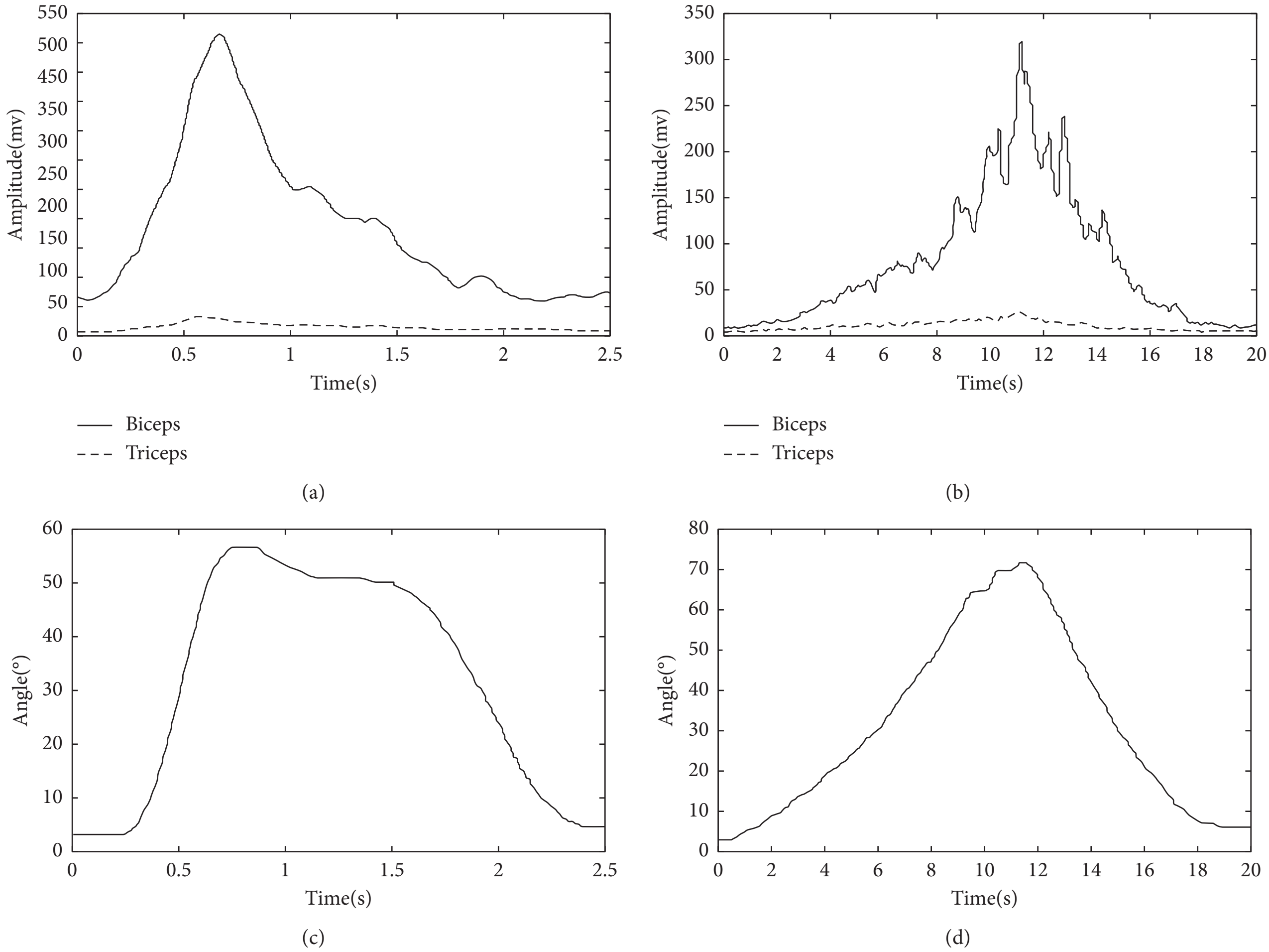

Figure 12: Dynamic contraction of (a) EMGs featuring value change in rapid swing, (b) EMGs featuring value change in slow swing, (c) elbow joint change in rapid swing, (d) elbow joint change in slow swing, with 5 kg load.

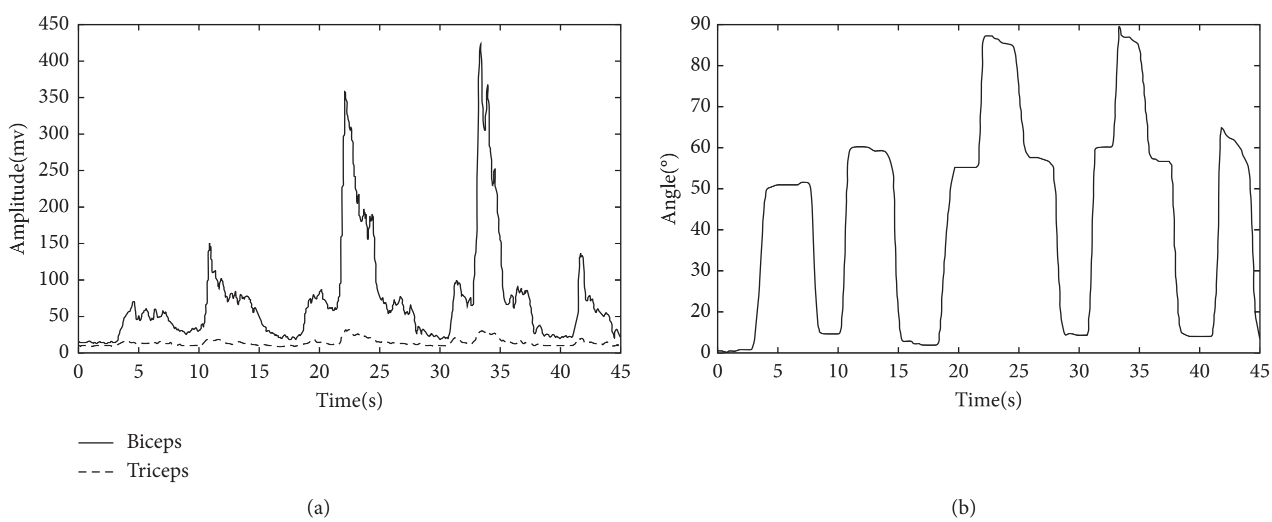

Figure 13: Discontinuous swing; (a) EMGs feature value change in discontinuous swing and (b) elbow joint change in discontinuous swing, with 3 kg load applied.

Table 1: Comparison of dynamic contraction under various loads.

Load (kg)	Rise time (s)		Fall time (s)		Maximum amplitude (mV)	
	Rapid	Slow	Rapid	Slow	Rapid	Slow
0	0.5	10	0.5	12	130	80
1	0.5	10	0.6	18	180	140
2	0.5	15	0.8	10	300	250
3	0.5	10	0.8	8	480	270
4	0.5	10	1	8	485	310
5	0.5	9	1	6	514	325

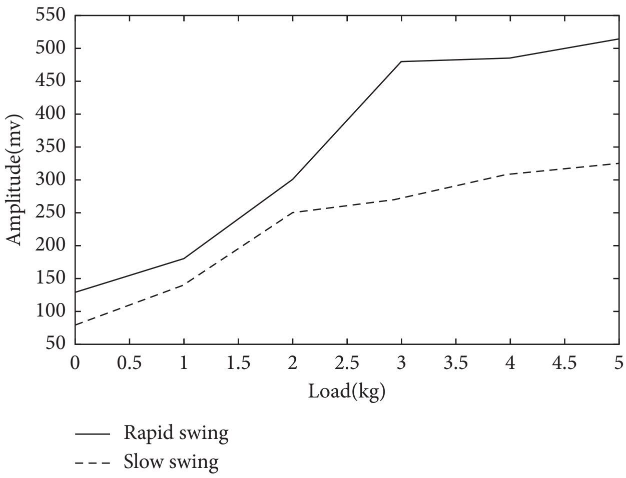

Figure 14: Maximum EMG under various loads.

5. Man-Machine Synergy Control

5.1. EMGs Mapping Relationships. When the tester is in the exoskeleton, muscle force can be subjectively conceived into five levels: powerless, weak, moderate, strong, and very strong, and its corresponding duty-ratio-controlled variables are 20, 40, 60, 80, and 100. The biceps (pulling up) and triceps (pulling down) EMGs strength can be estimated in such a case. The method for EMGs strength calculation is to average the EMGs characters of muscle force within 0.5 seconds.

$$\overline{\mathrm{EMG}} = \frac{\sum_{i=0}^{1000} \mathrm{EMG}(i)}{1000}, \quad (5)$$

where $\mathrm{EMG}(i)$ represents sampled data, and $\overline{\mathrm{EMG}}$ is the average of EMGs.

The sampled data are shown in Table 2.

From Figure 15, a nonlinear relationship between duty-ratio-controlled variables and average EMG characters can be derived. This suggests that EMGs generated by human perception of muscle force are nonlinear. If the exoskeleton is in strict accordance with linear control, we will quickly run into rotational speed increases with the elbow joint. Thus, it is easily operated, and the operation is linear control in human perception, and nonlinear EMGs are mapped to duty-ratio-controlled variables.

There are only 5 separated points in Figure 15. The average EMG characters can be contrasted with the duty-ratio-controlled variables, and the two appear in a continuum for continuous control; hence, interpolation is needed for the 5 separated points.

5.2. Polynomial Interpolation. A series of points also looks as an approximate expression when using interpolation. The choices of functional form can be various, such as trigonometric function and rational function. Algebraic polynomial interpolation is applied, as it is easily performed by the function of $f(x) = a_0 + a_1x + a_2x^2 + \ldots + a_nx^n$.

As the function has 5 points, according to the polynomial interpolation uniqueness condition, the fourth-order polynomial is satisfactory. Its key is to define the related coefficient of the polynomial function. There are many methods to solve the problem, such as multivariable polynomial system or Lagrangian method. The order of interpolation is small, and it is easy to find a solution for equations. We can obtain the polynomial coefficient by developing programs directly for equations in software, and the procedure is presented below.

There are 5 points, namely, (x_0, y_0), (x_1, y_1), (x_2, y_2), (x_3, y_3), and (x_4, y_4), which satisfy the function of $f(x) = a_0 + a_1x + a_2x^2 + a_3x^3 + a_4x^4$, giving the following equations [17]:

$$\begin{cases} a_0 + a_1x_0 + a_2x_0^2 + a_3x_0^3 + a_4x_0^4 = y_0, \\ a_0 + a_1x_1 + a_2x_1^2 + a_3x_1^3 + a_4x_1^4 = y_1, \\ a_0 + a_1x_2 + a_2x_2^2 + a_3x_2^3 + a_4x_2^4 = y_2, \\ a_0 + a_1x_3 + a_2x_3^2 + a_3x_3^3 + a_4x_3^4 = y_3, \\ a_0 + a_1x_4 + a_2x_4^2 + a_3x_4^3 + a_4x_4^4 = y_4. \end{cases} \quad (6)$$

Using the Gaussian elimination method of linear algebra, the combination of elimination method and recursive method as a solution to the above equations can yield the values of 5 parameters.

Given the parameters in Table 3 above as a reference, the mapping relation function image is illustrated in Figure 16.

As can be seen in Figure 16, the interpolation function goes through points that are detected using the interpolation method, and ideal nonlinear mapping can be realized around several measured points. These points easily fluctuate around the measured points. According to the triceps mapping relation in Figure 16, the average EMGs character is more than 50, and the corresponding duty-ratio-controlled variables exhibit a sharp drop, which is even negative.

This explains the problem of man-machine synergy control. The operator's upper limb swings up, stops in midstream, and then swings up again, which will lead to the upper limb's shaking. This is mainly because of a sudden change of the moving direction of human muscle dynamic contraction, causing a sharp maximum in EMGs. The duty-ratio-controlled variables of the triceps will offset those of the biceps first, and then, triceps EMGs are in the process of 50–80, falling off sharply. Subsequently, the net duty-ratio-controlled variables increase again, which causes vibration.

Table 2: Exertion rating and average EMGs characters.

Exertion rating	Duty-ratio-controlled variables	Biceps EMG ratio	Triceps EMG ratio
Powerless	20	11.9	4.8
Weak	40	21.3	9.7
Moderate	60	33.0	18.3
Strong	80	44.1	29.4
Very strong	100	79.1	49.4

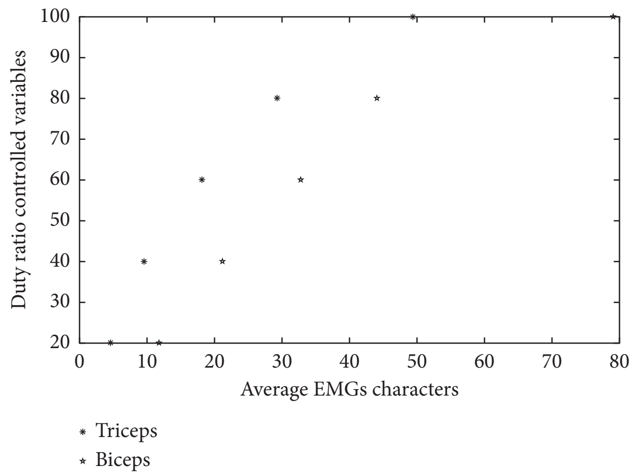

Figure 15: Scatter diagram of duty-ratio-controlled variables and average EMG characters.

Table 3: Mapping relation parameters.

Signal source	a_0	a_1	a_2	a_3	a_4
Biceps	−21.810601	4.827553	−0.138556	0.002629	−0.000018
Triceps	−11.075030	8.138877	−0.382913	0.009916	−0.000093

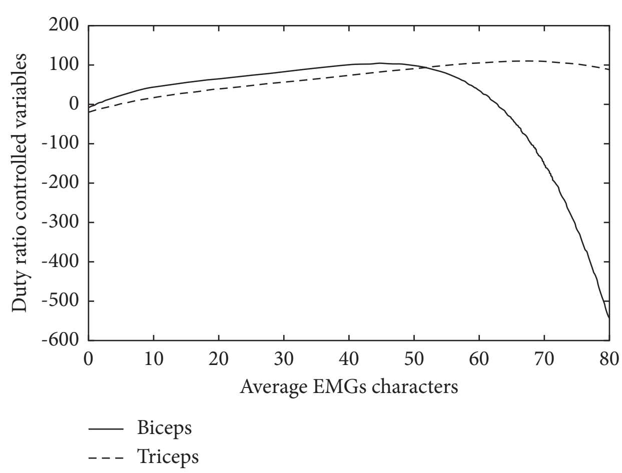

Figure 16: Duty-ratio-controlled variables and average EMGs characters.

To solve the problem of EMGs mapping uncertainty outside the range of interpolation, the answer is to cut out the EMGs' feature value. The oversized EMGs feature value matches the maximal duty-ratio-controlled variables directly. When EMGs are very small, the duty-ratio-controlled variables are set to the high-speed on-off valve dead zone critical point, which is 15.

5.3. Determination of Synergic Control Method. The synergic control method falls into three steps: feature extraction, nonlinear mapping, and comparison judgment.

Feature extraction only consists of the high-pass filter, full-wave rectifier, and low-pass filter, originally acquiring the EMGs data of two motions, the envelope curve of biceps and triceps EMGs, which are EMG_1 and EMG_2, respectively.

According to the method claimed above, the biceps and triceps ratings of perceived exertion average EMGs characters are $\mathrm{EMG}_{10} \ldots \mathrm{EMG}_{14}$ and $\mathrm{EMG}_{20} \ldots \mathrm{EMG}_{24}$, respectively, and then, in polynomial interpolation, the interpolation function coefficients are $a_{10} \ldots a_{14}$ and $a_{20} \ldots a_{24}$, and the mapping function is as follows:

$$\mathrm{Duty}_{\mathrm{emg1}}(x) = \begin{cases} 15, & x \le \mathrm{EMG}_{10}, \\ a_{10} + a_{11}x + a_{12}x^2 + a_{13}x^3 + a_{14}x^4, & \mathrm{EMG}_{10} < x < \mathrm{EMG}_{14}, \\ 100, & x \ge \mathrm{EMG}_{14}, \end{cases}$$
$$\mathrm{Duty}_{\mathrm{emg2}}(x) = \begin{cases} 15, & x \le \mathrm{EMG}_{20}, \\ a_{20} + a_{21}x + a_{22}x^2 + a_{23}x^3 + a_{24}x^4, & \mathrm{EMG}_{20} < x < \mathrm{EMG}_{24}, \\ 100, & x \ge \mathrm{EMG}_{24}. \end{cases} \quad (7)$$

After the nonlinear mapping of EMGs, the net duty-ratio-controlled variables $\mathrm{Duty}_{\mathrm{net}}$ can be calculated as

$$\mathrm{Duty}_{\mathrm{net}} = \mathrm{Duty}_{\mathrm{emg1}}(\mathrm{EMG}_1) - \mathrm{Duty}_{\mathrm{emg2}}(\mathrm{EMG}_2), \quad (8)$$

where $\mathrm{Duty}_{\mathrm{emg1}}(\mathrm{EMG}_1)$ and $\mathrm{Duty}_{\mathrm{emg2}}(\mathrm{EMG}_2)$ are the duty-ratio-controlled variables of the first and second high-speed on-off valve, respectively.

5.4. Forearm Lift-Up Motion When Unpowered with Various Loads. The biceps and triceps EMGs are taken as control input when the tester is in the exoskeleton while studying the load controlling results and the effect of weight reduction by the exoskeleton.

The experiment includes two parts: forearm EMGs unpowered with various loads and forearm EMGs powered by the exoskeleton with various loads.

The tester stands still, the surface electrodes are pasted to a relevant location outside of the biceps and triceps, the tester outputs upward force, and the exoskeleton swings up, recording EMGs and the angle in the whole process.

It can be derived from Figure 17 and 18 that the biceps EMGs increase with elbow joint angle and triceps EMGs change little in the process.

5.5. Forearm Lift-Up Motion When Powered with Various Loads. The EMGs and angle joint variation curves (powered, 5 kg) can be seen in Figures 19 and 20. When the operator lifts-up and puts down the forearm, muscles are activated. The movements are biceps upward and triceps downward, and the essential distinction is obvious, which is different from the powered condition. The load is not on the operator when powered, and the biceps does not need to be in tension all the time during lifting up and putting down the forearm; there is a great deal of difference in EMGs change. The wave deformation is very similar in the process of lifting up when powered, and the variance of maximum EMGs is much larger than the average EMGs.

5.6. Maximum EMGs Powered Efficiency. The average EMGs feature value describes EMGs in the whole process, and the maximum EMGs feature value describes the extent to which the muscles are activated during dynamic muscle contraction. The biceps maximum EMGs in lifting up under unpowered and powered conditions are compared to evaluate powered efficiency.

The maximum EMGs powered efficiency can be derived from Table 4. The maximum value of EMGs shows a sharp reduction between unpowered and powered condition, and the maximum EMGs powered efficiency can reach 78.66%. The less the maximum EMGs, the more comfortable for the operator, and the relatively smaller transient impact to the limb.

5.7. Powered Stability Analysis. The intensity of EMGs rises with the increase of load when unpowered; however, the muscle output force is approximating similar without much fluctuation when powered. To evaluate the fluctuation of the control system relative to load change, EMGs mean variance is calculated for various loads.

Table 5 describes powered stability. The mean of biceps EMGs is 26.05 during lifting up with the load increased from 0 kg to 10 kg, which is smaller than that for an unpowered condition without any load, and the standard deviation is 3.79. The mean of triceps EMGs is 19.01 during putting down, while the unpowered minimum biceps feature value is 25.3. With the increase of load, the force change is very small for the operator to control the exoskeleton, and the results for exoskeleton assistance are excellent.

5.8. Coordination Effect Analysis. In order to evaluate the advantage of the control method, man-machine synergy control is another aspect besides assistance. The aim of synergy control is that man should be synchronized with the exoskeleton, and the operator can achieve starting and stopping the control of the exoskeleton.

The discontinuous swing EMGs and angle joint variation curves are shown in Figures 21 and 22. The operator stops the exoskeleton midstream, and there is an angle overshoot, which diminishes gradually with the load increase and inertia moment.

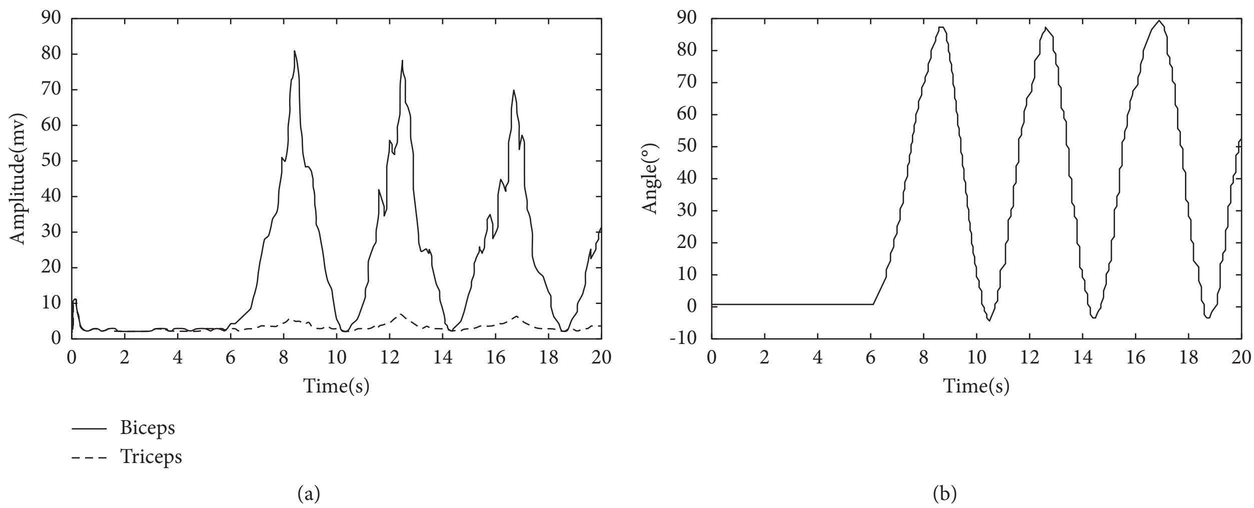

Figure 17: EMGs and angle joint variation curves of (a) EMGs and (b) angle joint; unpowered (3 kg).

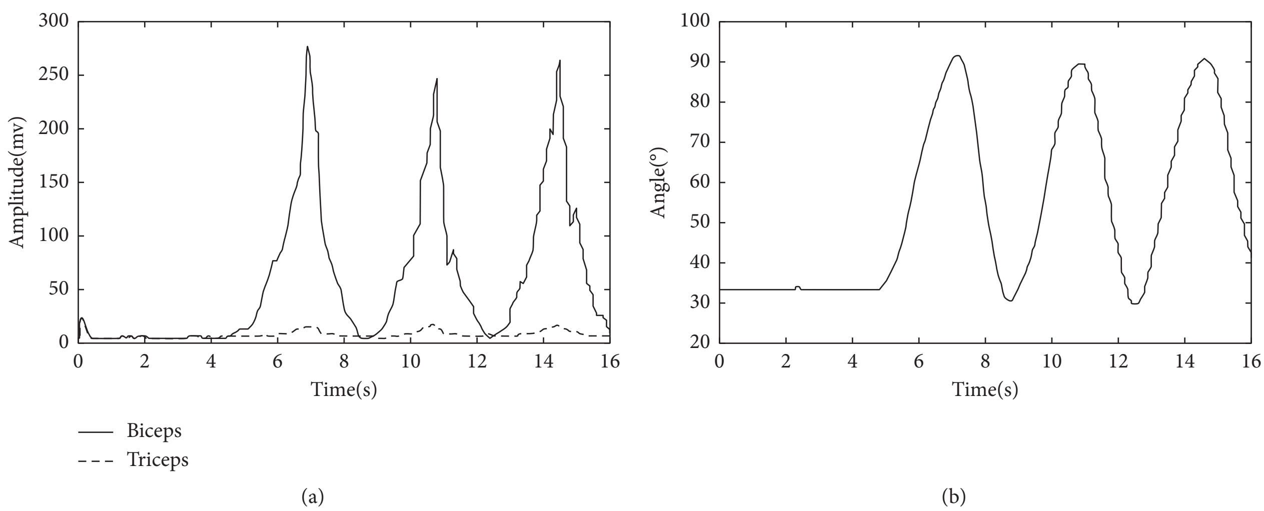

Figure 18: EMGs and angle joint variation curves of (a) EMGs and (b) angle joint; unpowered (5 kg).

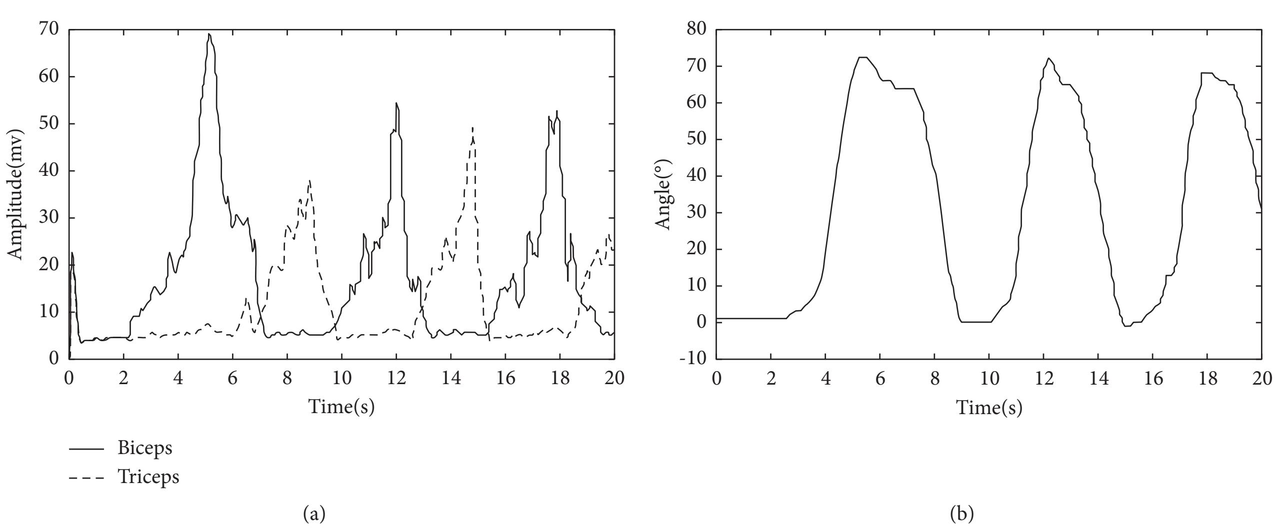

Figure 19: EMGs and angle joint variation curves of (a) EMGs and (b) angle joint; powered condition (3 kg).

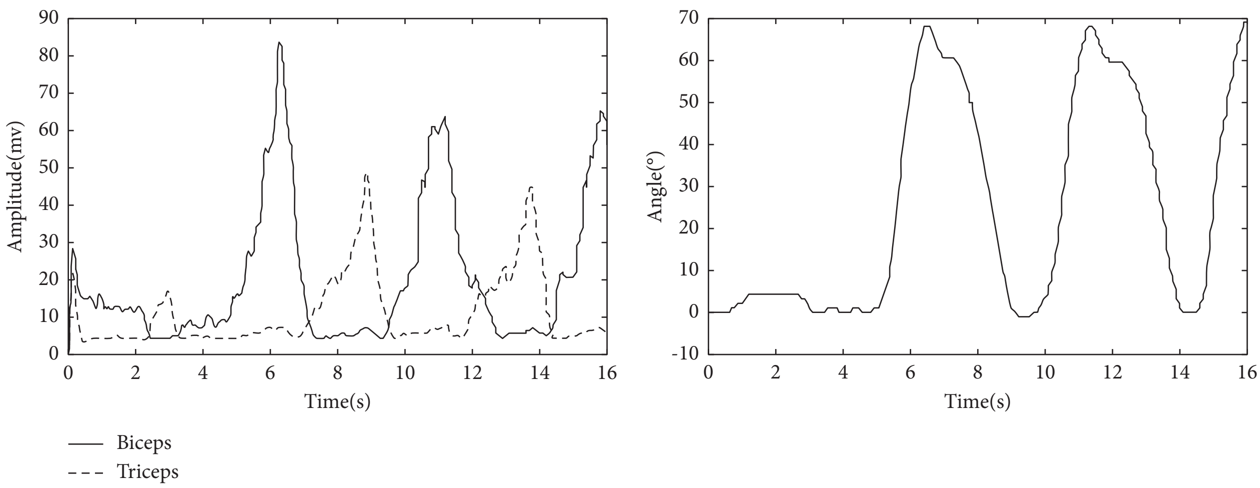

(a) (b)

Figure 20: EMGs and angle joint variation curves of (a) EMGs and (b) angle joint; powered condition (5 kg).

Table 4: Maximum EMGs powered efficiency.

Load (kg)	Lifting up		
	Unpowered	Powered	Powered efficiency
0	74.0	72.1	2.57
1	98.3	50.9	48.22
2	110	64.1	41.73
3	156	53.8	65.51
4	262	55.9	78.66
5	274	63.2	76.93

Table 5: Powered stability.

Statistics	Lifting up		Putting down	
	Biceps	Triceps	Biceps	Triceps
Average value	26.05	5.39	9.22	19.01
Variance	3.79	0.30	1.48	3.97

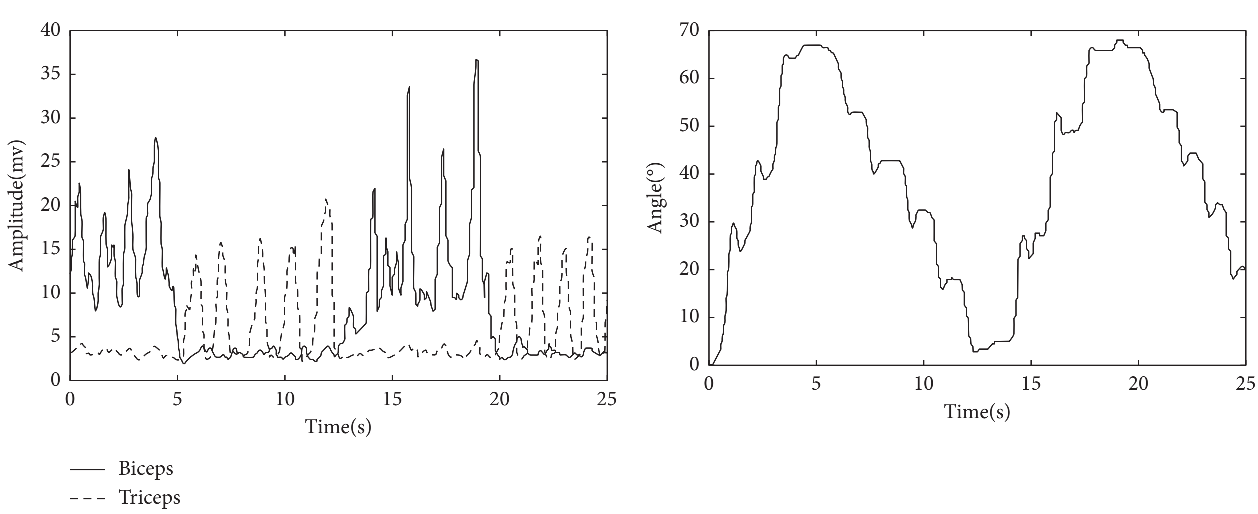

(a) (b)

Figure 21: Discontinuous swing EMGs and angle joint variation curves of (a) EMGs, (b) angle joint under 3 kg load.

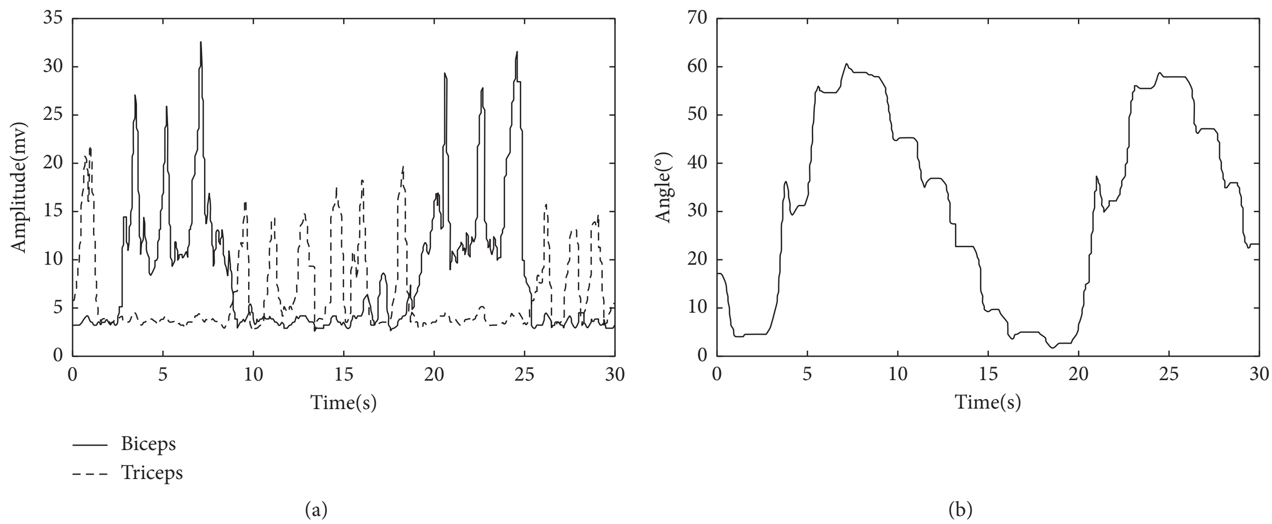

FIGURE 22: Discontinuous swing EMGs and angle joint variation curves of (a) EMGs, (b) angle joint under 5 kg load.

6. Conclusions

This study analyzed the amplitude and frequency characteristics of EMGs and proposed a suitable signal processing scheme. The acquisition instrument was selected, and the EMGs acquisition system was established. The biceps and triceps EMGs static contraction and dynamic contraction, and rotational speeds were analyzed under various loads (3 kg and 5 kg, respectively). The duty-ratio-controlled variables could be divided into five levels corresponding to the exertion rating from powerless to very strong in two EMGs characters, which can be reflected in the scatter diagram of duty-ratio-controlled variables and average EMGs characters. The net duty-ratio-controlled variables were adopted to control the on-off state and PWM duty ratio of the high-speed on-off valve. The maximum EMGs powered efficiency, powered stability analysis, and coordination effect all indicate that the pneumatic-powered exoskeleton is of good assistance, and synergic control also works perfectly in forearm lift-up movement powered under various loads, whether the elbow is in continuous swing or not.

We may extend the proposed methods to uncertain probabilistic linguistic environments in our future studies [18, 19], including decision-making with probabilistic hesitant fuzzy information based on multiplicative consistency, instead of the man-machine synergic control in a specific environment. We may also extend the proposed methods to probabilistic linguistic uncertain environments in our future studies, such as score function based on concentration degree for probabilistic linguistic term sets, evaluating the Internet of Things platforms using integrated probabilistic linguistic multicriteria decision-making method [20–23]. We can also introduce a nonlinear control algorithm in the controller design, such as fuzzy control, neural network control [24], and observer-based fuzzy adaptive control [25].

Data Availability

All data, models, or code generated or used to support the findings of this study are available from the corresponding author upon request.

Conflicts of Interest

The author(s) declare no potential conflicts of interest with respect to research, authorship, and/or publication of this article.

Acknowledgments

This project was supported by the Zhejiang Province Welfare Technology Applied Research Project (project no. GLF 19E050003), College Students' Science and Technology Innovation and XinMiao Project of Zhejiang Province (project no. 2021R417019), and Zhejiang Province Welfare Technology Applied Research Project (project no. GLF 20E090006).

References

[1] R. F. Antonio, L. P. Joan, and L. P. Josep, "Systematic review on wearable lower-limb exoskeletons for gait training in neuromuscular impairments," *Journal of NeuroEngineering and Rehabilitation*, vol. 18, p. 22, 2021.

[2] J. Narayan, B. Kalita, and S. K. Dwivedy, "Development of robot-based upper limb devices for rehabilitation purposes: a systematic review," *Augmented Human Research*, vol. 6, no. 1, p. 4, 2021.

[3] M. Dong, Y. Zhou, J. Li et al., "State of the art in parallel ankle rehabilitation robot: a systematic review," *Journal of NeuroEngineering and Rehabilitation*, vol. 18, no. 1, p. 52, 2021.

[4] N. P. Fromme, M. Camenzind, R. Riener, and R. M. Rossi, "Need for mechanically and ergonomically enhanced tremor-suppression orthoses for the upper limb: a systematic review,"

Journal of NeuroEngineering and Rehabilitation, vol. 16, no. 1, p. 93, 2019.

[5] C. Lambelet, D. Temiraliuly, M. Siegenthaler et al., "Characterization and wearability evaluation of a fully portable wrist exoskeleton for unsupervised training after stroke," *Journal of NeuroEngineering and Rehabilitation*, vol. 17, no. 1, p. 132, 2020.

[6] M. Rahmani and M. H. Rahman, "Adaptive neural network fast fractional sliding mode control of a 7-DOF exoskeleton robot," *International Journal of Control, Automation and Systems*, vol. 18, no. 1, pp. 124–133, 2020.

[7] F. Xiao, Y. Gao, Y. Wang, Y. Zhu, and J. Zhao, "Design and evaluation of a 7-DOF cable-driven upper limb exoskeleton," *Journal of Mechanical Science and Technology*, vol. 32, no. 2, pp. 855–864, 2018.

[8] O. Baser, H. Kizilhan, and E. Kilic, "Employing variable impedance (stiffness/damping) hybrid actuators on lower limb exoskeleton robots for stable and safe walking trajectory tracking," *Journal of Mechanical Science and Technology*, vol. 34, no. 6, pp. 2597–2607, 2020.

[9] B. J. Kruif1, E. Schmidhauser, K. S. Stadler, and L. O. Sullivan, "Simulation architecture for modelling interaction between user and elbow-articulated exoskeleton," *Journal of Bionics Engineering*, vol. 14, pp. 706–715, 2017.

[10] S. Kittisares, H. Nabae, G. Endo, K. Suzumori, and R. Sakurai, "Design of knee support device based on four-bar linkage and hydraulic artificial muscle," *Robomech Journal*, vol. 7, no. 1, p. 16, 2020.

[11] M. Ashmi, M. Anila, and K. S. Sivanandan, "Comparison of SMC and PID controllers for pneumatically powered knee orthosis," *Journal of Control, Automation and Electrical Systems*, vol. 32, no. 5, pp. 1153–1163, 2021.

[12] H. D. Lee, H. Park, B. Seongho, and T. H. Kang, "Development of a soft exosuit system for walking assistance during stair ascent and descent," *International Journal of Control, Automation and Systems*, vol. 18, no. 10, pp. 2678–2686, 2020.

[13] G. M. Bryan, P. W. Franks, S. Song et al., "Optimized hip-knee-ankle exoskeleton assistance reduces the metabolic cost of walking with worn loads," *Journal of NeuroEngineering and Rehabilitation*, vol. 18, no. 1, p. 161, 2021.

[14] Z. Yang, S. Guo, Y. Liu, H. Hirata, and T. Tamiya, "An intention-based online bilateral training system for upper limb motor rehabilitation," *Microsystem Technologies*, vol. 27, no. 1, pp. 211–222, 2021.

[15] S. X. Deng, J. Wang, and D. C. Qiao, *Sport Physiology*, Higher Education Press, Beijing, China, 3rd edition, 2015.

[16] X. Cui, *Signal Analysis and Processing*, China Power Press, Beijing, China, 3rd edition, 2016.

[17] D. F. Zhang, *MATLAB Numerical Method*, China Machine Press, Beijing, China, 2010.

[18] P. Li and H. Chen, "Evaluation of green building suppliers based on IVPLTS-CBR decision-making method," *International Journal of Intelligent Computing and Cybernetics*, vol. 15, 2021.

[19] V. C. Maduekwe and S. A. Oke, "Novel Taguchi scheme-based DEMATEL methods and DEMATEL method for the principal performance indicators of maintenance in a food processing industry," *International Journal of Intelligent Computing and Cybernetics*, vol. 14, no. 3, pp. 363–397, 2021.

[20] M. Lin, Z. Chen, Z. Xu, X. Gou, and F. Herrera, "Score function based on concentration degree for probabilistic linguistic term sets: an application to TOPSIS and VIKOR," *Information Sciences*, vol. 551, pp. 270–290, 2021.

[21] M. Lin, C. Huang, Z. Xu, and R. Chen, "Evaluating IoT platforms using integrated probabilistic linguistic MCDM method," *IEEE Internet of Things Journal*, vol. 7, no. 11, pp. 11195–11208, 2020.

[22] M. Lin, Y. Chen, and R. Chen, "Bibliometric analysis on Pythagorean fuzzy sets during 2013-2020," *International Journal of Intelligent Computing and Cybernetics*, vol. 14, no. 2, pp. 104–121, 2021.

[23] X. Q. Xu, J. L. Xie, N. Yue, and H. Wang, "Probabilistic uncertain linguistic TODIM method based on the generalized Choquet integral and its application," *International Journal of Intelligent Computing and Cybernetics*, vol. 14, pp. 122–144, 2021.

[24] Y. Chen, G. L. Tao, and H. Liu, "High precision adaptive robust neural network control of a servo pneumatic system," *Applied Sciences*, vol. 9, no. 17, p. 3472, 2019.

[25] F. L. Jiang, H. Liu, and D. X. Chai, "Humanoid lower limb: design, analysis, observer-based fuzzy adaptive control and experiment," *Mathematical Problems in Engineering*, vol. 2021, 15 pages, 2021.

Hindawi
Mathematical Problems in Engineering
Volume 2022, Article ID 7685033, 18 pages
https://doi.org/10.1155/2022/7685033

Research Article

A Divergence-Based Medical Decision-Making Process of COVID-19 Diagnosis

Bahram Farhadinia

Department of Mathematics, Quchan University of Technology, Quchan, Iran

Correspondence should be addressed to Bahram Farhadinia; bfarhadinia@qiet.ac.ir

Received 3 December 2021; Revised 12 January 2022; Accepted 18 January 2022; Published 11 February 2022

Academic Editor: Ali Ahmadian

This study is concerned with introducing a class of parametric and symmetric divergence measures under hesitant fuzzy environment. The proposed divergence measures have several interesting properties which make their use attractive. In order for exploring the features of proposed divergence measures for hesitant fuzzy sets (HFSs), we compare them with other existing ones in terms of divergence-initiated weighs and counter-intuitive cases. In the process of comparison, we first modify the conventional framework of hesitant fuzzy additive ratio assessment (HFARAS) using the proposed divergence measures, and then, the superiority of proposed measures is further demonstrated in a COVID-19 case study. There, we notify that the other existing divergence measures may not provide satisfactory results.

1. Introduction

These days, the COVID-19 pandemic is drastically impacting healthcare systems [1–3] worldwide. To solve the problems of this pandemic, many medical scientists are focusing their research on that, and for recognizing and diminishing the COVID-19 effects, a large number of researchers have prepared a variant of workable models. Fouladi et al. [4] considered ResNet, OxfordNet, convolutional neural network, convolutional autoencoder neural network, and machine learning methods in order to classify chest CT images of COVID-19. Melin et al. [5] predicted successfully the consequence of COVID-19 time series by the help of a multiple collaborative convolutional neural network tool which is described thoroughly by encountering the concept of fuzzy set. Abdel-Basst et al. [6] merged two techniques, namely, the Best-Worst Method (BWM) and Technique for Order Preference by Similarity to Ideal Solution (TOPSIS) method to explore the association between COVID-19 and different viral chest diseases in uncertainty environment. By implementation of a model of Internet-based reporting, Bonilla-Aldana et al. [7] gathered the data on COVID-19 to increase its effectiveness during the pandemic. Ashraf and Abdullah [8] proposed a number of tools for dealing with the emergency condition of COVID-19 using the concept of spherical fuzzy set. In the period of COVID-19 pandemic in China, Wu et al. [9] introduced a technique to plan several emergency production procedures for producing a proper medical mask. Mishra et al. [10] enhanced the additive ratio assessment model by encountering the divergence measure to evaluate the medicine being used to treat those patients involving the mild symptoms of COVID-19.

The additive ratio assessment (ARAS) technique [11] implements the concept of optimality degree for extracting a ranking. In brief, this technique is described as a fraction of two values: the sum of normalized weighted values for criteria corresponding to each alternative and the sum of normalized weighted values for the best alternative. Indeed, the ARAS framework has intuitive procedures yielding relatively exact outcomes in the process of choosing diversified alternatives.

Up to now, there exist a large number of fuzzy-based contributions dedicated to the ARAS technique. Following, Zavadskas and Turskis [11] who first argued that a complicated phenomenon in the real world could be realized by the help of simple comparisons, Turskis and Zavadskas [12] tried to select the logistic center location based on the combination of AHP and ARAS for data in the form of fuzzy sets. In the sequel, Stanujkic [13] generalized the ARAS framework to that of interval-valued fuzzy sets. Büyüközkan and Göçer [14] developed the ARAS framework to that of interval-valued intuitionistic fuzzy sets for evaluating the digital supply chains. Büyüközkan and Göçer [15] assessed the digital maturity scores of the firms on the basis of hesitant fuzzy ARAS framework. Iordache et al. [16] suggested an interval type II hesitant fuzzy ARAS framework for choosing the location of underground hydrogen storage. Liao et al. [17] offered an ARAS framework encountering the hesitant fuzzy linguistic term data to choose a digital finance supplier selection.

The technique of ASAS yields benefits which are association with criteria weights proportionally and straightly [11], scalability and flexibility [13, 14], and adaptability to various fuzzy environments [14]. It also yields weaknesses which are behaviour dependency on the different levels of knowledge elicited by decision makers [14] and behaviour dependency on given data-type of participants [18].

Divergence measure is generally used to quantify the distance between two distributions by evaluating the amount of their discrimination. There exist a set of diverse contributions which deal with the divergence applications in the context of research framework, especially the field of multiple criteria decision making.

In order to show the applicability of divergence measure under a hesitant fuzzy environment in which the criteria weights are to be computed in terms of the Shapley function, Mishra et al. [19] investigated the problem of service quality decision making. Then, Mishra et al. [19] offered another exponential HFS divergence measure to assess the green supplier problem. Furthermore, Mishra et al. [10] developed an ARAS technique by encountering a divergence-based procedure for assessing rationally the relative importance of criteria. In the sequel, Mishra et al. [20] defined a parametric hesitant fuzzy-based divergence measure for evaluating the criteria weights.

In any way, the weight determination process of criteria has a remarkable impact on the decision outcomes, and the divergence measure is a factor which plays an important role in the determination of criteria weight. As shown in Section 5, the abovementioned HFS divergence measures are limited in nature. Therefore, we have been in search of new divergence measures with fewer drawbacks.

In summary, the major distinctive features of the study are as follows:

(1) It introduces an innovative class of divergence measures for HFSs which are parametric and symmetric

(2) A number of interesting properties of proposed divergence measure are proved and discussed

(3) This contribution reviews and explores counter-intuitive cases of existing divergence measures under hesitant fuzzy environment

(4) The experimental results demonstrate that the parametric hesitant fuzzy divergence measure is more effective than the existing ones in decision-making situations

This contribution is set up as follows. We first recall the concept of HFS, and a brief review of some preliminaries is given in Section 2. In Section 3, an innovative class of hesitant fuzzy divergence measures is introduced parametrically and symmetrically. We modify the existing framework of hesitant fuzzy ARAS (HFARAS) using the proposed divergence measures in Section 4. Section 5 is devoted to present the application of proposed divergence measures in a case study of COVID-19 coronavirus. Finally, several conclusions are drawn in Section 6.

2. Preliminaries to Hesitant Fuzzy Sets (HFSs)

In this section, we review some basic notions and well-known results about HFSs that are used in the next discussion.

Let X be the reference set. A hesitant fuzzy set (HFS) on X is defined by Torra [21] in terms of a function that when it is applied to X, it returns a subset of $[0,1]$.

In fact, the notion of HFS is employed for handling a class of decision-making problems where the belongingness degree of an element to a set includes a variety of values.

Toward a better understanding, Xia and Xu [22] reconsidered the concept of HFS in the form of

$$H_A = \{\langle x, h_A(x)\rangle : x \in X\}, \quad (1)$$

where $h_A(x)$ stands for all possible membership degrees of $x \in X$ belonging to the set H_A, and it is afterwards named as the hesitant fuzzy element (HFE) of H_A.

Adding to the latter presented concept are the following set and arithmetic operations. Let $h_1 = \{h_1^{\delta(i)} \mid i = 1, \ldots, l_{h_1}\}$ and $h_2 = \{h_2^{\delta(i)} \mid i = 1, \ldots, l_{h_2}\}$ be two HFEs. Then, it is defined (i.e., [23]).

(i) Complement: $h_1^c = \cup_{h_1^{\delta(i)} \in h_1}\{1 - h_1^{\delta(i)}\}$

(ii) Union: $h_1 \cup h_2 = \cup_{h_1^{\delta(i)} \in h_1, h_2^{\delta(j)} \in h_2}\{\max\{h_1^{\delta(i)}, h_2^{\delta(j)}\}\}$

(iii) Intersection: $h_1 \cap h_2 = \cup_{h_1^{\delta(i)} \in h_1, h_2^{\delta(j)} \in h_2}\{\min\{h_1^{\delta(i)}, h_2^{\delta(j)}\}\}$

(iv) Addition: $h_1 \oplus h_2 = \cup_{h_1^{\delta(i)} \in h_1, h_2^{\delta(j)} \in h_2}\{h_1^{\delta(i)} + h_2^{\delta(j)} - h_1^{\delta(i)} h_2^{\delta(j)}\}$

(v) Multiplication: $h_1 \otimes h_2 = \cup_{h_1^{\delta(i)} \in h_1, h_2^{\delta(j)} \in h_2}\{h_1^{\delta(i)} h_2^{\delta(j)}\}$

(vi) Multiplication by scalar: $\lambda h_1 = \cup_{h_1^{\delta(i)} \in h_1}\{1 - (1 - h_1^{\delta(i)})^{\lambda}\}, \quad \lambda > 0$

(vii) Power: $h_1^{\lambda} = \cup_{h_1^{\delta(i)} \in h_1}\{(h_1^{\delta(i)})^{\lambda}\}, \quad \lambda > 0$

We explain below how the total ordering on HFEs was proposed and introduced. This was achieved by keeping in mind the score function of $h = \{h^{\delta(i)} \mid i = 1, \ldots, l_h\}$ given by [22]

$$s(h) = \frac{1}{l_h}\sum_{i=1}^{l_h} h^{\delta(i)}, \quad (2)$$

and its variance function [24] is defined by the following formulation:

$$\nu(h) = \frac{2.(l_h - 2)}{l_h!}\sqrt{\sum_{h^{\delta(i)},h^{\delta(j)}\in h}\left(h^{\delta(i)} - h^{\delta(j)}\right)^2}. \quad (3)$$

Indeed, the total ordering of HFEs $h_1 = \{h_1^{\delta(i)} \mid i = 1,\ldots,l_{h_1}\}$ and $h_2 = \{h_2^{\delta(i)} \mid i = 1,\ldots,l_{h_2}\}$ could be defined by using the following comparison scheme:

(i) If we have $s(h_1) < s(h_2)$, then it is concluded that $h_1 \prec_T h_2$

(ii) If we have $s(h_1) < s(h_2)$, then

  (i) For the relation $\nu(h_1) < \nu(h_2)$, we get $h_1 \prec_T h_2$

  (ii) For $\nu(h_1) = \nu(h_2)$, we conclude that $h_1 \approx_T h_2$

Now, we are in a position to explain the unified length scale of HFSs as follows: in most situations, we observe that $l_{h_1} \neq l_{h_2}$. In order for comparing h_1 and h_2 correctly, we may extend the shorter HFE until the length of both HFEs are the same [25–28]. Suppose that $l = \max\{l_{h_1}, l_{h_2}\}$. Then, the shorter HFE is extended by appending the same value repeatedly. The repeated value depends on the risk preference of the decision makers, that is, if we consider (i) the pessimistic case, then the repeated value is the shortest one; (ii) if the optimistic case is considered, then the largest value will be repeated, and (iii) in the general case, we consider the convex combination of maximum and minimum values of a HFE.

Suppose that $h_1 = \{h_1^{\delta(j)} \mid j = 1,\ldots,l\}$ and $h_2 = \{h_2^{\delta(j)} \mid j = 1,\ldots,l\}$ are two length-unified HFEs on X. The elementwise ordering of HFEs is defined by (i.e., [29])

$$h_1 \leq_E h_2 \text{ if and only if } h_1^{\delta(j)} \leq h_2^{\delta(j)}, \quad (4)$$

for any $j = 1,\ldots,l$.

Eventually, we represent the definition of two widely used aggregation operators of HFEs [25, 29]. Let $h_1 = \{h_1^{\delta(j)} \mid j = 1,\ldots,l\}$, $h_2 = \{h_2^{\delta(j)} \mid j = 1,\ldots,l\}$, and $h_m = \{h_m^{\delta(j)} \mid j = 1,\ldots,l\}$ be a set of m HFEs with the corresponding weights ϖ_i $(i = 1,\ldots,m)$. Then, it is defined.

(i) The hesitant fuzzy weighted averaging (HFWA) operator:

$$\begin{aligned}\mathrm{HFWA}(h_1, h_2, \ldots, h_m) &= \mathop{\oplus}_{i=1}^{m}(\varpi_i h_i) \\ &= \left\{1 - \prod_{i=1}^{m}\left(1 - h_i^{\sigma(j)}\right)^{\varpi_i} \mid j = 1,\ldots,l\right\}.\end{aligned} \quad (5)$$

(ii) The hesitant fuzzy weighted geometric (HFWG) operator:

$$\begin{aligned}\mathrm{HFWG}(h_1, h_2, \ldots, h_m) &= \mathop{\otimes}_{i=1}^{m}\left(h_i^{\varpi_i}\right) \\ &= \left\{\prod_{i=1}^{m}\left(h_i^{\sigma(j)}\right)^{\varpi_i} \mid j = 1,\ldots,l\right\}.\end{aligned} \quad (6)$$

3. A New Class of HFS Divergence Measures

Axiomatically, a divergence measure of two HFSs satisfies the following items similar to that of fuzzy sets [30] and intuitionistic fuzzy sets [31]:

(i) It is nonnegative and symmetric

(ii) It returns the zero value whenever the two sets coincide

In this contribution, we are going to develop a procedure that estimates the objective weights of criteria by using the concept of divergence measure, needless to say that the criteria weights are computed subjectively or objectively. The former technique computes the criteria weights by taking the thought of decision makers, while the latter technique characterizes the criteria weights by considering the mathematical assessments.

Let $h_1 = \{h_1^{\delta(j)} \mid j = 1,\ldots,l\}$ and $h_2 = \{h_2^{\delta(j)} \mid j = 1,\ldots,l\}$ be two length-unified HFEs as described above.

The following formula introduces a class of innovative divergence measures for HFSs:

$$\mathrm{Div}_\Gamma(h_1, h_2) = \frac{1}{l}\sum_{j=1}^{l}\left[\left(\frac{\gamma_1\Gamma\left(h_1^{\delta(j)}\right) + \gamma_2\Gamma\left(h_2^{\delta(j)}\right)}{\gamma_1 + \gamma_2}\right) - \Gamma\left(\frac{\gamma_1 h_1^{\delta(j)} + \gamma_2 h_2^{\delta(j)}}{\gamma_1 + \gamma_2}\right)\right], \quad (7)$$

where Γ is a real convex function, and γ_k $(k = 1, 2)$ are the positive and real numbers.

Among all the real convex functions, Γ may be chosen as follows:

(i) $\Gamma(h) = p_1 h + p_2$ for $p_1, p_2 \in \mathfrak{R}$ (affine function)

(ii) $\Gamma(h) = \exp(ph)$ for $p \in \mathfrak{R}$ (exponential function)

(iii) $\Gamma(h) = h^p$ for $p \geq 1$ (power function)

(iv) $\Gamma(h) = |h|^p$ for $p \geq 1$ (absolute-value function)

(v) $\Gamma(h) = -\log(h)$ (logarithmic function)

(vi) $\Gamma(h) = h \times \log(h)$ (combinatorial function)

To simplify the next discussion, hereafter, we only restrict Γ by its power type $\Gamma(h) = h^p$ for $p \geq 1$ together with $\gamma_1 = \gamma_2 = 1$. In view of this, we attain the following class of divergence measures for HFSs:

$$\mathrm{Div}_\Gamma(h_1,h_2)=\frac{1}{l}\sum_{j=1}^{l}\left[\left(\frac{\left(h_1^{\delta(j)}\right)^p+\left(h_2^{\delta(j)}\right)^p}{2}\right)-\left(\frac{h_1^{\delta(j)}+h_2^{\delta(j)}}{2}\right)^p\right],\quad p\geq 1. \tag{8}$$

Remark 1. It is interesting to note that the measure Div_Γ given by (8) will be the divergence measure of Mishra et al. [10] if we set $p=2$.

Before presenting the main properties of divergence measure Div_Γ given by (8), we are going to state the following lemma.

Lemma 1. *Assume that $h_j\geq 0$ for any $1\leq j\leq n$. Then, it holds that*

$$\sum_{j=1}^{n}\left(h_j\right)^p\leq\left(\sum_{j=1}^{n}h_j\right)^p\leq n^{p-1}\sum_{j=1}^{n}\left(h_j\right)^p,\quad p\geq 1. \tag{9}$$

Proof. To prove the left-hand inequality, we set $H:=\sum_{j=1}^n h_j$ and $H_j:=h_j/H$. Then, we easily find that $0\leq H_j\leq 1$ together with $\sum_{j=1}^n H_j=1$. Now, from the fact that $(H_j)^p\leq H_j$ for any $p\geq 1$, we conclude that $\sum_{j=1}^n(H_j)^p\leq\sum_{j=1}^n H_j=1$. This implies that $\sum_{j=1}^n(H_j)^p=\sum_{j=1}^n(h_j/H)^p\leq 1$, and therefore, $\sum_{j=1}^n(h_j)^p\leq H^p=(\sum_{j=1}^n h_j)^p$.

To prove the right-hand inequality, we apply Jensen's inequality

$$\Gamma\left(\frac{\sum_{j=1}^n\gamma_j h_j}{\sum_{j=1}^n\gamma_j}\right)\leq\frac{\sum_{j=1}^n\left(\gamma_j\Gamma\left(h_j\right)\right)}{\sum_{j=1}^n\gamma_j}, \tag{10}$$

to $\Gamma(x)=x^p$ with $\gamma_1=\cdots=\gamma_n=1/n$. Thus, we conclude that $(1/n\sum_{j=1}^n h_j)^p\leq\sum_{j=1}^n 1/n(h_j)^p$, which implies that $(\sum_{j=1}^n h_j)^p\leq n^{p-1}\sum_{j=1}^n(h_j)^p$.

Now, we establish the fundamental aim of this study which is given by the following theorem. □

Theorem 1. *Suppose that $h_1=\left\{h_1^{\delta(j)}\mid j=1,\ldots,l\right\}$ and $h_2=\left\{h_2^{\delta(j)}\mid j=1,\ldots,l\right\}$ are two length-unified HFEs. Then, the formula $Div_\Gamma(h_1,h_2)$ given by (8) presents a divergence measure for any $p\geq 1$.*

Proof. It needs to show that the formula $\mathrm{Div}_\Gamma(h_1,h_2)$ satisfies the two items given in the beginning of this section, that is, for any two HFEs $h_1=\left\{h_1^{\delta(j)}\mid j=1,\ldots,l\right\}$ and $h_2=\left\{h_2^{\delta(j)}\mid j=1,\ldots,l\right\}$, it must be held that

$$\mathrm{Div}_\Gamma(h_1,h_2)\geq 0; \tag{11}$$

$$\mathrm{Div}_\Gamma(h_1,h_2)=0\text{ if and only if } h_1\approx_E h_2. \tag{12}$$

The proof of relation (11): from Lemma 1, we find that $(\sum_{k=1}^2 h_k^{\delta(j)})^p\leq 2^{p-1}\sum_{k=1}^2(h_k^{\delta(j)})^p$ is true for any $j=1,\ldots,l$. Equivalently,

$$\left(\frac{h_1^{\delta(j)}+h_2^{\delta(j)}}{2}\right)^p\leq\frac{\left(h_1^{\delta(j)}\right)^p+\left(h_2^{\delta(j)}\right)^p}{2}, \tag{13}$$

holds true for any $j=1,\ldots,l$, and hence,

$$\mathrm{Div}_\Gamma(h_1,h_2)=\frac{1}{l}\sum_{j=1}^{l}\left[\left(\frac{\left(h_1^{\delta(j)}\right)^p+\left(h_2^{\delta(j)}\right)^p}{2}\right)-\left(\frac{h_1^{\delta(j)}+h_2^{\delta(j)}}{2}\right)^p\right]\geq 0,\quad\text{for any } p\geq 1. \tag{14}$$

The proof of relation (12): assume that $h:\approx_E h_1\approx_E h_2$ which means that $h^{\delta(j)}:=h_1^{\delta(j)}=h_2^{\delta(j)}$ for any $j=1,\ldots,l$. Therefore,

$$\mathrm{Div}_\Gamma(h,h)=\frac{1}{l}\sum_{j=1}^{l}\left[\left(\frac{\left(h^{\delta(j)}\right)^p+\left(h^{\delta(j)}\right)^p}{2}\right)-\left(\frac{h^{\delta(j)}+h^{\delta(j)}}{2}\right)^p\right]=0. \tag{15}$$

Conversely, we suppose that $\mathrm{Div}_\Gamma(h_1,h_2)=0$, that is,

$$\frac{1}{l}\sum_{j=1}^{l}\left[\left(\frac{\left(h_1^{\delta(j)}\right)^p+\left(h_2^{\delta(j)}\right)^p}{2}\right)-\left(\frac{h_1^{\delta(j)}+h_2^{\delta(j)}}{2}\right)^p\right]=0, \tag{16}$$

for any $p\geq 1$. This implies that

$$\left(\frac{\left(h_1^{\delta(j)}\right)^p+\left(h_2^{\delta(j)}\right)^p}{2}\right)-\left(\frac{h_1^{\delta(j)}+h_2^{\delta(j)}}{2}\right)^p=0, \tag{17}$$

for any $j=1,\ldots,l$.

The latter equality is possible if and only if the equalities $h_1^{\delta(j)}=h_2^{\delta(j)}$ $(j=1,\ldots,l)$ hold true. This finding implies that $h_1\approx_E h_2$. □

Theorem 2. *Suppose that $h_1=\left\{h_1^{\delta(j)}\mid j=1,\ldots,l\right\}$, $h_2=\left\{h_2^{\delta(j)}\mid j=1,\ldots,l\right\}$, and $h_3=\left\{h_3^{\delta(j)}\mid j=1,\ldots,l\right\}$ are three length-unified HFEs, and the formula $Div_\Gamma(h_1,h_2)$ given by (8) presents a divergence measure. Then, for any $h_1\prec_E h_2\prec_E h_3$, the following inequalities hold true:*

$$\begin{aligned}&\mathrm{Div}_\Gamma(h_1,h_2)\leq\mathrm{Div}_\Gamma(h_1,h_3);,\\&\mathrm{Div}_\Gamma(h_1,h_3)\leq\mathrm{Div}_\Gamma(h_2,h_3).\end{aligned} \tag{18}$$

Proof. Referring to the definition of elementwise ordering of HFEs given by (4), we observe that $h_1\leq_E h_2\leq_E h_3$ is valid if and only if $h_1^{\delta(j)}\leq h_2^{\delta(j)}\leq h_3^{\delta(j)}$ for any $j=1,\ldots,l$. Therefore, for any $p\geq 1$, we have

$$\begin{aligned}\mathrm{Div}_{\Gamma}(h_1,h_2) &= \frac{1}{l}\sum_{j=1}^{l}\left[\left(\frac{\left(h_1^{\delta(j)}\right)^p+\left(h_2^{\delta(j)}\right)^p}{2}\right)-\left(\frac{h_1^{\delta(j)}+h_2^{\delta(j)}}{2}\right)^p\right]\\ &\le \frac{1}{l}\sum_{j=1}^{l}\left[\left(\frac{\left(h_1^{\delta(j)}\right)^p+\left(h_3^{\delta(j)}\right)^p}{2}\right)-\left(\frac{h_1^{\delta(j)}+h_3^{\delta(j)}}{2}\right)^p\right] = Di\ v_{\Gamma}(h_1,h_3),\end{aligned} \tag{19}$$

and

$$\begin{aligned}\mathrm{Div}_{\Gamma}(h_1,h_3) &= \frac{1}{l}\sum_{j=1}^{l}\left[\left(\frac{\left(h_1^{\delta(j)}\right)^p+\left(h_3^{\delta(j)}\right)^p}{2}\right)-\left(\frac{h_1^{\delta(j)}+h_3^{\delta(j)}}{2}\right)^p\right]\\ &\le \frac{1}{l}\sum_{j=1}^{l}\left[\left(\frac{\left(h_2^{\delta(j)}\right)^p+\left(h_3^{\delta(j)}\right)^p}{2}\right)-\left(\frac{h_2^{\delta(j)}+h_3^{\delta(j)}}{2}\right)^p\right]\\ &= Di\ v_{\Gamma}(h_1,h_3).\end{aligned} \tag{20}$$

□

Theorem 3. *Suppose that* $h_1=\{h_1^{\delta(j)}\mid j=1,\dots,l\}$, $h_2=\{h_2^{\delta(j)}\mid j=1,\dots,l\}$, *and* $h_3=\{h_3^{\delta(j)}\mid j=1,\dots,l\}$ *are three length-unified HFEs, and the formula* $Div_{\Gamma}(h_1,h_2)$ *given by (8) presents a divergence measure. Then, the following equalities hold true:*

$$\mathrm{Div}_{\Gamma}(h_1\cup h_2,h_1\cap h_2)=\mathrm{Div}_{\Gamma}(h_1,h_2), \tag{21}$$

$$\mathrm{Div}_{\Gamma}(h_1\cup h_2,h_3)=\frac{1}{2}\left(\mathrm{Div}_{\Gamma}(h_1,h_3)+\mathrm{Div}_{\Gamma}(h_2,h_3)\right), \tag{22}$$

$$\mathrm{Div}_{\Gamma}(h_1\cap h_2,h_3)=\frac{1}{2}\left(\mathrm{Div}_{\Gamma}(h_1,h_3)+\mathrm{Div}_{\Gamma}(h_2,h_3)\right). \tag{23}$$

Proof. For any $j=1,\dots,l$ and $p\ge 1$, we propose the following proofs.

The proof of relation (21):

$$\begin{aligned}\mathrm{Div}_{\Gamma}(h_1\cup h_2,h_1\cup h_2) &= \frac{1}{l}\sum_{j=1}^{l}\left[\left(\frac{\left((h_1\cup h_2)^{\delta(j)}\right)^p+\left((h_1\cup h_2)^{\delta(j)}\right)^p}{2}\right)-\left(\frac{(h_1\cup h_2)^{\delta(j)}+(h_1\cap h_2)^{\delta(j)}}{2}\right)^p\right]\\ &= \frac{1}{l}\sum_{j=1}^{l}\left[\left(\frac{\left(\max\{h_1^{\delta(j)},h_2^{\delta(j)}\}\right)^p+\left(\min\{h_1^{\delta(j)},h_2^{\delta(j)}\}\right)^p}{2}\right)-\left(\frac{\max\{h_1^{\delta(j)},h_2^{\delta(j)}\}+\min\{h_1^{\delta(j)},h_2^{\delta(j)}\}}{2}\right)^p\right].\end{aligned} \tag{24}$$

In the case where $h_1^{\delta(j)}\le h_2^{\delta(j)}$, we easily conclude that

$$\begin{aligned}\max\{h_1^{\delta(j)},h_2^{\delta(j)}\}&=h_2^{\delta(j)},\\ \min\{h_1^{\delta(j)},h_2^{\delta(j)}\}&=h_1^{\delta(j)},\end{aligned} \tag{25}$$

and hence,

$$\mathrm{Div}_{\Gamma}(h_1\cup h_2,h_1\cap h_2)=\frac{1}{l}\sum_{j=1}^{l}\left[\left(\frac{\left(h_2^{\delta(j)}\right)^p+\left(h_1^{\delta(j)}\right)^p}{2}\right)-\left(\frac{h_2^{\delta(j)}+h_1^{\delta(j)}}{2}\right)^p\right]=\mathrm{Div}_{\Gamma}(h_1,h_2). \tag{26}$$

For the other case, that is, $h_1^{\delta(j)}\ge h_2^{\delta(j)}$, we conclude again the latter result. Therefore, we have

$$\mathrm{Div}_{\Gamma}(h_1\cup h_2,h_1\cap h_2)=\mathrm{Div}_{\Gamma}(h_1,h_2). \tag{27}$$

The proof of relation (22):

$$\begin{aligned}\mathrm{Div}_\Gamma(h_1\cup h_2,h_3)&=\frac{1}{l}\sum_{j=1}^{l}\left[\left(\frac{\left((h_1\cup h_2)^{\delta(j)}\right)^p+\left(h_3^{\delta(j)}\right)^p}{2}\right)-\left(\frac{(h_1\cup h_2)^{\delta(j)}+h_3^{\delta(j)}}{2}\right)^p\right]\\&=\frac{1}{l}\sum_{j=1}^{l}\left[\left(\frac{\left(\max\left\{h_1^{\delta(j)},h_2^{\delta(j)}\right\}\right)^p+\left(h_3^{\delta(j)}\right)^p}{2}\right)-\left(\frac{\max\left\{h_1^{\delta(j)},h_2^{\delta(j)}\right\}+h_3^{\delta(j)}}{2}\right)^p\right].\end{aligned}\tag{28}$$

In the case where $h_1^{\delta(j)}\le h_2^{\delta(j)}$, the following result is obtained:

$$\max\left\{h_1^{\delta(j)},h_2^{\delta(j)}\right\}=h_2^{\delta(j)},\tag{29}$$

which gives rise to

$$\mathrm{Div}_\Gamma(h_1\cup h_2,h_3)=\frac{1}{l}\sum_{j=1}^{l}\left[\left(\frac{\left(h_2^{\delta(j)}\right)^p+\left(h_3^{\delta(j)}\right)^p}{2}\right)-\left(\frac{h_2^{\delta(j)}+h_3^{\delta(j)}}{2}\right)^p\right]=\mathrm{Div}_\Gamma(h_2,h_3).\tag{30}$$

For the other case, that is, $h_1^{\delta(j)}\ge h_2^{\delta(j)}$, we achieve that

$$\mathrm{Div}_\Gamma(h_1\cup h_2,h_3)=\frac{1}{l}\sum_{j=1}^{l}\left[\left(\frac{\left(h_1^{\delta(j)}\right)^p+\left(h_3^{\delta(j)}\right)^p}{2}\right)-\left(\frac{h_1^{\delta(j)}+h_3^{\delta(j)}}{2}\right)^p\right]=\mathrm{Div}_\Gamma(h_1,h_3).\tag{31}$$

Now, it follows from (30) and (31) that

$$\mathrm{Div}_\Gamma(h_1\cup h_2,h_3)=\frac{1}{2}\left(\mathrm{Div}_\Gamma(h_1,h_3)+\mathrm{Div}_\Gamma(h_2,h_3)\right).\tag{32}$$

The proof of relation (23): the justification of relation (23) is similar to that of relation (22). □

Theorem 4. *Suppose that $h_1=\left\{h_1^{\delta(j)}\mid j=1,\ldots,l\right\}$, $h_2=\left\{h_2^{\delta(j)}\mid j=1,\ldots,l\right\}$, and $h_3=\left\{h_3^{\delta(j)}\mid j=1,\ldots,l\right\}$ are three length-unified HFEs, and the formula $Div_\Gamma(h_1,h_2)$ given by (8) presents a divergence measure. Then, the following inequalities hold true:*

$$\mathrm{Div}_\Gamma(h_1\cup h_3,h_2\cup h_3)\le\mathrm{Div}_\Gamma(h_1,h_2),\tag{33}$$

$$\mathrm{Div}_\Gamma(h_1\cap h_3,h_2\cap h_3)\le\mathrm{Div}_\Gamma(h_1,h_2).\tag{34}$$

Proof. For any $j=1,\ldots,l$ and $p\ge 1$, we offer the following proofs.

The proof of relation (33):

$$\begin{aligned}Di\ v_\Gamma(h_1\cup h_3,h_2\cup h_3)&=\frac{1}{l}\sum_{j=1}^{l}\left[\left(\frac{\left((h_1\cup h_3)^{\delta(j)}\right)^p+\left((h_2\cup h_3)^{\delta(j)}\right)^p}{2}\right)-\left(\frac{(h_1\cup h_3)^{\delta(j)}+(h_2\cup h_3)^{\delta(j)}}{2}\right)^p\right]\\&=\frac{1}{l}\sum_{j=1}^{l}\left[\left(\frac{\left(\max\left\{h_1^{\delta(j)},h_3^{\delta(j)}\right\}\right)^p+\left(\max\left\{h_2^{\delta(j)},h_3^{\delta(j)}\right\}\right)^p}{2}\right)-\left(\frac{\max\left\{h_1^{\delta(j)},h_3^{\delta(j)}\right\}+\max\left\{h_2^{\delta(j)},h_3^{\delta(j)}\right\}}{2}\right)^p\right].\end{aligned}\tag{35}$$

Accordingly, all the possible cases are as follows:

$$h_1^{\delta(j)}\le h_2^{\delta(j)}\le h_3^{\delta(j)},\tag{36}$$

$$h_2^{\delta(j)}\le h_1^{\delta(j)}\le h_3^{\delta(j)},\tag{37}$$

$$h_1^{\delta(j)}\le h_3^{\delta(j)}\le h_2^{\delta(j)},\tag{38}$$

$$h_2^{\delta(j)}\le h_3^{\delta(j)}\le h_1^{\delta(j)},\tag{39}$$

$$h_3^{\delta(j)}\le h_1^{\delta(j)}\le h_2^{\delta(j)},\tag{40}$$

$$h_3^{\delta(j)}\le h_2^{\delta(j)}\le h_1^{\delta(j)}.\tag{41}$$

From the first case to the last case which are labelled by (36)–(41), we conclude, respectively, that

$$\begin{aligned}
&\mathrm{Div}_\Gamma(h_1\cup h_3, h_2\cup h_3) = \mathrm{Div}_\Gamma(h_3,h_3),\\
&\mathrm{Div}_\Gamma(h_2\cup h_3, h_2\cup h_3) = \mathrm{Div}_\Gamma(h_3,h_3),\\
&\mathrm{Div}_\Gamma(h_1\cup h_3, h_2\cup h_3) = \mathrm{Div}_\Gamma(h_2,h_3),\\
&\mathrm{Div}_\Gamma(h_2\cup h_3, h_1\cup h_3) = \mathrm{Div}_\Gamma(h_1,h_3),\\
&\mathrm{Div}_\Gamma(h_1\cup h_3, h_2\cup h_3) = \mathrm{Div}_\Gamma(h_1,h_2),\\
&\mathrm{Div}_\Gamma(h_2\cup h_3, h_1\cup h_3) = \mathrm{Div}_\Gamma(h_2,h_1).
\end{aligned} \tag{42}$$

Clearly, the first case and the second case (i.e, equations (36) and (37)) give rise to $\mathrm{Div}_\Gamma(h_3,h_3)\le\mathrm{Div}_\Gamma(h_1,h_2)$, and moreover, the third case and the fourth case (i.e, equations (38) and (39)) result in $\mathrm{Div}_\Gamma(h_2,h_3), \mathrm{Div}_\Gamma(h_1,h_3)\le\mathrm{Div}_\Gamma(h_1,h_2)$. Therefore, by taking all the above results into consideration, we find that

$$\begin{aligned}
\mathrm{Div}_\Gamma(h_1\cup h_3, h_2\cup h_3) &= \mathrm{Div}_\Gamma(h_3,h_3) + \mathrm{Div}_\Gamma(h_3,h_3) + \mathrm{Div}_\Gamma(h_2,h_3)\\
&\quad + \mathrm{Div}_\Gamma(h_1,h_3) + \mathrm{Div}_\Gamma(h_1,h_2) + \mathrm{Div}_\Gamma(h_2,h_1)\\
&\le \frac{1}{6}\left(\underbrace{\mathrm{Div}_\Gamma(h_1,h_2)+\cdots+\mathrm{Div}_\Gamma(h_1,h_2)}_{6}\right) = \mathrm{Div}_\Gamma(h_1,h_2).
\end{aligned} \tag{43}$$

The proof of relation (34): it is proved in a similar way as the proof of inequality (33). □

4. Hesitant Fuzzy Additive Ratio Assessment (HFARAS)

In this part of contribution, we modify the framework of hesitant fuzzy additive ratio assessment (HFARAS) which was initiated by Mishra et al. [10]. They used mainly the concept of divergence measure for developing the complex multiple criteria decision-making methodology. This work concentrates more on the methodology of Mishra et al. [10], in which a class of fruitful divergence measures for HFSs is employed instead. The resulted methodology is constituted by the following steps:

Step 1. We initially form each individual decision matrix corresponding to the evaluation of experts ϵ_k $(k=1,\ldots,r)$ as follows:

$$^{\epsilon_k}D = \begin{bmatrix} C_1 & C_2 & \cdots & C_n\\ A_1 & ^{\epsilon_k}h_{11} & ^{\epsilon_k}h_{12} & ^{\epsilon_k}h_{1n}\\ A_2 & ^{\epsilon_k}h_{21} & ^{\epsilon_k}h_{22} & ^{\epsilon_k}h_{2n}\\ \vdots & \vdots & \vdots & \vdots\\ A_m & ^{\epsilon_k}h_{m1} & ^{\epsilon_k}h_{m2} & ^{\epsilon_k}h_{mn}\end{bmatrix}, \tag{44}$$

in which the HFS array $^{\epsilon_k}h_{ij}$ $(i=1,\ldots,m,\ j=1,\ldots,n)$ indicates the rating of alternative A_i corresponding to the criterion C_j with the weight of ω_j.

By the way, the degree of significant for each expert ϵ_k $(k=1,\ldots,r)$ is computed by the use of

$$\varpi_{\epsilon_k} = \frac{\sum_{t=1}^{l} {}^{\epsilon_k}h_{ij}^{\delta(t)}}{\sum_{k=1}^{r}\left(\sum_{t=1}^{l} {}^{\epsilon_k}h_{ij}^{\delta(t)}\right)}, \quad (i=1,\ldots,m, j=1,\ldots,n), \tag{45}$$

where $^{\epsilon_k}h_{ij} = \left\{^{\epsilon_k}h_{ij}^{\delta(t)} \mid t=1,\ldots,l\right\}$. Furthermore, it is easily seen that $\varpi_{\epsilon_k}\ge 0$ and $\sum_{k=1}^{r}\varpi_{\epsilon_k}=1$.

Step 2. We aggregate all the individual decision matrices into the aggregated matrix:

$$D = \begin{bmatrix} C_1 & C_2 & \cdots & C_n\\ A_1 & h_{11} & h_{12} & h_{1n}\\ A_2 & h_{21} & h_{22} & h_{2n}\\ \vdots & \vdots & \vdots & \vdots\\ A_m & h_{m1} & h_{m2} & h_{mn}\end{bmatrix}, \tag{46}$$

in which

$$h_{ij} = \left\{\cup_{^{\epsilon_1}h_{ij}^{\delta(t)}\in {}^{\epsilon_1}h_{ij},\ldots,{}^{\epsilon_r}h_{ij}^{\delta(t)}\in {}^{\epsilon_r}h_{ij}} \left\{1-\prod_{k=1}^{r}\left(1-{}^{\epsilon_k}h_{ij}^{\delta(t)}\right)^{\varpi_{\epsilon_k}}\right\} \mid t=1,\ldots,l\right\}, \tag{47}$$

for any $i = 1, \ldots, m$ and $j = 1, \ldots, n$.

4.1. The Intermediate Steps. Now, if we use the intermediate steps, then the weight of criteria is to be computed based on the two parameters: rationality degree and importance degree.

4.2. The Rationality Degree

(1) If we employ a divergence measure Div, we then find the support degree between the criteria C_j and C_l as

$$S\left(h_{ij}, h_{il}\right) = 1 - Di\ v\left(h_{ij}, h_{il}\right), \quad (i = 1, \ldots, m,\ j, l = 1, \ldots, n,\ j \neq l). \tag{48}$$

(2) Using the support degree S, we are able to calculate the total support degree,

$$TS\left(h_{ij}\right) = \sum_{l=1, l=j}^{n} S\left(h_{ij}, h_{il}\right), \quad (i = 1, \ldots, m,\ j, l = 1, \ldots, n), \tag{49}$$

for any h_{ij} over the criteria C_j.

(3) The utilization of total support degree TS leads to the rationality degree

$$R_j = \frac{1}{m} \sum_{i=1}^{m} TS\left(h_{ij}\right), \quad (j = 1, \ldots, n), \tag{50}$$

in which $0 \leq R_j \leq 1$.

(4) By using the rationality degree R_j, we attain the overall rationality degree

$$OR_j = \frac{R_j}{\sum_{j=1}^{n} R_j}, \quad (j = 1, \ldots, n), \tag{51}$$

where $0 \leq OR_j \leq 1$.

4.3. The Importance Degree

(1) We calculate the individual importance degree matrix ${}^{\epsilon_k}I$ as follows:

$${}^{\epsilon_k}I = \begin{bmatrix} C_1 & C_2 & \cdots & C_n \\ {}^{\epsilon_1} & {}^{\epsilon_1}I_1 & {}^{\epsilon_1}I_2 & {}^{\epsilon_1}I_n \\ {}^{\epsilon_2} & {}^{\epsilon_2}I_1 & {}^{\epsilon_2}I_2 & {}^{\epsilon_2}I_n \\ \vdots & \vdots & \vdots & \vdots \\ {}^{\epsilon_r} & {}^{\epsilon_r}I_1 & {}^{\epsilon_r}I_2 & {}^{\epsilon_r}h_n \end{bmatrix}, \tag{52}$$

where ${}^{\epsilon_k}I_j$ denotes the importance degree of criterion C_j given by the k^{th} expert.

Now, all the individual importance degree matrices can be aggregated into the matrix:

$$I = \left[\sum_{\epsilon_k} \begin{matrix} C_1 & C_2 & \cdots C_n \\ I_1 & I_2 & I_n \end{matrix}\right], \tag{53}$$

in which

$$I_j = \left\{ \cup_{{}^{\epsilon_1}I_j^{\delta(t)} \in {}^{\epsilon_1}I_j, \ldots, {}^{\epsilon_r}I_j^{\delta(t)} \in {}^{\epsilon_r}I_j} \left\{ 1 - \prod_{k=1}^{r} \left(1 - {}^{\epsilon_k}I_j^{\delta(t)}\right)^{\varpi_{\epsilon_k}} \right\} \mid t = 1, \ldots, l \right\}, \tag{54}$$

for any $j = 1, \ldots, n$.

(2) The utilization of aggregated degree I_j leads to the overall importance degree:

$$OI_j = \frac{s\left(I_j\right)}{\sum_{j=1}^{n} s\left(I_j\right)}, \quad (j = 1, \ldots, n), \tag{55}$$

where s denotes the score function given by (2), and moreover, $0 \leq OI_j \leq 1$.

Now, with the parameters of overall rationality degree OR_j and overall importance degree OI_j given, respectively, by (51) and (55), it derives the subjective weights of criteria as

$$\omega_j = \theta OR_j + (1 - \theta) OI_j, \quad (j = 1, \ldots, n), \tag{56}$$

where $0 \leq \theta \leq 1$ indicates the adjustment coefficient.

It is worthwhile to mention that the coefficient θ is chosen in accordance with the actual demand of decision maker, that is, the maximum value of θ stands for the superior influence of rationality degree of criteria in the assessment, and the minimum value of θ indicates the lesser influence of importance degree of criteria.

Step 3. We evaluate the j^{th} element of optimal significance rating by the help of

$$h_O^j = \begin{cases} \max\limits_{1 \leq i \leq m} \left\{h_{ij}\right\}, & j \in C_{\text{benefit}}, \\ \min\limits_{1 \leq i \leq m} \left\{h_{ij}\right\}, & j \in C_{\text{cost}}, \end{cases} \tag{57}$$

for $j = 1, \ldots, n$, which results in the optimal significance rating $h_O = \sum_{j=1}^{n} h_O^j$.

Step 4. We are able to normalize each array of aggregated hesitant fuzzy decision matrix by using the transformation

$$^{\aleph}h_{ij} = \begin{cases} \dfrac{h_{ij}}{\max_{1\le i\le m}\left\{s\left(h_{ij}\right)\right\}}, & j \in C_{\text{benefit}}, \\ 1 - \dfrac{h_{ij}}{\max_{1\le i\le m}\left\{s\left(h_{ij}\right)\right\}}, & j \in C_{\text{cost}}, \end{cases} \quad (58)$$

where s denotes the score function given by (2).

Step 5. We calculate the weighted normalized form of decision matrix as

$$^{\omega\aleph}h_i = \bigoplus_{j=1}^{n}\left(\omega_j^{\aleph}h_{ij}\right) = \left\{ \cup_{^{\aleph}h_{i1}^{\delta(t)}\in {}^{\aleph}h_{i1},\ldots,{}^{\aleph}h_{in}^{\delta(t)}\in {}^{\aleph}h_{in}} \left\{ 1 - \prod_{j=1}^{n}\left(1 - {}^{\aleph}h_{ij}^{\delta(t)}\right)^{\omega_j} \right\} \mid t = 1,\ldots,l \right\}, \quad (59)$$

for any $i = 1,\ldots,m$.

Step 6. We obtain the overall performance rating in terms of

$$OP_i = s\left(^{\omega\aleph}h_i\right), (i = 1,\ldots,m), \quad (60)$$

in which s stands for the score function given by (2).

With the help of parameter OP_i, we can estimate the preference of options. That means that the greatest value of OP_i specifies the best option, and its lowest value characterizes the worst one.

However, besides the above selection option, we may assess the optimal option in accordance with the relative impact of that option being called the utility degree and evaluated by

$$U_i = \frac{OP_i}{h_O}. \quad (i = 1,\ldots,m). \quad (61)$$

The largest value of U_i determines the desirable one.

5. Case Study of the COVID-19 Coronavirus

COVID-19 is the most recognized and thoroughly known virus by humans in the recent times. According to the World Health Organization report on November 29, 2020, more than 62,570,316 cases of COVID-19 across the world have been estimated which cause more than 1,466,426 deaths and 44,671,725 recovered persons [32]. Using data from the aforementioned report, most people with COVID-19 are associated with the symptoms and signs including fever (83%–99%), cough (59%–82%), fatigue (44%–70%), anorexia (40%–84%), shortness of breath (31%–40%), sputum production (28%–33%), and myalgias (11%–35%) [33, 34].

In this contribution, we have selected five medicines to manage the critical care of COVID-19 patients [35] including LPV/RTV-IFNb (A_1), favipiravir (A_2), LPV/RTV (A_3), remdesivir (A_4), and hydroxychloroquine (A_5).

However, what is to be noted here is that the antiviral drugs should be considered not only for their impact on signs but also for their probable side effects and performance. To do this task, we have chosen the following parameters: anorexia (C_1), cough (C_2), fatigue (C_3), fever (C_4), myalgia (C_5), shortness of breath (C_6), and sputum production (C_7) [15, 17, 33]. In order to select an ideal drug, Mishra et al. [10] presented the assessment values in the form of linguistic variables together with hesitant fuzzy preference degrees as those given in Table 1.

Now, if we employ the algorithm of hesitant fuzzy additive ratio assessment (HFARAS) presented thoroughly in Section 4 to the abovementioned problem, then each step of algorithm can be carried out as follows.

Step 7. On the basis of data given in Table 1 and relation (45), we get the degree of significant ϖ_{ϵ_k} for each expert ϵ_k $(k = 1, 2, 3)$ as

$$\varpi_{\epsilon_1} = 0.3372, \varpi_{\epsilon_2} = 0.2674, \varpi_{\epsilon_3} = 0.3953. \quad (62)$$

Moreover, Table 2 provides the evaluation of five drugs performance in accordance with the seven criteria for each of three experts.

Step 8. The opinions of three experts are aggregated using formula (47), and this leads to results expressible in the form given in Table 3.

5.1. Comparison of Divergence-Initiated Weights. In this part of Section 5, we are interested to perform a comparison between the weight values concluded from the proposed and the exiting divergence measures [19, 36] to demonstrate more capabilities of the proposed ones.

Let $h_1 = \left\{h_1^{\delta(j)} \mid j = 1,\ldots,l\right\}$ and $h_2 = \left\{h_2^{\delta(j)} \mid j = 1,\ldots,l\right\}$ be two length-unified HFEs. Mishra et al. [19] and Mishra et al. [36] introduced, respectively, the exponential form of HFE divergence measures:

Table 1: The assessment ratings of criteria.

Linguistic variable	Hesitant preference degree
Extremely preferred (EP)	(0.90, 1.00)
Strongly preferred (SP)	(0.80, 0.90)
Preferred (P)	(0.65, 0.80)
Medium (M)	(0.50, 0.65)
Undesirable (U)	(0.35, 0.50)
Strongly undesirable (SU)	(0.20, 0.35)
Extremely undesirable (EU)	(0.00, 0.20)

Table 2: The linguistic variable-based data of the evaluation matrix.

Criteria	Experts	Alternatives				
		A1	A2	A3	A4	A5
	$\epsilon1$	P	M	M	SP	M
C1	$\epsilon2$	M	P	SP	SM	P
	$\epsilon3$	M	P	M	SP	M
	$\epsilon1$	M	P	P	P	P
C2	$\epsilon2$	M	M	M	P	P
	$\epsilon3$	P	U	P	M	M
	$\epsilon1$	U	M	M	M	U
C3	$\epsilon2$	M	U	M	P	P
	$\epsilon3$	M	P	M	M	P
	$\epsilon1$	P	M	M	M	M
C4	$\epsilon2$	M	M	P	M	M
	$\epsilon3$	P	P	P	P	P
	$\epsilon1$	M	M	U	M	SU
C5	$\epsilon2$	U	SU	U	P	M
	$\epsilon3$	U	M	M	P	P
	$\epsilon1$	U	U	SU	P	U
C6	$\epsilon2$	M	U	P	M	P
	$\epsilon3$	SU	M	U	U	SU
	$\epsilon1$	U	M	SU	P	M
C7	$\epsilon2$	U	U	M	U	SU
	$\epsilon3$	SU	SU	U	M	U

Table 3: The aggregated form of experts' opinions.

Criteria	Alternatives				
	A1	A2	A3	A4	A5
C1	0.684	0.666	0.696	0.804	0.604
C2	0.608	0.554	0.633	0.649	0.690
C3	0.512	0.572	0.549	0.680	0.615
C4	0.633	0.608	0.633	0.624	0.644
C5	0.450	0.476	0.454	0.729	0.548
C6	0.423	0.454	0.469	0.600	0.547
C7	0.370	0.373	0.401	0.604	0.381

Table 4: The values of ω_j corresponding to the divergence measures Div_{M3} and Div_{M4}.

Criteria	ω_j^{M3}	ω_j^{M4}					
		$P = 1.0$	$P = 1.2$	$P = 1.4$	$P = 1.6$	$P = 1.8$	$P = 2.0$
C1	0.150	0.1502	0.1503	0.1503	0.1503	0.1503	NaN
C2	0.163	0.1629	0.1629	0.1628	0.1628	0.1628	NaN
C3	0.85	0.1449	0.1449	0.1449	0.1449	0.1449	NaN
C4	0.176	0.1758	0.1758	0.1758	0.1758	0.1758	NaN
C5	0.117	0.1177	0.1177	0.1178	0.1178	0.1178	NaN
C6	0.127	0.1271	0.1271	0.1272	0.1272	0.1272	NaN
C7	0.123	0.1214	0.1213	0.1212	0.1212	0.1212	NaN

NaN, "Not-A-Number."

$$\mathrm{Div}_{M1}\left(\left(h_1,h_2\right)\right)=\frac{1}{l}\sum_{j=1}^{l}\left[\begin{array}{l}1-\left(\dfrac{h_1^{\delta(j)}+h_1^{l-\delta(j)+1}}{2}\right)\exp\left(\dfrac{h_2^{\delta(j)}+h_2^{l-\delta(j)+1}-h_1^{\delta(j)}-h_1^{l-\delta(j)+1}}{2}\right)-\\ \left(\dfrac{2-h_1^{\delta(j)}-h_1^{l-\delta(j)+1}}{2}\right)\exp\left(\dfrac{h_1^{\delta(j)}+h_1^{l-\delta(j)+1}-h_2^{\delta(j)}-h_2^{l-\delta(j)+1}}{2}\right)\end{array}\right]$$

$$\frac{1}{l}\sum_{j=1}^{l}\left[\begin{array}{l}1-\left(\dfrac{h_2^{\delta(j)}+h_2^{l-\delta(j)+1}}{2}\right)\exp\left(\dfrac{h_1^{\delta(j)}+h_1^{l-\delta(j)+1}-h_2^{\delta(j)}-h_2^{l-\delta(j)+1}}{2}\right)-\\ \left(\dfrac{2-h_2^{\delta(j)}-h_2^{l-\delta(j)+1}}{2}\right)\exp\left(\dfrac{h_2^{\delta(j)}+h_2^{l-\delta(j)+1}-h_1^{\delta(j)}-h_1^{l-\delta(j)+1}}{2}\right)\end{array}\right], \tag{63}$$

$$\mathrm{Div}_{M2}\left(h_1,h_2\right)=\frac{1}{l\sqrt{e}\left(\sqrt{e}-1\right)}\sum_{j=1}^{l}\left[\begin{array}{l}\left(\dfrac{h_1^{\delta(j)}+h_1^{l-\delta(j)+1}+h_2^{\delta(j)}+h_2^{l-\delta(j)+1}}{4}\right)\exp\left(\dfrac{h_1^{\delta(j)}+h_1^{l-\delta(j)+1}+h_2^{\delta(j)}+h_2^{l-\delta(j)+1}}{4}\right)+\\ \left(\dfrac{4-h_1^{\delta(j)}+h_1^{l-\delta(j)+1}+h_2^{\delta(j)}+h_2^{l-\delta(j)+1}}{4}\right)\exp\left(\dfrac{4-h_1^{\delta(j)}+h_1^{l-\delta(j)+1}+h_2^{\delta(j)}+h_2^{l-\delta(j)+1}}{4}\right)\\ -\dfrac{1}{2}\left[\begin{array}{l}\left(\dfrac{h_1^{\delta(j)}+h_1^{l-\delta(j)+1}}{2}\right)\exp\left(\dfrac{h_1^{\delta(j)}+h_1^{l-\delta(j)+1}}{2}\right)+\left(\dfrac{2-h_1^{\delta(j)}-h_1^{l-\delta(j)+1}}{2}\right)\exp\left(\dfrac{2-h_1^{\delta(j)}-h_1^{l-\delta(j)+1}}{2}\right)+\\ \left(\dfrac{h_2^{\delta(j)}+h_2^{l-\delta(j)+1}}{2}\right)\exp\left(\dfrac{h_2^{\delta(j)}+h_2^{l-\delta(j)+1}}{2}\right)+\left(\dfrac{2-h_2^{\delta(j)}-h_2^{l-\delta(j)+1}}{2}\right)\exp\left(\dfrac{2-h_2^{\delta(j)}-h_2^{l-\delta(j)+1}}{2}\right)\end{array}\right]\end{array}\right]. \tag{64}$$

Before going more deeply into the definition of next existing divergence measures, we here point out that the latter measures cannot discriminate different HFEs correctly in some situations. This happens especially when a HFE contains elements with the condition

$$h_k^{\delta(j)}+h_k^{l-\delta(j)+1}=1, \tag{65}$$

for any $j=1,\ldots,l$ and $k=1,2$. In this situation,

$$\begin{aligned}&\mathrm{Div}_{M3}\left(h_1,h_2\right)=0,\\&\mathrm{Div}_{M4}\left(h_1,h_2\right)=0,\end{aligned} \tag{66}$$

which are not logical and give rise to inconsistent and inaccurate outcomes.

Bearing the abovementioned shortcoming of Div_{M1} and Div_{M2} in mind, we only examine in detail the next exiting divergence measures together with the proposed ones in the current contribution.

Now, we are going to review the following HFE divergence measures, which were, respectively, introduced by Mishra et al. [10] and Mishra et al. [20]:

$$\mathrm{Div}_{M3}\left(h_1,h_2\right)=\frac{1}{l\left(\sqrt{2}-1\right)}\sum_{j=1}^{l}\left[\sqrt{\left(\frac{\left(h_1^{\delta(j)}\right)^2+\left(h_2^{\delta(j)}\right)^2}{2}\right)}-\left(\frac{h_1^{\delta(j)}+h_2^{\delta(j)}}{2}\right)\right], \tag{67}$$

Table 5: The values of ω_j corresponding to the proposed divergence measure Div_Γ.

Criteria	ω_j^Γ					
	$P = 1.0$	$P = 1.2$	$P = 1.4$	$P = 1.6$	$P = 1.8$	$P = 2.0$
C1	0.1499	0.1499	0.1499	0.1500	0.1500	0.1500
C2	0.1630	0.1630	0.1630	0.1630	0.1630	0.1629
C3	0.1445	0.1446	0.1446	0.1446	0.1446	0.1447
C4	0.1756	0.1756	0.1756	0.1756	0.1756	0.1757
C5	0.1173	0.1174	0.1174	0.1174	0.1175	0.1175
C6	0.1267	0.1268	0.1268	0.1268	0.1269	0.1269
C7	0.1229	0.1228	0.1227	0.1225	0.1224	0.1223

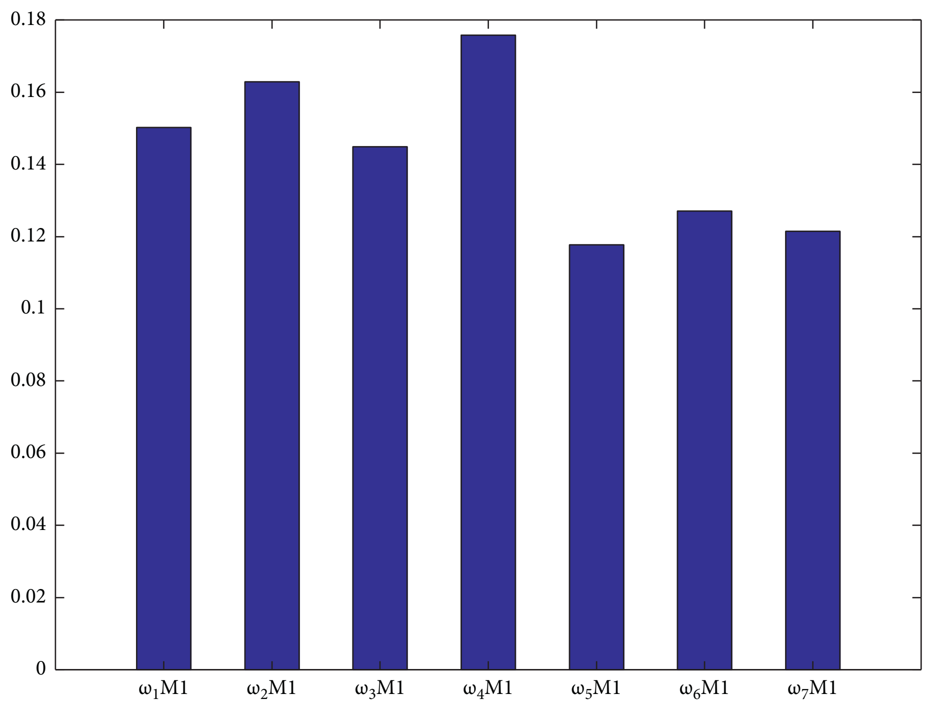

Figure 1: The combined criteria weights ω_j corresponding to the divergence measure Div_{M3}.

and

$$\mathrm{Div}_{M4}(h_1,h_2) = \frac{1}{l\left(2^{(1-(p/2))}-1\right)}\sum_{j=1}^{l}\left[\sqrt{\left(\frac{\left(h_1^{\delta(j)}\right)^2+\left(h_2^{\delta(j)}\right)^2}{2}\right)^p} - \left(\frac{\left(h_1^{\delta(j)}\right)^p+\left(h_2^{\delta(j)}\right)^p}{2}\right)\right], \quad p>0 \text{ and } (p\neq 2). \tag{68}$$

Let us return back again to the algorithm of HFARAS presented in Section 4, and we execute the steps from Step 8 to Step 12 of that framework.

In order to perform the intermediate steps and obtaining the rationality degree and the importance degree, we incorporate the divergence measures Div_{M3}, Div_{M4}, and Div_Γ given, respectively, by (67), (68), and (8) into (48). Then, to save more space for convenient storage, we present only the combined criteria weights ω_j $(j = 1,\ldots,n)$ which are given by (56). All the results are, respectively, given in Table 4 and Table 5, and they are correspondingly shown in Figures 1–3.

Step 9. It is needless to say that for the three different divergence-based processes, the relation (57) returns the optimal performance rating vector of drug options in the form of

$$h_O^j\,|_{j=1}^{7} = \{0.804, 0.690, 0.680, 0.644, 0.729, 0.600, 0.604\}, \tag{69}$$

which is extracted from Table 3.

Step 10. Since all the criteria are cost-based criteria, therefore, we do not need to normalize them.

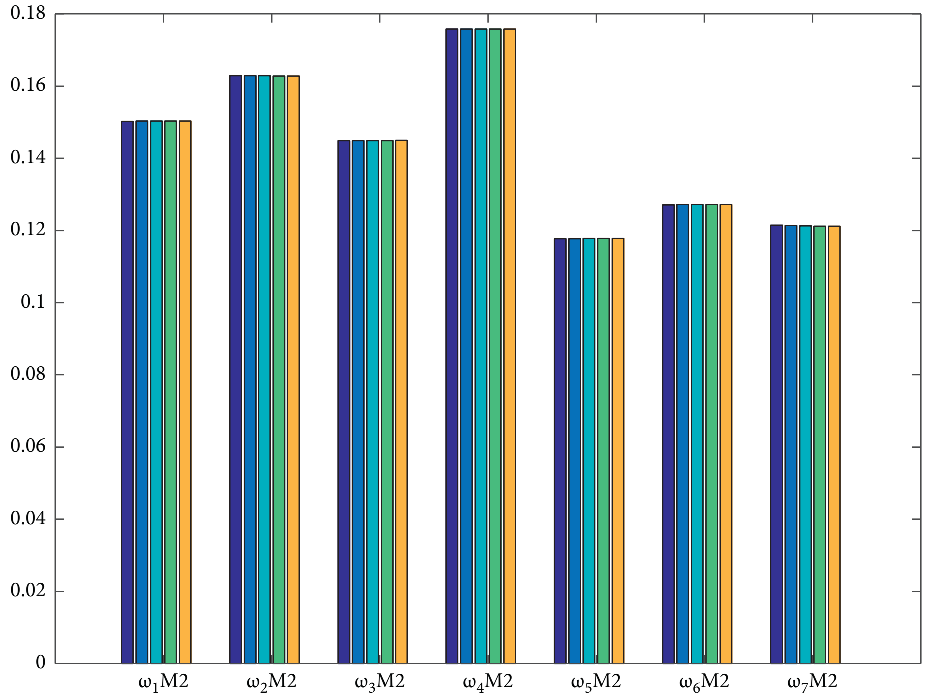

Figure 2: The combined criteria weights ω_j corresponding to the divergence measure Div_{M4}. The sixth column is not preserved due to "Not-A-Number" value.

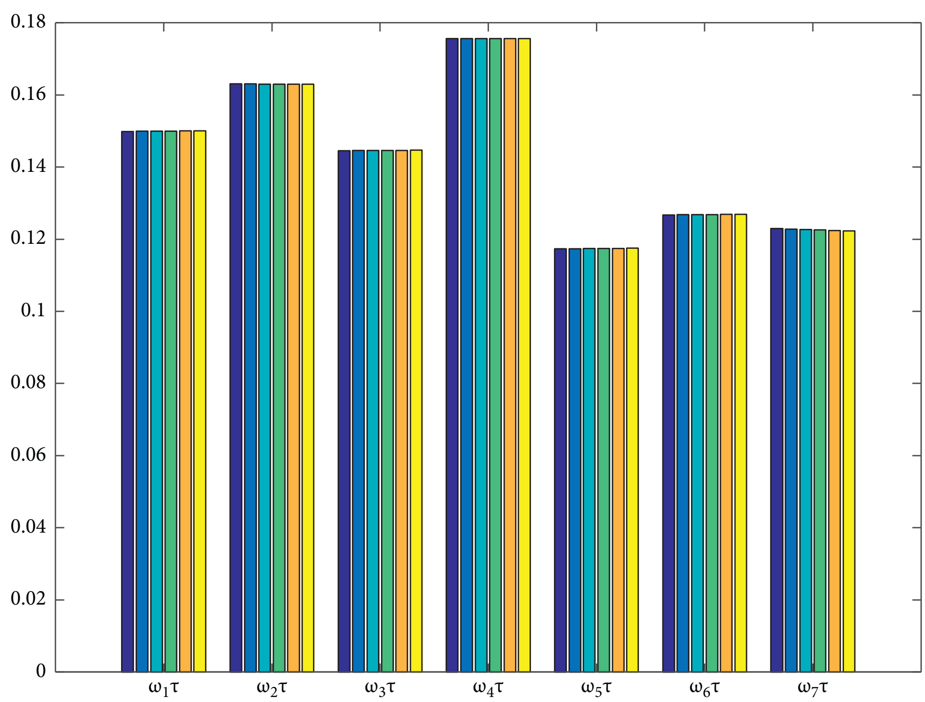

Figure 3: The combined criteria weights ω_j corresponding to the divergence measure Div_{Γ}.

Table 6: The weighted normalized form of decision matrix corresponding to the divergence measure Div_{M3}.

Criteria	Alternatives				
	A1	A2	A3	A4	A5
C1	0.1028	0.1001	0.1046	0.1208	0.0907
C2	0.0990	0.0902	0.1031	0.1057	0.1124
C3	0.0742	0.0829	0.0795	0.0985	0.0891
C4	0.1113	0.1069	0.1113	0.1097	0.1132
C5	0.0530	0.0560	0.0534	0.0858	0.0645
C6	0.0538	0.0577	0.0596	0.0763	0.0695
C7	0.0449	0.0453	0.0487	0.0733	0.0463

Table 7: The weighted normalized form of decision matrix corresponding to the divergence measure Div_{M4} (for $p = 1.0$).

Criteria	Alternatives				
	A1	A2	A3	A4	A5
C1	0.1028	0.1001	0.1046	0.1208	0.0907
C2	0.0990	0.0902	0.1031	0.1057	0.1124
C3	0.0742	0.0829	0.0795	0.0985	0.0891
C4	0.1113	0.1069	0.1113	0.1097	0.1132
C5	0.0530	0.0560	0.0534	0.0858	0.0645
C6	0.0538	0.0577	0.0596	0.0763	0.0695
C7	0.0449	0.0453	0.0487	0.0733	0.0463

Table 8: The weighted normalized form of decision matrix corresponding to the divergence measure Div_{Γ} (for $p = 1.0$).

Criteria	Alternatives				
	A1	A2	A3	A4	A5
C1	0.1025	0.0998	0.1043	0.1205	0.0905
C2	0.0991	0.0903	0.1032	0.1058	0.1125
C3	0.0740	0.0827	0.0793	0.0983	0.0889
C4	0.1111	0.1068	0.1111	0.1096	0.1131
C5	0.0528	0.0558	0.0533	0.0855	0.0643
C6	0.0536	0.0575	0.0594	0.0760	0.0693
C7	0.0455	0.0459	0.0493	0.0742	0.0468

The other data of divergence measures Div_{M4} and Div_{Γ} for $p = 1.2, 1.4, 1.6, 1.8, 2.0$ are saved and not expressed in Table 7 and Table 8 due to space limitations.

Step 11. The weighted normalized form of decision matrices corresponding to the divergence measures Div_{M3}, Div_{M4}, and Div_{Γ} are, respectively, given in Tables 6, 7, and 8.

Step 12. The preference orders for the drug options in accordance with the considered divergence measures Div_{M3}, Div_{M4}, and Div_{Γ} are determined as those shown in Figures 4–6.

As can be observed, the preference order for the drug options corresponding to all three cases remains the same as follows:

$$\begin{aligned}&\text{Remdesivir}\left(A_4\right) \succ \text{hydroxychloroquine}\left(A_5\right)\\&\succ \frac{\text{LPV}}{\text{RTV}}\left(A_3\right) \succ \frac{\text{LPV}}{\text{RTV}} - \text{IFN}b\left(A_1\right) \succ \text{favipiravir}\left(A_2\right),\end{aligned} \tag{70}$$

and the desirable drug option is remdesivir (A_4).

Although the final outcome of two existing divergence measures Div_{M3} and Div_{M4} is coincided with that of the proposed divergence measure Div_{Γ}, two major issues need to be addressed here:

(i) The parametric divergence measure Div_{Γ} provides us with a class of divergence values (based on the parameter $p \geq 1$) wider than that of the nonparametric divergence measure Div_{M3}, which is contained in the former as a special case;

(ii) Both divergence measures Div_{Γ} and Div_{M4} are parametric, but the latter one is meaningless when $p = 2$, and this shortcoming is not going to be visible in the former one.

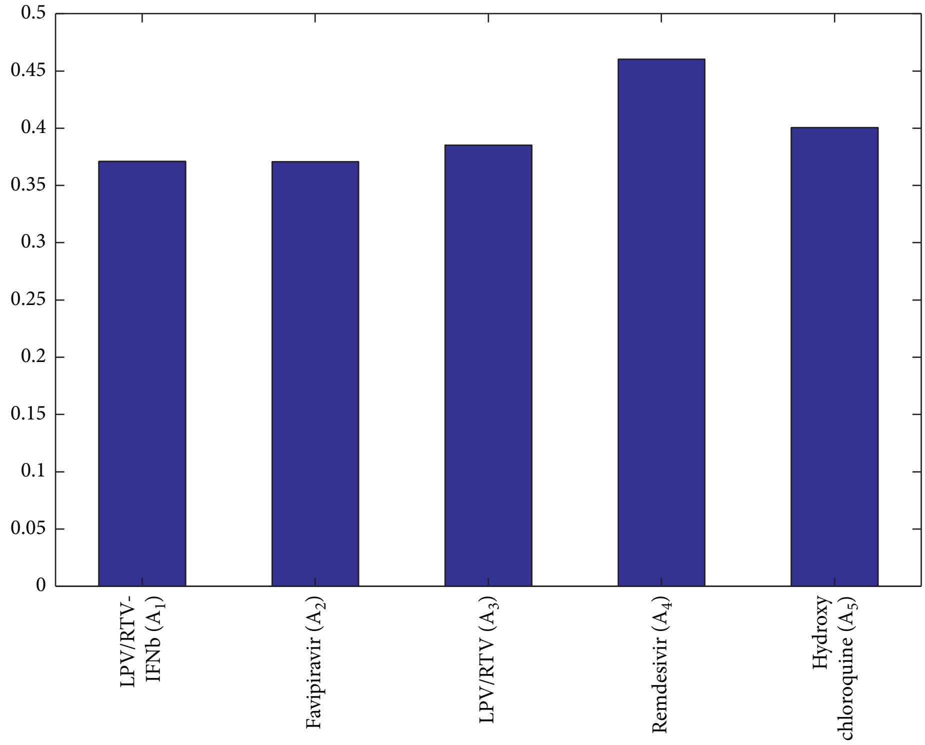

FIGURE 4: The value of alternatives corresponding to the divergence measure Div_{M3}.

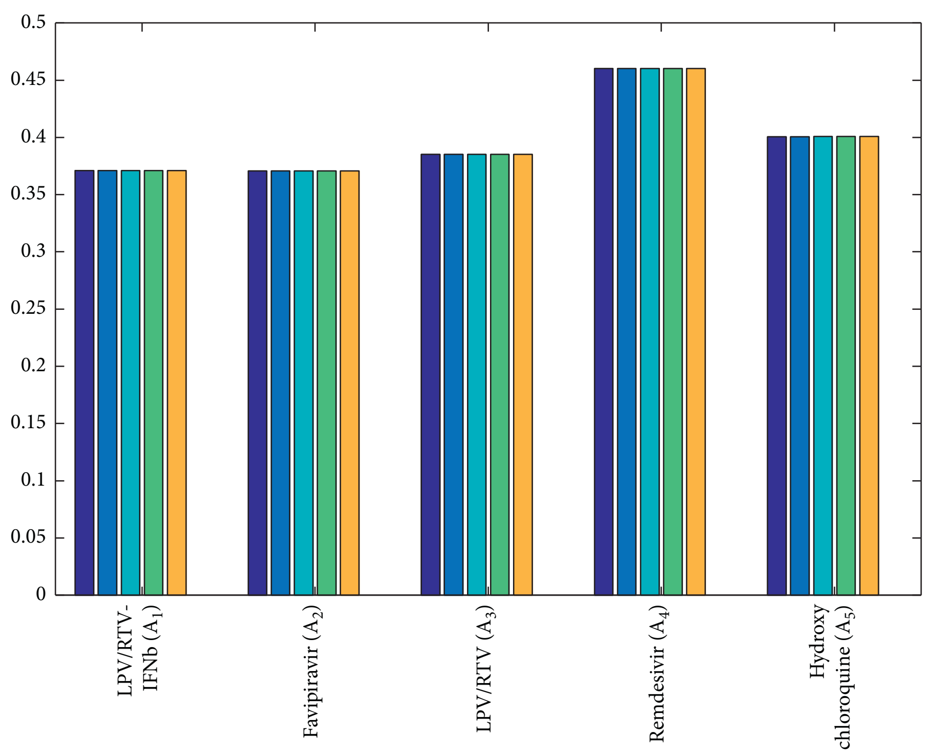

FIGURE 5: The value of alternatives corresponding to the divergence measure Div_{M4}. The sixth column is not preserved due to "Not-A-Number" value.

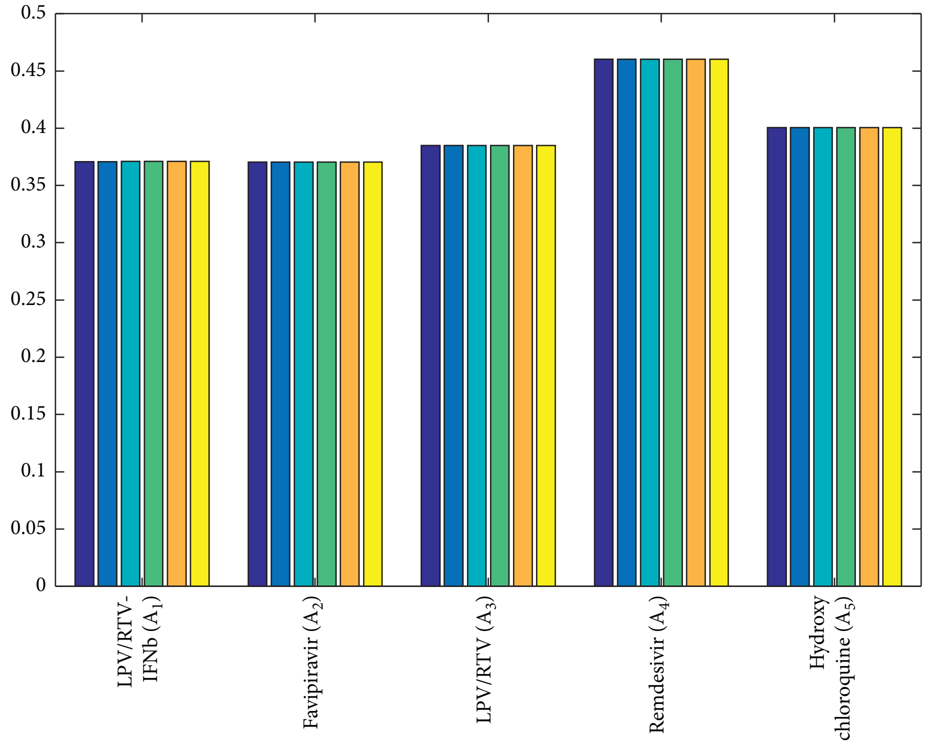

FIGURE 6: The value of alternatives corresponding to the divergence measure Div_{Γ}.

6. Conclusions

This contribution offers an ARAS framework being based on the HFS divergence measure for evaluating mainly the criteria weights. The prominent role of HFS divergence measures are apparent in their parametrically and symmetrically properties.

Other main contributions of the present work are summarized as follows:

(1) Investigating of several properties for the proposed divergence measures

(2) Pointing out the counter-intuitive cases corresponding to the existing divergence measures versus the proposed ones

(3) Illustrating the validity and more applicability of the proposed divergence-based decision-making methodology

The direction of future work of this research may be focused on the other applications such as renewable energy technology selection, optimal selection of antiviral therapy for the mild symptoms of COVID-19, and other applications in the process of bid evaluation [37] and reverse logistics [38], [39].

Data Availability

The data used to support the findings of this study are available from the corresponding author upon request.

Conflicts of Interest

The author declares that there are no conflicts of interest.

References

[1] S. Lashgari, J. Antuchevičienė, A. Delavari, and O. Kheirkhah, "Using QSPM and WASPAS methods for determining outsourcing strategies," *Journal of Business Economics and Management*, vol. 15, no. 4, pp. 729–743, 2014.

[2] S. Narayanamoorthy, J. V. Brainy, T. Manirathinam, S. Kalaiselvan, J. V. Kureethara, and D. Kang, "An adoptable multi-criteria decision-making analysis to select a best hair mask product-extended weighted aggregated sum product assessment method," *International Journal of Computational Intelligence Systems*, vol. 14, no. 1, p. 160, 2021.

[3] S. Zolfaghari and S. M. Mousavi, "A new risk evaluation methodology based on FMEA, MULTIMOORA, TPOP, and interval-valued hesitant fuzzy linguistic sets with an application to healthcare industry," *Kybernetes*, vol. 50, no. 9, pp. 2521–2547, 2021.

[4] S. Fouladi, M. J. Ebadi, A. A. Safaei, M. Y. Bajuri, and A. Ahmadian, "Efficient deep neural networks for classification of COVID-19 based on CT images: virtualization via software defined radio," *Computer Communications*, vol. 176, pp. 234–248, 2021.

[5] P. Melin, J. C. Monica, D. Sanchez, and O. Castillo, "Multiple ensemble neural network models with fuzzy response aggregation for predicting COVID-19 time series: the case of Mexico," *Healthcare*, vol. 8, no. 2, 2020.

[6] M. Abdel-Basst, R. Mohamed, and M. Elhoseny, "A model for the effective COVID-19 identification in uncertainty environment using primary symptoms and CT scans," *Health Informatics Journal*, vol. 26, no. 4, 2020.
[7] D. K. Bonilla-Aldana, Y. Holguin-Rivera, I. Cortes-Bonilla et al., "Coronavirus infections reported by ProMED, february 2000-january 2020," *Travel Medicine and Infectious Disease*, vol. 35, Article ID 101575, 2020.
[8] S. Ashraf and S. Abdullah, "Emergency decision support modeling for COVID-19 based on spherical fuzzy information," *International Journal of Intelligent Systems*, vol. 35, no. 11, 2020.
[9] C. Wu, M. Liao, M. Karatas, S. Chen, and Y. Zheng, "Real-time neural network scheduling of emergency medical mask production during COVID-19," *Applied Soft Computing*, vol. 97, 2020.
[10] A. R. Mishra, P. Rani, R. Krishankumar, K. S. Ravichandran, and S. Kar, "An extended fuzzy decision-making framework using hesitant fuzzy sets for the drug selection to treat the mild symptoms of Coronavirus Disease 2019 (COVID-19)," *Applied Soft Computing*, vol. 103, Article ID 107155, 2019.
[11] E. K. Zavadskas and Z. Turskis, "A new additive ratio assessment (aras) method in multicriteria decision-making/naujas adityvinis kriterijų santykių ivertinimo metodas (aras) daugiakriteriniams uždaviniams spręsti," *Technological and Economic Development of Economy*, vol. 16, no. 2, pp. 159–172, 2010.
[12] Z. Turskis and E. K. Zavadskas, "A new fuzzy additive ratio assessment method (Aras-f). Case study: the analysis of fuzzy multiple criteria in order to select the logistic centers location," *Transport*, vol. 25, no. 4, pp. 423–432, 2010.
[13] D. Stanujkic, "Extension of the ARAS method for decision-making problems with interval-valued triangular fuzzy numbers," *Informatica*, vol. 26, no. 2, pp. 335–355, 2015.
[14] G. Büyüközkan and F. Göçer, "An extension of ARAS methodology under interval valued intuitionistic fuzzy environment for digital supply chain," *Applied Soft Computing*, vol. 69, pp. 634–654, 2018.
[15] G. Büyüközkan and M. Güler, "Analysis of companies' digital maturity by hesitant fuzzy linguistic MCDM methods," *Journal of Intelligent and Fuzzy Systems*, vol. 38, no. 1, pp. 1119–1132, 2020.
[16] M. Iordache, D. Schitea, M. Deveci, İ. Z. Akyurt, and I. Iordache, "An integrated ARAS and interval type-2 hesitant fuzzy sets method for underground site selection: seasonal hydrogen storage in salt caverns," *Journal of Petroleum Science and Engineering*, vol. 175, pp. 1088–1098, 2019.
[17] H. Liao, Z. Wen, and L. Liu, "Integrating BWM and ARAS under hesitant linguistic environment for digital supply chain finance supplier section," *Technological and Economic Development of Economy*, vol. 25, no. 6, pp. 1188–1212, 2019.
[18] E. K. Zavadskas, Z. Turskis, T. Vilutienė, and N. Lepkova, "Integrated group fuzzy multi-criteria model: case of facilities management strategy selection," *Expert Systems with Applications*, vol. 82, pp. 317–331, 2017.
[19] A. R. Mishra, P. Rani, and K. R. Pardasani, "Multiple-criteria decision-making for service quality selection based on Shapley COPRAS method under hesitant fuzzy sets," *Granular Computing*, vol. 4, no. 3, pp. 435–449, 2019.
[20] A. R. Mishra, P. Rani, R. Krishankumar, E. K. Zavadskas, F. Cavallaro, and K. S. Ravichandran, "A hesitant fuzzy combined compromise solution framework-based on discrimination measure for ranking sustainable third-party reverse logistic providers," *Sustainability*, vol. 13, no. 4, Article ID 2064, 2021.
[21] V. Torra, "Hesitant fuzzy sets," *International Journal of Intelligent Systems*, vol. 25, pp. 529–539, 2010.
[22] M. Xia and Z. Xu, "Hesitant fuzzy information aggregation in decision making," *International Journal of Approximate Reasoning*, vol. 52, no. 3, Article ID 52395, 2011.
[23] Z. Xu, *Hesitant Fuzzy Sets Theory, Studies in Fuzziness and Soft Computing*, Springer, Berlin, Germany, 2014.
[24] H. Liao, Z. Xu, and X. J. Zeng, "Hesitant fuzzy linguistic VIKOR method and its application in qualitative multiple criteria decision making," *IEEE Transactions on Fuzzy Systems*, vol. 23, pp. 1343–1355, 2014.
[25] B. Farhadinia, H. Liao, and E. Herrera-Viedma, "A modified class of correlation coefficients of hesitant fuzzy information," *Soft Computing*, vol. 25, no. 10, pp. 7009–7028, 2021.
[26] B. Farhadinia and F. Chiclana, "A decision-making methodology based on the weighted correlation coefficient in weighted extended hesitant fuzzy environments," *International Journal of Intelligent Systems*, vol. 36, no. 4, pp. 1485–1534, 2021.
[27] B. Farhadinia and A. Taghavi, "A Single-valued extended hesitant fuzzy score-based technique for probabilistic hesitant fuzzy multiple criteria decision-making," *Complexity*, vol. 2021, Article ID 2454738, 19 pages, 2021.
[28] B. Farhadinia, U. Aickelin, and H. A. Khorshidi, "Uncertainty measures for probabilistic hesitant fuzzy sets in multiple criteria decision making," *International Journal of Intelligent Systems*, vol. 35, no. 11, pp. 1646–1679, 2020.
[29] B. Farhadinia, "Information measures for hesitant fuzzy sets and interval-valued hesitant fuzzy sets," *Information Sciences*, vol. 240, pp. 129–144, 2013.
[30] R. Kadian and S. Kumar, "Renyi's-Tsallis fuzzy divergence measure and its applications to pattern recognition and fault detection," *Journal of Intelligent and Fuzzy Systems*, vol. 39, no. 1, pp. 731–752, 2020.
[31] R. Kumari and A. R. Mishra, "Multi-criteria COPRAS method based on parametric measures for intuitionistic fuzzy sets: application of green supplier selection," *Iranian Journal of Science and Technology, Transactions of Electrical Engineering*, vol. 44, no. 4, pp. 1645–1662, 2020.
[32] Worldometer, "COVID-19 Coronavirus Pandemic," 2020, http://www.worldometers.info/coronavirus/#countries%3C.
[33] N. Chen, M. Zhou, X. Dong et al., "Epidemiological and clinical characteristics of 99 cases of 2019 novel coronavirus pneumonia in Wuhan, China: a descriptive study," *The Lancet*, vol. 395, no. 10223, pp. 507–513, 2020.
[34] W.-J. Guan, Z. Ni, Y. Hu et al., "Clinical characteristics of coronavirus disease 2019 in China," *New England Journal of Medicine*, vol. 382, no. 18, pp. 1708–1720, 2020.
[35] Who, "Novel Coronavirus (2019-nCoV) Situation Reports," World Health Organization, 2020, http://www.who.int/emergencies/diseases/novelcoronavirus-2019/situation-reports/.
[36] A. R. Mishra, P. Rani, K. R. Pardasani, and A. Mardani, "A novel hesitant fuzzy WASPAS method for assessment of green supplier problem based on exponential information measures," *Journal of Cleaner Production*, vol. 238, 2019.
[37] Z.-S. Chen, X. Zhang, R. M. Rodríguez, W. Pedrycz, and L. Martínez, "Expertise-based bid evaluation for construction-contractor selection with generalized comparative linguistic ELECTRE III," *Automation in Construction*, vol. 125, Article ID 103578, 2021.

[38] Z.-S. Chen, X. Zhang, K. Govindan, X.-J. Wang, and K.-S. Chin, "Third-party reverse logistics provider selection: a computational semantic analysis-based multi-perspective multi-attribute decision-making approach," *Expert Systems with Applications*, vol. 166, Article ID 114051, 2021.
[39] V. Kersuliene and Z. Turskis, "An integrated multi-criteria group decision making process: selection of the chief accountant," *Procedia Soc. Behav. Sci.*vol. 110, pp. 897–904, 2014.

Hindawi
Mathematical Problems in Engineering
Volume 2021, Article ID 4312842, 12 pages
https://doi.org/10.1155/2021/4312842

Research Article

Economic Management Data Envelopes Based on the Clustering of Incomplete Data

Shuo Dong [1] and Sang-Bing Tsai [2]

[1]School of Economics, Central University of Finance and Economics, Beijing 10081, China
[2]Regional Green Economy Development Research Center, School of Business, WUYI University, Nanping, China

Correspondence should be addressed to Shuo Dong; shuodong@email.cufe.edu.cn

Received 27 October 2021; Revised 17 November 2021; Accepted 22 November 2021; Published 3 December 2021

Academic Editor: Zhen Song Chen

In this paper, the economic management data envelope is analyzed by an algorithm for clustering incomplete data, a local search method based on reference vectors is designed in the algorithm to improve the accuracy of the algorithm, and a final solution selection method based on integrated clustering is proposed to obtain the final clustering results from the last generation of the solution set. The proposed algorithm and various aspects of it are tested in comparison using benchmark datasets and other comparison algorithms. A time-series domain partitioning method based on fuzzy mean clustering and information granulation is proposed, and a time series prediction method is proposed based on the domain partitioning results. Firstly, the fuzzy mean clustering method is applied to initially divide the theoretical domain of the time series, and then, the optimization algorithm of the theoretical domain division based on information granulation is proposed. It combines the clustering algorithm and the information granulation method to divide the theoretical domain and improves the accuracy and interpretability of sample data division. This article builds an overview of data warehouse, data integration, and rule engine. It introduces the business data integration of the economic management information system data warehouse and the data warehouse model design, taking tax as an example. The fuzzy prediction method of time series is given for the results of the theoretical domain division after the granulation of time-series information, which transforms the precise time-series data into a time series composed of semantic values conforming to human cognitive forms. It describes the dynamic evolution process of time series by constructing the fuzzy logical relations to these semantic values to obtain their fuzzy change rules and make predictions, which improves the comprehensibility of prediction results. Finally, the prediction experiments are conducted on the weighted stock price index dataset, and the experimental results show that applying the proposed time-series information granulation method for time series prediction can improve the accuracy of the prediction results.

1. Introduction

Clustering is an unsupervised data mining method. The basic idea is to measure the similarity between the data based on the intrinsic properties of the data and classify the samples with greater similarity into the same class and those with less similarity into different classes [1]. In the field of finance, clustering is widely used in problems, such as personal credit collection and risk identification of listed companies. However, in specific applications, traditional clustering algorithms cannot handle high-dimensional data well. The presence of a large amount of noise and redundant features makes it very unlikely that clusters exist in all dimensions. As the sample dimensionality increases, the distance difference between the samples becomes smaller, and the data becomes sparse in the high-dimensional space [2]. It is shown that in the processing of high-dimensional data, low-dimensional feature subspaces can approximate the high-dimensional data features. The subspace clustering methods follow this idea and seek to identify the different classes of clusters in different feature subspaces in the same dataset. Since the features of different classes of data may correspond to different feature subspaces, and the feature dimensions composing these feature subspaces may also be different, it is more difficult to identify the class clusters in the original feature space. The subspace clustering algorithm divides the original feature space to obtain several different feature subspaces and identifies the possible class clusters from the feature subspaces. Many subspace clustering algorithms have been proposed in the existing research for clustering high-dimensional data [3]. However, these algorithms are optimized for a single objective function and adopt a greedy search strategy, and thus, they have the disadvantages of being sensitive to the initial points and easily falling into local optima. Moreover, optimizing multiple objective functions simultaneously can improve the robustness of the algorithm to different data.

Clustering analysis is one of the important techniques in the field of data mining and machine learning and has been widely used in several fields, including information granulation, image processing, bioinformatics, security assurance, web search, etc. The so-called clustering is to divide the sample objects in a dataset into different class clusters, where the sample objects in similar clusters are highly similar, while those in different class clusters are less similar. The role of clustering as an unsupervised learning technique in identifying the unlabeled data structures cannot be ignored [4]. For different division methods of samples, the existing clustering methods can be classified as hierarchical clustering methods, divisive clustering methods, grid-based clustering methods, density-based clustering methods, and other clustering methods. The existing clustering algorithms can also be roughly classified into two main categories: hierarchical clustering methods and divisive clustering methods [5]. Besides, the clustering algorithms can be classified into hard clustering algorithms and soft clustering algorithms based on other classification criteria. After years of research and development, many clustering algorithms have been widely used. Although there are several clustering algorithms in the field of clustering analysis, each algorithm has its unique method for discovering the underlying data structure in a dataset. However, different algorithms processing the same dataset may produce different clustering results, and it is difficult for us to evaluate which clustering result is more consistent with the data structure of that dataset without supervised information [6]. Completely random missing means that the missing values are lost completely at random, and the tendency of the data points to be missing is independent of their hypothetical values and the values of other variables. Random missing means that the missing values are missing because of some observed data and the tendency of the data points to be missing is independent of the missing data, however, it is related to some observed data. Nonrandom missing means that the missing values are not lost randomly but for a reason. Usually, the reason is that the missing value depends on the assumed value or the value of another variable.

Because of the existence of data sets containing missing data, the traditional clustering algorithms are no longer able to deal with these data directly. Therefore, exploring how to solve the clustering problem of incomplete datasets has become a pressing challenge in the study of cluster analysis. In summary, the study of clustering methods for incomplete data has very wide scientific research value and practical application value. It is an information management technology whose main purpose is to support the management decisions through smooth, rational, and comprehensive information management. A data warehouse is a new application of database technology and not a replacement for the database. Data warehouse and operational database, respectively, undertakes two different tasks of high-level decision analysis and daily operational processing and play different roles. There is a close connection between the data warehouses and real time databases, and the data warehouses require real time databases to provide large amounts of historical data to provide answers, analysis, and prediction results for the various topics required.

The second part of this paper is the research status, the third part is the introduction of the related research algorithm structure, the fourth part is the analysis and explanation of the results, and the fifth part is the conclusion of this paper.

2. Current status of Research

With the rapid development of the internet technology and the improved performance of data storage devices in recent years, a large amount of data is generated and stored in various industries. Among these data, a large portion is time-tagged, i.e., a series of observations recorded in a chronological order, known as time series. How to effectively analyze and process the time series data to uncover potential and valuable knowledge and information to support more efficient production, operation, management, and decision-making activities of the enterprises is one of the important tasks in today's big data era [7]. Traditional time series analysis mainly uses statistical models to analyze and process time series, and with the rapid development of artificial intelligence, time series analysis methods based on data mining and machine learning theory have gradually become mainstream, forming a research branch of time series data mining. In the system sense, time series refers to the response of a system at different times [8]. From the viewpoint of system operation, the definition points out that time series are arranged in a certain order. The "certain order" here can be either a time order or a physical quantity with various meanings, such as representing temperature, velocity, or other monotonically increasing values. The time series is an objective record of the historical behavior of the system under study, which contains the structural characteristics of the system and its operation laws [9]. In summary, the time series has the following characteristics: the data or the position of the data points in the series depends on time, that is, the values of the data depend on the change of time but not necessarily a strict function of time. The values or the position of the data points at each moment have certain randomness, and it is impossible to predict the historical values with complete accuracy. The values or the position of the data points at the preceding and following moments (not necessarily adjacent moments) have a certain correlation, and this correlation is the dynamic regularity of the system. As a whole, the time series tend to show some kind of trend or cyclical variation [10].

In general, we cannot completely avoid the missing samples, similarly, in the association rule algorithm or decision tree algorithm, the missing data will directly affect the calculation of confidence, support of the frequent itemset, or the selection of the splitting attributes of the tree nodes. Therefore, the handling of missing values plays a crucial role in whether the clustering process can be carried out smoothly [11]. Therefore, the handling of missing values plays a crucial role in the success of the clustering process. The effective processing of incomplete data has become hot research in the field of pattern recognition. The modeling method generally analyzes the patterns of data in the dataset by finding them, establishing a suitable mathematical model, and calculating the corresponding missing attribute filler values by the established model, with the disadvantage that it is only suitable for the datasets of moderate size and with certain patterns. In addition to the above-mentioned methods, in recent years, with the rising popularity of machine learning, many missing value processing methods have been derived in combination with machine learning methods [12]. How credit card issuers specifically manage these risks concerning the probability of occurrence and the types of risks is also a focus of academic research. Recognizing these risks and improving the system of risk response appears to be crucial. From the point of view of cost reduction, credit card risk management needs to find the balance between the risk revenue and the expected cost of risk to maximize revenue with risk minimization, reduce costs in the balance, improve the efficiency of bank operations, and use digital models to assess the risk revenue of the cost of risk accompanying the credit card business based on theoretical research [13]. However, Yikin looks at the three perspectives of internal operational risk, external systemic risk, and technical operational risk for analysis and proposes the basic ideas of risk control under the network model of multiple risk interactions [5].

The populated incomplete dataset was processed using integrated clustering methods to obtain multiple clustering results. The consistent partitioning of each clustering result is performed using voting. Firstly, label matching is done for each class of clusters in different clustering results. Then, the intersection of the same labeled class clusters is obtained, and the samples in the intersection are divided into the core domain of the corresponding class clusters. The remaining samples decide whether they belong to the core domain or the boundary domain of the class clusters according to the relationship between the number of votes obtained by voting and the set threshold value. Determining the core-domain and boundary-domain samples of the class clusters results in a three-branch clustering result. The feasibility of the algorithm is demonstrated by evaluating the clustering results by clustering validity metrics.

3. Economic Management Data Envelopment Analysis for Incomplete Data Clustering

In this section, we give a detailed description of the main algorithms and structures. Although we have just proposed a high-quality clustering criterion, it is still difficult for us to quantify it. The final evaluation of the quality of the clustering is often the satisfaction of the stakeholders after the clustering. If the demander is satisfied with your clustering results and obtains valuable information from it, then the clustering is effective and high-quality.

3.1. Design of Clustering Algorithms for Incomplete Data. The missing values in a dataset can be classified as completely random missing, random missing, and completely non-random missing in terms of the distribution of missingness. Completely random missing means that the missing data is random, and the missing data does not depend on any incomplete or complete variables. Random missing means that the missing data is not completely random, i.e., the missing data of that type depends on other complete variables. Completely nonrandom missing means that the missing of the data depends on the incomplete variables themselves [14]. The data objects studied in this chapter are incomplete information systems under completely random missingness, i.e., the missingness of the data is random and the missingness of the data does not depend on any incomplete or complete variables. In most cases, a high percentage of missingness is often accompanied by inefficient clustering results, and when the missingness rate of the dataset is high, the accuracy for filling the missing values of the sample objects decreases. It can also directly cause a decrease in the performance of the clustering algorithm. Therefore, we set the missing rate of the dataset between 5% and 30%, i.e., the missing attribute values of the sample objects need to satisfy two conditions [15]. Any sample object must retain at least one full attribute value. Each attribute has at least one corresponding complete value in the incomplete dataset. In other words, a sample cannot be missing all attribute values and all samples cannot be missing the same attribute. This chapter and the next chapter preprocess the dataset to the incomplete dataset following the two basic conditions for missing the attribute values and the missing rate range value requirement for the dataset.

For a sample point, in addition to the inherent characteristics of the sample itself, it will be influenced by other samples. If there are more samples of a certain category around the sample, then the denser the distribution, the more likely the sample belongs to this category. Conversely, if the number of samples of a certain category around the sample is sparse and the distribution is sparser, it is less likely the sample belongs to this category. Therefore, the effective use of sample distribution information can make the clustering results more accurate. Therefore, when calculating the distance between a sample point and the cluster center, the distance calculation can be improved by introducing the proximity category information in the form of a ratio. The distance formula with the sample distribution information can make certain adjustments to the distance measurement process with the changes in the data set, thus obtaining a more accurate distance value [16]. In the process of filling incomplete datasets, the information of missing attributes can also be collected from their nearest neighbor samples. The denser the distribution of the nearest neighbor samples, the higher the possibility of finding valid attribute information and the closer the filled value is to the true value. Inspired by this idea, this paper proposes a fuzzy mean algorithm for the incomplete data based on the sample spatial distance. The algorithm uses the nearest neighbor rule to fill the missing attributes of the incomplete data and introduces the sample spatial distribution information into the clustering process from two aspects. One is to determine the clustering influence value of the sample based on the sample nearest neighbor density, which is added to the clustering objective function in the form of weights, and the other is to correct the class information based on the sample nearest distance between the sample and the clustering center so that the process of distance metric can be adjusted somewhat with different data sets, and different sample spatial information is further introduced into the clustering process as shown in Figure 1.

Autonomous motivation significantly and positively predicts creative thinking. Controlled motivation has no significant predictive effect on creative thinking. Autonomous motivation plays a complete mediating role between moderate control and creative thinking, and it partly plays a mediating role between moderate autonomy/high autonomy and creative thinking. However, determining the number of nearest neighbors of a sample becomes a new problem. The number of nearest neighbors needs to be specified artificially, and if the number of the selected nearest neighbor samples is too small, there is a possibility that not enough attribute information is obtained to fill the missing values, resulting in too large a gap between the filled values and the true values. However, if too many nearest neighbor samples are selected, the filled attribute features will be confused by too many sample subclasses. It has a certain degree of impact on the accuracy of the algorithm.

$$D_{ik} = \frac{1}{\sum_{j=1}^{s} I_{jk}} \sqrt{\sum_{j=1}^{s} \left(I_{jk} + x_{jk}\right)^2 I_{jk}},$$
$$x_{jk} = \frac{1}{N} \sum_{j=1}^{s} I_{jk}, \tag{1}$$

D_{ik} represents the flux, and I_{jk} represents the economic value in the j^{th} column and k^{th} row. In this way, the attributes of the complete data and the information of the attributes that are not missing in the incomplete data are fully utilized. The nearest neighbor samples of the incomplete data are identified, and the missing part of the incomplete data is filled using the average of the information of the complete attributes of the N nearest neighbor samples. It makes the filling effect more reasonable and realistic.

$$H_{ik} = N_k^i \cdot N_k,$$
$$d_{ik}^* = d_{ik} - a\left(1 - H_{ik}\right), \tag{2}$$

H_{ik} represents the flow rate, and d_{ik} represents the year. After the information granulation operation on the time series, the original time series is transformed into granular time series. The next step is to measure the similarity between the granular time series. The commonly used time series similarity measures are Euclidean distance, dynamic time-bending distance, cosine similarity distance, etc. Since the number of information grains and the size of the time window contained in the granular time series obtained from the two-time series after the information granulation operation may be different, this section proposes a new similarity measure, i.e., the linear information granulation-based time series similarity measure. For many practical data classification problems, samples originating from different classes often partially overlap in the feature space [17]; see Figure 1.

Although the training samples in the overlapping regions have accurate category labels, these samples do not reflect the exact distribution of the categories, i.e., the information provided by the samples in these overlapping regions of the categories is inaccurate. Therefore, a reasonable modeling of the imprecise training data in these overlapping regions is needed to achieve the effective utilization of this part of the training data.

Incomplete training data usually refers to the fact that the obtained training data is not sufficient to provide an effective portrayal of the true conditional probability distribution. In general, fewer training samples and higher feature dimensions are the main factors that cause the incompleteness of training data. Therefore, how to obtain better classification performance based on incomplete training data is an important topic in the design of classification methods. Unreliable training data usually means that the obtained training data has large noise in terms of categories or features. Category noise refers to the training samples being labeled as the wrong category, while feature noise refers to the deviation of some feature values of the samples from the normal range. Therefore, to obtain better classification performance based on unreliable training data, robust classification methods need to be designed to suppress the data noise.

$$J_m(U,V) = \sum_{k=1}^{n} \sum_{i=1}^{n} w_k u_{ik}^m d_{ik}^2,$$
$$u_{ik} = \left(\sum_{l=1}^{c} \frac{d_{ik}^*}{d_{lk}^*}\right)^{2/1+m}, \tag{3}$$
$$v_i = \frac{\sum_{k=1}^{n} w_k w_k u_{ik}^m d_{ik}^2}{\left(\sum_{l=1}^{c} d_{ik}^* / d_{lk}^*\right)^{2/1+m}},$$

$J_m(U,V)$ represents the fixed flow, w is the weight, u represents the proportion of different positions, and v represents the corresponding rate. The rules configuration

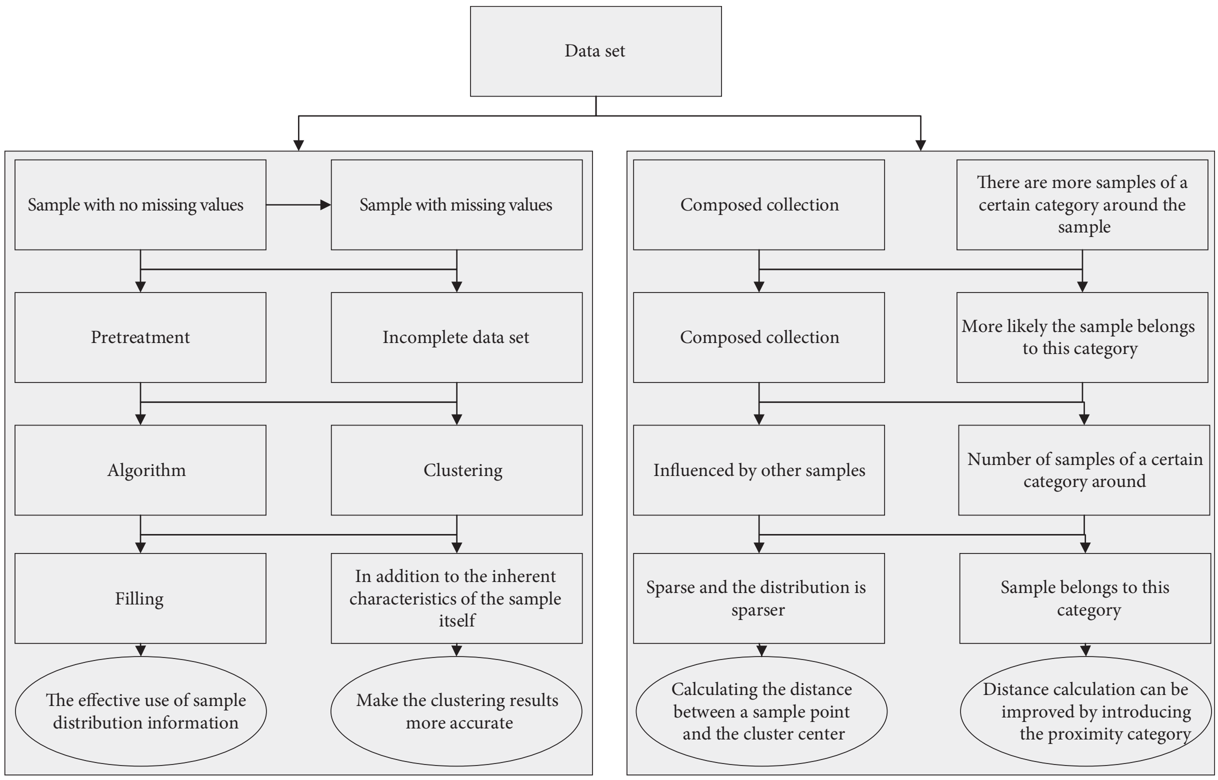

Figure 1: The framework of complete data clustering algorithm.

management of the economic data reporting system is divided into two parts: one is the configuration management of the rules for the splitting of reporting documents, and the other is the configuration management of the rules for the verification of reporting documents. These two rules are managed and configured separately while performing normative constraints for a report. The splitting rules mainly describe the parsing rules of the business unit report, such as the interval symbol between data, the split symbol between each data item, the report description item, etc. The verification rules mainly describe some requirements for the corresponding data items of the report, such as the type, name, definition, and constraints of the data items; the rule configuration is where the user input is a specific application. When the business data reported by the business unit is verified by the splitting rules and data verification rules, the system will automatically store the economic data in the corresponding original economic database for future extraction to the data warehouse as shown in Figure 2.

Since the processed data are in large batches, when storing the data into the database, one can imagine how inefficient the system would be if it were simply inserted with one SQL statement. Therefore, in this part, it can be considered to improve the speed of data depositing in terms of performance. It may be useful to intervene in the concept of the data persistence layer in terms of technical implementation. The design goal of the data persistence layer is to provide a high-level, unified, secure, and concurrent data persistence mechanism for the entire project. The users of the economic operation platform system are the municipal and district local taxation bureaus, national taxation bureaus, industrial and commercial bureaus, the development and reform commission, the bureau of statistics, and relevant leaders at all levels. From the viewpoint of the users of the system, the level of use and computer knowledge of the users of the economic operation platform is relatively high, and many business units, such as the state taxation bureau, local taxation bureau, and the industry and commerce bureau have established their professional business systems. Some have participated in the construction of the government portal system and the construction of the office automation system, which has promoted the improvement of the level of computer use. In terms of the frequency of use of the system, the most frequent use would be the statistical analysis part of the system, i.e., the frequency of operation of the system by NDRC and leaders at all levels would be greater.

3.2. Economic Management Data Envelope Design. The data integration rules of the original platform are cured in the program by the programmer. Although the current data integration is achieved, when the data of each department needs to be newly integrated according to the new economic rules, or when new departments are added to this system, the horizontal association requirements of the data between the

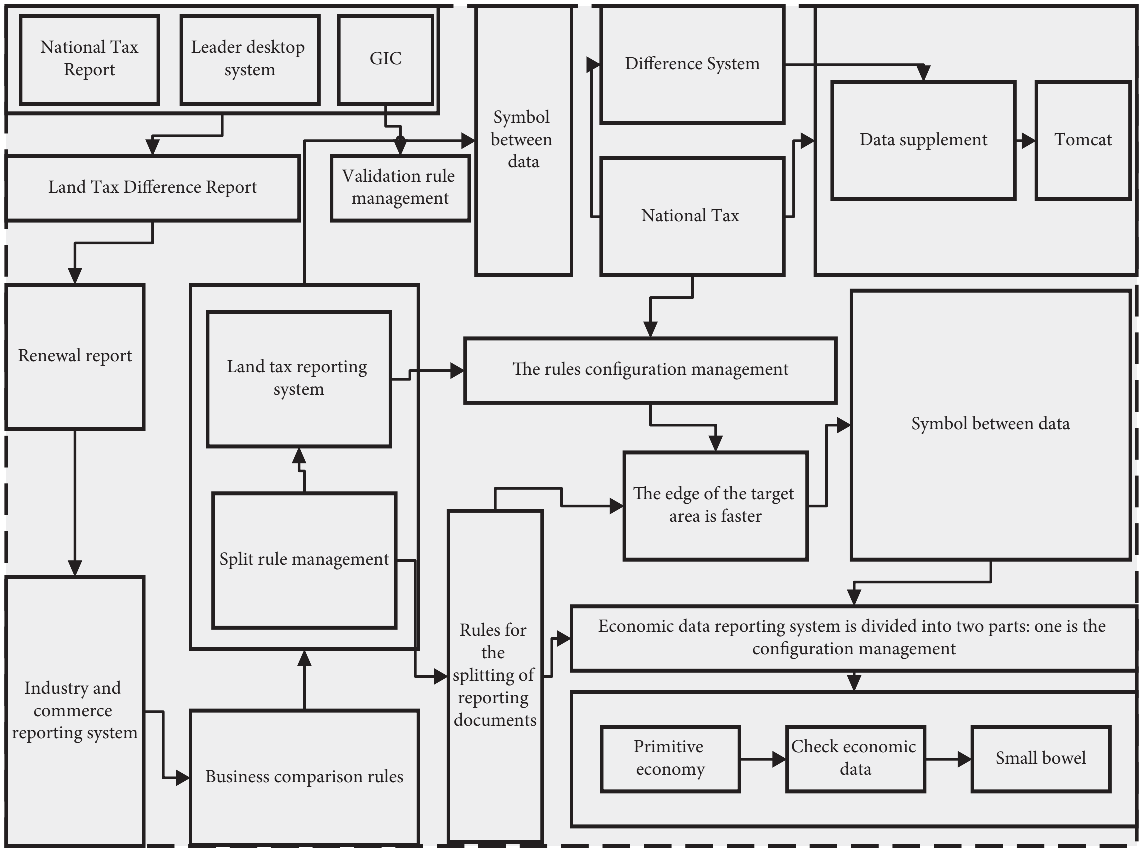

Figure 2: Economic platform architecture.

departments will be greatly increased. At this time, the update of the data integration module will face a lot of repetitive work, which will bring a lot of inconvenience to the operation and maintenance of the system. In the data integration, the data of each department is linked horizontally and new economic data is generated. It has certain economic data analysis functions [18,19]. However, with the continuous updating of economic rules and the addition of new departments and data, the system will gradually become huge and the data will become more complicated. In this case, the management of the database group in the original design will become difficult, and the analysis of economic data will put forward higher requirements. Hence, there is an urgent need for a technology that can effectively solve massive data storage and can effectively realize data mining and analysis. Therefore, we need to improve the platform to solve these problems [20].

If a unified economic database with regional attributes is to be established instead of a single economic vertical database, a horizontal correlation of multiple vertical data will be required to create a large integrated economic database. The core purpose of horizontal data processing is to eliminate the sectoral attributes of the data itself so that the data established with horizontal correlation has regional economic attributes. At present, several cities in China have already established preliminary economic data exchange systems. For example, Qingdao has established an economic data exchange system with four departments, including industry and commerce, taxation, and quality inspection. A part of our data source comes from our own collation, and the other part is open-source data. The practical effects and operational results reflected by the initial economic data exchange systems established in several cities show that it is feasible to establish a large horizontal economic data exchange system and management system. At present, many economic theories can only be understood by professional economic experts. The conclusions of many theories have a reference role for the regional governments to manage the economy. The system needs to correlate some standard general economic theories with the regional economic state and deduce some reference opinions for the regional governments to use as shown in Figure 3.

In a market economy, people in a transaction will have different information, and the fact that some people have information that others do not will create information asymmetry. The two results of information asymmetry are moral hazard and adverse selection. With imperfect access to information, a credit card holder may refuse to disclose all personal information to the bank so that the bank cannot get accurate information to evaluate whether the cardholder can have a credit card. Thus, in the credit card market, the mixed information leaves banks with no way to determine which cardholder has higher integrity and better cash flow. On the other hand, information asymmetry can also cause potential problems in the ex-ante credit card segment. If, after a successful credit card application, the cardholder's

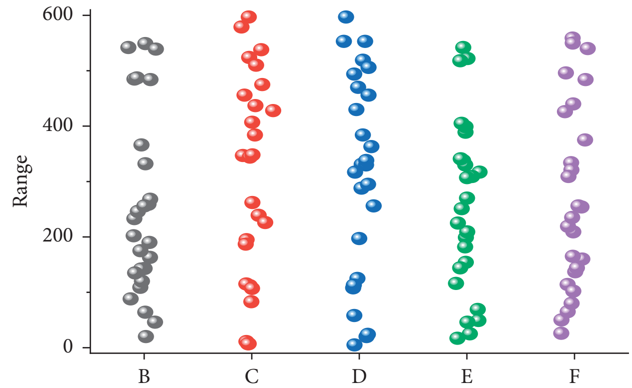

Figure 3: Schematic diagram of the feature subspace.

repayment ability fluctuates because of a combination of factors, such as job changes, cash flow turnover, and changes in income trends, then the bank is often unable to capture that part of the information and maintains the credit limit at a similar level [19]. The bank is often unable to capture this information, and the credit limit remains at a similar level as before, while the cardholder's repayment ability has changed. This information asymmetry also hides the potential risk of credit failure and default.

From the perspective of big data, banks, and other card-holding institutions, to achieve a penetrating supervision of the cardholders, they can obtain comprehensive information of cardholders from all aspects. It not only contains financial data directly affecting the repayment ability but also includes their consumption habits, work habits, social environment, moral risks, and many other data collections, thus constituting a comprehensive information judgment system. It is conducive to reducing the risk brought by information asymmetry to banks. With deeper application in the financial field, each financial institution has built its own big data platform one after another, using the computing power of the platform to standardize and centralize the data originally scattered in various business systems using a unified data platform or data warehouse. By a scenario-based design, the making of each business scenario can be described and applied by models using their existing data for a model test and complete the application of relevant business. The application of big data in the banking industry is mainly in various aspects such as accurate marketing, refined management, low-cost management, and centralized management of banks. Banks can make precise marketing strategies for individuals using information technology and have a valuable prediction and judgment for each customer's preference and ability. As per the big data model, banks can record credit card information while also providing feedback on these bearers' consumption behaviors. It is summarized and organized, especially in terms of risk control for loans, as shown in Figure 4.

Data integration in the regional economic management system is mainly to solve the problem of data ambiguity ambiguity among economic data scattered among various economic management departments describing the same economic affairs and to horizontally associate the scattered economic data with the same business meaning to generate new economic data, i.e., to perform data aggregation [20]. The form of the dispersed economic data is shown in Figure 4. The main work to achieve the disambiguation and data integration of a regional dispersed economic data is to identify and locate the original dispersed economic data and define and identify the business association relationships between the dispersed data. Among the more general solutions available, it is more practical and feasible to use the principle of rule engines to solve it.

Operational risk is the loss caused by the bank's internal systems, resulting in inadequate internal processes and external events, such as deficiencies in related information systems and staff errors. Operational risk can be manifested in the form of losses caused to customers by the design or implementation of a customized product or by the lack of training of the bank's internal staff, which makes its employees not aware of the risks they should have and the gaps or imperfections in internal processes, as well as the risks caused by errors in the authorization and approval of information systems and the technical environment.

4. Analysis of Results

4.1. Performance Results of Incomplete Data Clustering Algorithm. Figure 5 shows the experimental results of the algorithm KM-IMI and the algorithm KM-CD on the metrics DBI, AS, and ACC, where the experiments are done 100 times on each data set. The mean and best values of these three metrics are obtained. The underlined data in the figure indicates that the clustering effect of the KM-IMI algorithm is not as good as the clustering effect of the KM-CD algorithm. By observing the underlined data, we can directly see that the clustering results of the data sets Iris, Wine, WDBC, Pen digits, and Page Blocks on the mean of the ACC evaluation metrics on the KM-IMI algorithm are not as effective as on the algorithm KM-CD. Although the two datasets, Pen digits and Page Blocks, are less effective than the KM-IMI algorithm on the mean of the ACC metrics and on their best values, the difference is only between 0.01 and 0.02. It is easy to find that one of the reasons is that there is a positive relationship between the missing rate and the accuracy, i.e., the higher the missing rate, the lower the

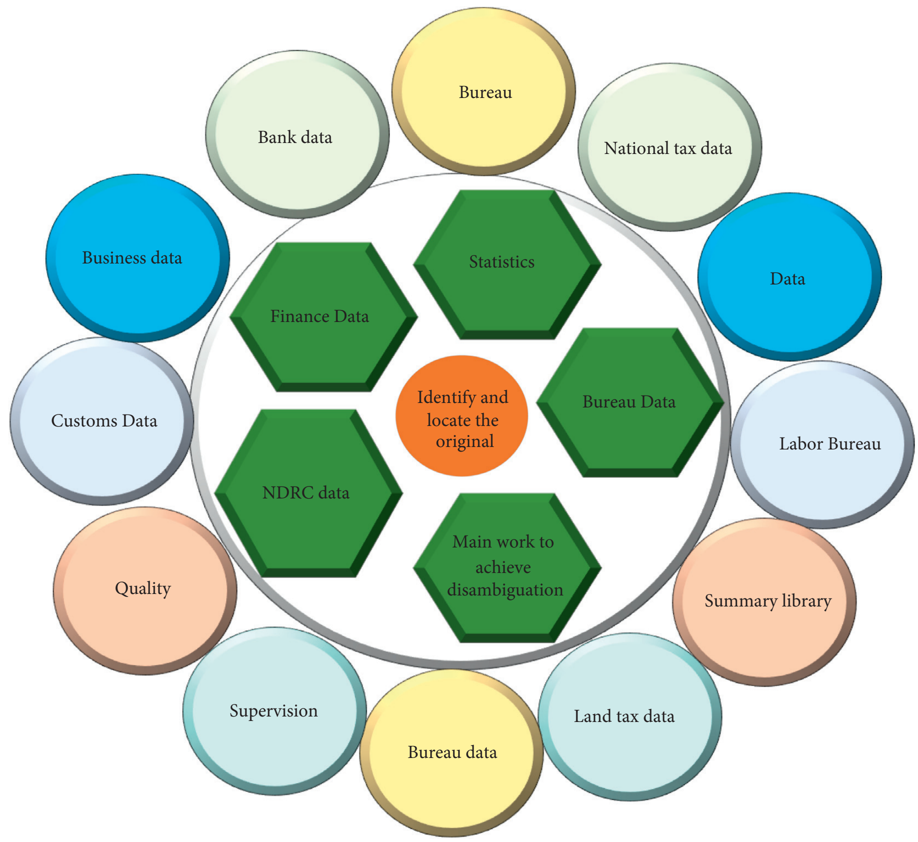

Figure 4: Original and aggregated repository clusters for the economic platform.

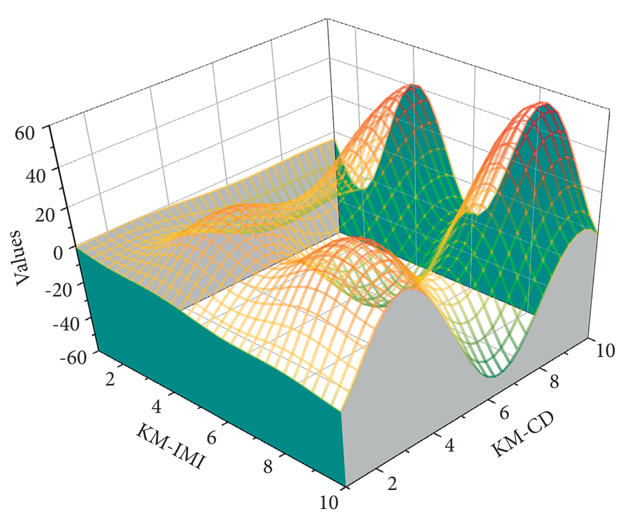

Figure 5: Experimental results on the dataset.

accuracy of the clustering results. It directly leads to the degradation of the performance of the clustering algorithm. The mean and best values of the algorithm KM-IMI on the metrics DBI and AS outperformed the algorithm KM-CD on most of the datasets, except for the underlined data. It is worth mentioning that in the dataset Banknote, CMC outperforms the mean and best values on all three indicators. Based on the above analysis, we can conclude that the improved clustering algorithm for the mean interpolation of incomplete data, i.e., KM-IMI can effectively solve the clustering problem of incomplete data as shown in Figure 5.

Observe Figure 6, the mean and best values of the experimental results for the data on the UCI dataset for the indicators ACC and FMI, where the bolded data indicate the better experimental results. The experiments were performed 100 times under different data set missing rates, and

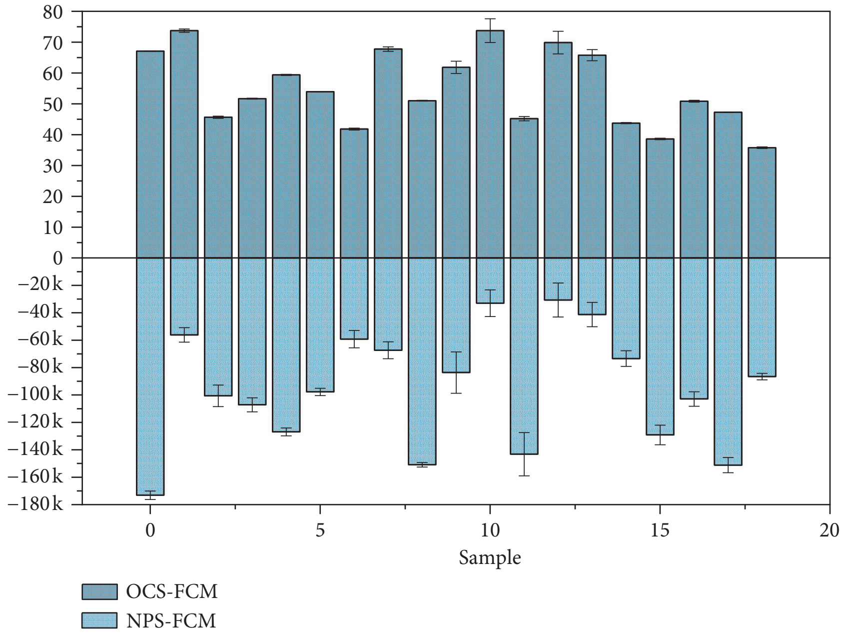

FIGURE 6: Average ACC.

the mean and best values were found from these 100 experiments, i.e., the mean and best values of ACC and FMI were obtained. From the figure, we can directly observe that the bolded experimental results are basically from the algorithm. Thus, we can conclude that the experimental results of the algorithm on the metrics ACC and FMI are better than the algorithms OCS-FCM and NPS-FCM, both in terms of the mean and best values of the metrics. Also, we observe that the data distribution of the algorithm is relatively stable with the values of ACC and FMI gradually decreasing as the missing rate of the data set increases. The data of the NPS-FCM algorithm is not so stable, which means that using the nearest neighbor approach to fill incomplete data is very much variable, and the nearest neighbor objects of the missing data samples are not stable, especially in the Pen digits dataset. The two algorithms compared are implemented based on the FCM algorithm. Using this algorithm, it is difficult to obtain good clustering results on non-spherical datasets. The algorithms are based on integrated clustering and can effectively improve the robustness of the clustering results, stability, and quality of the clustering results; see Figure 6.

The three-branch decision clustering uses the core and boundary domains to describe the relationship between the sample objects and class clusters. It is more appropriate than using an ensemble to represent a class cluster. At the same time, integrated clustering is an effective approach in dealing with clustering problems. The chapter proposes a three-branch integrated clustering algorithm for incomplete data by combining three-branch decision clustering with integrated clustering. Firstly, the attribute values corresponding to the missing data objects are filled according to the incomplete data filling method proposed in Chapter 2, i.e., based on the mean values of the attributes of all the sample objects in the clustering results of the complete data set. Then, the optimal estimates are obtained using the perturbation analysis of the clustering center. The three-branch integrated clustering method is used, i.e., if the class labels of the data objects agree after multiple clustering, then the object is classified into the core of the corresponding class cluster domain. Otherwise, the object is classified into the boundary domain.

4.2. Results of the Economic Management Data Envelope. Firstly, the data in the data warehouse comes from various data sources, including various heterogeneous database systems, data file data, other data, etc. Using data extraction tools, by the process of data extraction, cleansing, conversion, and loading, the data is loaded into the data warehouse according to different business themes, i.e., different analysis needs, to achieve integrated storage and facilitate data sharing. Then, various analysis tools are applied, such as retrieval query tools, OLAP tools for multidimensional data, statistical analysis tools, and data mining tools, to present the analysis results in the form of intuitive charts. These analytical tools, such as data mining tools, are highly functional with the help of a human.

At present, there are few information management systems for managing regional economies, and some local governments have established their own regional economic management systems according to their actual situation and needs. These systems are derived from the actual business needs of a competent economic department. Some of them also integrate the work needs of other economic management departments, and the main method used is the aggregation and analysis of economic data utilizing large data centralization. There is no data warehouse design for these information systems, however, the national information systems such as the construction of the four major databases

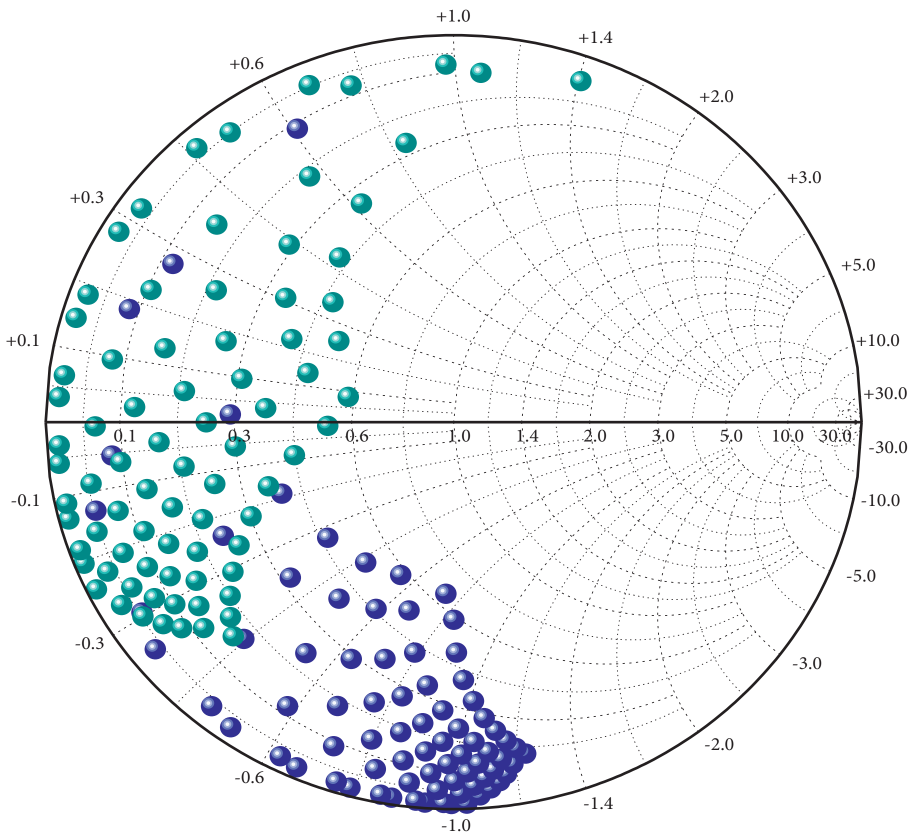

Figure 7: Tests for each method at different characteristic noise levels.

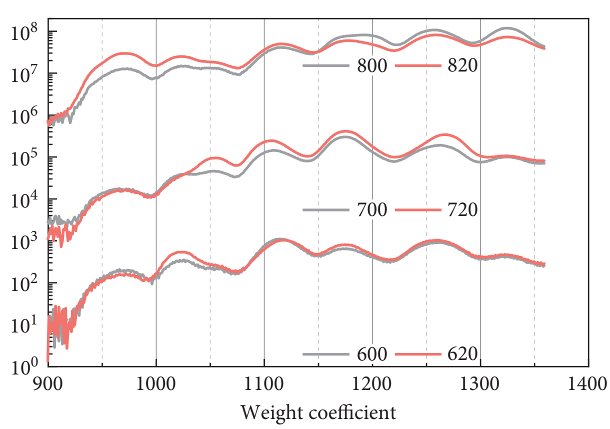

Figure 8: Classification error as the weight coefficient changes from 0 to 1.

adopt the data warehouse design. However, the station is higher and generally adopted by provincial units and municipalities. This system is still a blank field because it is standing in the perspective of the local government as shown in Figure 7.

The results under the same class noise condition are similar and most of the datasets proposed in this paper obtain better classification results under any feature noise level. To show more clearly, the robustness of different methods to feature noise gives the relative accuracy loss of each classification method at different feature noise levels. Based on a similar statistical analysis approach, firstly, we analyze whether there is a significant difference between the methods on the whole using the Friedman test. The running time of the training and classification phases depends mainly on the number of rules generated. More rules mean more time is needed to train the rule base and more time is needed when classifying an input sample. Therefore, we can analyze the impact of these factors on the time complexity from the perspective of the number of training samples, several features, and some fuzzy divisions of the dataset on the number of rules.

Figure 8 gives the classification errors during the change of weight coefficients from 0 to 1 for different data noise levels. The optimal values of the weight coefficients for different data noise levels are taken differently. As the noise level increases, the optimal value of the weight coefficient tends to become smaller. This is because the reliability of DBRB generated based on the training data decreases at high noise levels, and therefore, the noise-independent KBRB is needed to play a greater role in determining the final classification results; see Figure 8.

Credit business is a complete system, and through a big data system, it can become an organic integration of the whole business system. Big data technology can run through the whole credit business process, which can realize effective information collection and analysis before the loan, information sharing and transmission during the loan, and information monitoring and feedback after the loan. It can greatly improve the management efficiency of the loan business. After combining data analysis and questionnaire survey to analyze the problems in the bank credit business risk management from both objective and subjective aspects, it is necessary to further analyze the causes of these problems and provide a more reference piece value basis for the subsequent countermeasure formulation.

5. Conclusion

In this paper, two new methods for clustering incomplete data are proposed based on the nearest neighbor correlation of samples. However, there are still difficult problems that need to be studied. Since the incomplete samples themselves have uncertainty in the attribute space distribution, how to put aside subjectivity to choose a suitable similarity measure to determine the nearest neighbor samples of the incomplete samples is an important issue that deserves further research. Based on the existing economic platform, this thesis investigates the feasibility of building a data warehouse on the regional government economic operation platform, discusses the methods and steps of integrating business data and building a data warehouse, designs the data model and architecture of the tax data warehouse, and investigates the technical difficulties in the design of data storage and gives specific implementation methods. The key technologies in the design and implementation of building the data warehouse system are analyzed, and the theory of data warehouse is used to guide the design and development of the regional government economic operation platform system. The strategy of business data integration of the regional government economic operation platform system is studied, and the construction of the data integration platform based on the rule engine technology is analyzed and demonstrated, designed, and implemented. The data warehouse design was completed, focusing on solving technical difficulties, such as topic analysis and dimension table design. Based on this research, a unified data storage structure of the regional government economic operation platform system will be formed to provide a standard and comprehensive data source for data analysis and utilization, as well as future government decision-making. Compared with other studies, the efficiency and accuracy of our research results showed, approximately, a 10% improvement.

Data Availability

The data used to support the findings of this study are included within the article.

Conflicts of Interest

No competing interests exist concerning this study.

Acknowledgments

This paper was not funded by any organization.

References

[1] Y. Zhang, W. Wu, R. T. Toll et al., "Identification of psychiatric disorder subtypes from functional connectivity patterns in resting-state electroencephalography," *Nature Biomedical Engineering*, vol. 5, no. 4, pp. 309–323, 2021.

[2] I. A. Udugama, C. L. Gargalo, Y. Yamashita et al., "The role of big data in industrial (Bio)chemical process operations," *Industrial & Engineering Chemistry Research*, vol. 59, no. 34, pp. 15283–15297, 2020.

[3] M. Balistrocchi, R. Metulini, M. Carpita, and R. Ranzi, "Dynamic maps of human exposure to floods based on mobile phone data," *Natural Hazards and Earth System Sciences*, vol. 20, no. 12, pp. 3485–3500, 2020.

[4] J. Chen, X. Lian, H. Su, Z. Zhang, X. Ma, and B. Chang, "Analysis of China's carbon emission driving factors based on the perspective of eight major economic regions," *Environmental Science and Pollution Research*, vol. 28, no. 7, pp. 8181–8204, 2021.

[5] W. Yu, Z. Zhang, and Q. Zhong, "Consensus reaching for MAGDM with multi-granular hesitant fuzzy linguistic term sets: a minimum adjustment-based approach," *Annals of Operations Research*, vol. 300, no. 2, pp. 443–466, 2021.

[6] M. Hussein, R. R. Stewart, D. Sacrey, J. Wu, and R. Athale, "Unsupervised machine learning using 3D seismic data applied to reservoir evaluation and rock type identification," *Interpretation*, vol. 9, no. 2, pp. T549–T568, 2021.

[7] F. Torti, A. Corbellini, and A. C. Atkinson, "fsdaSAS: a package for robust regression for very large datasets including the batch forward search," *Stats*, vol. 4, no. 2, pp. 327–347, 2021.

[8] A. Sayghe, Y. Hu, I. Zografopoulos et al., "Survey of machine learning methods for detecting false data injection attacks in power systems," *IET Smart Grid*, vol. 3, no. 5, pp. 581–595, 2020.

[9] R. Metulini and M. Carpita, "A spatio-temporal indicator for city users based on mobile phone signals and administrative data," *Social Indicators Research*, vol. 156, no. 2, pp. 761–781, 2021.

[10] A. Ben Abdelkrim, T. Tribout, O. Martin, D. Boichard, V. Ducrocq, and N. C. Friggens, "Exploring simultaneous perturbation profiles in milk yield and body weight reveals a diversity of animal responses and new opportunities to identify resilience proxies," *Journal of Dairy Science*, vol. 104, no. 1, pp. 459–470, 2021.

[11] X. Qinlin, T. Chao, W. Yanjun, X. Li, and L. Xiao, "Measurement and comparison of Urban Haze governance level and efficiency based on the DPSIR model: a case study of 31 cities in North China," *Journal of Resources and Ecology*, vol. 11, no. 6, pp. 549–561, 2020.

[12] D. S. Davis, R. J. DiNapoli, M. C. Sanger, and C. P. Lipo, "The integration of lidar and legacy datasets provides improved explanations for the spatial patterning of shell rings in the American Southeast," *Advances in Archaeological Practice*, vol. 8, no. 4, pp. 361–375, 2020.

[13] L. K. Chen, A. C. Hwang, W. J. Lee et al., "Efficacy of multidomain interventions to improve physical frailty, depression and cognition: data from cluster-randomized controlled trials," *Journal of cachexia, sarcopenia and muscle*, vol. 11, no. 3, pp. 650–662, 2020.

[14] J. Cawley, D. Frisvold, and D. Jones, "The impact of sugar-sweetened beverage taxes on purchases: evidence from four city-level taxes in the United States," *Health Economics*, vol. 29, no. 10, pp. 1289–1306, 2020.

[15] G. He, S. Wang, and B. Zhang, "Watering down environmental regulation in China," *Quarterly Journal of Economics*, vol. 135, no. 4, pp. 2135–2185, 2020.

[16] A. Adhvaryu, N. Kala, and A. Nyshadham, "The light and the heat: productivity co-benefits of energy-saving technology," *The Review of Economics and Statistics*, vol. 102, no. 4, pp. 779–792, 2020.

[17] G. F. Fan, Y. H. Guo, J. M. Zheng, and W. C. Hong, "A generalized regression model based on hybrid empirical mode decomposition and support vector regression with back-propagation neural network for mid-short-term load forecasting," *Journal of Forecasting*, vol. 39, no. 5, pp. 737–756, 2020.

[18] P. C. Medina, "Side effects of nudging: evidence from a randomized intervention in the credit card market," *Review of Financial Studies*, vol. 34, no. 5, pp. 2580–2607, 2021.

[19] S. D. Bennett, J. H. Cross, A. E. Coughtrey et al., "MICE—mental Health Intervention for Children with Epilepsy: a randomised controlled, multi-centre clinical trial evaluating the clinical and cost-effectiveness of MATCH-ADTC in addition to usual care compared to usual care alone for children and young people with common mental health disorders and epilepsy—study protocol," *Trials*, vol. 22, no. 1, pp. 1–16, 2021.

[20] F. Wang, D. Wang, G. Guo, M. Zhang, J. Lang, and J. Wei, "Potential distributions of the invasive barnacle scale ceroplastes cirripediformis (Hemiptera: coccidae) under climate change and implications for its management," *Journal of Economic Entomology*, vol. 114, no. 1, pp. 82–89, 2021.

Hindawi
Mathematical Problems in Engineering
Volume 2021, Article ID 9628251, 12 pages
https://doi.org/10.1155/2021/9628251

Research Article

Cross-Efficiency Evaluation under Probabilistic Hesitant Fuzzy Environment and Its Application to the Portfolio Selection Process

Yutong Zhang,[1] **Wei Zhou**,[1] **Danxue Luo**,[1] **and Xiaorong He**[2]

[1]*Business School, Yunnan University of Finance and Economics, Kunming 650221, China*
[2]*School of Information Engineering, Nanjing Audit University, Nanjing, Jiangsu 211815, China*

Correspondence should be addressed to Danxue Luo; 1034159312@qq.com

Received 16 September 2021; Accepted 5 November 2021; Published 26 November 2021

Academic Editor: Ali Ahmadian

In the case of insufficient quantitative data, qualitative evaluation information is very important for investment decision-making. However, if it is completely based on qualitative evaluation information, the results may be subjective. In response to this problem, this paper proposes a method, namely, probabilistic hesitant fuzzy cross-efficiency evaluation (PHFCEE) method, based on probabilistic hesitant fuzzy theory, cross-efficiency data envelopment analysis (CEDEA). This method uses probabilistic hesitant fuzzy sets to collect qualitative evaluation information and then uses the cross-efficiency DEA model to fuse quantitative data and qualitative information. And finally, an investment portfolio is built based on the cross-efficiency value and its variance. In addition, this article gives the specific operating steps of the PHFCEE method and uses the construction of a portfolio of 10 stocks in the China CSI 300 Index as an example to illustrate the effectiveness of this method.

1. Introduction

The investment portfolio can effectively diversify risks [1]. At present, a large number of suitable tools and sophisticated models have been used for portfolio construction and selection research [2]. However, most of the methods that have been constructed require sufficient quantitative data [3, 4]. In fact, in the research process, there are situations where important indicators are difficult to quantify, there is no data, or there is little data [5, 6]. For example, the level of the team is difficult to measure with quantitative data, and the company that has just gone public has no financial data, etc. In addition, quantitative data are almost all historical data, which has certain limitations and one-sidedness in reflecting expected information and uncertain information. Based on the consideration of the above issues, we constructed the PHFCEE model and apply it to portfolio selection. We use expert evaluation to measure some qualitative indicators and then use CEDEA to fuse quantitative data and expert evaluation information and finally build an investment portfolio based on cross-efficiency values and constraints. This article will use probability fuzzy theory to describe the expert's evaluation information. It is an interesting method to combine qualitative evaluation with quantitative data to construct a portfolio. Because experts have knowledge, experience, wisdom, and thinking and judgment capabilities that far exceed those of ordinary investors, they can grasp the essence and key points from complex information and give a more objective evaluation. The quantitative data can effectively reflect historical information and further ensure the objectivity of the model results.

At present, according to the type and quantity of data required by the model, the research of portfolio model can be roughly divided into the following three categories: First, a portfolio model that requires a large amount of time-series data to calculate statistical indices. Representative methods are Markowitz's portfolio model and its extended models, such as Huang [7], Zhao and Xiao [8], and Kuzmanovic et al. [9]. Second, the investment portfolio model proposed is based on the nonstatistical model, which requires relatively little data. Nonstatistical methods used in portfolio models include neural networks [10], CEDEA [11], genetic algorithms [12], and fuzzy theory [13, 14]. Third, some qualitative portfolio models were developed based on fuzzy environments, such as Wang and Zhu [15], Chiarawongse et al. [16], and Zhou and Xu [3, 4].

However, fuzzy data is usually used to describe uncertain information provided by experts, investors, or decision-makers [17, 18], which is subjective. Therefore, we believe that integrating some quantitative data into the model can build a more effective investment portfolio. Fuzzy theory is widely used in various fields because it can describe uncertain information. In the field of investment, interval fuzzy sets [19–21], hesitant fuzzy sets [22, 23], intuitionistic fuzzy sets [24, 25], and probabilistic hesitant fuzzy sets [18, 26] are often used to describe all kinds of evaluation information. These documents provide a theoretical basis for this article to describe qualitative information using fuzzy theory. Taking into account the inconsistent preferences of the expert group when making complex multiattribute decision-making, this paper chooses to use probabilistic hesitant fuzzy sets to describe the evaluation information of the expert group.

In addition, there are differences between the evaluation information of experts and the measurement methods of quantitative data. Therefore, it is necessary to find a model to fuse the two kinds of information. Sexton et al. [27] proposed a CEDEA model that can consider both self-evaluation and mutual evaluation, which provides an effective method for this paper to evaluate efficiency using data covering both quantitative and qualitative information. The CEDEA model has the characteristics of dimensionless, and it is also a method of measuring the overall organizational efficiency on multiple metrics and synthesizing a single index. These characteristics provide a theoretical basis for the fusion of data in this paper. In addition, the CEDEA model has been applied to portfolio evaluation or selection [11, 28, 29]. These articles provide a valuable reference for us to use the calculation results of cross-efficiency DEA to construct investment portfolios.

Based on the above background and literature review, this paper will combine probabilistic hesitant fuzzy theory, CEDEA model, and mean-variance to construct a new portfolio method. Its main function is to construct a portfolio based on quantitative data and qualitative evaluation information. As an illustration of the methodology presented in this article, we report a case study involving 10 companies in the China CSI 300 Index. In addition, the possible advantages of this article are as follow: First, the model uses both quantitative data and qualitative evaluation to describe important information about investment products or projects, which will show product features more comprehensively. This will help decision-makers or investors to make more accurate judgments. Second, the model uses the cross-efficiency DEA model to fuse two forms of data. Third, the model can be used for portfolio construction with only one data form or mixed data information form.

The rest of this article is structured as follows: Section 2 introduces the basic knowledge of hesitant fuzzy, probabilistic hesitant fuzzy, and CEDEA model. In Section 3, we build a method, named PHFCEE model, and introduce the steps to use it for portfolio selection. Section 4 provides a practical case to demonstrate the effectiveness and operability of this model. Section 5 introduces the conclusions, shortcomings, and prospects of this article.

2. Preliminary Concepts

As an effective multicriteria decision-making method, the cross-efficiency DEA is often used in portfolio selection and construction. But when using this method, it is mostly based on objective statistical data, and the statistical data has certain one-sidedness and limitations. In order to overcome this shortcoming, this paper introduces the probabilistic hesitant fuzzy data with subjective information into the CEDEA model to form a new method of portfolio construction based on comprehensive information. This part will briefly introduce the basic theories and concepts involved in the new method, that is, hesitant fuzzy, probabilistic hesitant fuzzy, and the CEDEA model.

2.1. Hesitant Fuzzy Set (HFS) and Probabilistic Hesitant Fuzzy Set (PHFS). To solve the problem of inconsistent preferences of experts in complex multiattribute decision-making, Torra [30, 31] proposed the hesitant fuzzy set, whose core idea is that all the preferences of experts are taken as membership values. This concept is expressed as follows:

Definition 1 (see [30, 31]). Given any nonempty set S, the hesitant fuzzy set $H(s)$defined in the collection S can be expressed as

$$H(s) = \{ < s, h(s) > | s \in S\}, \tag{1}$$

where $h(s) = (\gamma^{\tau} | \tau = 1, 2, \cdots, \ell)$, s is an element in the set S,$h(s)$ is the hesitant fuzzy element, $\gamma \in [0, 1]$ is the degree of membership, and arranged in ascending order, and τ represents the sort position of γ. $H(s)$ is the set of $h(s)$, and $h(s)$ is the set of γ.

Example 1. If an expert's rating on the return on assets of an enterprise is 0.5 or 0.6, the corresponding hesitant fuzzy element can be expressed as $h(s) = \{0.5, 0.6\}$.

According to Definition 1 and Example 1, all membership degrees in HFS have the same importance or the same probability. However, when evaluating assets, it is usually carried out by multiple experts, and experts have a certain tendency to score. *Example 2.* If the expert's score for a certain company's return on assets is more inclined to 0.6, this means that the degree of membership of 0.6 is more important or the probability of occurrence is greater. *Example 3.* Suppose that the set of scores given by Expert 1 and Expert 2 on the return on assets of a certain enterprise are $\{0.5, 0.6\}$ and $\{0.6, 0.7\}$, respectively. Then, the hesitant fuzzy element composed of the comprehensive information of Expert 1 and Expert 2 is denoted as $h(s) = \{0.5, 0.6, 0.7\}$. Among them, 0.6 appears in both score sets, indicating that it has a more important degree.

From the above analysis, it can be seen that the degree of membership in the HFS, that is, the expert score, fails to reflect the tendency of the expert score and the number of experts. This will result in the loss of a large amount of decision-making information. Therefore, this paper further uses PHFS to synthesize the evaluation information of the expert group. This concept can be expressed as follows.

Definition 2 (see [32]). Given any nonempty set S, the probabilistic hesitant fuzzy set $\dot{H}(s)$ defined on set S can be expressed as

$$\dot{H}(s) = \{ < s, h(p(s)) > | s \in S\}, \tag{2}$$

where $h(p(s)) = (\gamma^{\tau}|p^{\tau}|\tau = 1, 2, \cdots \ell)$, s is an element in the set S , $h(p(s))$ is the hesitant probabilistic fuzzy element, $\gamma \in [0, 1]$ is the degree of membership arranged in ascending order, and τ represents the sort position ofγ. When $p^{\tau} = c$,$c = 1/\ell(\tau = 1, 2, \cdots \ell)$, the probabilistic hesitant fuzzy set $\dot{H}(s)$ degenerates into the hesitant fuzzy set $H(s)$.

Example 4. Based on Example 3, the probabilistic hesitant fuzzy element can be expressed as $h(p(s)) = \{0.5|0.25, 0.6|0.5, 0.7|0.25\}$, where the membership degrees are 0.5, 0.6, and 0.7, respectively. The probability of 0.5 is 0.25, the probability of 0.6 is 0.5, and the probability of 0.7 is 0.25. It is found that the probability of 0.6 is higher than other membership degrees.

2.2. Cross-Efficiency DEA Model (CEDEA). CEDEA can not only effectively measure efficiency, but also provides a method to systematically choose a weight when there are multiple metrics. All these provide the basis for this article to build a portfolio based on objective data and subjective judgments. The calculation steps of the CEDEA model are briefly described as follows [27].

Suppose that there are as many as l DMUs whose efficiency needs to be measured, denoted as DMU_r, $(r = 1, 2, \cdots, l)$; each DMU evaluated has$m$ kinds of inputs and n kinds of outputs, denoted as$x_i\,(i = 1, 2, \cdots, m)$ and $y_j\,(j = 1, 2, \cdots, n)$, respectively; the weights of inputs and outputs are $\alpha_i\,(i = 1, 2, \cdots, m)$ and $\beta_j\ (j = 1, 2, \cdots, n)$, respectively.

First, solve the efficiency value e_{tt} of DMU_t based on the linear programming form of the CCR model [33]:

$$\begin{aligned} & e_{tt} = \mathrm{Max} \sum_{j=1}^{n} \beta_j y_{jt}, \\ & \text{s.t.} \begin{cases} \sum_{j=1}^{n} \beta_j y_{jt} - \sum_{j=1}^{n} \alpha_i x_{ir} \le 0, \\ \sum_{i=1}^{m} \alpha_i x_{it} = 1, \\ \alpha_i \ge 0,\ \beta_j \ge 0, \\ i = 1, 2, \cdots, m,\ j = 1, 2, \cdots, n,\ t, r = 1, 2, \cdots, l, \end{cases} \end{aligned} \tag{3}$$

where e_{tt} is the efficiency value of DMU_t and x_{it}, x_{ir} are the m kinds of inputs of $\mathrm{DMU}_t$and DMU_r, respectively, and y_{jt}, y_{jr} are the n outputs of DMU_t and DMU_r, respectively, α_i and β_j are the weights of input and output, respectively, $t, r = 1, 2, \cdots, l$, $i = 1, 2, \cdots, m$ and $j = 1, 2, \cdots, n$.

Second, the optimal weights α_{it}^* and β_{jt}^* of DMU_t calculated in model (3) are substituted into the following equation to calculate the mutual evaluation efficiency value e_{tr} between DMU_t and DMU_r:

$$e_{tr} = \frac{\sum_{j=1}^{n} \beta_{jt}^* y_{jr}}{\sum_{i=1}^{m} \alpha_{it}^* x_{ir}}, \quad t, r = 1, 2, \ldots, l; t \neq r. \tag{4}$$

Third, to calculate the cross-efficiency value $\overline{e}_r$ of DMU_r, the formula is as follows:

$$\overline{e}_r = \frac{1}{l} \sum_{t=1}^{l} e_{tr} = \frac{1}{l} \sum_{t=1}^{l} \frac{\sum_{j=1}^{n} \beta_{jt}^* y_{jr}}{\sum_{i=1}^{m} \alpha_{it}^* x_{ir}}. \tag{5}$$

In addition, calculate the degree of deviation of cross efficiency of DMU_r, that is, the variance. The formula is as follows:

$$\sigma_r^2 = \frac{1}{l} \sum_{t=1}^{l} (e_{tr} - \overline{e}_r)^2. \tag{6}$$

This section briefly introduces the definitions of hesitant fuzzy set and probabilistic hesitant fuzzy set and the application steps of the CEDEA model. This provides a theoretical basis for constructing the PHFCEE method.

3. PHFCEE Model Construction and Portfolio Selection

At present, portfolio selection and efficiency evaluation are mostly based on objective statistical data, ignoring the one-sidedness and limitations of statistical data. However, the probabilistic hesitant fuzzy theory can effectively deal with the fuzzy subjective evaluation information of experts. Therefore, this paper introduces it into the CEDEA model and puts forward the PHFCEE model. The essence of the model is to take the multiangle and multifactor fuzzy evaluation data of the expert group as the output or input in the CEDEA model at the same time. Then, the portfolio is constructed based on the efficiency value and its variance, which is estimated by the PHFCEE model.

In the whole method, first of all, each expert evaluates the attributes of the asset to form a hesitant fuzzy set, and then based on all the hesitant fuzzy sets obtained by the expert group, a comprehensive hesitant fuzzy set is formed. Finally, the probabilistic hesitant fuzzy set is formed by calculating the probability. Definitions 4–6 are proposed to show more clearly how the model integrates information and obtains the probability of membership. The relevant definitions are as follows.

Definition 4. Given that S is a nonempty set. The comprehensive hesitant fuzzy set $\widetilde{H}$ defined on set S can be expressed as

$$\widetilde{H} = \{ < s, h'(s) > | s \in S\}, \tag{7}$$

where $h'(s)(h'(s) = \{{}^1h(s) \cup {}^2h(s) \cup \cdots \cup {}^kh(s)\}$ is the comprehensive hesitant fuzzy element and ${}^kh(s)$ represents a hesitant fuzzy element.

Definition 5. Given any comprehensive hesitant fuzzy element $h'(s) = (\gamma^{\tau}|\tau = 1, 2, \cdots \ell)$, let $h' = h'(s)$, where membership degrees can be defined as follows:

$$\begin{aligned} &\gamma^{\tau'} \in \left\{\gamma_1^{\tau_1} \cup \gamma_2^{\tau_2} \cup \cdots \cup \gamma_k^{\tau_k}\right\},\\ &\sum_{a=1}^{k} \tau_a \geq \ell' \geq \ell(\tau_a = 1, 2, \cdots \ell; a = 1, 2, \cdots k). \end{aligned} \tag{8}$$

where $\gamma^{\tau'}$ is membership degrees of the comprehensive hesitant fuzzy element, $\gamma_k^{\tau_k}$ corresponds to the hesitant fuzzy element of the kth expert, τ_a, τ' is the ranking of the membership degree, which is sorted by default from small to large, and ℓ , ℓ' are the number of membership degree and comprehensive membership degree, respectively.

Definition 6. Given an arbitrary probabilistic hesitant fuzzy element $h(p(s)) = (\gamma^{\tau}|p^{\tau}|\tau = 1, 2, \cdots \ell)$, let $\widetilde{h'} = h(p(s))$ such that the probability corresponding to its membership degree can be defined as

$$p^{\tau'} = \frac{N\left(\gamma^{\tau'}\right)}{\sum_{a=1}^{k} \tau_a}, \tag{9}$$

where $N(\gamma^{\tau'})$ represents the frequency of the same membership value s in the k hesitant fuzzy elements of the attribute and $\sum_{a=1}^{k} \tau_a$ represents the sum of the number of all the subhesitant fuzzy elements.

Because the CEDEA model cannot effectively deal with the fuzzy data of probabilistic hesitant degree, this paper obtains its expected value based on probability to represent the expert group's score of asset attributes. Above, the S nonempty collection defined represents the property collection of the asset.

Definition 7. Given an arbitrary probabilistic hesitant fuzzy element $h(p(s)) = (\gamma^{\tau'}|p^{\tau'}|t\tau'n = q1, 2h, \ldots x\ell')$, the score function is defined as

$$E\left(\widetilde{h'}\right) = \sum_{\tau=1}^{\ell} \gamma^{\tau'} p^{\tau'}. \tag{10}$$

Definition 8. Given any nonempty set Y, defining the corresponding set Y of scores on the sets$(s \in S)$, it can be expressed as

$$Y = \left\{ < s, E\left(\widetilde{h'}\right) > | s \in S \right\}. \tag{11}$$

Then, the score set of all assets can be represented by a matrix, and at the same time, $y' = E(\widetilde{h'})$:

$$\begin{bmatrix} s_{11} & s_{12} & \cdots & s_{1b} \\ s_{21} & s_{22} & \cdots & s_{2b} \\ \vdots & \vdots & \cdots & \vdots \\ s_{l1} & s_{l2} & \cdots & s_{lb} \end{bmatrix} \begin{bmatrix} y_{11}' & y_{12}' & \cdots & y_{1n''}' \\ y_{21}' & y_{22}' & \cdots & y_{2n''}' \\ \vdots & \vdots & \cdots & \vdots \\ y_{l1}' & y_{l2}' & \cdots & y_{ln''}' \end{bmatrix}, \tag{12}$$

where it corresponds s_{lb} to y_{lb} one by one. s_{lb} represents the l attribute of the b asset; then y_{lb}' corresponds to the comprehensive score given by the expert group.

Secondly, based on the above definition and formula, the PHFCEE method containing probabilistic fuzzy information data is constructed, and its linear programming form is as follows:

$$\begin{aligned} &e_{tt}^* = Max \sum_{j=1}^{n'} \beta_j y_{jt} + \sum_{b=1}^{n''} \beta_b y_{bt}',\\ &s.t. \begin{cases} \sum_{j=1}^{n'} \beta_j y_{jt} + \sum_{b=1}^{n''} \beta_b y_{bt}' - \sum_{i=1}^{m} \alpha_i x_{ir} \leq 0, \\ \sum_{i=1}^{m} \alpha_i x_{it} = 1, \\ \alpha_i \geq 0,\ \beta_j \geq 0, \beta_b \geq 0 \end{cases} \quad i = 1, 2, \cdots, m; j = 1, 2, \cdots n'; b = 1, 2, \cdots, n''; t, r = 1, 2, \cdots, l; t \neq r, \end{aligned} \tag{13}$$

where e_{tt}^* is the optimal efficiency value of the t asset (DMU$_t$), x_{it} and x_{ir} have m kinds of inputs of assets, y_{jt} and y_{jr} have n' kinds of the objective statistical data output of assets, y_{bt}, y_{br} are n'' kinds of the subjective fuzzy data output of assets, α_i is input weights, and β_j and β_b are output weights.

Through model (13), the optimal efficiency value e_{tt}^* and the corresponding optimal weights α_{it}^*, β_{jt}^*, β_{bt}^* DMU$_t$ are obtained, and the mutual evaluation efficiency $\dot{e}_{tr}$ of DMU$_r$, as shown in Table 1, is further calculated.

$$\dot{e}_{tr} = \frac{\sum_{j=1}^{n'} \beta_{jt}^* y_{jr} + \sum_{b=1}^{n''} \beta_{bt}^* y_{br}'}{\sum_{i=1}^{m} \alpha_{it}^* x_{ir}}, \quad t, r = 1, 2, \cdots, l; t \neq r. \tag{14}$$

The cross-efficiency $\widetilde{\widetilde{e}}_r$ of DMU$_r$ and its variance $\widetilde{\sigma}_r^2$ are calculated as follows:

$$\tilde{\bar{e}}_r = \frac{1}{l}\sum_{t=1}^{l} e_{tr} = \frac{1}{l}\sum_{t=1}^{l}\frac{\sum_{j=1}^{n'}\beta_{jt}^{*}y_{jr} + \sum_{b=1}^{n''}\beta_{bt}^{*}y_{br}'}{\sum_{i=1}^{m}\alpha_{it}^{*}x_{ir}},$$
$$\tilde{\sigma}_r^2 = \frac{1}{l}\sum_{t=1}^{l}\left(\dot{e}_{tr} - \tilde{\bar{e}}_r\right)^2. \tag{15}$$

Finally, the cross-efficiency value $\tilde{\bar{e}}_r$ and its variance $\tilde{\sigma}_r^2$ are defined as the return and risk of financial assets, respectively [11]. Based on the mean-variance framework, a portfolio selection method including probability model information and cross efficiency can be established. We provide the portfolio selection method of maximizing return and the portfolio selection method of minimizing risk, as follows.

The revenue maximization under constraint conditions:

$$\begin{aligned} e^{\#} &= \max\sum_{r=1}^{l} w_r\tilde{\bar{e}}_r \\ s.t &\left\{ \sum_{r=1}^{l} w_r\tilde{\bar{e}}_r \geq \frac{1}{l}\sum_{r=1}^{l}\tilde{\bar{e}}_r, \sum_{r=1}^{l} w_r^2\tilde{\sigma}_r^2 \leq \frac{1}{l^2}\sum_{r=1}^{l}\tilde{\sigma}_r^2, \sum_{r=1}^{l} w_r = 1, w_r \geq 0, r = 1, 2, \cdots, l. \right. \end{aligned} \tag{16}$$

Risk minimization under constraints:

$$\begin{aligned} e^{\diamond} &= \min\sum_{r=1}^{l} w_r^2\tilde{\sigma}_r^2 \\ s.t &\left\{ \sum_{r=1}^{l} w_r\tilde{\bar{e}}_r \geq \frac{1}{l}\sum_{r=1}^{l}\tilde{\bar{e}}_r, \sum_{r=1}^{l} w_r^2\tilde{\sigma}_r^2 \leq \frac{1}{l^2}\sum_{r=1}^{l}\tilde{\sigma}_r^2, \sum_{r=1}^{l} w_r = 1, w_r \geq 0, r = 1, 2, \cdots, l, \right. \end{aligned} \tag{17}$$

where w_r is the weight of the DMU_r, that is, the investment proportion of the corresponding financial assets; l is the number of assets; the purpose function is to maximize the return $e^{\#}$and minimize the market risk $e^{\diamond}$; the constraint conditions mean that the expected return of the portfolio should not be lower than the average return, and the risk should not be higher than the average risk, so the sum of the investment proportion of the assets is 1.

To better illustrate the operability and practicability of the above method, this paper gives specific steps. Suppose there are as many as l decision-making units (DMU_r, $r = 1, 2, \cdots, l$), among which there are m inputs (x_i, $i = 1, 2, \cdots, m$), and there are n' objective outputs (y_j, $j = 1, 2, \cdots, n'$) and n'' subjective fuzzy inputs (y_b', $b = 1, 2, \cdots, n''$). At the same time, fuzzy input corresponds to the comprehensive evaluation of attributes of the n''decision-making units by the expert group (G), in which the attributes are (s_b, $b = 1, 2, \cdots, n''$), k members of the expert group ($G_a, a = 1, 2, \cdots, k$), the comprehensive score is ($E_b(\#h')$, $b = 1, 2, \cdots n''$), the hesitant fuzzy set is H_k, the comprehensive hesitant fuzzy set is $\tilde{H}$, and the probabilistic hesitant module set $\dot{H}$.

(i) The first step is to obtain the hesitant fuzzy set of all attributes of the decision-making unit from the members of the expert group.

$$H_a = \begin{array}{c} \\ DM\,U_1 \\ DM\,U_2 \\ \vdots \\ DM\,U_l \end{array}\begin{array}{c} \begin{array}{cccc} s_1 & s_2 & \cdots & s_{n''} \end{array} \\ \begin{bmatrix} {}^a h(s_{11}) & {}^a h(s_{12}) & \cdots & {}^a h(s_{1n''}) \\ {}^a h(s_{21}) & {}^a h(s_{22}) & \cdots & {}^a h(s_{2n''}) \\ \vdots & \vdots & \cdots & \vdots \\ {}^a h(s_{l1}) & {}^a h(s_{l2}) & \cdots & {}^a h(s_{ln'}) \end{bmatrix} \end{array}, \tag{18}$$

where${}^a h(s_{rb}) = (\gamma_{ln''}^{\tau_a} | \tau_a = 1, 2, \cdots u; a = 1, 2, \cdots k; r = 1, 2, \cdots, l; b = 1, 2, \cdots, n'')$.

(ii) the second step, according to Definition 4 and Definition 5, the hesitant fuzzy set $H_a(a = 1, 2, \cdots k)$ of the expert members is combined to form a comprehensive hesitant fuzzy set $\tilde{H}$ for all attributes of all decision-making units. And then,

$$h'(s)=\left\{{}^{1}h(s)\cup{}^{2}h(s)\cup\cdots\cup{}^{k}h(s)\right\},$$

$$\widetilde{H}=\begin{bmatrix}\{{}^{1}h(s_{11})\cup\cdots\cup{}^{k}h(s_{11})\} & \cdots & \{{}^{1}h(s_{1n''})\cup\cdots\cup{}^{k}h(s_{1n''})\}\\ \{{}^{1}h(s_{21})\cup\cdots\cup{}^{k}h(s_{21})\} & \cdots & \{{}^{1}h(s_{2n''})\cup\cdots\cup{}^{k}h(s_{2n''})\}\\ \vdots & \vdots & \vdots\\ \{{}^{1}h(s_{l1})\cup\cdots\cup{}^{k}h(s_{l1})\} & \cdots & \{{}^{1}h(s_{ln''})\cup\cdots\cup{}^{k}h(s_{ln''})\}\end{bmatrix}\Rightarrow\widetilde{H}=\begin{bmatrix}h'(s_{11}) & h'(s_{12}) & \cdots & h'(s_{1n''})\\ h'(s_{21}) & h'(s_{22}) & \cdots & h'(s_{2n''})\\ \vdots & \vdots & \vdots & \vdots\\ h'(s_{l1}) & h'(s_{l2}) & \cdots & h'(s_{ln'})\end{bmatrix}, \tag{19}$$

where$h'(s_{rb}) = (\gamma^{\tau}|\tau=1,2,\cdots,\ell; r = 1,2,\cdots,l; b=1,2,\cdots,n'')$.

(iii) The third step is to calculate the probability of the membership degree in the comprehensive hesitant fuzzy element according to Definition 6, that is, equation (10), to form a probabilistic hesitant fuzzy set $\dot{H}$ as follows:

$$\dot{H}=\begin{bmatrix}h(p(s_{11})) & h(p(s_{12})) & \cdots & h(p(s_{1n''}))\\ h(p(s_{21})) & h(p(s_{22})) & \cdots & h(p(s_{2n''}))\\ \vdots & \vdots & \vdots & \vdots\\ h(p(s_{l1})) & h(p(s_{l2})) & \cdots & h(p(s_{ln''}))\end{bmatrix}=\begin{bmatrix}\{\gamma_{11}^{1}|p_{11}^{1},\cdots,\gamma_{11}^{\ell}|p_{11}^{\ell}\} & \cdots & \{\gamma_{1n''}^{1}|p_{1n''}^{1},\cdots,\gamma_{1n''}^{\ell}|p_{1n''}^{1}\}\\ \{\gamma_{21}^{1}|p_{21}^{1},\cdots,\gamma_{21}^{\ell}|p_{21}^{\ell}\} & \cdots & \{\gamma_{2n''}^{1}|p_{2n''}^{1},\cdots,\gamma_{2n''}^{\ell}|p_{2n''}^{1}\}\\ \vdots & \vdots & \vdots\\ \{\gamma_{l1}^{1}|p_{l1}^{1},\cdots,\gamma_{l1}^{\ell}|p_{l1}^{\ell}\} & \cdots & \{\gamma_{ln''}^{1}|p_{ln''}^{1},\cdots,\gamma_{ln''}^{\ell}|p_{ln''}^{1}\}\end{bmatrix}. \tag{20}$$

(iv) In the fourth step, according to Definition 7 and Definition 8, the probabilistic hesitant fuzzy set$\dot{H}$is calculated, and the comprehensive evaluation information of the expert group is obtained, which is shown as follows:

$$E(\dot{H})=\begin{bmatrix}E(\#h'_{11}) & E(\#h'_{12}) & \cdots & E(\#h'_{1n''})\\ E(\#h'_{21}) & E(\#h'_{22}) & \cdots & E(\#h'_{2n''})\\ \vdots & \vdots & \vdots & \vdots\\ E(\#h'_{l1}) & E(\#h'_{l2}) & \cdots & E(\#h'_{ln''})\end{bmatrix}\Rightarrow Y=\begin{bmatrix}y'_{11} & y'_{12} & \cdots & y'_{1n''}\\ y'_{21} & y'_{22} & \cdots & y'_{2n''}\\ \vdots & \vdots & \vdots & \vdots\\ y'_{l1} & y'_{l2} & \cdots & y'_{ln''}\end{bmatrix}, \tag{21}$$

where $y'_{rb}=E(\#h'_{rb})$, $(r=1,2,\cdots,l; b=1,2,\cdots,n'')$.

(v) In the fifth step, x_i, y_j, $y'_b(i=1,2,\cdots,m; r=1,2,\cdots,l; b=1,2,\cdots,n'')$ is substituted into model (12) to estimate the optimal efficiency value $\mathrm{DMU}_t\,(t=1,2,\cdots,l)$ of the evaluated asset e_{tt}^{*} and its corresponding optimal weight α_{it}^{*}, β_{jt}^{*}, β_{bt}^{*}.

(vi) In the sixth step, the optimal weight of $\mathrm{DMU}_t\,(t=1,2,\cdots,l)$ is substituted into equation (13) to calculate the mutual evaluation efficiency of $\dot{e}_{tr}(r\neq t)$, as shown in Table 1.

(vii) In the seventh step, the crossover efficiency values $\widetilde{\overline{e}}_r$ and variance $\widetilde{\sigma}_r^2$ are calculated according to equations (14) and (15), as shown in Table 2.

(viii) In the eighth step, the cross-efficiency value $\widetilde{\overline{e}}_r$ and variance $\widetilde{\sigma}_r^2$ estimated by the cross-efficiency DEA are defined as the return and risk of the investment, respectively, and then the investment weight is calculated based on the investor's investment purpose model (16) or (17). Model (16) maximizes the profit and model (7) minimizes the risk.

4. Illustrated Example

Investors often build their portfolios based on quantitative data and information and lack of adoption and analysis of qualitative information. The main reason is that qualitative information is difficult to quantify. To solve this problem, the method of expert evaluation is introduced to evaluate the attribute information that cannot be quantified, and the fuzzy methods of hesitant and probabilistic hesitant are used to collect and quantify the evaluation information with preference. To fuse and analyze the quantitative data and qualitative information, this paper further introduces the CEDEA model, which has the advantage of dimensionless. Based on this, this paper proposes the PHFCEE model to measure the cross-efficiency (benefit) and variance (risk) containing quantitative and qualitative information. Finally,

Table 1: Mutual evaluation efficiency matrix among decision-making units.

Assets	DMU_1	DMU_2	$\cdots$	DMU_l
DMU_1	$\dot{e}_{11}$	$\dot{e}_{12}$	$\cdots$	$\dot{e}_{1l}$
DMU_2	$\dot{e}_{21}$	$\dot{e}_{22}$	$\cdots$	$\dot{e}_{2l}$
$\vdots$	$\vdots$	$\vdots$	$\cdots$	$\vdots$
DMU_l	$\dot{e}_{l1}$	$\dot{e}_{l2}$	$\cdots$	$\dot{e}_{ll}$

Note. The diagonal is the self-evaluation efficiency of the asset; the nondiagonal element is the mutual evaluation efficiency between the assets.

Table 2: Cross efficiency and variance.

Assets	DMU_1	DMU_2	$\cdots$	DMU_l
$\overline{e}_r$	$\tilde{\overline{e}}_1$	$\tilde{\overline{e}}_2$	$\cdots$	$\tilde{\overline{e}}_l$
$\tilde{\sigma}_r^2$	$\tilde{\sigma}_1^2$	$\tilde{\sigma}_2^2$	$\cdots$	$\tilde{\sigma}_l^2$

the calculation results of the PHFCEE model are substituted into the portfolio model constructed in the third part to calculate the final portfolio components and weights.

To demonstrate the effectiveness of the method proposed in this paper, we select 10 stocks in the CSI 300 index for a case study. The corresponding enterprises (code/variable life) are Industrial and Commercial Bank of China (601398/DMU1), China Pacific Insurance (601601/DMU2), Shanghai Pharmaceutical (601607/DMU3), China Zhongzhi (601618/DMU4), China Life Insurance (601628/DMU5), China Construction (601668/DMU6), Shanghai Electric (601727/DMU7), Everbright Securities (601788/DMU8), China Exemption (601888/DMU9), and Zijin Mining (601899/DMU10). In addition, because the general CEDEA model cannot deal with data with negative values, this paper excludes enterprises with missing values and negative values when screening sample data. Finally, the ten enterprises shown above are formed as samples. According to the annual report of the enterprise in 2020, the relevant financial data are obtained to calculate the input and output indicators required by the PHFCEE model. Indicators that will reflect the operational ability, solvency, and growth ability of the enterprise [11, 34, 35] are considered as input to the PHFCEE model. The profitability of the enterprise and the market reaction of the stock is taken as the output of the objective data of the model. In addition, this paper also takes the output of the subjective data of the model through the evaluation of experts from the aspects of enterprise prospect, enterprise innovation, team level, and so on. Specific information on the relevant indicators is shown in Table 3.

In Table 3, except for the expert evaluation section, the corresponding financial data in other sectors can be calculated from the annual report data published by enterprises between March and April each year. This paper takes the annual report data of 10 enterprises in 2020 as an example. The expert evaluation section consists of a team of three experts to evaluate the selected enterprises from three aspects: enterprise prospect, enterprise innovation, and team level, in which the evaluation result of each expert is expressed in the form of the hesitant fuzzy set. The evaluation result of the expert group is expressed by the comprehensive hesitant fuzzy set, and the evaluation result of the expert group considering the importance of membership is expressed by the probabilistic hesitant fuzzy set. According to the specific steps of the method given in the third part of the article, the analysis of this case is as follows.

The first step is to obtain the evaluation results of 10 enterprises by three experts from three aspects: enterprise prospect, enterprise innovation, and team level, using hesitant fuzzy set H_1, H_2, and H_3 Express. The correspondence is shown in Tables 4–6, respectively. The second step, based on Definitions 4 and 5, merges the hesitant fuzzy elements for the same attribute in the hesitation fuzzy set and of the three experts and finally combines the comprehensive hesitation fuzzy set, which contains the evaluation results of all attributes of 10 enterprises, as shown in Table 7.

The third step is to calculate the probability of each membership degree in the comprehensive hesitant fuzzy set according to equation (10), to form a probabilistic hesitant fuzzy set $\dot{H}$ that contains more expert group evaluation information, as shown in Table 8.

The fourth step is based on Definitions 7 and 8 and probabilistic hesitant fuzzy set $\dot{H}$. The comprehensive scores for each attribute of 10 enterprises are calculated, respectively, and the results are shown in Table 9.

In the fifth step, the input and output data of 10 enterprises are substituted into model (12) to estimate the optimal self-evaluation efficiency value e_{tt}^* and the optimal weight α_{it}^*, β_{jt}^*, β_{bt}^*, and substitute it into model (13) to calculate the mutual evaluation efficiency between enterprises $\dot{e}_{tr} (r \neq t)$. The estimated results run through MATLAB are shown in Table 10. In this table, the value on the diagonal is the self-evaluation efficiency of the enterprise, and the nondiagonal data of each row is the mutual evaluation efficiency of other enterprises to the corresponding enterprises of the bank.

The sixth step is to calculate the cross-efficiency value $\tilde{\overline{e}}_r$ and variance $\tilde{\sigma}_r^2$ between enterprises according to equation (15) and equation (16) and sort them from large to small, as shown in Table 11.

According to Table 11, the three enterprises with the largest cross-efficiency values are DMU1, DMU5, and DMU2, and their corresponding variances are 0.2031 (10), 0.3457 (4), and 0.3428 (5), respectively. Thus, it can be seen that except for the relatively high return and relatively low risk of enterprise DMU1, the income and risk of other enterprises show different characteristics.

In the seventh step, the cross-efficiency value $\tilde{\overline{e}}_r$ and variance $\tilde{\sigma}_r^2$ are regarded as the risk and return of the investment, respectively, and substituted into model (17) or model (18) to calculate the investment weight w. It is assumed that there are no taxes, no transaction costs, no short selling, and full liquidity when constructing the investment portfolio.

Table 3: Details of input and output metrics.

Types	Aspect	Financial indicators or evaluation indicators	Variable abbreviation
Input	Operation ability	Asset turnover rate	x_1
	Debt paying ability	Asset-liability ratio	x_2
	Growth ability	Income growth rate	x_3
Output	Profitability	Net profit margin	y_1
	Stock	Stock price	y_2
	Expert evaluation	Enterprise prospect (s_1)	y_3
		Enterprise innovation (s_2)	y_4
		Team level (s_3)	y_5

Table 4: Results of Expert 1 assessment.

Enterprises	s_1	s_2	s_3
DMU1	(0.5, 0.6)	(0.3, 0.4)	(0.5, 0.6)
DMU2	(0.6, 0.7)	(0.6)	(0.4, 0.5, 0.6)
DMU3	(0.6, 0.7)	(0.4)	(0.5)
DMU4	(0.7, 0.8)	(0.6, 0.7)	(0.5, 0.7)
DMU5	(0.6, 0.7)	(0.5, 0.6)	(0.4, 0.6)
DMU6	(0.6, 0.75)	(0.3)	(0.4, 0.3)
DMU7	(0.4, 0.5)	(0.4, 0.45)	(0.4)
DMU8	(0.55)	(0.3)	(0.4, 0.50)
DMU9	(0.7)	(0.5, 0.6)	(0.5)
DMU10	(0.4, 0.5)	(0.4, 0.5)	(0.5, 0.4)

Table 5: Results of Expert 2 assessment.

Enterprises	s_1	s_2	s_3
DMU1	(0.3, 0.5)	(0.6, 0.9)	(0.4, 0.6, 0.8)
DMU2	(0.4, 0.6, 0.7)	(0.2, 0.6)	(0.3, 0.7)
DMU3	(0.4, 0.5)	(0.5, 0.8)	(0.4, 0.5)
DMU4	(0.7, 0.8)	(0.5, 0.6, 0.7)	(0.2, 0.4)
DMU5	(0.4, 0.7)	(0.5)	(0.5, 0.8)
DMU6	(0.65)	(0.5, 0.6)	(0.6)
DMU7	(0.3, 0.5)	(0.6, 0.7)	(0.45, 0.7)
DMU8	(0.6, 0.75)	(0.3, 0.65)	(0.55)
DMU9	(0.4, 0.6)	(0.7)	(0.65)
DMU10	(0.5)	(0.4)	(0.4, 0.85)

Table 6: Results of Expert 3 assessment.

Enterprises	s_1	s_2	s_3
DMU1	(0.5, 0.6)	(0.3)	(0.4, 0.6, 0.7)
DMU2	(0.3)	(0.6, 0.8)	(0.5)
DMU3	(0.5, 0.7)	(0.4)	(0.6)
DMU4	(0.5, 0.6)	(0.7)	(0.4, 0.6)
DMU5	(0.4, 0.5)	(0.6)	(0.5, 0.55)
DMU6	(0.45, 0.7)	(0.3, 0.5)	(0.4, 0.65)
DMU7	(0.3, 0.4, 0.65)	(0.55, 0.8)	(0.4, 0.7)
DMU8	(0.3)	(0.6)	(0.4)
DMU9	(0.4)	(0.35)	(0.5, 0.75)
DMU10	(0.45)	(0.4)	(0.6)

In this paper, 5, 6, 7, and 8 enterprises with high cross-efficiency are selected to construct the investment portfolio, and the investment weights under different constraints are obtained, as shown in Tables 12 and 13. From the observation, we can see something important. First, with the increase of the number of stocks in the portfolio, the weight of the corresponding stocks of each enterprise is decreasing accordingly. Second, no matter how many stocks are included in the investment portfolio, whether the purpose of the portfolio construction is to maximize the return or

Table 7: Comprehensive evaluation results of the expert group.

Enterprises	s_1	s_2	s_3
DMU1	(0.3, 0.5, 0.6)	(0.3, 0.4, 0.6, 0.9)	(0.4, 0.5, 0.6, 0.7, 0.8)
DMU2	(0.3, 0.4, 0.6, 0.7)	(0.2, 0.6, 0.8)	(0.3, 0.4, 0.5, 0.6, 0.7)
DMU3	(0.4, 0.5, 0.6, 0.7)	(0.4, 0.5, 0.8)	(0.4, 0.5, 0.6)
DMU4	(0.5, 0.6, 0.7, 0.8)	(0.5, 0.6,0.7)	(0.2, 0.4, 0.5, 0.6, 0.7)
DMU5	(0.4, 0.5, 0.6, 0.7)	(0.5, 0.6)	(0.4, 0.5, 0.55, 0.6, 0.8)
DMU6	(0.3, 0.5, 0.6, 0.65, 0.75)	(0.3, 0.5, 0.6)	(0.3, 0.4, 0.6, 0.65)
DMU7	(0.3, 0.4, 0.5, 0.65)	(0.4, 0.45, 0.55, 0.6, 0.8)	(0.4, 0.45, 0.7)
DMU8	(0.3, 0.55, 0.6, 0.75)	(0.3, 0.6, 0.65)	(0.4, 0.50, 0.55)
DMU9	(0.4, 0.6, 0.7)	(0.35, 0.5, 0.6, 0.7)	(0.5, 0.65, 0.75)
DMU10	(0.4, 0.45, 0.5)	(0.4, 0.5)	(0.4, 0.5, 0.6, 0.85)

Table 8: Results of comprehensive evaluation of Expert groups with preferences ($\dot{H}$).

Enterprises	s_1	s_2	s_3
DMU1	(0.3|0.17, 0.5|0.5, 0.6|0.33)	(0.3|0.4, 0.4|0.2, 0.6|0.2, 0.9|0.2)	(0.4|0.25, 0.5|0.375, 0.6|0.125, 0.7|0.125, 0.8|0.125)
DMU2	(0.3|0.17, 0.4|0.17, 0.6|0.33, 0.7|0.33)	(0.2|0.2, 0.6|0.6, 0.8|0.2)	(0.3|0.17, 0.4|0.17, 0.5|0.34, 0.6|0.17, 0.7|0.17)
DMU3	(0.4|0.17, 0.5|0.33, 0.6|0.17, 0.7|0.33)	(0.4|0.5, 0.5|0.25, 0.8|0.25)	(0.4|0.25, 0.5|0.5, 0.6|0.25)
DMU4	(0.5|0.17, 0.6|0.17, 0.7|0.33, 0.8|0.33)	(0.5|0.17, 0.6|0.33,0.7|0.5)	(0.2|0.17, 0.4|0.34, 0.5|0.17, 0.6|0.17, 0.7|0.17)
DMU5	(0.4|0.33, 0.5|0.17, 0.6|0.17, 0.7|0.33)	(0.5|0.5, 0.6|0.5)	(0.4|0.17, 0.5|0.34, 0.55|0.17, 0.6|0.17, 0.8|0.17)
DMU6	(0.3|0.2, 0.5|0.2, 0.6|0.2, 0.65|0.2, 0.75|0.2)	(0.3|0.4, 0.5|0.4, 0.6|0.2)	(0.3|0.2, 0.4|0.4, 0.6|0.2, 0.65|0.2)
DMU7	(0.3|0.29, 0.4|0.29, 0.5|0.29, 0.65|0.14)	(0.4|0.2, 0.45|0.2, 0.55|0.2, 0.6|0.2, 0.8|0.2)	(0.4|0.5, 0.45|0.25, 0.7|0.25)
DMU8	(0.3|0.25, 0.55|0.25, 0.6|0.25, 0.75|0.25)	(0.3|0.5, 0.6|0.25, 0.65|0.25)	(0.4|0.5, 0.50|0.25, 0.55|0.25)
DMU9	(0.4|0.5, 0.6|0.25, 0.7|0.25)	(0.35|0.25, 0.5|0.25, 0.6|0.25, 0.7|0.25)	(0.5|0.5, 0.65|0.25, 0.75|0.25)
DMU10	(0.4|0.25, 0.45|0.25, 0.5|0.5)	(0.4|0.75, 0.5|0.25)	(0.4|0.4, 0.5|0.2, 0.6|0.2, 0.85|0.2)

Table 9: The comprehensive score of each attribute of 10 enterprises.

Enterprises	s_1	s_2	s_3
DMU1	0.50	0.5	0.55
DMU2	0.47	0.56	0.51
DMU3	0.53	0.525	0.5
DMU4	0.61	0.633	0.476
DMU5	0.51	0.55	0.5695
DMU6	0.56	0.32	0.47
DMU7	0.44	0.56	0.4875
DMU8	0.55	0.4625	0.4625
DMU9	0.53	0.5375	0.6
DMU10	0.46	0.425	0.55

minimize the risk, the investment weight of the enterprise DMU1 is the largest. Third, under the condition of income maximization, the investment right of DMU1 is more important than the investment weight of risk minimization.

Combined with the analysis of Tables 11 and 12, when investors aim to maximize returns, each portfolio will increase the investment weight of stocks with higher returns on the premise of not exceeding the average risk. Similarly, combined with the analysis of Tables 11 and 13, when investors aim to minimize risk, each investment portfolio will increase the investment weight of less risky stocks on the premise that the return is not lower than the average return. The above results are consistent with the facts, which shows the rationality of the portfolio construction model.

In addition, the return and risk of the portfolio are calculated according to the required weight and compared with the return and risk of the equal weight investment; the results are shown in Table 14. The analysis shows that the investment weight calculated based on model (16) and model (17) is lower than the equal weight investment in terms of return and risk. The investment return of income maximization is higher than that of risk minimization, and the risk of risk minimization is lower than that of return maximization. The comparison results in Table 14 are in line with expectations, which once again illustrates the rationality and effectiveness of the portfolio construction in this paper.

Compared with the quantitative portfolio selection methods such as modern portfolio theory [36–38], the

Table 10: Table of efficiency values among 10 enterprises.

	DMU1	DMU2	DMU3	DMU4	DMU5	DMU6	DMU7	DMU8	DMU9	DMU10
DMU1	1.0000	0.9638	0.6461	0.6414	0.9851	1.0000	0.6650	0.7968	0.4023	0.7068
DMU2	0.0273	1.0000	0.2707	0.6739	0.9719	0.8599	0.4330	0.4024	0.1481	0.6817
DMU3	0.0026	0.7010	1.0000	0.7823	0.7675	1.0000	0.1046	0.1231	0.0667	0.3541
DMU4	0.0033	0.9315	0.1510	1.0000	0.9513	1.0000	0.1949	0.2170	0.0642	0.4431
DMU5	0.0349	0.9592	0.2608	0.7115	1.0000	0.9156	0.4894	0.4971	0.1499	0.7432
DMU6	0.0068	0.4896	0.1281	0.5017	0.5548	0.9710	0.1065	0.2148	0.1264	0.4592
DMU7	0.0071	0.5451	0.0326	0.5156	0.7367	0.5156	1.0000	0.7148	0.1163	0.5809
DMU8	0.0401	0.4958	0.0442	0.5193	0.6546	0.6872	0.7149	1.0000	0.4085	0.5764
DMU9	0.0221	0.3701	0.0227	0.3975	0.6199	0.4619	0.3385	0.3840	1.0000	0.5624
DMU10	0.0340	0.6866	0.0748	0.7118	0.9283	0.8379	0.3749	0.4561	0.2667	1.0000

Table 11: Cross efficiency (benefit), variance (risk), and ranking.

Enterprises	$\tilde{\tilde{e}}_r$	Sort	$\tilde{\sigma}_r^2$	Sort
DMU1	0.7807	1	0.2031	10
DMU2	0.5469	3	0.3428	5
DMU3	0.4902	7	0.4008	2
DMU4	0.4956	6	0.4249	1
DMU5	0.5762	2	0.3457	4
DMU6	0.3559	10	0.2937	8
DMU7	0.4765	8	0.3273	6
DMU8	0.5141	5	0.2957	7
DMU9	0.4179	9	0.2839	9
DMU10	0.5371	4	0.3470	3

Table 12: Investment weight of income maximization.

Enterprises	w	Enterprises	w	Enterprises	w	Enterprises	w
DMU1	0.3671	DMU1	0.3427	DMU1	0.3099	DMU1	0.2723
DMU2	0.1541	DMU2	0.1364	DMU2	0.1238	DMU2	0.1119
DMU5	0.1607	DMU5	0.1435	DMU5	0.1301	DMU5	0.1171
DMU10	0.1497	DMU10	0.1320	DMU10	0.1198	DMU10	0.1085
DMU8	0.1684	DMU8	0.1472	DMU8	0.1337	DMU8	0.1217
—	—	DMU4	0.0982	DMU4	0.0892	DMU4	0.0815
—	—	—	—	DMU3	0.0934	DMU3	0.0854
—	—	—	—	—	—	DMU7	0.1016

Table 13: Risk-minimized portfolio weight.

Enterprises	w	Enterprises	w	Enterprises	w	Enterprises	w
DMU1	0.2897	DMU1	0.2545	DMU1	0.2254	DMU1	0.1977
DMU2	0.1716	DMU2	0.1508	DMU2	0.1335	DMU2	0.1172
DMU5	0.1702	DMU5	0.1495	DMU5	0.1324	DMU5	0.1162
DMU10	0.1696	DMU10	0.1489	DMU10	0.1319	DMU10	0.1157
DMU8	0.1990	DMU8	0.1748	DMU8	0.1548	DMU8	0.1358
—	—	DMU4	0.1216	DMU4	0.1077	DMU4	0.0945
—	—	—	—	DMU3	0.1142	DMU3	0.1002
—	—	—	—	—	—	DMU7	0.1227

PHFCEE model proposed in this paper uses more comprehensive information, and then the derived results meet the real needs of investors and companies because this model not only uses quantitative data reflecting historical information but also uses hesitant fuzzy sets to describe some qualitative factors that cannot be measured with quantitative data. Compared with the qualitative portfolio model proposed by Zhou and Xu [3, 4] and others, the given model also uses some quantitative financial data to ensure the objectivity of the given results. The incomplete rationality of experts could lead to subjectivity in the evaluation information provided by experts and decision-makers, which can

Table 14: Comparison of income and risk.

Amount	The average return on investment	Weighted return under income maximization	Weighted return under risk minimization	The average investment in risk	Weighted risk under profit maximization	Weighted risk under risk minimization
5	0.59100	0.63046	0.61143	0.06058	0.06016	0.05827
6	0.57511	0.62008	0.59735	0.05387	0.05356	0.05124
7	0.56298	0.60773	0.58511	0.04776	0.04748	0.04543
8	0.55216	0.59277	0.57178	0.04168	0.04145	0.03989

further affect the optimal results. Then, we add objective quantitative data into the model. Concerning these comparisons, the investment portfolio derived by this model could be more realistic and reasonable than that got by the other two types of models.

5. Conclusions

A portfolio approach that utilizes qualitative information is an effective venture capital technique when quantitative data are scarce or unavailable. However, the approach of building a portfolio using only qualitative information is somewhat subjective. To solve this problem, this paper proposes the PHFCEE model. The acquisition of qualitative information and the effective fusion of two data forms are the key technologies for portfolio construction. Then, we introduce probabilistic hesitant fuzzy set and the CEDEA model. Next, based on the cross-efficiency value and its variance, the investment portfolio ratios considering the investors' risk preferences are constructed. Lastly, a real example has been provided to demonstrate the feasibility of the proposed models.

The mixed-data portfolio model based on the probabilistic hesitant fuzzy environment in this paper has some disadvantages, such as simple modeling rules, simple probabilistic calculation, and excessively ideal constraints. Therefore, in future work, the research will further consider the mixed-data portfolio model under the environment with incomplete or no-probability information and intend to develop a new probability solution algorithm. It will be worthwhile and interesting work.

Data Availability

The data used to support the findings of this study are available from the corresponding author upon request.

Conflicts of Interest

The authors declare that they have no conflicts of interest regarding the publication of this paper.

Acknowledgments

This work was supported by the Natural Science Foundation of China (nos. 72071176 and 71840001), the Humanities and Social Sciences in Universities of Jiangsu Province, China (no. 2019SJA0337), and the Natural Science Research Project of Universities in Jiangsu Province, China (no. 19KJB120008).

References

[1] X. Zhou, J. Wang, and X. Yang, "Portfolio selection under different attitudes in fuzzy environment," *Information Sciences*, vol. 462, pp. 278–289, 2018.
[2] S. Guo, L. Yu, and X. Li, "Fuzzy multi-period portfolio selection with different investment horizons," *European Journal of Operational Research*, vol. 254, no. 3, pp. 1026–1035, 2016.
[3] W. Zhou and Z. S. Xu, "Portfolio selection and risk investment under the hesitant fuzzy environment," *Knowledge-Based Systems*, vol. 144, pp. 21–31, 2018.
[4] W. Zhou and Z. S. Xu, "Hesitant fuzzy linguistic portfolio model with variable risk appetite and its application in the investment ratio calculation," *Applied Soft Computing*, vol. 84, Article ID 105719, 2019.
[5] L. Dimova, P. Sevastianov, and D. Sevastianov, "MCDM in a fuzzy setting: investment projects assessment application," *International Journal of Production Economics*, vol. 100, no. 1, pp. 10–29, 2006.
[6] P. Hildebrandt and T. Knoke, "Investment decisions under uncertainty-a methodological review on forest science studies," *Forest Policy and Economics*, vol. 13, no. 1, pp. 1–15, 2011.
[7] X. X. Huang, "A new perspective for optimal portfolio selection with random fuzzy returns," *Information Science*, vol. 177, pp. 5404–5414, 2007.
[8] P. Zhao and Q. Xiao, "Portfolio selection problem with value-at-risk constraints under non-extensive statistical mechanics," *Journal of Computational and Applied Mathematics*, vol. 298, pp. 64–71, 2016.
[9] M. Kuzmanovic, D. Makajic-Nikolic, and N. Nikolic, "Preference based portfolio for private investors: discrete choice analysis approach," *Mathematics*, vol. 8, no. 1, p. 30, 2020.
[10] A. Fernandez and S. Gomez, "Portfolio selection using neural networks," *Computers and Operations Research*, vol. 34, no. 1, pp. 1177–1191, 2005.
[11] S. Lim, K. W. Oh, and J. Zhu, "Use of DEA cross-efficiency evaluation in portfolio selection: an application to Korean stock market," *European Journal of Operational Research*, vol. 236, no. 1, pp. 361–368, 2014.
[12] P. Sinha, A. Chandwani, and T. Sinha, "Algorithm of construction of optimum portfolio of stocks using genetic algorithm," *International Journal of Systems Assurance Engineering and Management*, vol. 6, pp. 35–44, 2015.
[13] Y. J. Liu and W. G. Zhang, "Fuzzy portfolio selection model with real features and different decision behaviors," *Fuzzy Optimization and Decision Making*, vol. 17, pp. 317–336, 2018.
[14] B. Wang, Y. Li, S. M. Wang, and J. Watada, "A multi-objective portfolio selection model with fuzzy value-at-risk ratio," *IEEE Transactions on Fuzzy Systems*, vol. 26, pp. 3673–3687, 2018.

[15] S. Wang and S. Zhu, "On fuzzy portfolio selection problems," *Fuzzy Optimization and Decision Making*, vol. 1, pp. 361–377, 2002.

[16] A. Chiarawongse, S. Kiatsupaibul, S. Tirapat, and B. V. Roy, "Portfolio selection with qualitative input," *Journal of Banking & Finance*, vol. 36, no. 2, pp. 489–496, 2012.

[17] M. W. Lin, Y. Q. Chen, and R. Q. Chen, "Bibliometric analysis on Pythagorean fuzzy sets during 2013–2020," *International Journal of Intelligent Computing and Cybernetics*, vol. 14, no. 2, pp. 104–121, 2021.

[18] M. Liu, C. H. Zhang, and C. H. Yu, "Knowledge diffusion trajectories in the Pythagorean fuzzy field based on main path analysis," *International Journal of Intelligent Computing and Cybernetics*, 2021.

[19] L. T. Zhou, Y. F. Wang, and Y. Jiang, "Investment project assessment by a MAGDM method based on the ranking of interval type-2 fuzzy sets," *Journal of Intelligent and Fuzzy Systems*, vol. 35, no. 2, pp. 1875–1888, 2018.

[20] A. Serguieva and J. Hunter, "Fuzzy interval methods in investment risk appraisal," *Fuzzy Sets and Systems*, vol. 142, no. 3, pp. 443–466, 2004.

[21] X. Q. Xu, J. L. Xie, and Y. Na, "Probabilistic uncertain linguistic TODIM method based on the generalized Choquet integral and its application," *International Journal of Intelligent Computing and Cybernetics*, vol. 14, no. 2, pp. 122–144, 2021.

[22] S. Yang and Y. Ju, "A GRA method for investment alternative selection under Dual hesitant fuzzy environment with incomplete weight information," *Journal of Intelligent and Fuzzy Systems*, vol. 28, no. 4, pp. 1533–1543, 2015.

[23] P. Zhou, J. Luo, and F. Cheng, "Analysis of risk priorities for renewable energy investment projects using a hybrid IT2 hesitant fuzzy decision-making approach with alpha cuts," *Energy*, vol. 4, Article ID 120184, 2021.

[24] L. Wang and J. Pu, "Research on the investment performance evaluation of corporate venture capital with intuitionistic fuzzy information," *Journal of Intelligent & Fuzzy Systems: Applications in Engineering and Technology*, vol. 30, no. 3, pp. 1783–1790, 2016.

[25] M. Zhao, G. Wei, and C. Wei, "Improved TODIM method for intuitionistic fuzzy MAGDM based on cumulative prospect theory and its application on stock investment selection," *International Journal of Machine Learning and Cybernetics*, vol. 12, pp. 891–901, 2020.

[26] W. Y. Wu, Z. W. Ni, and F. F. Jin, "Investment selection based on Bonferroni mean under generalized probabilistic hesitant fuzzy environments," *Mathematics*, vol. 9, p. 107, 2021.

[27] T. R. Sexton, R. H. Silkman, and A. J. Hogan, "Data envelopment analysis: critique and extensions," *New Directions for Evaluation*, vol. 32, pp. 73–105, 1986.

[28] H. Essid, J. Ganouati, and S. Vigeant, "A mean-maverick game cross-efficiency approach to portfolio selection: an application to Paris stock exchange," *Expert Systems with Applications*, vol. 113, pp. 161–185, 2018.

[29] Z. Mashayekhi and H. Omrani, "An integrated multi-objective Markowitz-DEA cross-efficiency model with fuzzy returns for portfolio selection problem," *Applied Soft Computing*, vol. 38, pp. 1–9, 2016.

[30] V. Torra, "Hesitant fuzzy sets," *International Journal of Intelligent Systems*, vol. 25, no. 6, pp. 529–539, 2010.

[31] V. Torra and Y. Narukawa, "On hesitant fuzzy sets and decision," in *Proceedings of the 18th IEEE International Conference on Fuzzy Systems*, pp. 1378–1382, IEEE, Jeju Island, Korea, August 2009.

[32] Z. S. Xu and W. Zhou, "Consensus building with a group of decision makers under the hesitant probabilistic fuzzy environment," *Fuzzy Optimization and Decision Making*, vol. 16, no. 4, pp. 481–503, 2017.

[33] A. Charnes, W. W. Cooper, and E. Rhodes, "Measuring the efficiency of decision making units," *European Journal of Operational Research*, vol. 2, no. 6, pp. 429–444, 1978.

[34] N. C. P. Edirisinghe and X. Zhang, "Generalized DEA model of fundamental analysis and its application to portfolio optimization," *Journal of Banking & Finance*, vol. 31, no. 11, pp. 3311–3335, 2007.

[35] N. C. P. Edirisinghe and X. Zhang, "Portfolio selection under DEA-based relative financial strength indicators: case of US industries," *Journal of the Operational Research Society*, vol. 59, no. 6, pp. 842–856, 2008.

[36] J. B. Clempner and A. S. Poznyak, "Sparse mean-variance customer Markowitz portfolio optimization for Markov chains: a Tikhonov's regularization penalty approach," *Optimization and Engineering*, vol. 19, no. 2, pp. 383–417, 2018.

[37] L. G. Hong, S. Juneja, and G. W. Liu, "Kernel smoothing for nested estimation with application to portfolio risk measurement," *Operations Research*, vol. 65, no. 3, pp. 657–673, 2017.

[38] H. M. Markowitz, "Portfolio selection, journal of finance," vol. 7, pp. 77–91, 1952.

Hindawi
Mathematical Problems in Engineering
Volume 2021, Article ID 8789355, 11 pages
https://doi.org/10.1155/2021/8789355

Research Article

An Empirical Study on Interactive Flipped Classroom Model Based on Digital Micro-Video Course by Big Data Analysis and Models

Na Tian[1] **and Sang-Bing Tsai**[2]

[1]*Gingko College of Hospitality Management, Chengdu 610000, China*
[2]*Regional Green Economy Development Research Center, School of Business, Wuyi University, Nanping, China*

Correspondence should be addressed to Na Tian; tinna8296134@163.com

Received 8 October 2021; Revised 26 October 2021; Accepted 10 November 2021; Published 25 November 2021

Academic Editor: Mingwei Lin

This paper provides an in-depth analysis and study of the interactive flipped classroom model for a digital micro-video for a big data English course. To improve the learning efficiency of English courses and reduce the learning pressure of students, the thesis also uses certain techniques to apply audiovisual language to the production of specific micro-class videos, broadcast the successfully recorded micro-class courses to students, and then use the questionnaire to randomly distribute the designed audiovisual language use questionnaire. Micro-classes earnestly perform data statistics for students and finally conduct data analysis to summarize and verify the effects of micro-class audiovisual language use. The improved algorithm can effectively reduce the fluctuation of the consumption of various resources in the cluster and make the services in the cluster more stable. The new distributed interprocess communication based on protocol and serialization technology is more efficient than traditional communication based on protocol standards, reduces bandwidth consumption in the cluster, and improves the throughput of each node in the cluster. The content design and scripting of micro-video teaching resources are based on this. Then, the production process of micro-video teaching resources is explained, according to the selection of tools, the preparation, recording, editing, and generation of materials.

1. Introduction

With the large-scale promotion and use of information technology and network technology, video data have taken up 70% of the Internet traffic. In the field of life, short video and real-time live streaming are becoming increasingly popular; in the field of surveillance, network surveillance cameras are spread all over the city; in the field of office, cloud video conferencing is also gradually approaching people's work. In the future, there will be increased video data, and these video data have high timeliness. Unlike text information, video data have multidimensional, large volume, high hidden characteristics; compared with text data, video data are more complex and require higher computational requirements [1]. It is inefficient to analyze the cameras in urban corners by hand alone, so how to mine the information in these unstructured data through computer technology in time to further improve the work productivity has also become a major challenge for enterprises and related research institutions [2]. However, these frameworks have been developed over the years, and to make the frameworks have better generality, the community developers have not made optimization for specific scenarios (e.g., video processing), and users need to optimize the configuration according to their business scenarios and modify the source code if necessary [3]. At the same time, according to the theory and practice of micro-video teaching, there is a natural combination of micro-video teaching and scaffolded teaching, and the combination of the two will significantly improve the teaching efficiency of English listening classroom. In terms of specific practices, first, complex learning tasks can be decomposed through scaffolded teaching to gradually guide learners to deeper understanding. Then micro-videos are used in each level of the decomposed tasks, allowing students to improve their listening skills by watching them and creating a contextualized listening learning atmosphere.

On the one hand, because the micro-course is composed of streaming video, the aesthetic standard of video audiovisual language is applicable; on the other hand, the use of film and television works with a large number of rich audiovisual language to shoot the storyline of the micro-course; the audiovisual language in line with the human visual and auditory sense helps students learn micro-course knowledge. It is an important research topic to apply the audiovisual language filming method in micro-course production to improve students' learning effect and highlight the focus of teaching content knowledge [4]. With the rise of the concept of flipped classroom teaching and the rapid development of large-scale open online courses, micro-courses are also becoming another breakthrough in the exploration of educational reform. The advent of the "micro" era has affected people in every aspect. With the rapid development of network communication technology, micro-courses are also developing rapidly, and with their short characteristics, they effectively solve the micro-needs of learners. Through theoretical research and comparative analysis of the audiovisual language elements in the excellent micro-course videos and comparison with the rich audiovisual language in film and television works, the study of the unique audiovisual language in micro-courses and the search for the use of audiovisual language in micro-course production can provide some reference to reduce the fatigue of learners in long micro-courses.

The importance of learning English grammar is self-evident. However, from my own teaching experience and the current situation of local students learning English, the teaching and learning of English grammar are not particularly satisfactory [5]. First, due to the heavy workload and the reform of English examination papers, some teachers and students have the concept of "light on grammar, grammatical plates and light on special sentences," which is manifested by the fact that everyone pays more attention to big grammar, such as the three main clauses, verbs, and nonverbal verbs, and marginalizes special sentences. The first relevance of this study is to emphasize the importance of special sentences in grammar learning; even though micro-videos and flipped classrooms have emerged in recent years, their effectiveness is still unknown, and people are afraid to implement them. Therefore, the second relevance of this study is to provide a reference for teachers who want to make a change in teaching special sentences as grammar, especially for those who have accumulated many high-quality grammar micro-videos in provincial micro-video competitions, and want to implement them specifically in their teaching. Under the concept of the flipped classroom, students learn by watching the micro-video first, then answer questions, and consolidate their knowledge through discussion or asking the teacher for advice; students' initiative can be strengthened, and students' deep understanding of grammar knowledge can be achieved; and students' main position can be highlighted, and students can use the fragmented time to learn everywhere, which can free up more time in class to strengthen.

2. Current Status of Research

To facilitate this, the videos were posted online for their independent learning, and as the number of hits increased, he began to think about the advantages of this teaching method. Inspired by the videos, many teachers have tried to change the way they taught in the classroom by having students watch the videos at home before class to grasp the main points of the lesson and to assess their proficiency through appropriate exercises; then in class, they focus on problem-solving and collaborative communication between the teacher and the students. Prensky et al. mentioned that with the development of science, technology, and the Internet, this generation of youth is different from their parents' generation [6]. In the face of this explosion of knowledge, although some people complain about their concentration and attention span, others argue that it is not because they are not concentrating but because they have more options, their attention span has changed, and their needs are different [7]. There are so many things that appeal to them in the face of a colorful world. Faced with this world of light and darkness, it is no longer possible for them to be as simple as the past generation, and their independent thinking and individuality gradually emerge [8]. Education, then, must be branded with the digital age to capture and engage students, and Salman Khan and others mention that there is both serendipity and inevitability in being an early researcher in the flipped classroom [9]. The serendipity lies in the fact that he did not realize that he would have such a big impact until then. He simply hoped to use his recorded instructional videos to tutor his relatives on their homework, but he did not expect to receive good results. The necessity lies in the fact that as an education practitioner, he has always believed that what exists may not be justified. The drawbacks of traditional education, which have become apparent, cannot ignore just because people have become accustomed to its existence [10].

The analysis and collation of the scholars' understanding of flipped classrooms show that everyone's understanding of flipped classrooms is similar, based on the development of science and technology, the catalyst of the change of knowledge learning mode, plus the escort of independent learning [11]. Combined with the analysis and collation, the author then synthesizes his own practical experience and believes that the existence of flipped classrooms has its inevitability. For students at a better level like the one the author is dealing with, one will find that the current generation is different from the previous one in many ways [12]. The previous generation may not know what big data, 5G, and the Internet are; they already live in a smart city and feel them everywhere; and they often scoff at some shallow understanding and memorization [13]. Sometimes, within the class, while the teacher drones on about some grammar rules, many students are already off to do their own thing [14]. For them, flipping the classroom is not a bad way to learn. Because it realigns the time inside and outside the classroom, the teacher no longer has the power to make decisions about learning, and instead, it is transferred to the students. With this model of teaching and learning, the valuable time within the classroom, students can focus more on active project-based learning, working together to solve problems and thus gain a deeper understanding [15].

It can effectively reduce the pressure on the server, but it will increase the requirements for the hardware configuration of the user's device, and if the configuration is too low, the user experience will be greatly reduced. At the same time, this approach can only integrate some lightweight algorithms; otherwise, it will increase the requirements for the user's terminal device configuration and even cause hardware loss. After years of development, the stream computing framework has become increasingly complex, although it has become richer and richer in functions, and the technology is maintained by large enterprises, and SMEs or research institutions do not have enough resources to maintain it, and it is difficult to troubleshoot problems [16]. Moreover, the development of current stream computing frameworks is mainly borrowed from the Internet, and there is a lack of product-tested stream computing frameworks for real-time video stream data processing scenarios. All three solutions for video stream processing have their applicable scenarios, and different R&D vendors will adopt different strategies to improve user experience. However, the greatest scope for development is the clustering of video streams, which is a key research direction for companies with video businesses today. The method of clustering processing has no upper limit on the throughput rate and processing delay in theory, and the size of the throughput rate can be controlled by dynamically adjusting the number of service nodes in the cluster, and the cluster can be flexibly adapted to various scenarios through intelligent dynamic configuration.

3. A Study on Interactive Flipped Classroom Model for Big Data English Course with Digital Micro Video

3.1. Big Data Platform Design for Digital Micro-Video. First, we need to design and implement the basic functions of this video big data intelligent analysis platform, mainly including five modules, which are: real-time statistics, real-time monitoring, query retrieval, resource management, and system settings. Some of the function modules contain some subfunctions; query retrieval subfunctions include: historical alarms, capture retrieval, 1:1 comparison, and personnel database comparison; resource management subfunctions include: personnel database management, control management, and bayonet management; and system settings subfunctions include: department management and user management. In addition to the basic functions of the system, based on the capture records in the system, it is also necessary to implement some functions of target person analysis [17]. When the number of cameras deployed in the area reaches a certain level, personnel behavior analysis can be analyzed. The system architecture design is the beginning of developing a software system and is also crucial to the implementation and performance of the system. Properly designed architecture not only allows for smooth and efficient development of subsequent functions but also allows for more stable operation during the operational phase of the system, saves physical resources such as servers, and has higher availability and fault tolerance. In addition, when facing changes in requirements, a good architecture makes it easier for the system to cope with these changes so that it can bring more adaptation with fewer changes. It can be said that architecture design is the top priority in software system development. When implementing this video big data intelligent analysis platform, we need to fully consider the stability and scalability of the system to ensure that the system can run stably for a long time, and it is also best to upgrade the system without interrupting the services provided to the public [18]. When adding cameras to the system, both the processing of video and face data or the relevant capture records and pictures of storage will increase the burden on the system; at this time, the system scalability is also very important. To ensure that when adding real-time video to the system for analysis, the system operation is not interrupted, and the service is not interrupted, so the system needs to have the ability to dynamically expand the capacity.

Micro-video teaching resources should have a scientific process as the mainline of production, according to which the production process is concretized. The production of micro-video teaching resources includes the selection of tools, preparation of materials, and a series of recording, editing, and finally generating the video format required for teaching. Micro-video teaching resources should have a scientific process as the mainline of production, according to which the specific production process is launched. The production of micro-video teaching resources includes the selection of tools, the preparation of materials, and a series of recordings, editing, and the final generation of the video format required for teaching. This is the work of collecting and preparing materials such as pictures, videos, audios, and PPT courseware needed in the stage of making micro-video teaching resources, which is related to the specific recording practice in the next stage, so it is necessary to be well prepared. When collecting materials, we should take the needs of learners as the primary principle, consider the cognitive development of secondary school learners, and try to focus on interesting and popular materials, to be easy to understand and unique [19]. In the cluster, if a new node appears, to prevent the new node from scheduling too many nodes, we will monitor the scheduling success event of the scheduler, obtain the scheduling result, and mark the number of scheduled pods for each node in the past period, such as the number of pods scheduled within 1 min, 5 min, and 30 min, the hotspot value of the node is measured and then compensated to the node's preference score, so this will become increasingly stable. This is the stage of concretizing the practice of micro-video teaching resources. The author uses the pre-selected tools for recording work, and editing can be done within the recording software or using other post-editing tools to insert the required images, audio, animation, and so on. After finishing the editing work, the required format is generated, and if there are special format requirements, format conversion can be done using Format Factory software. After the initial completion, the micro-video teaching resources are shown to some learners; the viewing experience is collected; the resources are adjusted and improved according to other teachers' suggestions; and the content and form of the micro-video teaching resources has to be continuously optimized until the final version is generated, to obtain the desired teaching effect in the practice stage of the resources, as shown in Figure 1.

Since a cluster environment is more complex compared to a standalone environment and the cluster contains various resource conditions that affect each other, a distributed processing system needs to be able to not only complete the tasks submitted by users but also dynamically balance the cluster load and rationally allocate cluster resources so that the efficiency of task processing in the cluster can be improved. We can optimize the cluster load by intelligently scheduling tasks through load balancing algorithms. Allocation and scheduling of tasks in a distributed system require the use of load balancing algorithms. The load balancing algorithm studied in this paper will combine the weighted voting method based on real-time resource monitor and system load prediction by deep learning-based time series prediction algorithm so that the tasks can be allocated reasonably. Since a cluster environment is more complex compared to a standalone environment and the cluster contains various resource conditions that affect each other, a distributed processing system needs to be able to not only complete the tasks submitted by users but also dynamically balance the cluster load and rationally allocate cluster resources so that the efficiency of task processing in the cluster can be improved. We can optimize the cluster load by intelligently scheduling tasks through load balancing algorithms (see Figure 1).

Allocation and scheduling of tasks in a distributed system require the use of load balancing algorithms. The load balancing algorithm studied in this paper will combine the weighted voting method based on real-time resource monitor and system load prediction by deep learning-based time series prediction algorithm so that the tasks can be allocated reasonably.

The weighted voting method is to assign a weight value to each condition in advance. Let there be n conditions related to the resource consumption of the service node and each resource is given a weight value. Then the final service computing node's resource consumption can be calculated by the following equation:

$$P = \sum_{i=0}^{n} P_i \times W_i^2. \tag{1}$$

The advantage of performing load balancing in this way is that the hardware configuration of each node in the cluster can vary, as the final task is assigned based on the percentage of available resources to the total resources. The dynamic load balancing algorithm designed in this paper does not rely completely on load prediction algorithms, as there are no accurate prediction algorithms available. The load balancing algorithm starts by obtaining the current resource utilization status of each service node in the cluster, then predicts the candidate nodes, selects the node that is least likely to generate a resource utilization spike in the future period, and finally assigns the task to that node.

$$P_b = \frac{\left(\sum_{i=1}^{n} T + \sum_{i=1}^{n} R\right)}{(n \times I \times Tb)}, \tag{2}$$

$$R = P_b \times W_b - P_m \times W_m - P_c \times W_c. \tag{3}$$

From the functions of each part of the system, we can see that the system is closely focused on face data, and many functions are closely related to capture records or dynamic face data. For example, the alarm is judged according to the dynamic face capture data, and the functions such as trajectory analysis, analysis of the same pedestrian, analysis of the landing point, and frequent passing are also based on the analysis and calculation of the capture records. Face capture records are very important to the whole system. In addition, as the number of cameras connected to the system increases, the number of face captures will also increase, and the dynamic face data that needs to be processed by the system in real-time will also increase. If the dynamic face data is not processed properly, the light will make the capture retrieval, alarm, and other functions delayed and heavy perhaps with the increasing number of data to be processed, until the whole system dragged down. Therefore, dynamic face data processing can be said to be the top priority in the whole system implementation process, as shown in Figure 2.

After collecting the data through TensorFlow's data-cleaning interface, it is possible to separate the data set into test data (20%) and training data (80%); since the data are temporally attributed in this scenario, there is no mashing of the data, and parameters need to be introduced in this interface to get the same structure for all the same inputs.

$$p_t' = \frac{p_t + \max(p)}{\max(p) + \min(p)}, \tag{4}$$

$$W_t = \left(p_{t-w}^1, p_{t-w}^2, p_{t-w}^3, \ldots, p_{t-w}^w\right), \tag{5}$$

$$p_t^w = f\left(p_{t-w}^1 - p_{t-w}^2 + p_{t-w}^3 - p_{t-w}^w\right). \tag{6}$$

Students' interest in learning is the one with the highest mean among the four dimensions, from which students are more inclined to agree that micro-video scaffolded instruction can increase students' interest in learning (see Figure 2).

In addition, the standard deviation of the effect of micro-video scaffolded instruction on students' interest in learning is 0.71505 lower than the standard deviation of the other

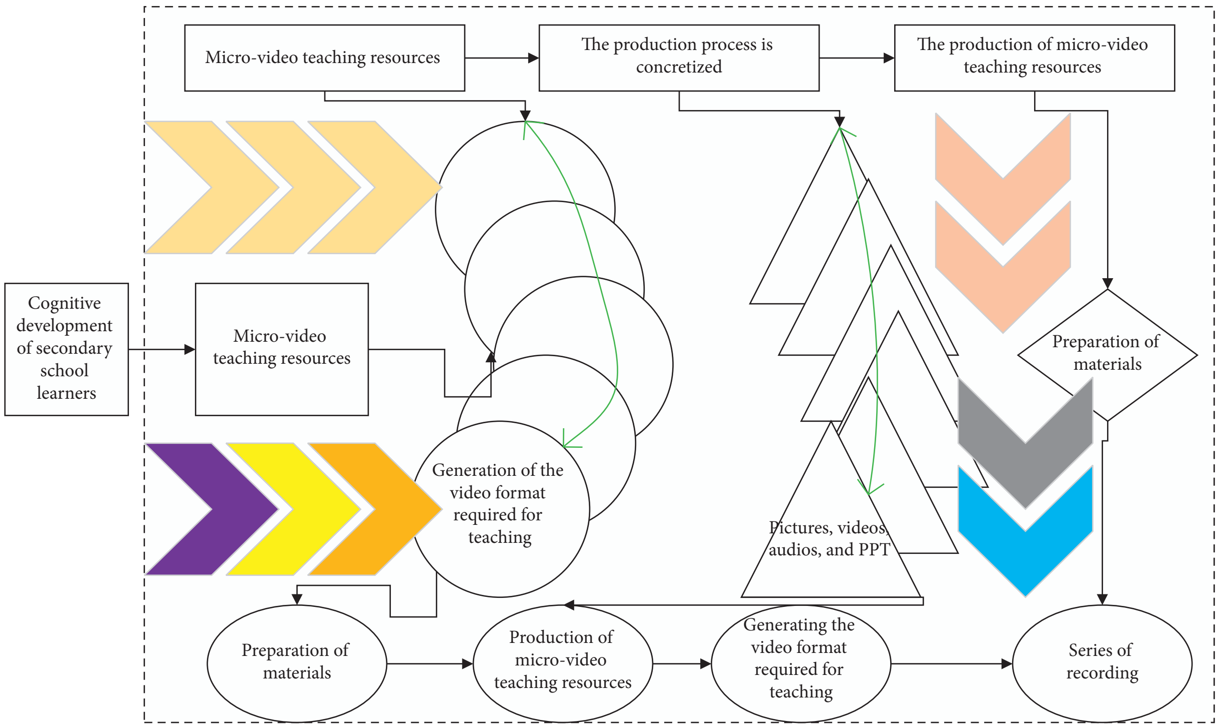

Figure 1: Stream computing architecture.

three dimensions, which leads to the conclusion that students are more inclined to agree that micro-video scaffolded instruction has the effect of increasing interest in learning.

$$3 \leq W \leq W_{\min}. \tag{7}$$

It can be seen that the model-based prediction algorithm has some accuracy in predicting the overall trend of the load situation, but it also has some error, so the final load balancing algorithm does not fully rely on this prediction algorithm, and then when assigning tasks, it will first discard the part of nodes with heavier load calculated by the prediction algorithm, then obtain the load situation of the remaining cluster nodes through the dynamic load balancing algorithm, and finally assign the tasks to the service nodes with the lowest load.

3.2. Design of an Interactive Flipped Classroom Model for English Courses. The mechanism of the more mature Kafka has been thoroughly studied, and our research goal is not the mechanism of Kafka. The connection of the three modules in the flipped classroom model is done through information technology; without the support of information technology, the flipped classroom model cannot be implemented. IT is a powerful lever for instructional designers to create a learning environment for students [20]. IT makes it possible for teachers to track and supervise students' learning online, to guide and help them online, to test and evaluate their learning results online, and to ensure personalized independent learning and collaborative group learning for students. The self-study and questioning stages are entirely at the students' own pace. First, the subject class representative will lead the interpretation of the learning objectives and arrange the learning tasks, and students will follow the learning objectives for self-study of the material. Students can read the textbook first to master the knowledge content and then complete the study plan independently, or they can read the textbook according to the study plan questions and then complete the study plan independently. The difficult problems encountered in the process of reading the textbook on their own can be studied with the help of micro-lessons recorded by the teacher in advance. The micro-lesson can be paused and rewatched repeatedly, and the problems in the lesson plan can be improved and revised after reading and understanding. After the micro-lesson, there are still questions that are not understood, or new questions arise, which need to be discussed and exchanged among group members. Generally, the students who finish the learning task first to communicate can be followed as models, and the communication experience is shared among the group members or the group. Of course, there may be questions that students do not understand or additional questions that arise, and students will need to write these down on a "question feedback slip." In addition, students will need to complete online tests prepared by the teacher in advance to test their learning. Teachers need to collect and summarize students' questions, data from the platform, and feedback from the learning plan. The teacher will design the breakthrough points and personalized tutorials after fully understanding the students' learning situation.

The micro-video-based flipped classroom teaching model should include three components: pre-class, in-class, and post-class. The components of the pre-lesson session include teacher's production of teaching micro-video,

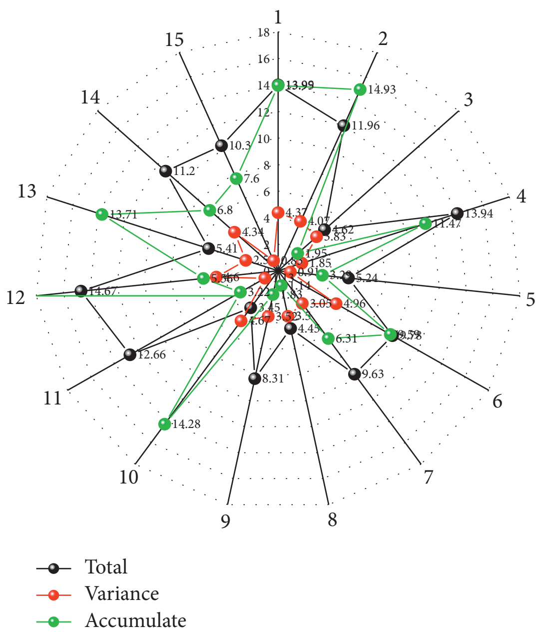

Figure 2: Explanation of the total variance of the factors.

teacher's design of pre-lesson independent learning task list, students' viewing of teaching micro-video, students' completion of the pre-lesson independent learning task list, students' marking of doubts, asking questions, and so on. The components of the midlesson session include warm-up of learning contents, students' independent work, group collaborative learning, display of learning results, teacher's guidance and counseling, teacher's evaluation, and feedback. The components of the post-lesson session include students' production work, students' sharing of work, teachers' evaluation of work, students' mutual evaluation of work, midterm, final exams, and so on. On this basis, the author combines the theory of ubiquitous learning, the theory of associationist learning and proficiency learning, as well as the theory of motivation, and constructs a flipped classroom teaching model based on micro-video, as shown in Figure 3.

The biggest difference between micro-video-based flipped classroom teaching mode and traditional classroom teaching is the part of knowledge transfer. In traditional classroom teaching, knowledge transfer is in the middle of the class, while micro-video-based flipped classroom teaching is done before the class, and the tasks of teachers and students change before the class. In traditional classroom teaching, the teacher's task is to remind students to preview what they are going to learn, with no specific instructions on how to preview and how to preview, and when students preview, they only preview the material, or even some students do not preview at all, causing the pre-class preview session to become a bubble. There are many tasks that teachers and students need to do in the pre-class session of micro-video-based flipped classroom teaching. First, teachers should make the micro-video a week before and distribute the video to students 2–3 days before; students get the micro-video and independent learning task list and then do independent learning before class; teachers should keep online guidance and supervision; students mark the problems they encounter when doing independent learning; and finally, teachers need to collect students' feedback and suggestions (see Figure 4).

Teaching evaluation refers to the process of measuring and value judgment on the process of teaching activities and their results following certain teaching objectives and using scientific and feasible standards and methods. Two points can be seen from the above definition: First, teaching evaluation is carried out following teaching objectives, and clear teaching objectives are the prerequisite for teaching evaluation. Therefore, the classification theory and method of teaching objectives and the development and changes of contemporary educational objectives concept dominate the process and method of teaching evaluation, developing their cognitive ability and the ability to criticize and create beauty mastering the systematic basic knowledge of culture and science, forming basic skills and techniques, developing their cognitive ability students' bodies to get normal development and healthy growth, gradually forming correct aesthetic views and the ability to feel the beauty and appreciate the beauty and create beauty, and gradually developing socialist moral behavior and ideological quality, the basis for the formation of a materialist worldview, and the comprehensive and harmonious development of their personalities [21]. Its factors are very rich, and teaching evaluation should be based on many factors that respond to the teaching objectives, as shown in Figure 4.

What teachers should do in this feedback session is to get questions and feedback to adjust their micro-video based on the effectiveness of the students' viewing of the instructional micro-video. Based on students' suggestions and comments on the instructional micro-video, the style, technique, format, and effectiveness of their instructional micro-video should be adjusted or changed. Students will record what

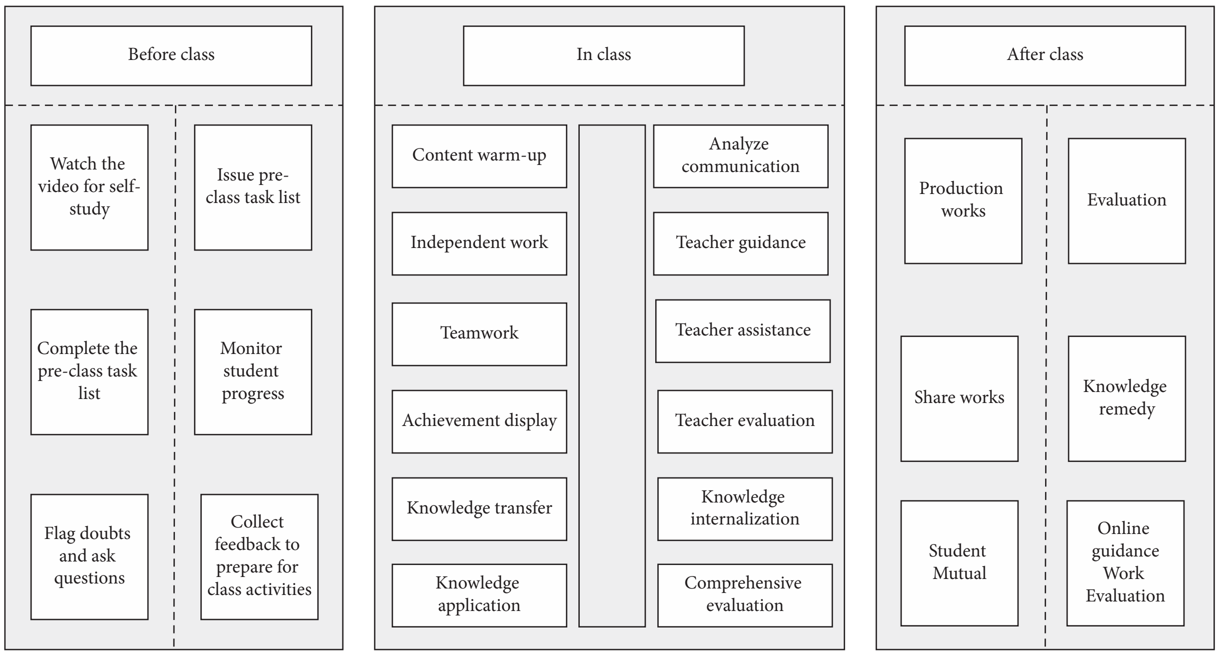

Figure 3: Micro-video-based flipped classroom teaching model.

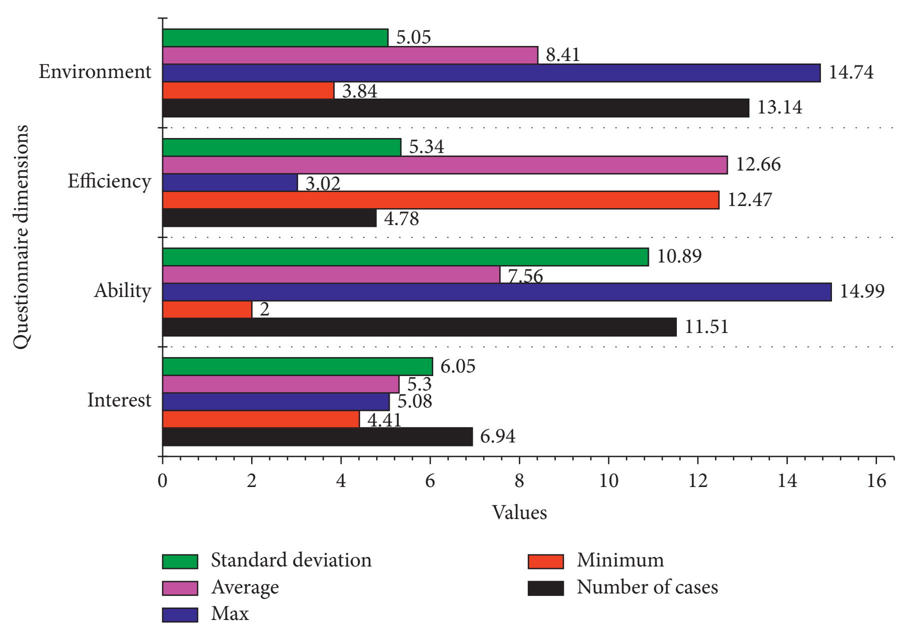

Figure 4: Impact of micro-video scaffolded instruction in the listening classroom.

they understood, what they did not understand, and what they want to study in-depth when they watch the instructional micro-video, and teachers will collect this feedback to prepare their in-class activities. In addition, teachers should create a comprehensive reward mechanism to increase students' enthusiasm and motivation by offering rewards for good performance, such as students who watch instructional micro-videos particularly attentively and who ask good questions or suggestions.

The students in the researcher's school have no problem in mastering basic grammar, such as lexis, tenses, and so on. Among the syntax, they have a good grasp of the frequently used and important definite clauses, but they have some difficulty in learning other macro-sentence types, such as noun clauses, and 90% of them cannot understand special sentences, which shows that the author's previous analysis of the students' learning situation is right.

4. Analysis of Results

4.1. Big Data Platform Performance Results for Digital Micro-Video. As the static load balancing algorithm does not consider the difference in the performance configuration of the service nodes in the cluster, it assigns tasks without any difference, resulting in node 3 reaching a bottleneck due to its performance, and the load situation is close to 100% at first, at which time node 3 can no longer accept tasks, but the computing resources of nodes 1 and 2 are still very sufficient at this time. Next, we use the same simulation to test the dynamic load balancing algorithm based on real-time resource monitoring; the test results are shown in Figure 5; from Figure 5, we can see that the overall resource consumption of the three service nodes is on the rise; although the fluctuation of no. 3 is relatively large (mainly due to the lack of CPU performance), there is no CPU burst when using the static load balancing algorithm. The dynamic load balancing algorithm gives priority to assigning tasks to the remaining nodes when node 3 has the highest resources, and the use of a dynamic load balancing algorithm can generally ensure the stable operation of the cluster (see Figure 5).

After applying the prediction-based load balancing algorithm, compared to the dynamic load balancing algorithm, the resource consumption of each node in the cluster becomes relatively smooth in general without particularly large fluctuations, except that the resource consumption of assigned tasks is relatively obvious due to the relatively poor performance of node 3, the other two nodes are relatively smooth, and when a load of a certain machine is relatively large, the algorithm will assign tasks to other nodes, so the node resource consumption rises for a while and then drops significantly.

Considering the efficiency of distributed interprocess communication in different scenarios, this paper adopts two middleware communication methods, message queue, and serialized network communication and uses different serialization algorithms and compression algorithms for messages with different attributes to further improve the throughput and transmission efficiency. The message queue has already had a more mature Kafka, so this paper does not do a deep study on this. The choice of the communication method between service nodes is crucial in distributed stream computing application scenarios. In this paper, based on the traditional remote procedure call method, we improve it for the latest HTTP 2.0 standard to improve the overall throughput rate and transmission efficiency of distributed applications.

The interface was tested before and after the optimization of the capture count to verify the impact of placing the count results in the Redis cache on the performance of the interface. The response time of the interface at different levels was recorded in the test database, and the system was warmed up by running the test 100 times before the test and then tested 100 times at each level, recording the time taken for each call and taking the average. The test data is shown below: this experiment is to simulate the communication process of two distributed processes in a cluster with two servers, by sending a large amount of image data simultaneously from one server to another server using the traditional network communication method and our designed serialized network communication method, respectively, and compare the difference in communication efficiency between the two; the experimental results are shown in Figure 6.

From the experimental results, we can see that the traditional protocol-based network communication method is less efficient than the protocol-based serialized network communication method in the scenario of transmitting a large amount of binary data, and the larger the data size, the more obvious the advantage of this serialized network communication method. And in the case of more cameras in the system access, the number of capture records generated in the system every day may reach millions. And then with the accumulation of time, the total number of captures in the system may reach tens of millions or even hundreds of millions. At this time, the database to do statistics on such a huge number of records will undoubtedly be slow. Once the interface response speed is full to a certain extent, the overall performance of the system may be affected.

4.2. Results of the Interactive FlippedCmodel for English Courses. For computer application courses, students' proficiency in hands-on operation is poor, and students hope that the time allocated for computer operation is greater than the time taught by teachers in class, so that students can have more opportunities for independent practice, which is consistent with the concept of "students are the main body of learning" in the above micro-video-based flipped classroom teaching model. From Figure 7, only 15.0% of the students like or like very much the current traditional teaching classroom; 85.0% of the students think that the current traditional teaching model is average or dislike or dislike very much; moreover, only 11.0% of the students say that the current traditional teaching mode can stimulate their learning interest; and as many as 89.0% of the students think that the traditional teaching mode cannot stimulate their learning interest well. This shows that students expect a new teaching model based on the traditional teaching mode, and this mode should make students more interested in learning and increase their motivation to learn. Although 88.0% of the students did not understand the concept and implementation process of the flipped classroom, 87.0% of the students were more interested in learning about the flipped classroom; 79.0% of the students were more or very interested in the "flipped classroom" of this course; 97.0% of the students expressed their willingness to experience the flipped classroom teaching mode; and 46.0% of the students were interested in the "flipped classroom" of this course. The students were able to have a correct understanding of the meaning of "flipped classroom."

After independent work and exploration, students have constructed their cognitive structure or knowledge system, but to complete the deep internalization of knowledge, students need to communicate and help each other. Therefore, communication and mutual assistance among group members are needed in a session, and students who have completed three topics can help other members of the group. This kind of peer-to-peer communication and mutual help helps students dissect and explain the knowledge points and helps group members who did not find the correct answers at the beginning sort out their questions to form the correct perception. At the

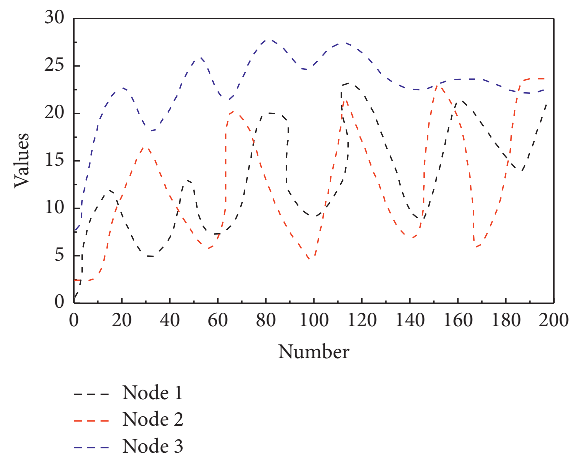

Figure 5: Dynamic load balancing.

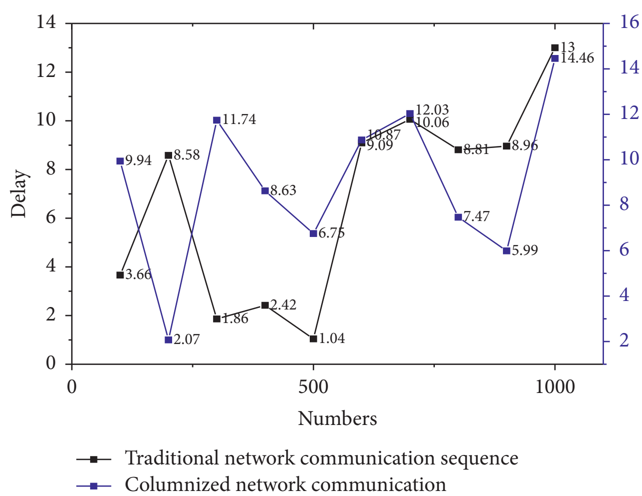

Figure 6: Experimental results of comparison of communication methods.

same time, the author will also join the students' group discussions to give timely guidance and help clarify students' misconceptions.

Students will develop their own or group learning outcomes after independent and collaborative group learning. In the above two sessions, what problems students solved and what problems remained unsolved, each group sends a representative out to present their learning outcomes and ask their questions. The presentation is done by the live demonstration method, where each group's representative goes to the teacher's machine and demonstrates the group's results to all the students, and the author evaluates the level of each group's demonstration and demonstrates results, and the groups evaluate each other (see Figure 7).

In Figure 7, what we show is the specific value under different headings. Due to a large number of types, this method is used for visual analysis. We can see that the values under different headings are not related in any way. As can be seen from Figure 8, after the micro-video-based flipped classroom teaching, the students in the experimental class preferred and liked the micro-video-based flipped classroom teaching model, which was more favored by the first-year students than the traditional teaching model. The results of the analysis showed that the overall mean value of the learning effectiveness section was 4.1543, which was higher than the value of 4 for the "meet" option on the five-point scale, with a standard deviation of 0.1392 and variance of 0.0190, indicating that the respondents generally believed that the use of micro-video teaching resources in the classroom had a positive impact on their ability to improve. The learners' hands-on, self-learning, and problem-solving skills were significantly improved, further explaining the reason for the relatively high overall performance of the learners. The question with the lowest score was "I think the use of micro-video teaching resources helps to enhance my observation and analysis skills," with a score of 3.9787, indicating that micro-video teaching resources have yet to be improved in enhancing learners' observation and analysis skills (see Figure 8).

Second, the sound effects can be used to cut the knowledge chapters, so that students can better appreciate the micro-course.

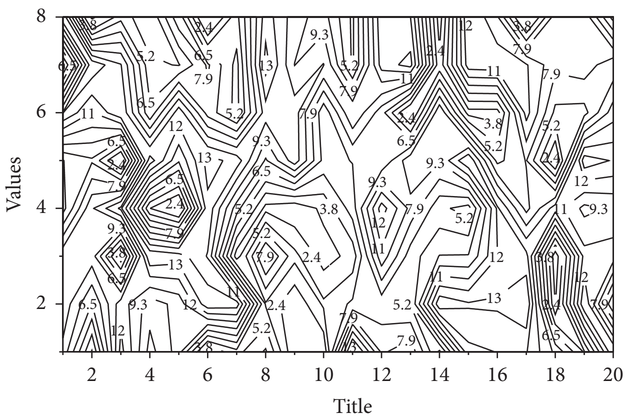

Figure 7: Pre-test statistics.

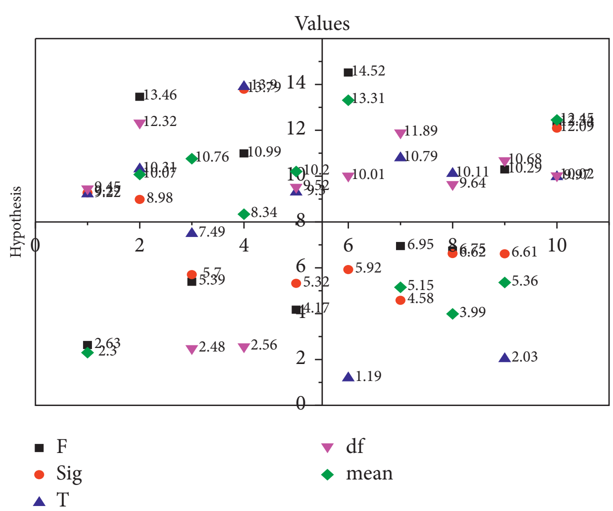

Figure 8: T-test results.

5. Conclusion

The use of micro-video scaffolding in the junior high school English listening classroom can significantly improve students' learning performance. Analysis of the pre- and post-test scores revealed that although both classes improved their English listening test scores in the first semester compared to the pre-experimental period, the further comparison revealed that the experimental class students' English listening scores improved more. In addition, the interview with the students of the experimental class revealed that the students of the class were generally more active in completing the tasks assigned by the teacher and were also able to participate in learning activities more actively and positively. What is more important is that both classes used the same teaching materials, but the only difference was the teaching method. This shows that the use of micro-video scaffolding teaching in junior high school English listening classrooms can stimulate students' motivation to learn English listening, improve learning efficiency, and eventually improve listening performance. The only difference between the two classes is the teaching method. This shows that the use of micro-video scaffolding in junior high school English listening classroom teaching can motivate students to learn English listening, improve learning efficiency, and eventually improve listening performance. The results of the students' reading motivation questionnaire after using the hybrid teaching model of micro-video-scaffolded classroom show that students' English reading motivation in the three dimensions of learning attitude, learning reasons, and learning behavior has been improved and maintained at a high level, mainly because students are more interested in learning English reading, learning English reading more out of deep internal learning motivation, completing the reading task on time, and taking the initiative to read outside the classroom.

Data Availability

The data used to support the findings of this study are included within the article.

Conflicts of Interest

No conflicts of interest exist concerning this study.

Acknowledgments

This paper was not funded by any organization.

References

[1] Z. Xu and Y. Shi, "Application of constructivist theory in flipped classroom-take college English teaching as a case study," *Theory and Practice in Language Studies*, vol. 8, no. 7, pp. 880–887, 2018.

[2] X. Ma, Y. Su, J. Liu, and S. Li, "Design and test of flipped classroom learning support model in mobile learning environment," *Creative Education*, vol. 10, no. 2, pp. 246–261, 2019.

[3] Y. Wang, "A study on college English high-efficiency class based on blended teaching mode of flipped classroom," *Theory and Practice in Language Studies*, vol. 10, no. 9, pp. 1066–1071, 2020.

[4] J. Qin and Z. Jia, "Learner-generated behaviours in a flipped learning: a focus on computer culture foundation course," *International Journal of Continuing Engineering Education and Life Long Learning*, vol. 30, no. 1, pp. 1–14, 2020.

[5] A. D. Fang, G. L. Chen, Z. R. Cai, L. Cui, and L. Harn, "Research on blending learning flipped class model in colleges and universities based on computational thinking—"Database principles" for example," *Eurasia Journal of Mathematics, Science and Technology Education*, vol. 13, no. 8, pp. 5747–5755, 2017.

[6] J. Liu, "The implementation of flipped classroom teaching mode in basic English teaching for Tibetan college students," *Theory and Practice in Language Studies*, vol. 9, no. 8, pp. 1009–1014, 2019.

[7] F. Jin, "Exploring the blended teaching mode under the guidance of OBE theory—taking the course of English newspaper reading I in Zhejiang Yuexiu university as an example," *Open Journal of Modern Linguistics*, vol. 11, no. 4, pp. 511–519, 2021.

[8] D. Zhao and X. Liang, "The research on the professional development of information technology teachers based on the implementation of flipped classroom teaching model," *International Journal of Social and Humanistic Computing*, vol. 3, no. 2, pp. 176–190, 2019.
[9] M. Chen, B. Li, Y. Hu, and Z. Ren, "A teaching ecosystem of engineering graphics based on the deeper learning cycle model and asynchronous SPOC," *Journal for Geometry and Graphics*, vol. 23, no. 2, pp. 259–267, 2019.
[10] Z. Fan and F. Shu-Xiong, "The process of personalized learning based on flipped classroom," *Sino-US English Teaching*, vol. 14, no. 4, pp. 233–238, 2017.
[11] N. Gao, "Construction and implementation of teaching mode for digital Mapping based on interactive micro-course technology," *International Journal of Emerging Technologies in Learning (iJET)*, vol. 13, no. 2, pp. 21–32, 2018.
[12] M. Huang and C. Lijian, "The path of building curriculum resources of adult colleges and universities based on MOOC in the intelligent era," *Canadian Social Science*, vol. 16, no. 6, pp. 32–38, 2020.
[13] W. Zhang and L. E. Vesnina, "Online teaching Russian practical grammar at a Chinese university during the epidemic," *Russian Language Studies*, vol. 18, no. 4, pp. 383–408, 2020.
[14] Z. Wei, "Discussion on the effective application of information technology in informatization EFL teaching," *Theory and Practice in Language Studies*, vol. 8, no. 10, pp. 1294–1300, 2018.
[15] J. Xiao, M. Cao, X. Li, and P. Hansen, "Assessing the effectiveness of the augmented reality courseware for starry sky exploration," *International Journal of Distance Education Technologies*, vol. 18, no. 1, pp. 19–35, 2020.
[16] J. Cai, S. Zhu, Y. M. Tian, and H. H. Yang, "Learning from practice: improving blended learning strategies in an educational technology course," *International Journal of Innovation and Learning*, vol. 21, no. 4, pp. 467–480, 2017.
[17] S. Shi and Z. A. B. Zainuddin, "A review of the research on blended learning in physical education in China and international," *Journal of Critical Reviews*, vol. 7, no. 11, pp. 672–686, 2020.
[18] P. J. García Nieto, E. García-Gonzalo, J. P. Paredes-Sánchez, A. Bernardo Sánchez, and M. Menéndez Fernández, "Predictive modelling of the higher heating value in biomass torrefaction for the energy treatment process using machine-learning techniques," *Neural Computing & Applications*, vol. 31, no. 12, pp. 8823–8836, 2019.
[19] L. M. Maiyar, S. Cho, M. K. Tiwari, K.-D. Thoben, and D. Kiritsis, "Optimising online review inspired product attribute classification using the self-learning particle swarm-based Bayesian learning approach," *International Journal of Production Research*, vol. 57, no. 10, pp. 3099–3120, 2019.
[20] E. M. Golafshani and G. Pazouki, "Predicting the compressive strength of self-compacting concrete containing fly ash using a hybrid artificial intelligence method," *Computers and Concrete*, vol. 22, no. 4, pp. 419–437, 2018.
[21] F. Daneshfar and S. J. Kabudian, "Speech emotion recognition using discriminative dimension reduction by employing a modified quantum-behaved particle swarm optimization algorithm," *Multimedia Tools and Applications*, vol. 79, no. 1, pp. 1261–1289, 2020.